Universidade de Lisboa

Faculdade de Medicina de Lisboa

Kyotorphin as a new pharmacological therapeutic strategy for Alzheimer's Disease

Rita Alexandra Figueira Belo

Orientador: Professora Doutora Maria José de Oliveira Diógenes Nogueira

Co-Orientadores: Professora Doutora Vera Luísa Santos Neves

Professora Doutora Ana Maria Ferreira Sebastião

Tese especialmente elaborada para obtenção do grau de

Doutor em Ciências Biomédicas

Especialidade em Neurociências

2022

Universidade de Lisboa

Faculdade de Medicina de Lisboa

Kyotorphin as a new pharmacological therapeutic strategy for Alzheimer's Disease

Rita Alexandra Figueira Belo

Orientador: Professora Doutora Maria José de Oliveira Diógenes Nogueira
Co-Orientadores: Professora Doutora Vera Luísa Santos Neves
Professora Doutora Ana Maria Ferreira Sebastião

Tese especialmente elaborada para obtenção do grau de Doutor em Ciências Biomédicas Especialidade em Neurociências

Júri: Doutora Catarina Alexandra dos Reis Vale Gomes, Professora Auxiliar da Faculdade de Farmácia da Universidade de Coimbra

Doutora Isaura Ferreira Tavares, Professora Catedrática da Faculdade de Medicina da Universidade do Porto

Doutora Joana Fernandes Esteves Soares Coelho, Investigadora Pós-Doc do Instituto de Medicina Molecular João Lobo Antunes, Unidade associada à Faculdade de Medicina da Universidade de Lisboa

Doutora Maria José de Oliveira Diógenes Nogueira, Professora Associada com Agregação da Faculdade de Medicina da Universidade de Lisboa

Doutor Nuno Fernanco Duarte Cordeiro Correia dos Santos, Professor Associado com Agregação da Faculdade de Medicina da Universidade de Lisboa

FCT Fundação para a Ciência e a Tecnologia
MINISTÉRIO DA CIÊNCIA, TECNOLOGIA E ENSINO SUPERIOR

2022

As opiniões expressas nesta publicação são da exclusiva responsabilidade do seu autor.

All opinions expressed in this document are of the sole responsibility of its author.

A impressão desta dissertação foi aprovada pelo Conselho Científico da Faculdade de Medicina de Lisboa em reunião de 25 de Janeiro de 2022.

The experimental work herein described was performed during February 2016 and February 2020, at Instituto de Medicina Molecular / João Lobo Antunes, Faculdade de Medicina da Universidade de Lisboa, except when otherwise stated, under the supervision of Doctor Maria José Diógenes, and co-supervision of Doctor Vera Neves and Doctor Ana Maria Sebastião.

“Here is my secret,

A very simple secret.

It is only with the heart that on can see rightly.

***What is essential is invisible to the eye**.”*

The Little Prince

Cheers to **FRIENDSHIP***!*

Um brinde à **AMIZADE***!*

Um bem que parece
ser cada vez mais raro

The **Acknowledgments** section
is at the end of this document

Contents

Index of Figures

Index of Tables

a.a.	Amino acids
aCSF	Artificial cerebrospinal fluid
AD	Alzheimeir's Disease
ANOVA	Analysis of variance
Arg or L-Arg	Arginine or L-Arginine
ATP	Adenosine 5'-triphosphate
Aβ	Amyloid beta
$A\beta_{olig}$	Oligomeric forms of amyloid beta
BBB	Blood-brain barrier
BDNF	Brain-derived neurotrophic factor
BSA	Bovine serum albumin
CA1	*Cornu Ammonis* 1
Ca^{2+}	Calcium ion
$CaCl_2$	Calcium chloride
CCK-8	Cell counting kit-8
cGMP	Cyclic guanosine monophosphate
CNS	Central nervous system
CSF	Cerebrospinal fluid
DIV	Days *in vitro*
EDTA	Ethylenediaminetetraacetic acid
F-actin	Filamentous actin
FBS	Fetal bovine serum
fEPSP	Field-excitatory postsynaptic potentials
Fura 2AM	Fura 2-acetoxymethyl
HBSS	Hank’s balanced salt solution
HCl	Hydrochloric acid
HEPES	4-(2-hydroxyethyl)-1-piperazineethanesulfonic acid
HPLC	High-performance liquid chromatography
i.c.v.	Intracerebroventricular
i.cist.	Intracisternal
i.p.	Intraperitoneal
i.v.	Intravenous
I/O	Input/Output
$InsP_3$	Inositol 1,4,5-triphosphate

$InsP_3R$	$InsP_3$ receptor
K^+	Potassium ion
KCl	Potassium chloride
KTP	Kyotorphin or *L*-tyrosine-*L*-arginine
KTP_{ant}	KTP receptor antagonist or *L*-leucine-*L*-arginine
KTPase	KTP-degrading aminopeptidase
KTP-NH_2	Amidated-Kyotorphin
KTPr	KTP receptor
LTP	Long-term potentiation
MAP2	Microtubule-associated protein 2
MCI	Mild-cognitive impairment
Met-enk, met-enk, Enk	Met-enkephalin
Mg^{2+}	Magnesium ion
$MgCl_2$	Magnesium chloride
$MgSO_4$	Magnesium sulfate
MTT	3-(4,5-dimethylthiazol-2-yl)-2,5-diphenyltetrazolium bromide
Na^+	Sodium ion
Na_3VO_4	Trisodium vanadate
NaCl	Sodium chloride
NaF	Sodium fluoride
NaH_2PO_4	Monosodium phosphate
$NaHCO_3$	Sodium bicarbonate
NaOH	Sodium hydroxide
NFTs	neurofibrillary tangles
NMDAR	*N*-methyl-*D*-aspartate receptor
NO	Nitric oxide
NORT	Novel Object Recognition test
OFT	Open Field test
PBS	Phosphate-buffered saline
PEPT2	Peptide transporters 2
PFA	Paraformaldehyde
pH	Potential of hydrogen
PLC	Phospholipase C
PPF	Paired-pulse facilitation
PSFV	Presynaptic fiber volley

p-Tau	Hyperphosphorylated tau
PTP	Post-tetanic potentiation
rpm	Revolutions per minute
RT	Room temperature
SDS	Sodium dodecyl sulphate
SEM	Standard error of the mean
TBS-T	Tris-buffered saline with Tween-20
TFA	Trifluoroacetic acid
TrkB-FL	Tropomyosin receptor kinase B-full length
TrkB-ICD	Tropomyosin receptor kinase B-intracellular domain
TRPC1	Transient receptor potential C1
Tyr or L-Tyr	Tyrosine or *L*-tyrosine
TyrRS	Tyrosyl-tRNA synthetase
UV	Ultraviolet
v/v	volume/volume
w/v	weigth/volume
WB	Western-blot
YM-SAT	Y-Maze Spontaneous Alternation test

Resumo

A quiotorfina (KTP, *L*-tirosina-*L*-arginina) é um dipéptido endógeno descrito, pela primeira vez em 1979, como sendo uma potente molécula analgésica. O seu efeito analgésico é semelhante ao dos opioides, ocorrendo através da libertação indireta de Met-encefalinas (Met-enk), sendo reversível pela ação da naloxona. Atualmente é aceite que a KTP atua através da activação de um receptor acoplado a uma proteína Gi (KTPr), capaz de induzir o influxo de Ca^{2+} através de um processo mediado pela fosfolipase C. Além disso, a ação do KTPr pode ser antagonizada pelo dipéptido *L*-Leucina-*L*-Arginina (KTP_{ant}).

Nas últimas décadas, vários estudos têm revelado o papel da KTP na modulação de diversos mecanismos do sistema nervoso central (SNC) e periférico. A KTP tem sido descrita como tendo acção antiepiléptica, termorreguladora, anti-hibernação, comportamental e moduladora de stress, sendo estes efeitos não mediados pela ação de opióides. No entanto, a grande maioria dos estudos sobre a KTP têm explorado a sua potencial aplicação no tratamento da dor. Mais recentemente, a relação entre a dor e a Doença de Alzheimer (DA), duas condições de extrema relevância epidemiológica, sugeriu o uso de fármacos relacionados com a KTP como uma nova estratégia terapêutica para a DA.

As evidências mostram que a dor crónica agrava a DA, e que a limitação em expressar verbalmente e percecionar a dor dos doentes com DA pode levar a um agravamento da doença. A DA tem vindo a provar-se ser uma doença neurodegenerativa complexa, onde a presença de placas amilóides cerebrais, principalmente constituídas pelo péptido beta amilóide (Aβ), e os emaranhados neurofibrilares, formados pela proteína tau hiperfosforilada (p-Tau), são as duas principais características histopatológicas desta doença. Adicionalmente, sabe-se que a excitotoxicidade, bem como a desregulação da sinalização do factor neurotrófico derivado do cérebro (BDNF), estão envolvidas em doenças neurodegenerativas como a DA. À semelhança do que foi observado em doentes com dor persistente, os doentes com DA apresentam uma diminuição dos níveis de KTP no líquido cefalorraquiano (LCR), sendo esta alteração inversamente proporcional ao aumento dos níveis de p-Tau no LCR desses mesmos doentes.

Recentemente, a KTP foi sugerida como sendo um agente neuroprotetor endógeno. Em particular, quando injectada intracerebroventricularmente (i.c.v.), a KTP melhora os défices de memória num modelo da DA esporádica em rato. No entanto, a KTP tem uma capacidade muito limitada para atravessar a barreira hematoencefálica (BHE). O potencial terapêutico da KTP como fármaco com possíveis aplicações no SNC contribuiu para o desenvolvimento de derivados sintéticos da KTP que atravessam a BHE. Assim, o derivado

amidado da KTP, a quiotorfina-amidada (KTP-NH_2), foi desenhado e produzido com o intuito de superar a BHE.

Neste trabalho, o objetivo principal foi explorar o uso terapêutico da KTP-NH_2 como um novo fármaco para o tratamento da DA. A caracterização e comparação do impacto da KTP e da KTP-NH_2 na função sináptica foi primeiramente avaliada em condições miméticas às fisiológicas. Dado o interesse particular no tratamento da DA, o potencial neuroprotetor de ambos os péptidos foi avaliado sobre a fisiopatologia de DA induzida pelo péptido Aβ (Capítulo 3). Por fim, este trabalho correlacionou os mecanismos sinápticos protegidos pela ação da KTP-NH_2 contra a toxicidade induzida pelo péptido Aβ, e a melhoria dos défices de memória observados após a administração sistémica de KTP-NH_2 num modelo da forma esporádica de DA em rato (Capítulo 4).

Registos eletrofisiológicos obtidos na área CA1 de fatias de hipocampo, preparadas a partir de murganhos adultos machos C57BL/6J, e pré-expostas ou superfundidas com KTP e KTP-NH_2, permitiram caracterizar o efeito de ambos os péptidos na função sináptica em condições não patológicas. Os resultados revelaram que perfusão dos péptidos, em concentrações que variaram entre os 5 nM os 50 µM, afectou a transmissão sináptica basal num processo dependente da concentração dos mesmos. Enquanto a KTP aumentou ligeiramente a transmissão sináptica, com um efeito máximo medido a 50 nM, a KTP-NH_2 causou a sua diminuição gradual. Para concentrações de 5 mM, largamente em excesso ao que se será provável ocorrer endogenamente, a ação dos péptidos rapidamente inibiu a transmissão sináptica, sendo esses efeitos reversíveis. De facto, este efeito inibitório foi total ou parcialmente eliminado com a respectiva remoção da KTP ou da KTP-NH_2. Assim, em condições não patológicas, estes resultados apontam para a existência de diferenças entre os mecanismos sinápticos de ambos os péptidos. No entanto, nem a KTP (50 nM), nem a KTP-NH_2 (50 nM) afetaram significativamente 1) a eficiência da transmissão sináptica, avaliada por curvas de *input/output*; 2) a plasticidade de curto prazo, avaliada através da potenciação pós-tetânica e facilitação mediada por pares de sinais; ou 3) a libertação de glutamato. Juntos, esses dados apontam para que o efeito de ambos os péptidos na transmissão sináptica não seja mediado por mecanismos pré- ou pós-sinápticos.

A plasticidade sináptica é um mecanismo chave nos processos de memória e aprendizagem. A potenciação de longo prazo (em inglês *long-term potentiation*, ou LTP) foi avaliada em fatias de hipocampo, pré-expostas por 3h ou agudamente superfundidas com KTP (50 nM) ou KTP-NH_2 (50 nM). Para testar condições fisiopatológicas miméticas de DA, as fatias de hipocampo foram pré-tratadas com espécies oligoméricas do péptido Aβ (200 nM), uma das espécies solúveis do péptido Aβ mais tóxicas. Adicionalmente, as espinhas

dendríticas foram avaliadas em cultura de neurónios corticais após o tratamento com KTP (50 nM) ou KTP-NH_2 (50 nM), e na presença ou ausência do péptido Aβ (25 μM) por 24h. Os resultados demonstraram que a KTP-NH_2, mas não a KTP, teve um efeito neuroprotetor contra os défices induzidos pelo péptido Aβ na magnitude da LTP. No entanto, essas diferenças contrastaram com o efeito neuroprotector molecular semelhante. A acção de ambos os péptidos restaurou a densidade de espinhas dendríticas afectada pela ação do péptido Aβ, sem induzir efeitos tóxicos nos neurónios. Para se avaliar se o efeito neuroprotetor da KTP-NH_2 (50 nM) sobre a LTP poderia ser antagonizado pelo KTP_{ant}, as fatias foram pré-tratadas durante 30 min com KTP_{ant} (250 nM). Os resultados mostraram que o KTP_{ant} antagonizou o efeito neuroprotetor da KTP-NH_2 sobre os défices induzidos pelo péptido Aβ na LTP. No entanto, não ficou claro se, sozinho, o KTP_{ant} teve uma ação neuroprotetora preventiva contra o péptido Aβ, ou sobre qual foi o mecanismo afectado que induziu toxicidade pela adição prévia do KTP_{ant} antes da adição da KTP-NH_2.

O aumento dos níveis intracelulares de Ca^{2+} é uma constante nos processos mediados por KTP. Assim, a técnica de imagiologia de cálcio foi utilizada para se exclarecer se o aumento dos níveis de Ca^{2+} poderia ser causado diretamente pela atividade da KTP e/ou se tais aumentos seriam necessários para o surgimento das ações mediadas pela KTP. Os resultados revelaram que nem a presença da KTP (50nM) ou da KTP-NH_2 (50nM) afetaram os níveis intracelulares de Ca^{2+} em neurónios, não havendo alterações significativas na homeostase neuronal de Ca^{2+}.

A sobreativação das calpaínas ocorre devido ao aumento dos níveis intracelulares de Ca^{2+}, geralmente como consequência da excitotoxicidade induzida pelo péptido Aβ. Assim, a ação de ambos os péptidos (50 nM) foi avaliada sobre a atividade *in vitro* das calpaínas em homogenatos de tecido cortical de murganhos. No entanto, os resultados revelaram que nem a KTP nem a KTP-NH_2 afetaram a ativação das calpaínas e, consequentemente, não evitaram a clivagem do receptor de BDNF, em inglês *tropomyosin receptor kinase B-full length* (TrkB-FL), um receptor com conhecida acção neuroprotectora e é um substrato de calpaínas em condições de toxicidade induzida pelo péptido Aβ.

Finalmente, num modelo da forma esporádica de DA em rato, a administração sistémica de KTP-NH_2 protegeu contra os défices na memória de trabalho espacial e memória episódica, sem afetar a actividade motora ou induzir um comportamento ansiogénico nestes animais. O efeito neuroprotetor induzido pela KTP-NH_2 foi correlacionado com a prevenção dos défices moleculares induzidos pelo péptido Aβ tanto na magnitude da LTP em fatias hipocampais pré-tratadas como na perda de espinhas dendríticas em cultura de neurónios corticais.

Concluindo, este trabalho reuniu novas evidências sobre os efeitos neuromoduladores da KTP e da KTP-NH_2 sobre a função sináptica, destacando as ações neuroprotetoras da KTP-NH_2. Em condições miméticas às fisiológicas, a ausência de efeitos sobre a função sináptica reforça o potencial terapêutico de ambos os péptidos, sugerindo a inexistência de efeitos secundários sobre a transmissão sináptica. Tanto a nível molecular como funcional, os resultados atestam o efeito neuroprotetor da KTP-NH_2 (Capítulo 3), corroborando com os resultados obtidos pela sua administração sistémica num modelo da forma esporádica de DA em rato (Capítulo 4), o que fornece importantes evidências para o uso da KTP-NH_2 como um possível fármaco no tratamento da DA, entre outras. À luz da complexa fisiopatologia da DA, no futuro será importante determinar se o efeito neuroprotector da KTP-NH_2 é potenciado num tratamento independente, ou se as suas ações devem ser integradas num regime de politerapia. Entre outros aspectos, a identificação da janela de tempo para intervenção terapêutica com KTP-NH_2 no tratamento da DA será fundamental para determinar se sua ação é preventiva ou se é capaz de reverter os défices moleculares e cognitivos presentes na fisiopatologia da DA.

Palavras-chave: Quiotorfina, Quiotorfina-amidada, Doença de Alzheimer, Plasticidade Sináptica, Neuroproteção

Abstract

Kyotorphin (KTP, *L*-tyrosyl-*L*-arginine) is an endogenous dipeptide, described for the first time in 1979, as a potent analgesic molecule. Its naloxone-reversible opioid-like analgesic effect is indirectly mediated by the inducing the release of Met-enkephalin (Met-enk). It is currently accepted that KTP acts through a specific Gi-coupled receptor (KTPr), inducing Ca^{2+} influx in a phospholipase C-mediated process. Moreover, this KTPr-mediated action can be antagonized by the dipeptide *L*-Leucine-*L*-Arginine (KTP_{ant}).

Over the last decades, several studies have been revealing KTP role in the modulation of several mechanisms in the central and peripheric nervous systems. KTP has been described as having an antiepileptic, thermoregulatory, anti-hibernation, behavioral and stress modulatory actions, being these non-opioid-mediated effects. However, the vast majority of KTP research has been explored its potential application in pain treatment. More recently, the link between pain and Alzheimer's Disease (AD), two conditions with high epidemiologic relevance, supported the use of KTP-related drugs as new therapeutic strategies for AD.

Evidence shows that chronic pain aggravates AD, and the limited capacity of AD patients to verbally express and perceive pain can worsen disease progression. AD has proven to be a highly complex neurodegenerative disease, of which brain amyloid plaques, mainly constituted by amyloid beta (Aβ) peptide, and neurofibrillary tangles formed by hyperphosphorylated tau (p-Tau) protein, are the two histopathological hallmarks of this disease. Additionally, excitotoxicity, as well as dysregulation of brain-derived neurotrophic factor (BDNF) signaling, are known to be involved in neurodegenerative disorders such as AD. Similarly to what was observed in patients with persistent pain, AD patients have decreased cerebrospinal fluid (CSF) KTP levels, which are inversely correlated to the increase of p-Tau levels in CSF of those patients.

Recently, KTP was suggested to be an endogenous neuroprotective agent. In particular, when intracerebroventricular (i.c.v.) injected, KTP ameliorated memory impairments in a rat model of sporadic AD. However, KTP has a limited capacity to cross the blood-brain barrier (BBB). The potential therapeutic value of KTP as a central nervous system (CNS) drug led to the development of synthetic KTP derivatives, which might cross the BBB. Accordingly, the KTP amidated-derivative, the Amidated-Kyotorphin ($KTP\text{-}NH_2$), was designed and produced to overcome the BBB.

In this work, the main goal was to explore the therapeutic use of $KTP\text{-}NH_2$ as a new drug for AD treatment. It started with the characterization and comparison of the impact of KTP and $KTP\text{-}NH_2$ in synaptic function under physiological mimetic conditions. Then, given the particular interest of this work in AD treatment, the neuroprotective potential of both peptides

was evaluated upon Aβ-induced AD (Chapter 3). Finally, this work correlated the synaptic mechanisms protected by KTP-NH_2 action against Aβ-induced toxicity, and the ameliorated memory impairments observed after the systemic administration of KTP-NH_2 in a model of sporadic AD in rat (Chapter 4).

Electrophysiological recordings obtained in the CA1 area of hippocampal slices prepared from adult male C57BL/6J mice, pre-exposed or superfused with KTP and KTP-NH_2, allowed the characterization of the effects of both peptides on synaptic function under non pathological conditions. Results revealed that for concentrations ranging from 5 nM to 50 µM, the peptides affected the basal synaptic transmission in a concentration-dependent manner. While KTP slightly increased synaptic transmission, with a maximal effect measured at 50 nM, KTP-NH_2 had a gradual inhibitory effect. At concentrations of 5 mM, largely in excess of what is likely to occur endogenously, peptides' action rapidly inhibited synaptic transmission, being these effects reversible. In fact, this inhibitory effect was totally or partially eliminated with the respective removal of KTP or KTP-NH_2. Thus, under non-pathological conditions, these findings suggested a different effect on synaptic mechanisms. However, neither KTP (50 nM), nor KTP-NH_2 (50 nM), significantly affected: 1) synaptic transmission efficiency, evaluated by input/output curves; 2) short-term plasticity, evaluated by post-tetanic potentiation and paired-pulse facilitation; or 3) glutamate release. Together, these findings suggested that the effects of both peptides on synaptic transmission were likely not directly mediated by pre- or post-synaptic mechanisms.

Synaptic plasticity is a key mechanism in memory and learning processes. Long-term potentiation (LTP) was evaluated in hippocampal slices, which were either pre-exposed for 3h or acutely superfused with KTP (50 nM) or KTP-NH_2 (50 nM). For testing mimetic AD pathophysiological conditions, hippocampal slices were pre-treated with oligomeric Aβ peptide species (200 nM), one of the most soluble toxic Aβ species. Additionally, dendritic spines were evaluated in cultured cortical neurons, after the treatment with KTP (50 nM) or KTP-NH_2 (50 nM), and in the presence or absence of Aβ peptide (25 µM) for 24h. Results demonstrated that KTP-NH_2, but not KTP, had a neuroprotective effect against Aβ-induced impairments on LTP magnitude. However, these differences contrasted with the similar molecular neuroprotective effect. The action of both peptides restored the density of dendritic spines affected by the action of the Aβ peptide, without inducing toxic effects on neurons. To evaluate whether the neuroprotective effect of KTP-NH_2 (50 nM) over LTP could be antagonized by KTP_{ant}, slices were pre-treated for 30 min with KTP_{ant} (250 nM). The results revealed that KTP_{ant} antagonized the neuroprotective effect of KTP-NH_2 over Aβ peptide-induced impairments in LTP. However, it is still unclear if KTP_{ant}, alone, had a

preventive neuroprotective action against Aβ peptide, or which affected mechanism might prompt toxicity when KTP_{ant} was added *prior* to KTP-NH_2.

Elevation of intracellular Ca^{2+} levels are a hallmark of KTP-mediated processes. Thus, calcium imaging technique was used to understand whether the increase in Ca^{2+} levels could be directly caused by KTP activity and/or whether such increases would be necessary for the emergence of KTP-mediated actions. The results revealed that neither the presence of KTP (50 nM) nor KTP-NH_2 (50 nM) affected Ca^{2+} intracellular levels in neurons, so there were no significant changes in neuronal calcium homeostasis.

Calpain overactivation happens due to increased intracellular Ca^{2+} levels, usually as a consequence of Aβ peptide-induced excitotoxicity. As such, the action of both peptides (50 nM) over calpain *in vitro* activity was assessed using mice cortical tissue homogenates. Results revealed that neither KTP nor KTP-NH_2 impacted calpain activation and, consequently, did not prevent calpain-induced cleavage of the BDNF receptor, the tropomyosin receptor kinase B-full length (TrkB-FL), which has a well-known neuroprotective role, and it is a substrate for calpains under Aβ-induced toxicity.

Finally, in a rat model of sporadic AD, systemic administration of KTP-NH_2 protected against spatial working-memory and episodic memory deficits, without affecting motor activity or inducing an anxiety-like behavior in the animals. Moreover, this KTP-NH_2-induced neuroprotective effect was correlated with the prevention of Aβ-induced deficits, in both LTP magnitude of pre-treated hippocampal slices and spine density of cortical neuronal cultures.

In conclusion, the present work collected novel evidence of KTP and KTP-NH_2 neuromodulatory effects over synaptic function, highlighting the neuroprotective actions of KTP-NH_2. Under physiological mimetic conditions, the absence of effects over synaptic function bolsters the therapeutic potential of both peptides, suggesting the absence of side-effects upon synaptic transmission. At molecular and functional levels, these findings supported the KTP-NH_2 neuroprotective effect (Chapter 3), confirming the results obtained through its systemic administration in a rat model of sporadic AD (Chapter 4), which provides important evidence for the use of KTP-NH_2 as a drug for treatment of AD and, eventually, other diseases. In light of the complex pathophysiology of AD, in the future, it will be important to determine whether KTP-NH_2 neuroprotective effect is potentiated as a standalone treatment, or if its actions should be included as a broader multidrug treatment regimen. Among other aspects, in the treatment of AD, identifying the time-window for therapeutic intervention with KTP-NH_2 will be essential to ascertain whether its action relies on the prevention or if this drug is able to recover the molecular and cognitive deficits present in AD pathophysiology.

Keywords

Kyotorphin, Amidated-kyotorphin, Alzheimer's Disease, Synaptic Plasticity, Neuroprotection

In research, the design of a new study rarely emerges from a vacuum. It always starts with a *question*, and specific tasks naturally emerge based on some hypothesis that can be supported by experimental evidence. As expected, new scientific evidence commonly raises new questions and hypotheses to be tested. We can enter in a never-ending loop of consecutive iterations, especially in basic science where we still have so much to discover. This work was not an exception to this *phenomenon*. It started as a collaboration between the fields of *pharmacology & neurosciences* and *biochemistry*, and more specifically between Ana M. Sebastião's and Miguel Castanho's Laboratories at iMM | JLA.

This *story* started a few years before the beginning of my work, when a new molecule - the Amidated-Kyotorphin (KTP-NH_2) was developed at Miguel Castanho's Lab, as an interesting synthetic derivative of Kyotorphin (KTP). KTP is an endogenous dipeptide with the inability to cross the brain-blood barrier (BBB), which drastically reduces its therapeutic value. To overcome this difficulty, KTP-NH_2 was synthetized. Besides being capable of crossing the BBB, KTP-NH_2 has been studied for some years, showing a surprisingly neuroprotective effect against memory impairments present in a dementia rat model. Given that Alzheimer's' Disease (AD) is the major cause of dementia nowadays, the interest of evaluating the potential therapeutic use of KTP-NH_2 to treat AD patients was set out.

The motivation of this work was to study the neuroprotective effect of KTP-NH_2 in the context of AD. In addition, having in mind that little was known about the physiological actions of KTP-NH_2 and KTP (the endogenous peptide form), the effects of both peptides were characterized and compared in the synaptic function.

This thesis was organized in 6 chapters. It starts with the **introduction** chapter, providing a context for this study. Although this chapter can be somehow exhaustive in some topics, the information was selected to give a broad vision of the past, present, and future landscape of the research in KTP and KTP-NH_2. It was focused on aspects that can help understanding this work, namely its scientific motivation, rationality, and main findings.

The chapter of **objectives** presentes both general and specific aims. Given the high exploratory component of this work, some results led to new questions and, consequently, to the design of new experiments to answer them. However, the aims converged to a better understanding of KTP and KTP-NH_2 actions upon central nervous system.

Then, the **results** of this work were presented within the next two chapters. During the development of this work, we were able to prepare an original research article (Chapter 3), and publish another (Chapter 4). Chapters 3 and 4 include the sections of these scientific

papers (introduction, materials and methods, results, and discussion), with slightly structural adaptations to the original manuscripts. Each of those chapters have a brief *chapter rationale and publication information* section, where all authors' contributions were clearly described, as well as the funding support.

Chapter 3 – Characterization of KTP and KTP-NH_2 effects in synaptic functions under non-pathological conditions and Aβ-induced pathophysiology

Belo RF, Miranda-Lourenço C, Costa-Coelho T, de Almeida-Borlido C, Vaz SH, Martins V, de Alves Pereira B, Pérez-Peinado C, Valle J, Vicente Miranda H, Fonseca-Gomes J, Ferreira CB, Andreu D, Heras M, Bardaji E, Castanho MARB, Neves V, Sebastião AM, and Diógenes MJ (*in preparation*).

Chapter 4 – The neuroprotective effect of KTP-NH_2 systemic treatment

Belo RF*, Martins MLF*, Shvachiy L, Costa-Coelho T, de Almeida-Borlido C, Fonseca-Gomes J, Neves V, Vicente Miranda H, Outeiro TF, Coelho JE, Xapelli S, Valente CA, Heras M, Bardaji E, Castanho MARB[§], Diógenes MJ[§] and Sebastião AM[§] (2020) The Neuroprotective Action of Amidated-Kyotorphin on Amyloid β Peptide-Induced Alzheimer's Disease Pathophysiology. Front. Pharmacol. 11:985. doi: 10.3389/fphar.2020.00985 (Appendix).

Chapter 5 includes a **conclusion** of the main findings obtained along chapter 3 and 4, and the **future perspectives,** where I briefly presented the ongoing work, among other ideas and thoughts, which summarized my personal vision on how this work will pave the way for future studies.

The last chapter includes the **references** used along this dissertation. All figures presented along this thesis were created by me, unless otherwise stated. Figure and table indexes were adapted to flow over the manuscript.

Finally, the experimental work was developed between February 2016 and February 2020, at iMM | JLA, under the supervision of Doctor Maria José Diógenes, and co-supervision of Doctor Vera Neves and Doctor Ana Maria Sebastião, except from a 2-months period (June and July 2017), when I worked under the supervision of Doctor David Andreu, at Peptide Synthesis Core Facility, Universitat Pompeu Fabra, Barcelona Biomedical Research Park (Barcelona).

Funding

I was funded by Fundação para a Ciência e a Tecnologia (FCT), between March 2016 and February 2020 (PD/BD/114337/2016). My 2-months short internship in Barcelona was supported by a Marie Sklodowska-Curie Mobility Grant (INPACT-H2020-RISE, 2014).

Between March 2020 and April 2021, I was supported with a fellowship from Genome^{PT} - POCI-01-0145-FEDER-022184, supported by COMPETE 2020 – Operational Programme for Competitiveness and Internationalisation (POCI), Lisboa Portugal Regional Operational Programme (Lisboa2020), Algarve Portugal Regional Operational Programme (CRESC Algarve2020), under the PORTUGAL 2020 Partnership Agreement, through the European Regional Development Fund (ERDF).

Finally, all the work presented in this dissertation was financially supported by several grants and funding agencies, being this information detailed at the *rationale and publication information* section of chapter 3 and 4.

Other Publications

During this period, I also collaborated in other projects. Here I list both published and submitted research articles until the date of this dissertation submission:

Paulo SL*, Miranda-Lourenço C*, Belo RF*, Rodrigues RS, Fonseca-Gomes J, Tanqueiro SR, Geraldes V, Rocha I, Sebastião AM, Xapelli S, Diógenes MJ (2021) High caloric diet induces memory impairment and disrupted synaptic plasticity in aged rats. *Curr. Issues Mol. Biol.*, 43(3), 2305-2319. doi: 10.3390/cimb43030162

Miranda-Lourenço C*, Ribeiro-Rodrigues L*, Fonseca-Gomes J*, Tanqueiro SR*, Belo RF*, Ferreira CB*, Rei N*, Ferreira-Manso M, Almeida-Borlido C, Costa-Coelho T, Felicidade Freitas C, Zavalko S, Mouro FM, Sebastião AM, Xapelli S, Rodrigues TM, Diógenes MJ (2020) Challenges of BDNF-based therapies: From common to rare diseases. *Pharmacological Research*, 105281. doi: 10.1016/j.phrs.2020.105281

Ferreira CB*, Marttinen M*, Coelho JE*, Paldanius K, Takalo M, Mäkinen P, Leppänen L, Miranda-Lourenço C, Fonseca-Gomes J, Tanqueiro SR, Vaz SH, Belo RF, Sebastião AM, Leinonen V, Soininen H, Pike I, Haapasalo A, Lopes LV, de Mendonça A, Diógenes MJ, Hiltunen M (2021) S327 phosphorylation of the presynaptic protein SEPTIN5 increases in the early stages of neurofibrillary pathology and alters the functionality of SEPTIN5. *Neurobiology of Disease*, 163:105603. doi: 10.1016/j.nbd.2021.105603

Sá de Almeida J, Vargas M, Fonseca-Gomes J, Tanqueiro SR, Belo RF, Miranda-Lourenço C, Sebastião AM, Diógenes MJ and Pais TF (2020) Microglial Sirtuin 2 Shapes Long-Term Potentiation in Hippocampal Slices. *Front. Neurosci.* 14:614. doi: 10.3389/fnins.2020.00614

* co-first author

Chapter 1

Introduction

1.1. Kyotorphin: more than an analgesic molecule

Kyotorphin (KTP) was described for the first time in 1979, by Hiro Amano's group, in Kyoto University (Takagi et al., 1979a). This dipeptide has been studied over the last decades, revealing its role on the modulation of several mechanisms, which consolidates its proposed function as a neurotransmitter (Ueda, 2021).

1.1.1. Historical overview

During the American Revolution, opium, and later morphine, were widely used to alleviate pain in wounded soldiers (Ueda, 2021). By the late 1800s, and around 100 years after the successful isolation and crystallization of morphine from opium (Schmitz, 1985), morphine overused and its addiction had become a huge global problem. In the late 1960s, academics were highly motivated to develop new opiates or morphine derivatives that did not cause addiction, tolerance, and dependence. In the early 1970s, the discovery for the first time of morphine (opiate)-binding receptors in the mammalian brain (Hughes et al., 1975) paved a new research line where KTP discovery can be included.

In 1986, the World Health Organization presented clinical guidelines to recommend the use of morphine pills in pain treatment. Importantly, there are many reported side-effects associated with morphine administration including sedation, dizziness, constipation, nausea, urinary retention, motor impairment, respiratory depression, addition, and tolerance (Benyamin et al., 2008). However, tolerance is responsible for the dose escalation needed when opioids are chronically administrated, which increases not only the incidence but also the severity of side-effects. Unfortunately, due to addiction, opiate overuse is still a major cause of death in several countries. Nevertheless, its use continues to be highly significant for pain management in palliative care (Ueda, 2021).

1.1.2. Discovery and isolation

In 1975, Ueda and Amano's team started to search endogenous morphine-like substances present in bovine brain extracts using an adapted method developed by Kosterlitz's team (Takagi et al., 1966). This method consisted in a bioassay system for observing the inhibitory effects of the studied extracts on ileum contraction caused by electrical stimulation. Importantly, knowing that the drug naloxone had a reversible inhibitory action on morphine analgesic effect, it was commonly used as a positive control. Specifically, in the presence of morphine-like substances, naloxone can restore ileum electrical-induced contraction. In these studies, the presence of several unidentified compounds in the brain extract could mask this naloxone-reversible action. To overcome this problem, Ueda and Amano's team developed a novel method consisting on the intracisternal (i.cist.) injection of the studied extracts in rodents to assess their analgesic naloxone-reversible effect (Ueda et al., 1979).

In addition, for the assessment of anti-nociceptive effect, the authors also applied a tail-pinch test, intended to target the central pain processing instead of reflecting a spinal reflex (Takagi et al., 1966), as depicted in Figure 1 - Analgesic effect (yellow panel). Finally, using both assays, the authors proceeded with profiling the analgesic effect of fractionated substances, that were obtained through performing successively chromatographic techniques using the studied bovine brain extracts (Shiomi and Ueda, 1985; Takagi et al., 1979b); Figure 1 - First Detection and Isolation (green panel). Then, the final fraction obtained by this process unveiled the presence of a single compound with endorphin-like properties (Shiomi and Ueda, 1985). This was identified as a dipeptide constituted by a *L*-tyrosine-*L*-arginine, which was later named as *Kyotorphin* (KTP) – a combination of the words *Kyoto* (Japan) and [mor]*phine* (Takagi et al., 1979a); Figure 1 (blue panel).

1.1.3. Distribution and subcellular localization

Although initially discovered and isolated from brain tissue of bovines (Takagi et al., 1979b), KTP was later found in several other mammalian brains including in humans (Dzambazova and Bocheva, 2010). The KTP distribution across brain regions was firstly assessed in rat, after dividing their brains into eight parts (Glowinski and Iversen, 1966), and high-performance liquid chromatography (HPLC) coupled to a electrochemical detector was used to detect aromatic residues, such as in the tyrosine of KTP (Ueda et al., 1980). The KTP concentration is different among different brain regions and spinal cord, ranging for a maximum in midbrain (719.5 ng/g) and a minimum concentration in striatum (45.5 ng/g); Figure 1 - Brain and spinal cord distribution (pink panel). As expected, the highest levels of KTP are correlate with the most sensitive areas to morphine or electrical stimulation-induced analgesia, such as the lower brain stem and the spinal cord, particularly the dorsal half (Shiomi et al., 1981a, 1981b; Ueda et al., 1980). However, around 50% of total brain KTP is found in cortex, where opiate receptors and enkephalins levels are low, suggesting other non-opioid physiological actions for KTP (Ueda et al., 1980). Furthermore, KTP is also found in pituitary (Shiomi et al., 1981b), and adrenal glands (Kawabata et al., 1996), suggesting a peripheral role.

Depending on the cellular fraction analyzed, KTP concentration is higher in the crude mitochondrial P2 fraction (92.2 % of the total), followed by the nuclear P1 fraction (7.4%), and the microsome + cytosol S2 fraction (0.4%) (Ueda et al., 1982). Importantly, KTP is highly concentrated in the synaptosomal fraction of synaptic terminals (Ueda et al., 1982, 1986b, 1987a); Figure 1 - Subcellular localization (pink panel). KTP can be incorporated into rat brain synaptosomes and be released in a Ca^{2+}-dependent process upon a K^{+} depolarization, indicating that KTP might be released from neuronal endings (Ueda et al., 1986a); Figure 2 (0).

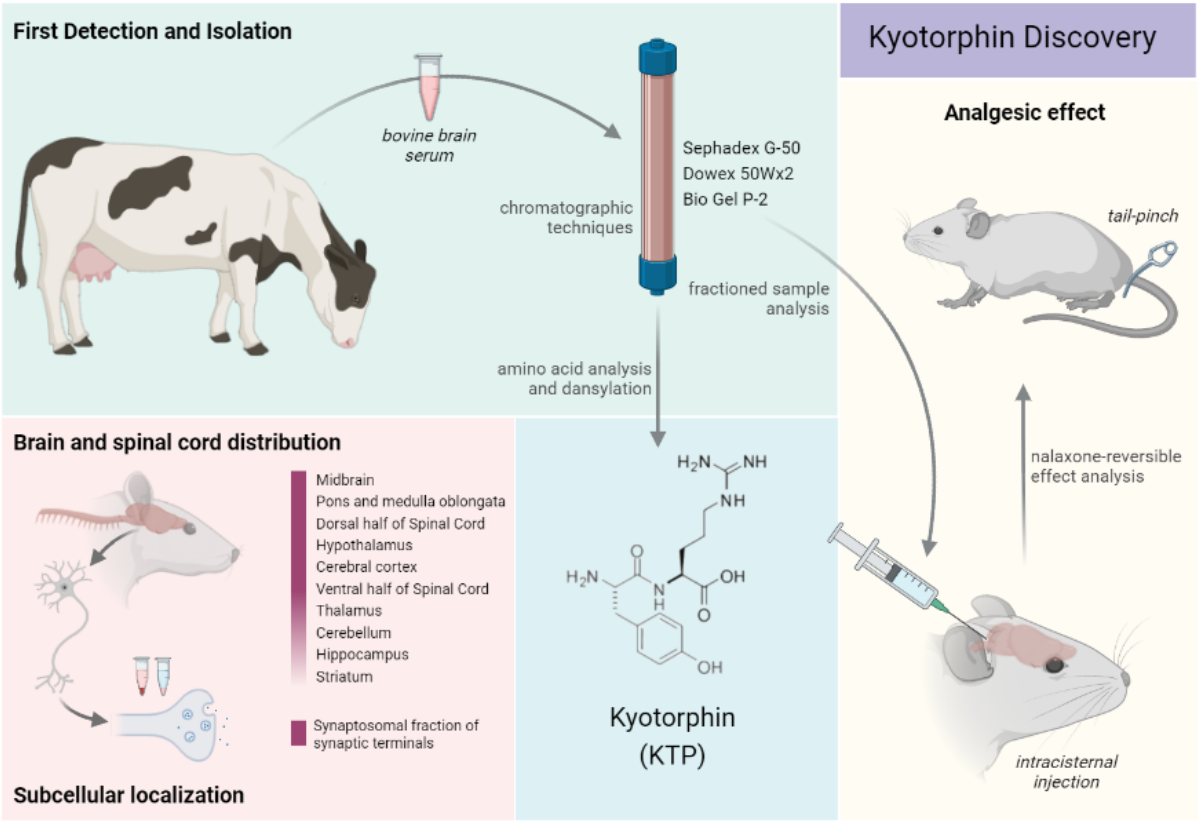

Figure 1. Kyotorphin Discovery. First Detection and Isolation (green panel): Bovine brain extracts were consecutively fractioned through performing successively chromatographic techniques and the analgesic effect of the fractionated substances was studied (Shiomi and Ueda, 1985; Takagi et al., 1979b). **Analgesic effect (yellow panel):** The naloxone-reversible analgesic potential of each substance was analyzed using a tail-pinch test after the intracisternal injection in mice (Takagi et al., 1966). **Kyotorphin (blue panel)**: Molecular structure of Kyotorphin (KTP). The authors identified a single substance in the fraction obtained after Sephadex G-50, Dowex 50W2, and Bio Gel P-2 chromatographic techniques were applied. The amino acid analysis and dansylation to determine the N-terminal amino acid revealed a dipeptide constituted by a *L*-tyrosine-*L*-arginine, confirmed by comparing the retention factor value of a synthetic compound using high-performance liquid chromatography (HPLC) (Takagi et al., 1979a). **Brain and spinal cord distribution (pink panel):** KTP distribution around the brain and the spinal cord is different, as represented by the pink column gradient. KTP concentration (ng/g tissue) is higher in midbrain and lower in striatum, as the following: 719.5 in the midbrain, 556.5 in the pons and medulla oblongata, 405.1 in the dorsal half of the spinal cord, 391.8 in the hypothalamus, 367.1 in the cerebral cortex, 230.2 in the ventral half of the spinal cord, 119.3 in the thalamus, 101.8 in the cerebellum, 61.8 in the hippocampus, and 45.5 in the striatum (Ueda et al., 1980). **Subcellular localization (pink panel):** KTP is highly concentrated in the synaptosomal fraction of synaptic terminals (Ueda et al., 1982, 1986b, 1987a).

1.1.4. Biosynthesis

KTP can be either biosynthesized by an ATP-dependent synthetase from tyrosine and arginine amino acids (a.a.), or it can be produced from the enzymatic processing of polypeptides (Ueda et al., 1986b). A specific KTP synthetase was firstly identified in rat brains, with an ATP and $MgCl_2$-dependent enzymatic activity (Ueda et al., 1987b; Tsukahara et al., 2018). Its enzymatic activity converted *L*-tyrosine (*L*-Tyr) and *L*-arginine (*L*-Arg) into KTP (Figure 2 (1)).

The distribution of KTP synthetase is correlated with the KTP levels around the brain, where its enzymatic activity is highest in midbrain, medulla oblongata, and synaptosome fractions (Ueda et al., 1980). However, its molecular characterization has not been entirely determined. An *in vitro* experiment showed that tyrosyl-tRNA synthetase (TyrRS) from *Bacillus stearothermophilus* can catalyze KTP synthesis (Kitabatake et al., 1987; Ueda et al., 1987b), whereas *Streptomyces septatus* aminopeptidase can synthesize several other dipeptides instead of KTP (Arima et al., 2006). In mammals, the TyrRS is a potential KTP synthetase (Tsukahara et al., 2018). Interestingly, in PC12 cells treated with a siRNA antisense for TyrRS, the activity of human recombinant TyrRS was selectively blocked for KTP synthesis, without affecting cell survival and proliferation, or the synthesis of several other tyrosine-containing dipeptides (e.g. tyrosine-tyrosine, tyrosine-proline, and tyrosine tryptophan) (Tsukahara et al., 2018). As expected, the expression of TyrRS mRNA is also higher in the midbrain and medulla oblongata, which correspond to rat brain regions where KTP synthetase activity is also higher (Ueda et al., 1987b). Additionally, its enzymatic catalyze is also detected in rat adrenal glands and spinal cord, which provides additional support for KTP possible role in the peripheral system (Kawabata et al., 1996).

As already mentioned, some evidence points towards KTP being produced from precursor polypeptides degradation by membrane-bound aminopeptidases or cytosolic Ca^{2+}-activated proteases (Ueda et al., 1985b; Yoshihara et al., 1990; Akasaki et al., 1995); Figure 2 (2). In fact, the accumulation of KTP, released from brain slices, is time-dependent in the presence of bestatin, which is a membrane-bound aminopeptidase inhibitor (Ueda et al., 1985b). Similarly, this also occurs in synaptosomes, possibly due to the activation of calcium-activated neutral proteases, calpain-1 or calpain-2 (Yoshihara et al., 1988). Interestingly, a novel type of calpain lacking the caseinolytic activity was identified as the one responsible for this accumulation (Yoshihara et al., 1990); Figure 2 (2). Nevertheless, calpastatin appeared as a subtract for this novel calpain and/or as a precursor of KTP. Since calpain activation requires a higher Ca^{2+} level than the neurons resting state concentration, calpain-calpastatin system activation can be driven by active neurons (see “working hypothesis” highlighted on Figure 2).

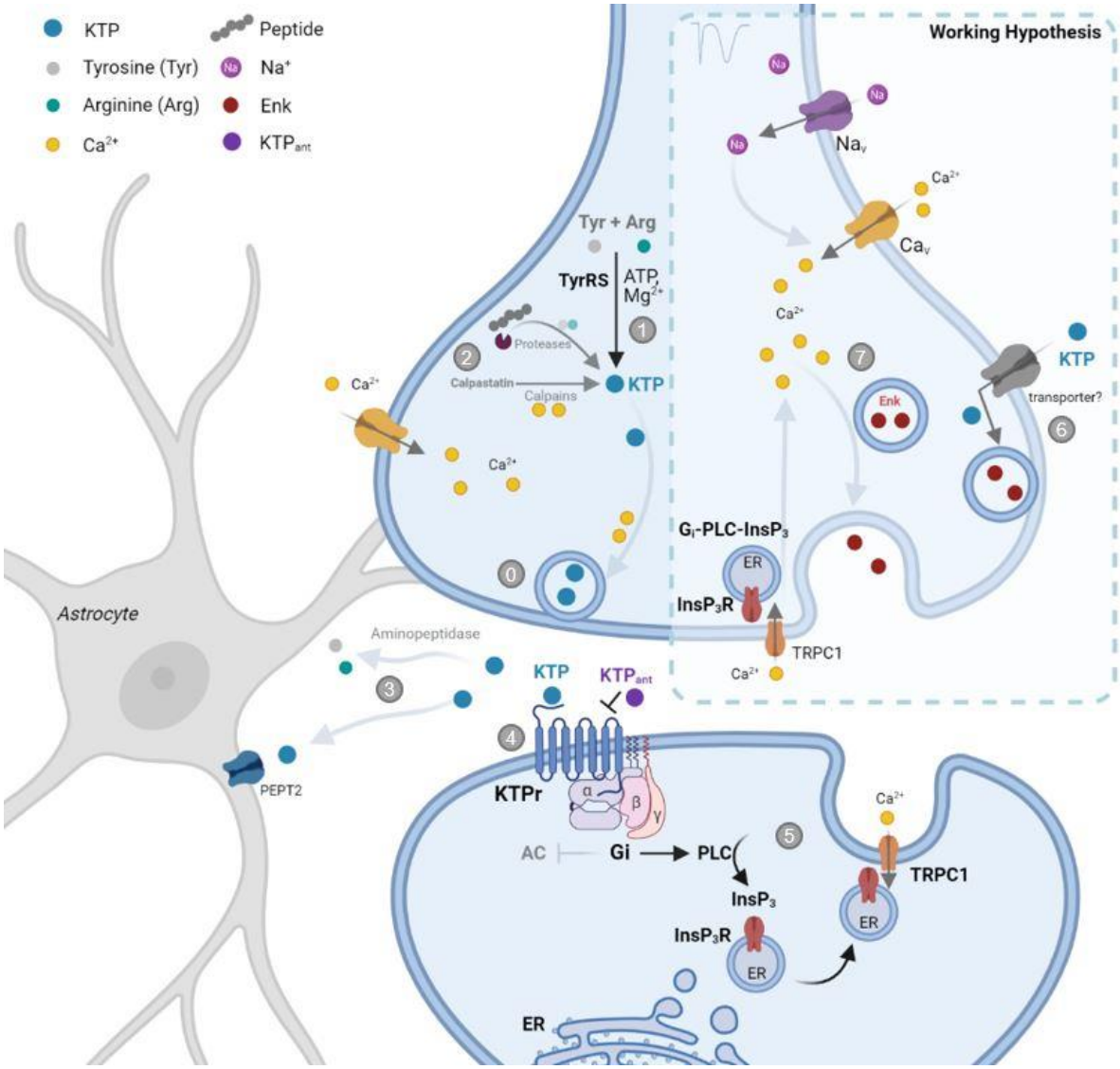

Figure 2. Kyotorphin biosynthesis, clearance, and signaling pathway activation. **(0)** Kyotorphin (KTP) can be released from neuronal endings in a Ca^{2+}-dependent process upon a K^+ depolarization (Ueda et al., 1986a). **(1)** KTP can be synthetized by a tyrosyl-tRNA synthetase (TyrRS) from *L*-Tyrosine (Tyr) and *L*-Arginine (Arg), in a Mg^{2+} and ATP-dependent mechanism (Ueda et al., 1987b; Tsukahara et al., 2018). **(2)** KTP can be produced from the degradation of precursor polypeptides by membrane-bound aminopeptidases or cytosolic Ca^{2+}-activated proteases (Akasaki et al., 1995; Ueda et al., 1985b; Yoshihara et al., 1990). Additionally, calpastatin appeared as a subtract for a novel type of calpain, lacking the caseinolytic activity, and as a precursor of KTP (Yoshihara et al., 1990). **(3)** KTP clearance happens mainly due to degradation by aminopeptidases (Ueda et al., 1985a), or KTP can be uptaken by astrocytes, or excreted to the cerebrospinal fluid through peptide transporters 2 (PEPT2) (Xiang et al., 2010). **(4)** Despite the inability to fully characterize the KTP receptor (KTPr), collected evidence indicates that KTPr is a Gi/o-coupled receptor, which activity is antagonized by the dipeptide *L*-Leucine-*L*-Arginine, or KTP antagonist (KTP_{ant}). **(5)** KTPr activates Gi-mediated phospholipase C (PLC), leading to an increase of inositol 1,4,5-triphosphate ($InsP_3$) levels, consequent $InsP_3$ receptor ($InsP_3R$) activation, and, ultimately to a Ca^{2+} influx, from extracellular

space. This Ca^{2+} influx is driven by the conformational coupling of the vesicular $InsP_3R$ and the transient receptor potential C1 (TRPC1) (Zarayskiy et al., 2007), and by the opening of PLC-mediated $InsP_3R$-gated Ca^{2+} channel (Ueda et al., 1995a, 1995b). **(6)** KTP is possible incorporated by neurons through unidentified transporters (Thakkar et al., 2008), and **(7)** it has a role on Met-enkephalin (Enk) vesicular incorporation and release (Axelrod et al., 1962). Figure inspired and adapted from (Ueda, 2021); AC – Adenylate cyclase; ER – endoplasmic reticulum.

1.1.5. Clearance

KTP inactivation mainly occurs due to peptidases degradation (Figure 2 (3)). In fact, KTP is subject to a rapid degradation in the presence of diluted suspensions of rat brain homogenates (Ueda et al., 1985a), and in lung and skin from rats (Orawski and Simmons, 1992).

Several studies have been reported the KTP degradation by aminopeptidases, trying to identify and characterize the specific KTP-degrading aminopeptidase (KTPase), and its activity inhibitors (Vaught and Chipkin, 1982; Matsubayashi et al., 1984; Ueda et al., 1985a; Akasaki et al., 1991; Akasaki and Tsuji, 1991; Orawski and Simmons, 1992; Akasaki et al., 1995). Interestingly, KTPase activity is inhibited by bestatin but not by puromycin, a potent inhibitor of soluble aminopeptidases. In fact, the co-administration of bestatin (i.cist.) potentiated KTP analgesic effect, but the systemic pre-treatment with naloxone abolished this effect (Ueda et al., 1985a). A more recent study successful purification of a specific bestatin-sensitive KTPase (Akasaki et al., 1995).

Additionally, KTP can be excreted to the cerebrospinal fluid (CSF), or up taken by astrocytes, through peptide transporter 2 (PEPT2) (Xiang et al., 2010). PEPT2 relies on pH gradient to transport di- and tripeptides, being considered a high-affinity and a low-capacity transporter. It is found in the brain, and more specifically in astrocytes, ependymal cells, epithelial cells of choroid plexus, kidney and retina (Berger and Hediger, 1999; Dieck et al., 1999; Liu et al., 1995). Since PEPT2 is not present at blood brain barrier (BBB), it cannot directly transport peptides from blood to central nervous system (CNS) (Berger and Hediger, 1999). The indirect interaction between KTP and PEPT2 was firstly described through a competitive study in rat synaptosomes (Fujita et al., 2004, 1999). Later, KTP uptake by PEPT2 was measured with peptides-induced inward currents (Thakkar et al., 2008). Importantly, the enhancement of KTP antinociceptive effect was observed in PEPT2 KO mice (Jiang et al., 2009).

1.1.6. Signaling Pathway

1.1.6.1. Receptor and antagonist

One of the most puzzling aspects of KTP signaling pathway is the inability to fully characterize the high-affinity KTP receptor (KTPr), despite all evidence pointing towards its existence (Ueda, 2021). Studies using ^{3}H-KTP revealed that KTP is able to bind to cells membranes in the brain, with both low- and high-affinity (Kitabatake et al., 1987; Ueda et al., 1989). The high-affinity binding of KTP suggests a receptor-mediated binding (Ueda et al., 1989), which levels are correlated with KTP (Ueda et al., 1980), and KTP synthetase levels (Ueda et al., 1987b). Moreover, dipeptides with tyrosine or arginine in their composition also bind to the putative KTPr, with *L*-leucine-*L*-arginine (Leu-Arg) presenting the higher affinity, followed by KTP, *L*-tyrosine-*L*-leucine, and *L*-tyrosine-*L*-lysine (Ueda et al., 1989).

Interestingly, KTP binding was blocked in the presence of guanosine triphosphate (GTP) gamma and $MgCl_2$, suggesting that the KTP receptor is coupled with G proteins - or it is a G protein-coupled receptor (Ueda et al., 1989). In fact, KTP showed a concentration-dependent effect on GTPase activity, which was not observed when Leu-Arg was used. Therefore, both high affinity for binding to KTPr and the inability of inducing GTPase activity, suggested Leu-Arg as an antagonist for KTPr (KTP_{ant}) (Ueda et al., 1989).

Importantly, depending on the specific G-protein coupled to the KTP receptor, the signaling pathway activated by KTP might have different outcomes. As such, the authors demonstrated that, similarly to the μ-opioid receptors (Ueda et al., 1990, 1988), the KTP receptor is Gi/o-coupled (Figure 2 (4)). In addition, KTP also induces Gi-mediated activation of phospholipase C (PLC), whose activity is measured by inositol 1,4,5-triphosphate ($InsP_3$) levels. Remarkably, KTP_{ant} is also able to reverse KTP-induced PLC activation in synaptosomal membranes (Ueda et al., 1989).

Later studies further support the hypothesis of KTPr being either a specific opioid receptor, or a receptor formed by δ- and μ-opioid receptors oligomerization (Machuqueiro and Baptista, 2007; Rackham et al., 1982). Nevertheless, although the binding pocket of KTPr must be different from the one in opioid receptors (Takagi et al., 1979b; Rackham et al., 1982; Ueda and Inoue, 2000), conformational studies confirmed their structural similarity (Machuqueiro and Baptista, 2007), which was already expected since both KTP and morphine share similar chemical structures.

1.1.6.2. Ca^{2+} influx

Under physiological condition, KTP-mediated G_i-PLC-$InsP_3$ activation provokes a Ca^{2+} influx, from extracellular space into the cytosol, through $InsP_3$-mediated $InsP_3$ receptor ($InsP_3R$) activation (Ueda et al., 1996). As detailed in Figure 2 (5), this Ca^{2+} influx is driven by the conformational coupling of the vesicular $InsP_3R$ and the transient receptor potential C1 (TRPC1) (Zarayskiy et al., 2007), and by the opening of PLC-mediated $InsP_3R$-gated Ca^{2+} channel (Ueda et al., 1995a, 1995b). Moreover, KTP also induced $^{45}Ca^{2+}$ release from $^{45}Ca^{2+}$-preloaded vesicles (Ueda et al., 1996).

1.1.6.3. Met-enkephalin release

As already pointed out, KTP shows a naloxone-reversible opioid-like analgesic effect (Rackham et al., 1982; Takagi et al., 1979b). In fact, when intracerebroventricular (i.c.v.) injected, KTP has an analgesic effect 4.2 times more potent than Met-enkephalin (Met-enk) (Takagi et al., 1979b), which is a neurotransmitter pentapeptide able to regulate pain transmission in the CNS (Takagi et al., 1979a; Lewis and Stern, 1983). Despite the mechanisms underlying this effect have been investigated since KTP discovery, they remain unclear in several aspects.

Although KTP itself does not appear to directly bind to opioid receptors, its indirect-action relies on Met-enk- and β-endorphin-mediated activation of δ- and/or μ-opioid receptors (Takagi et al., 1979b; Rackham et al., 1982; Ribeiro et al., 2011b). In addition, several studies confirmed a KTP-mediated Met-enk release (Takagi et al., 1979b; Shiomi et al., 1981a; Janicki and Lipkowski, 1983), in a process mediated by endogenous opioids. As such, in guinea pig striatal slices, Met-enk release increased in 1.6- or 3.4-fold, depending of 1 or 10 μM KTP superfusion, respectively (Shiomi et al., 1981a). Both $CaCl_2$ removal and the addition of tetrodotoxin stopped KTP-induced Met-enk release, suggesting a role on spontaneous excitatory activity. This can be explained by the tetrodotoxin-sensitive voltage-dependent Na^+ channels activation mediated by excitatory neurotransmitters release, such as glutamate (Shiomi et al., 1981a). In fact, when slices were stimulated, the addition of 1 μM KTP potentiated Met-enk electrical stimulation-induced release (3.6-fold), whereas a 2-fold increase was observed in slices electrical stimulation at 10 Hz. Similarly, 10 μM KTP also increased by 2.2-fold Met-enk release in spinal cord preparation (Shiomi et al., 1981a).

Regarding spinal cord, KTP has an excitatory effect on spontaneous activity of neurons located on the nucleus reticularis paragigantocellularis of the medulla oblongata, but it decreases neuronal activity in lamina V type neurons in the spinal dorsal horn (Satoh et al., 1980). These effects are also antagonized by naloxone, offering indirect evidence for the involvement of Met-enk.

In addition, KTP might also have an inhibitory action on some enkephalinases and, consequently, in the reduction of the Met-enk enzymatic degradation (Perazzo et al., 2017b; Vaught and Chipkin, 1982), which can lead to a relatively long-lasting analgesic effect (Hazato et al., 1986; Takagi et al., 1979b).

As suggested recently (Ueda, 2021), studies are needed to better understand if KTP-induced Met-enk release requires both activation of G_i-PLC-$InsP_3$ mechanism and physiological depolarization of nerve terminals (see "working hypothesis" highlighted on Figure 2). In addition, it is possible that KTP might be incorporated by neurons through unidentified transporters (Figure 2 (6)), and not through PEPT2 (Thakkar et al., 2008). PEPT2 is usually involved in the process of enkephalin clearance (Thakkar et al., 2008), and it has a role on Met-enk vesicular incorporation and release (Figure 2 (7)), as observed in the case of tyramine-induced noradrenaline release (Axelrod et al., 1962). Moreover, it is also not clear how KTP selectively induces the Met-enk release without affecting noradrenaline, gamma-aminobutyric acid (GABA), or *D*-aspartate when they were preloaded into vesicles (Janicki and Lipkowski, 1983).

1.1.6.4. Peripheral Action

At peripheral level, KTP was able to increase both amplitude and quantal content of the fast excitatory postsynaptic potentials from bullfrog sympathetic ganglion cells, without affecting resting membrane potential, input membrane resistance, action potentials amplitude and duration, and cellular ganglia-acetylcholine sensitivity (Hirai and Katayama, 1985). Another study showed that KTP inhibited noradrenaline-induced proliferation in brown fat cell cultures, which also indicates the existence of KTPr in these cells and, probably, on other peripheral tissues (Bronnikov et al., 1997).

Interestingly, KTP showed a non-opioid dependent analgesic effect in mice tested with a peripheral pain reflex, since naloxone was unable to prevent it (Inoue et al., 1997). This data suggested that KTP mechanism of action might have two distinct pathways leading to analgesia depending on the opioids' receptors activation and other opioid-independent mechanism. Nevertheless, when peripherally administrated at extremely low doses (on femtomolar range), KTP elicited nociceptive responses in a mechanism dependent of the releasing of substance P by primary afferent neurons endings (Inoue et al., 1999; Ueda and Inoue, 2000). In fact, KTP showed a bell-shaped dose-response curve when peripheral pain was tested through intraplantar injection in mice (Inoue et al., 1999). The observed KTP dual role on analgesic mechanisms was suggested to be mediated by different G proteins activation, leading to a differential effect in PLC activation, which is highly dependent of KTP used dose.

1.1.7. Other physiological effects

The wide physiological effects of KTP are dependent on several factors, namely the animal species used (mammals, amphibia, or fish), and the experimental conditions, such as KTP concentration and temperature. During the last years, several studies have been exploring other KTP non-opioid-mediated effects, such as its potential as antiepileptic, thermoregulator, and anti-hibernation, behavioral and stress modulator.

The antiepileptic and anticonvulsant potential of KTP was firstly explored in 1995 (Godlevsky et al., 1995). The impact of KTP (and other derivatives) was assessed in picrotoxin-induced convulsions after injection in mice lateral ventricle or into hippocampal CA1 (*Cornu Ammonis 1*) area. The KTP antiepileptic effect was dose- and target site-dependent. These findings were later confirmed, when KTP (i.c.v.) showed an anticonvulsant effect in a pentylenetetrazol seizure rat model (Bocheva and Dzambazova-Maximova, 2004).

Moderated concentrations of KTP were found in hypothalamus (Ueda et al., 1980), an important area for thermoregulation and stress regulation, which promoted several studies on those processes. Regarding the thermoregulation, the studies were contradictory (Dzambazova and Bocheva, 2010). On one hand, at 22ºC room temperature (RT), KTP injection (i.c.v.) in unrestrained cats third ventricle did not change body temperature (Clark and Ponder, 1980), but, at 24ºC RT, it caused a dose-dependent hypothermic response in mice (Sakurada et al., 1983). This response was also higher than when induced by Met-enk. Then, the administration of thyrotropin hormone, a pituitary hormone with the regulatory role on thyroid gland growth and function, prevented this naloxone-irreversible KTP hypothermic effect, suggesting a pituitary-thyroid regulatory effect instead of the opioid receptors' activation. KTP also inhibited noradrenaline-induced proliferation of cultured brown preadipocytes and brown adipose tissue *in vivo*, in a process dependent of Ca^{2+} signaling, suggesting the existence of KTPr in brown adipose tissue, which is an essential source in heat production process (Bronnikov et al., 1997, 2006).

Stress is known to be a physiological transitory state essential to restore the homeostasis of a system after an intrinsic or extrinsic stimulus (stressors) (Murison, 2016; Yaribeygi et al., 2017). The stress response includes triggering several compensatory mechanisms, ranging from molecular allostasis to adaptive behavior, to account for the survival of the individual and the species (Murison, 2016). Thus, stress is not a maladaptive response but rather a complex adaptive response, which is highly dependent on the type, timing, and severity of the stressor applied. Within this context, the administration of KTP and *L*-Arg (i.c.v.) in rats normally hydrated increased plasmatic oxytocin (OT) levels, a stress-hormone in rodents, without affecting vasopressin levels (Summy–Long et al., 1998), which induces vasoconstriction and regulates blood pressure by increasing it. This study revealed that both

KTP and *L*-Arg excess levels in CNS might mimic a stress response through the activation of the sympathetic nervous system, triggering the release of OT, and elevating both blood pressure and plasmatic glucose levels. On the other hand, KTP might attenuate vasopressin release by directly act into magnocellular neurons or by indirectly modulate a pressor-regulatory compensatory reflex.

KTP was also suggested as an anti-stressor molecule, reducing the secretion of both adrenocorticotropic hormone (ACTH) and corticosterone, known to have a role on the regulation of basal activity of the hypothalamic-pituitary-adrenal (HPA) axis. Rats treated with KTP immediately after exposure of acute immobilization, cold and heat stresses had restored levels of plasmatic ACTH and corticosterone when compared to stressed animals, suggesting that KTP prevented the HPA axis activation (Dzhambazova, 2015).

The behavioral effect of KTP was explored in different species (Dzambazova and Bocheva, 2010). Mice treated with KTP had no changes in motor abilities evaluated through the open-field test (Shi et al., 1991). However, when injected at high doses, KTP induced sedation and reduced motor activity in mice (Sakurada et al., 1983). Interestingly, its presence abolished the extinction of the avoidance response to pole-jumping in rats (Yamamoto et al., 1982); and even affected the learning of an aversive taste in chicks (Kastin et al., 1981). More recently, studies in rats and goldfish reported the suppression of exploratory activity by KTP action, presumably mediated by monoaminergic brain systems, such as the serotonergic system (Kolaeva et al., 2000).

In the brain of hibernating animals, KTP can act as an electron-acceptor, which may affect its regulation of Ca^{2+} currents in excitable tissues such as the heart (Marinov and Ziganshin, 1997). In fact, KTP was able to block Ca^{2+} influx currents in cold- and warm-blooded species (Dzambazova and Bocheva, 2010), and, more specifically, in frogs, and rats and ground squirrels (Ignat'ev et al., 1998), respectively. These findings supported KTP's role in the anti-hibernation process, such as in thermoregulation, and heart functioning. Moreover, KTP had a dose-dependent cardiac effect in rats, which indicated a possible indirect regulatory role in β-adrenergic action by triggering endogenous opioid release in rat cardiac muscle (Li et al., 2006).

1.1.8. Classification as a neurotransmitter

Over these years, several studies have been profiling the characteristics of KTP and its mechanisms of action to better understand if this peptide can be classified as a neurotransmitter (Salio et al., 2006; Ueda, 2021). Accordingly, as already mentioned, despite being an analgesic molecule, several studies have been unravelling novel physiological functions of KTP on the CNS. In summary, KTP presents several characteristics that can

attest its role as a neuromodulator and, as some authors argue, some of them suggesting KTP as a neurotransmitter (Ueda, 2021).

- KTP induces a significant higher release of Met-Enk in brain and spinal cord tissue;
- Although is potent analgesic effect, KTP is unevenly distributed in the brain, being more than 50% of its total amount in areas where it will presumably act in an opioid-independently manner;
- KTP can be produced by a specific synthetase from *L*-tyrosine and *L*-arginine, or through the enzymatic cleavage of polypeptides precursors;
- KTP is also mainly located in the synaptosome fraction or nerve-ending, and it can be preloaded into the synaptosome and released in a Ca^{2+}-dependent process upon a high K^{+} depolarization;
- KTP has a specific G-coupled receptor (KTPr), which activation triggers a G_i-PLC-mediated activation and inhibition of adenylyl cyclase (AC), and provokes a Ca^{2+} influx;
- KTP_{ant} (*L*-Leu-*L*-Arg) is a specific KTPr antagonist;
- KTP can be cleared by either aminopeptidase action, uptake by astrocytes or excreted to CSF through PEPT2 action.

1.2. Therapeutic potential of Kyotorphin

Peptides assume a vast role of biological functions in diverse physiological processes, acting as regulators, neurotransmitters, or growth factors among others, and their application is recognized across all biomedical sciences, ranging from therapeutic drugs to nutritional uses (Salio et al., 2006; Merighi et al., 2011; Santos et al., 2012). Among peptides' family, the use of di- and tripeptides on drug discovery and development raised a special interest, due to their possible oral administration, cost-effective synthesis (with a low-cost mass production), and simplicity to perform molecular structural and quantitative structure-activity studies (Santos et al., 2012). Peptides have high selectivity to targets, show an efficient activity, which, together with their low toxicity, made them very attractive as potential drugs. To improve their pharmacological properties and even add biological functions, small peptides can be easily transformed into derivatives by chemical transformations, such as cyclization, hydroxylation, amidation, acylation and binding to some other hydrophobic groups, (Santos et al., 2012). As a dipeptide formed by two a.a. (*L*-tyrosine-*L*-arginine), KTP was not an exception for this raised interest.

1.2.1. Pharmacological limitation

Several studies attested the effects of KTP following its systemic administration, such as intraperitoneal (i.p.), intravenous (i.v.) and oral, and the results were somehow disappointing. KTP has very weak activity when administered systemically: a high dose of 200 mg/kg was needed for a brief analgesic effect in rodents (Chen et al., 1998). The striking difference in activity between KTP effect when systemic administrated *versus* i.c.v. injected assigned its limited capacity to cross the BBB, preventing it from reaching the brain (Jiang et al., 2009; Serrano et al., 2014a, 2014b). In addition, this can also be a consequence of its susceptibility to various clearance mechanisms.

BBB, a physical barrier constituted by specialized endothelial cells tightly attached, is one of the first defence lines in the CNS, filtering and regulating compounds exchanges, and hampering pathogenesis invasion (Terstappen et al., 2021). This constitutes one major limitation when developing drugs to be delivered on the CNS. Nevertheless, the potential therapeutic value of KTP as a CNS drug (explored in the next topic), combined with this limitation contributed to the development of several KTP derivatives.

1.2.2. Synthetic derivatives

During the last decades, several groups have been working in different strategies to modify KTP, such as 1) to conjugate KTP with lipophilic groups (Chen et al., 1998; Wang et al., 2001; Lopes et al., 2006b; Ribeiro et al., 2011a; Serrano et al., 2014b); 2) chirality (Lopes et al., 2006a; Rybal'chenko et al., 1999); 3) cationicity improvement (Ribeiro et al., 2011b); and

4) the use of unnatural a.a. and substitution of peptides bonds (Dzimbova et al., 2014; Serrano et al., 2014b). Interestingly, some of these changes aimed to add new functions to the original peptide (Perazzo et al., 2017a). From the several synthetic KTP derivatives developed, this work was focused on the Amidated-Kyotorphin (KTP-NH_2).

1.2.2.1. Amidated-Kyotorphin

The KTP-NH_2 was synthesized with the substitution of KTP carboxylic group (-OH) with an amine group (-NH_2), which increased the peptide global net charge (from +1 to +2 at physiological pH) (Ribeiro, 2012). This also changed its hydrophobicity while partially maintained its molecular structure. As such, this structural change promoted KTP-NH_2 interaction with biological membranes, which increased its capability to cross the BBB (Ribeiro et al., 2011a, 2011b; Serrano et al., 2014b). Figure 3 presents both chemical structures of KTP and KTP-NH_2.

1.2.3. Functional studies

Recent studies profiled the analgesic effect of KTP-NH_2 when systemically administrated (oral and i.p.) in acute, sustained, and chronic neuropathic and inflammatory pain models (Ribeiro et al., 2011a, 2011b). The equi-effective dose of KTP-NH_2 (32.3 $mg.kg^{-1}$) was about fivefold more than of morphine (5 $mg.kg^{-1}$), when i.p. injected in an animal model of acute pain. As expected, oral administration required higher doses to achieve similar efficacy. In animal models of chronic pain, the analgesic effect of KTP-NH_2 was only observed after a week of daily i.p. treatment (32.3 $mg.kg^{-1}$). Despite naloxone administration prevented analgesia, the authors reported that KTP-NH_2 binding to opioids receptors was minimal (Ribeiro et al., 2011b). Furthermore, the putative neuroprotective actions of KTP-NH_2 were explored in more recent studies, which will be presented in later sections.

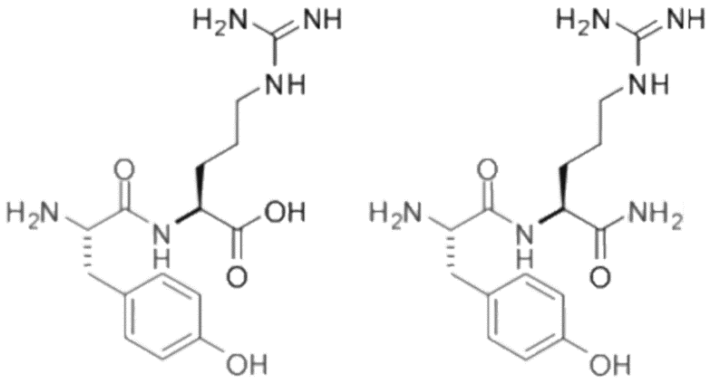

Figure 3. Chemical structure of Kyotorphin (left) and Amidated-Kyotorphin (right). Adapted from PepDraw (Freeman, 2015).

1.2.4. Side-effects

The side-effects of this small and cost-effective molecule remain doable, with studies reporting a reduction in micturition, and without causing toxicity, and unaffecting motor responses, blood pressure, and food and water intake (Ribeiro et al., 2011b, 2013). In addition, contrary to morphine, after systemic administration, KTP-NH_2 did not cause constipation, which offers an advantageous alternative over the current opioids treatment (Ribeiro et al., 2013).

1.3. Pain and Alzheimer's Disease: can Kyotorphin be the solution?

As already mentioned, the interest on KTP goes behind its analgesic properties, raising a crescent attention for its other physiological functions described, such as non-opioid actions without enkephalin release, or actions unrelated with pain processing (Dzambazova and Bocheva, 2010). The next subsections briefly explore the therapeutic use of KTP for pain and focus on its possible use for Alzheimer's Disease (AD) treatment.

1.3.1. Pain treatment: the obvious application

The vast majority of KTP research has been related to its potential application on pain treatment (Dzambazova and Bocheva, 2010). Nowadays, pain is considered the 5th vital sign and although it is persistently affecting a substantial part of the population is still undervalued (Finnerup et al., 2018). According to the *International Association for the Study of Pain* revised definition, pain can be referred to as "an unpleasant sensory and emotional experience associated with, or resembling that associated with, actual or potential tissue damage" (Raja et al., 2020). In a raw context, pain usually triggers an adaptive response to protect the individual against the harmful stimulus. Noteless, pain is always a personal experience, and its perception is highly influenced by biological, psychological, and social factors. Although verbalization of pain is a common behavior to express pain, the absence of it does not mean the absence of the individual experience of pain. Foremost, regardless of their side-effects, the use of opioids is still essential for pain relief, but alternative drugs are highly needed for long-lasting chronic pain illness.

Patients with persistent pain had decreased levels of KTP in CSF (0.24 ± 0.04 pmol.ml^{-1}) when compared to normal human CSF (1.19 ± 0.51 pmol.ml^{-1}) (Nishimura et al., 1991). This finding adds support to evidence suggesting that KTP acts as an endogenous neuromodulator of pain processes. Thus, people suffering from pain might benefit from therapies that restore or increase the endogenous levels of KTP. As such, the use of arginine-based therapies was explored by some researchers as an approach to indirect stimulate KTP endogenous production.

1.3.1.1. Arginine-based therapies

The production of KTP through its TyrRS synthetase is three-fourfold more than the one resulting from polypeptides degradation (Ueda et al., 1987b). The *L*-Arg levels needed to foster this enzymatic reaction (Tsukahara et al., 2018; Ueda et al., 1980) are clearly higher than the reported levels found in the human plasma for the enzymatic (Schmidt et al., 2016). Thus, several studies supported the possibility of using *L*-Arg as a KTP precursor.

In mice, the arginine (Arg) oral administration (1 g.kg^{-1}) induced an increase on KTP levels in midbrain, medulla oblongata and olfactory bulb of those animals (Tsukahara et al., 2018),

which is related with the already reported TyrRS levels. Interestingly, these results also indicated that the Arg consumption had a dose-dependent analgesic effect in thermal nociception (Tsukahara et al., 2018).

Additionally, the systemic i.c.v. administration of *L*-Arg induced an analgesia effect in mice submitted to thermal and mechanical nociception tests (Neyama et al., 2018). These effects were reversible by naloxone and *N*-methyl-*L*-Leu-*L*-Arg (NMLR) administration, a synthetic-stable KTPr antagonist (Ueda et al., 2000). In preproenkephalin- or proopioimelanocortin knockout mice the Arg-induced analgesia was attenuated, suggesting that Arg triggered opioid-like analgesia through an indirect activation of the KTPr, being this a process mediated by endogenous opioid release (Neyama et al., 2018).

Other authors also reported Arg-induced analgesia (Kawabata et al., 1993). In patients with persistent pain, i.v. administration of *L*-Arg induced a naloxone-reversible analgesia effect (Arima et al., 1996; Takagi et al., 1990). Interestingly, Arg also mediates gastrointestinal relaxation, which makes it very attractive for pain relief in terminal patients as a morphine-combine therapy, since it can reduce the morphine-induced constipation (Calignano et al., 1991).

1.3.1.2. Nitric Oxide

It is also known that *L*-Arg is a substrate for nitric oxide synthase (NOS), leading to the formation of nitric oxide (NO). In fact, both *L*-Arg and NO have been reported as having a dual role on pain processing, acting as analgesic agents as well as nociceptive promoters (Kawabata et al., 1993). Figure 4 illustrates the possible mechanism for *L*-Arg as a KTP- or a NO-induced precursor, which was presented for the first time in 1993 (Kawabata et al., 1993). Briefly, in the brain, *L*-Arg can be either considered an antinociceptive inducer, acting via KTP-Met-enk pathway, or a pro-nociceptive inducer when acting via NO-cyclic guanosine monophosphate (cGMP) pathway. Other authors confirmed the involvement of NO in the KTP-induced antinociception mechanism (Bocheva et al., 2003; Bocheva and Lazarova, 2003).

Nowadays, NO is considered both a neurotransmitter and a secondary signaling molecule, having an essential role either on physiological and pathophysiological processes, such as in regulation of cell survival, differentiation and proliferation of neurons (Tripathi et al., 2020). NO has a relevant function on pain processing in CNS, and it has been implicated in synaptic plasticity processes, among others (Janicki and Jeske-Janicka, 1998). Furthermore, some authors defended that KTP undergoes a fast degradation and that the originated *L*-Arg induces the NO formation (Arima, 1996; Takagi and Nomura, 1997). Thus, NO formation can

be the reason for the naloxone-resistant and opioid independent KTP analgesic effect at peripheral level.

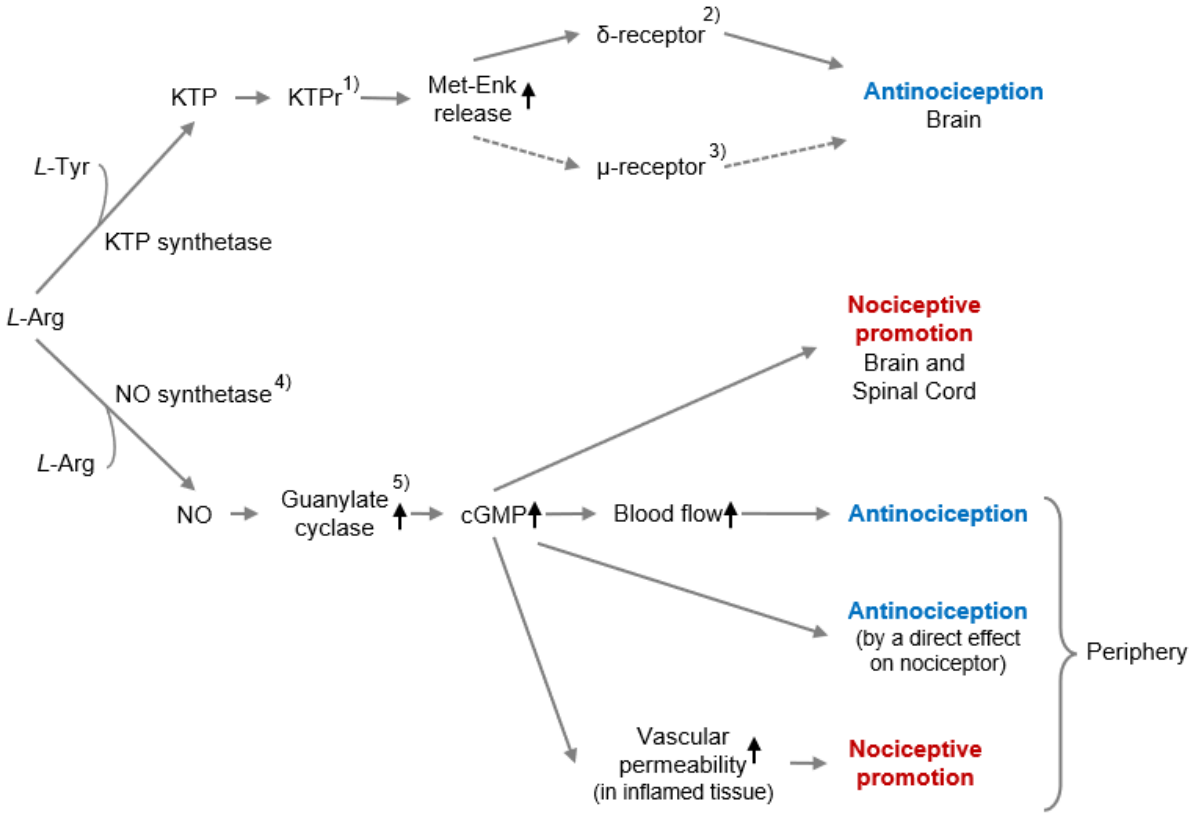

Figure 4. Possible mechanism for *L*-Arginine metabolism in both central and peripheric nervous systems. *L*-Arginine (*L*-Arg) can be a subtract for either nitric oxide (NO) synthase or for kyotorphin (KTP) synthetase. In the brain, *L*-Arg can act via KTPr-Met-enk pathway, inducing an opioid-dependent antinociceptive effect, or act via NO-cyclic guanosine monophosphate (cGMP) pathway, promoting a nociceptive effect. Moreover, at peripheral level, NO production leads to both antinociception and nociceptive action, depending on if the increase level of cGMP is acting to increase the blood flow and/or through nociceptors activation, or it is increasing the vascularity permeability in an inflamed tissue, respectively. Points of action of inhibitors and blockers used: (1) *L*-leucyl-*L*-arginine (KTP_{ant}); (2) naltrindole and naloxone; (3) naloxone; (4) L-NG-nitroarginine methyl ester; (5) methylene blue. Adapted from (Kawabata et al., 1993).

1.3.2. Alzheimer's Disease: the desirable application

KTP has been pointed as a possible neuroprotector factor against neurodegeneration, neuroinflammation, and neuronal death (Dzambazova and Bocheva, 2010). During the last decade, several studies attested KTP interest for AD treatment (Ueda, 2021).

This neurodegenerative disease was described for the first time in 1907 by a German psychiatrist, Alois Alzheimer. When Alzheimer was working in Frankfurt, he had the opportunity to meet Auguste Deter, a 51-year-old woman who presented short-term memory loss that rapidly deteriorated into severe dementia. After her death in 1906, Alzheimer was able to perform her brain autopsy and to identify several pathological aspect, including cortex shrinkage and the presence of senile plaques and neurofibrillary tangles (NFTs) (Alois Alzheimer Biography, 2016). These two have become the histopathological hallmark of this disease, which is now known as *Alzheimer's Disease* (Citron, 2010; Price et al., 1991).

1.3.2.1. Epidemiology

AD is a chronic progressive neurodegenerative disease and the most common cause of dementia in elderly, with death occurring, on average, 4-8 years after diagnosis. Nowadays, only in the USA, 5.8 million people are living with Alzheimer's dementia, of whom only 3% are under 65 years old (Alzheimer's Association, 2019).

Importantly, age is the greatest risk factor for developing AD (Sengoku, 2020), but AD is not a normal part of aging (Hebert et al., 2010). By 2050 it is expected that both incidence and prevalence of AD will be higher due to the expected increase in the older population over 60 years old (Alzheimer's Association, 2020; Mayeux and Stern, 2012). Additionally, women have a higher probabilistic risk of being diagnosed with AD, which can be partially explained by their higher life-expectancy when compared with men (Mielke et al., 2018).

1.3.2.2. Etiology

AD can be classified according to the age of onset, which is highly dependent on genetic predisposition (Sims et al., 2020). Early-onset AD, also referred as familial AD, is usually developed in people between 30 and 60 years old, and genetics plays a major contribution for the etiology of these AD cases. On the other hand, late-onset AD, also referred as sporadic AD, accounts for the most of AD cases (around 95%), with people being diagnosed around 65 years old (Bali et al., 2012).

Several mutations on genes expressing AD-related protein have been identified. The most common are in amyloid precursor protein (*APP*) gene, with 22 reported mutations, and in presenilin genes 1 and 2 (*PSEN1* and *PSEN2*) genes, with 32 and 19 reported mutations, respectively, being all transmitted in an autosomal dominant process (Canevelli et al., 2014; Lanoiselée et al., 2017). Both *APP* and *PSEN1* mutations are linked to early-onset dementia,

and generally account for a faster disease progression, leading to less frequent clinical symptoms such as legs' muscles weakness and stiffness, and prominent language impairment (Canevelli et al., 2014). Additionally, *APP* gene is located in chromosome 21 thus, research conducted with Down Syndrome's patients, a trisomy of the chromosome 21, offers an invaluable insight of AD pathophysiology. As such, the additional copy of the *APP* gene is already identified as the responsible inducer of AD-related dementia manifestation developed in the lifetime of these individuals (Lott and Head, 2019). Contrary, *PSEN2* mutations, rarely found in familial AD cases, are usually associated with late-onset AD (Canevelli et al., 2014).

Less than 1% of AD cases have origin in known genetic mutations (Sims et al., 2020), and Apolipoprotein E (*APOE*) genotype is the strongest genetic risk factor for sporadic AD. Of the three common *APOE* alleles (*ε2*, *ε3*, *ε4*), *APOEε4* allele has a dose-dependent associated with the decrease in the onset-age, and the presence of one or two *ε4* alleles increases AD risk by 3- and 12-fold, respectively, but the presence of the *APOEε2* allele is associated with AD decreased risk (Corder et al., 1993; Strittmatter et al., 1993). Additionally, a specific *TREM2* gene variant, that encodes an inflammatory response-mediator receptor in myeloid cells, increases AD risk similarly as having one *APOEε4* allele (Guerreiro et al., 2013; Jonsson et al., 2013). Interestingly, having first-degree relatives with late-onset AD increases around twice the expected lifetime risk of developing the disease, although no Mendelian inheritance transmission pattern is found (Bekris et al., 2010).

Over the last years, genome-wide association studies (GWAS) have identified several common and rare genetic variants as AD risk factors, including in amyloidogenic production and clearance pathways, lipid production, inflammatory response, and endocytosis (Karch and Goate, 2015). Despite the individual expression of common genetic variants slightly increasing the risk of developing AD, when combined they can almost double that risk (Escott-Price et al., 2015).

Finally, we are witnessing a current shift towards the understanding of this disease, which is now perceived as a multifactorial disease, and where 70% of risk factors are related to genetic variants (Lane et al., 2018; Sims et al., 2020). Nevertheless, the presence of cerebrovascular disease and its antecedents, clinical history of hypertension, smoking, obesity, and dyslipidaemias account as other non-genetic risk factors reported (Xu et al., 2015).

1.3.2.3. Pathology and Pathogenesis

As already mentioned, the two histopathological hallmarks of AD are the presence of brain amyloid plaques and NFTs. Plaques are primarily formed by the aggregation of the

extracellular misfolded amyloid beta (Aβ) peptide with 40 or 42 a.a. (Aβ40 or $Aβ_{1-40}$, Aβ42 or $Aβ_{1-42}$, respectively) (Citron, 2010; Price et al., 1991). This is partially originated by the aberrant proteolytic cleavage of the transmembrane APP (Chen et al., 2017). The APP is a large glycoprotein, coded by the *APP* gene, with an important physiological role on neuronal development, signaling, intracellular trafficking, among others. In neurons, this protein can be sequentially cleavage by β- and γ-secretases, and, upon synaptic activity, Aβ peptide production and secretion are known to be stimulated (Gouras et al., 2015; Serrano-Pozo et al., 2011). The increased Aβ42/Aβ40 ratio found in plaques happens due to Aβ42 higher insolubility and tendency for fibrillization (Lane et al., 2018; Takahashi et al., 2017). Moreover, AD patients with described mutations in *APP*, *PSEN1*, and *PSEN2* genes have an Aβ peptide overproduction, and specially of the Aβ42 fragment (Masters et al., 2015), that accumulates in CNS and leads to a higher plasmatic Aβ42/Aβ40 ratio (Gómez-Isla et al., 1999; Potter et al., 2013).

NFTs are essentially formed by the misfolded hyperphosphorylated tau (p-Tau) protein (Citron, 2010; Price et al., 1991). These tangles usually appear accompanied by neuropil threads, which are thought to be the result of dendrites and axon breakdown products (Serrano-Pozo et al., 2011). Moreover, NFTs are less AD-specific than amyloid plaques since they are also observed in other neurodegenerative diseases, such as several subtypes of frontotemporal dementia and corticobasal degeneration (Gouras et al., 2015).

Plaques' accumulation starts in the basal portions of the frontal, temporal, and occipital lobes. Later, plaques are detected in the limbic system, being the hippocampal mildly impaired, and, finally, they appear in subcortical areas, such as in the primary isocortical areas, and molecular layer of the cerebellum and subcortical nuclei (striatum, thalamus, hypothalamus, subthalamic nucleus, and red nucleus) (Braak and Braak, 1991; Thal et al., 2002). On the other hand, the accumulation of NFTs starts in the medial temporal lobes, affecting the hippocampus, and spreads to other areas of the neocortex (Masters et al., 2015). Interestingly, plaques deposits reach a plateau early after the appearance of the first cognitive symptoms, without showing a correlation with the severity or the duration of the associated dementia (Hyman et al., 1993; Ingelsson et al., 2004; Serrano-Pozo et al., 2011). In contrast, NFTs formation occurs in parallel to both neuronal and synapse loss, and it is better correlated with the clinical symptoms and disease progression (Ingelsson et al., 2004).

The deposition of Aβ peptide in cerebral blood vessels leads to cerebral amyloid angiopathy (Noguchi-Shinohara et al., 2016). The presence of granulovascular degeneration, consisting of large double-membrane bodies accumulation, and Hirano Bodies, that are eosinophilic rod-like cytoplasmic inclusions observed in the cytoplasm of hippocampal pyramidal neurons are other microscopic alterations associated to AD brains (Serrano-Pozo et al., 2011).

In addition to protein aggregation-induced neurotoxicity, alteration of glial response, imbalance of neuronal calcium homeostasis, cholinergic dysfunction, and extensive neuronal and synaptic loss are also observed (Sims et al., 2020). The disruption of NO homeostasis is also known to accelerate the development of AD (De La Torre and Stefano, 2000).

Excitotoxicity as well as dysregulation of brain-derived neurotrophic factor (BDNF) signaling are known to be involved in neurodegenerative disorders such as AD (Budni et al., 2015; Jerónimo-Santos et al., 2015). BDNF is an important neurotrophic factor with a well-studied regulatory action on neuronal survival, differentiation and maturation, and synaptic plasticity (Binder and Scharfman, 2004). This neurotrophin enhances hippocampal long-term potentiation (LTP) through the activation of the tropomyosin receptor kinase B-full length (TrkB-FL), contributing to synaptic plasticity facilitation (Fontinha et al., 2008; Minichiello, 2009; Lu et al., 2015). Importantly, Aβ peptide triggers excitotoxicity through *N*-methyl-*D*-aspartate receptor (NMDAR)-mediated Ca^{2+} influx, leading to an overactivation of calpain. This causes a pathological cleavage of TrkB-FL, with a formation of a membrane TrkB truncated fragment and of its intracellular domain fragment (TrkB-ICD), which impairs synaptic plasticity by abolish LTP and decrease neuronal spine density (Fonseca-Gomes et al., 2019; Jerónimo-Santos et al., 2015; Tanqueiro et al., 2018).

AD patients show a generalized brain atrophy, being the hippocampi one of the most affected areas (Citron, 2010). The synaptic loss triggered by amyloid and tau pathologies (Forner et al., 2017; Overk and Masliah, 2014), is preceded by the loss of pyramidal and cholinergic neurons, which is predominant in cortex and hippocampal CA1 region. This degeneration strongly correlates with the progressive cognitive decline in AD patients, firstly characterized by impairments in memory, spatial orientation, attention, and executive functions.

Despite the collected evidence, AD full pathogenesis is yet to be clarified. From all proposed hypotheses, the amyloid cascade has been shaping the mechanistic research as well as the drug discovery research over the last 25 years (Sims et al., 2020). According, Aβ-induced toxicity triggers a complex cascade of events leading to neurodegeneration, which ultimately drives into the cognitive dysfunction observed in AD patients (Hardy and Higgins, 1992). Other theories include the cholinergic hypothesis, where a selective dysfunction of this type of neurons is suggested to be the cause for the AD patients cognitive decline (Terry and Buccafusco, 2003), and the mitochondria-associated endoplasmic reticulum membrane hypothesis, which implies that metabolic changes affecting the homeostasis of these cellular structures lead to alterations on APP processing and tau phosphorylation, contributing to AD pathology (Area-Gomez et al., 2018; Area-Gomez and Schon, 2017).

1.3.2.4. Diagnosis and biomarkers

Non-cognitively impaired elderly might also present neuropathological hallmarks of AD, such as amyloid plaques and NFTs (Mufson et al., 2016), offering another puzzling evidence for this disease. The criteria for AD diagnosis have been revised over the last years, in particular, by the *International Working Group*, and the *National Institute of Ageing-Alzheimer Association*. The latest proposed criteria for monitoring AD progression subdivides it into three phases: 1) preclinical AD, mild-cognitive impairment (MCI), and dementia due to AD (Figure 5 (A)).

AD patients might have no symptoms for years (preclinical or prodromal phase), which might be explained by the activation of several molecular compensatory mechanisms (Bobkova and Vorobyov, 2015). However, during this stage, several changes in AD biomarkers measured in the brain, CSF, and blood can already be detected in these patients (Figure 5 (B)). By the time that the first cognitive symptoms appear, the disease is already set, biomarkers levels are higher, and patients show symptoms of MCI that still do not affect most of their daily activities. Then, AD patients start to develop all dementia symptoms and to lose their individuality. AD became a highly demanding disease for society, mainly due to the full dependence of these patients in later stages of the disease progression (Alzheimer's Association, 2019).

Nowadays, clinical diagnosis criteria include cognitive assessment, to identify AD-associated impairments, specifically short-term memory loss. The presence of AD biomarkers, and/or cerebral structural abnormalities or injuries, imply the need of complementary exams to correctly assess the AD diagnosis. Blood tests are usually performed to exclude other conditions that may contribute to similar cognitive symptoms (Lane et al., 2018; Mucke, 2009). Cerebral imaging studies are also recommended for AD diagnosis and to evaluate disease progression (Blennow and Zetterberg, 2018; Huang and Mucke, 2012). Structural abnormalities and degenerative atrophy can be identified in structural magnetic resonance imaging (MRI) studies (Hort et al., 2010). These studies can be also used for differential diagnosis and evaluate the cerebrovascular compromising that might mimic or co-occur with AD (Lane et al., 2018). Additionally, positron-emission tomography (PET) can be performed to detect amyloid deposits, where the compounds used bind to fibrillar β-amyloid (Ikonomovic et al., 2016).

Finally, the presence of higher levels of tau, p-Tau and decreased levels of Aβ42 in CSF can also be used to diagnose AD (Blennow and Zetterberg, 2018). These CSF biomarkers can predict the favourable AD progression from individuals with MCI (Olsson et al., 2016), which are extremely helpful for clinicians to identify the expected 15% of MCI cases that will eventually progress to AD (Davatzikos et al., 2011).

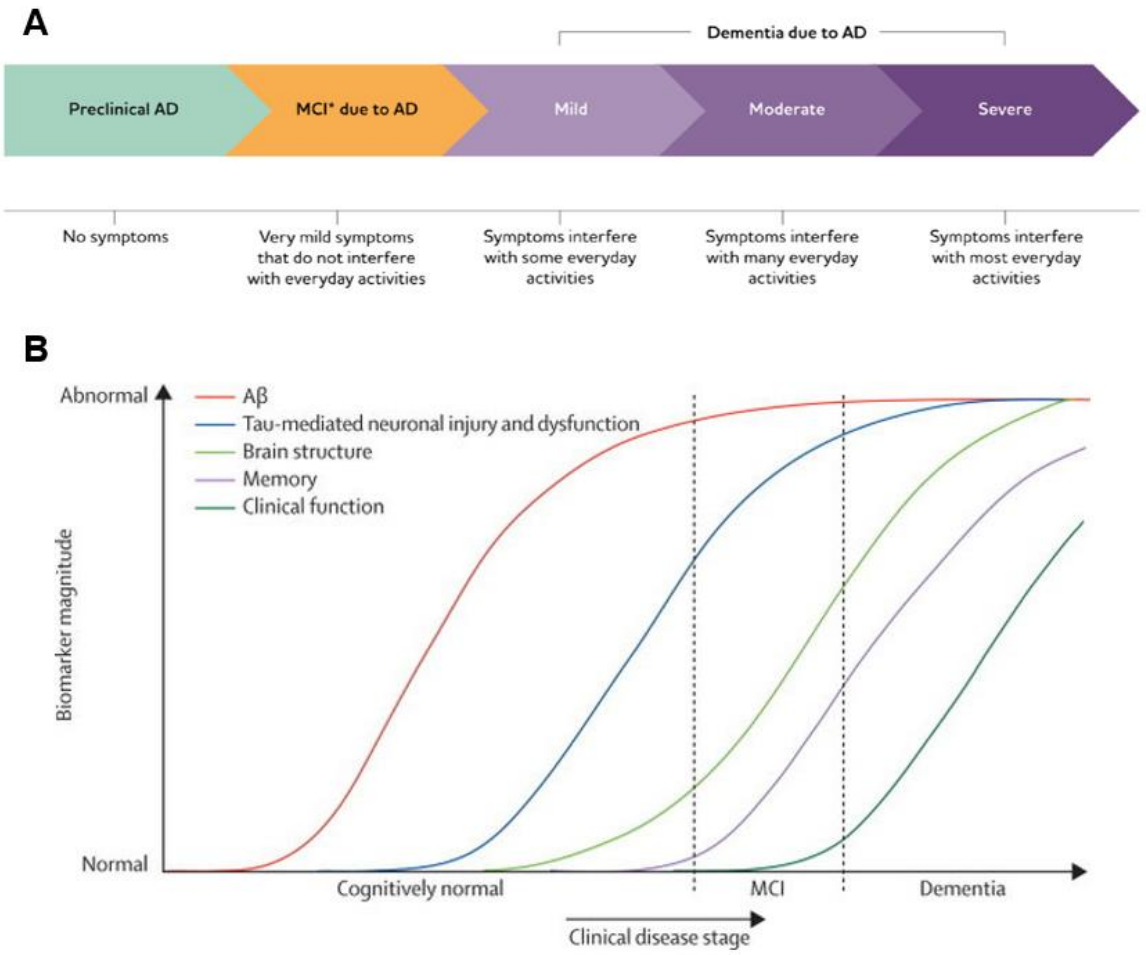

Figure 5. Alzheimer's Disease progression. (A) Alzheimer's Disease (AD) symptomatology continuum associated to its currently accepted classification: preclinical, mild cognitive impairment (MCI), and dementia. (Alzheimer's Association, 2020). **(B)** Biomarkers for AD pathological cascade model (Jack et al., 2013).

1.3.2.5. Current treatment options

AD has no cure and the available pharmacological treatments are limited and only slightly attenuate the symptoms (Alzheimer's Association, 2019). Worldwide, scientific research on AD and AD-related fields represents a collective effort to find more appropriated treatments. However, the high complexity of this disease has proven to be a challenge. Over the last years, we have witnessed the devastating results in clinical trials failures using the most promising drugs to fight AD, mainly designed to overcome amyloid and tau pathologies.

Nevertheless, four drugs are currently approved for the clinical use in AD patients to temporarily ameliorate their symptoms: Rivastigmine, Donepezil, Galantamine, and Memantine (Massoud and Léger, 2011). The first three are acetylcholinesterase inhibitors, hampering the acetylcholine degradation, an essential neurotransmitter for postsynaptic stimulation (Birks and Harvey, 2006; Seltzer, 2007; Onor et al., 2007; Birks et al., 2009; Loy and Schneider, 2006; Robinson and Plosker, 2006). They induce a transient increase of

acetylcholine at synaptic level, acting as a compensatory therapy for the loss of cholinergic neurons in AD. In contrast, Memantine is indicated for moderate to severe AD-related dementia (Epperly et al., 2017). It is a NMDAR antagonist, and its action counteracts the glutamate-induced excitotoxicity through mainly blocking the extra-synaptic glutamate NMDAR (Johnson and Kotermanski, 2006; Tanqueiro et al., 2018). This excitotoxicity is observed in later stages of AD and it contributes to a faster disease progression (Kavirajan, 2009; Massoud and Léger, 2011).

Several additional pharmacologic factors might have a protective role on AD progression, such as undertaking oestrogen, statins, antihypertensive medications, and non-steroidal anti-inflammatory drugs. In addition, being intellectually and/or physically active, by receiving cognitive training, emotional, physical, and social stimulation, and music therapy, alongside with having a diet rich in folate, vitamin E/C and coffee have shown to be protective against AD and increasing the general quality of life of these patients (Mayeux and Stern, 2012; Xu et al., 2015; Zucchella et al., 2018).

1.3.3. Link between pain and Alzheimer's Disease

The prevalence of persistent pain increases with age, aggravated by the inherent difficulties of clinicians to assess and manage pain, leaving a significant percentage of elderlies untreated (Kaye et al., 2010). Further evidence show that chronic pain aggravates AD, and the limited capacity to verbally express and percept the pain and discomfort of these patients can lead to a pain underestimation, which can worsen the disease progression without adequate treatment (Borsook, 2012).

Similarly to what was observed in patients with persistent pain (Nishimura et al., 1991), AD patients have decreased levels of KTP in CSF (Santos et al., 2013), which may be a consequence of the disease-specific cortical thinning and hippocampal volume loss. In fact, decreased cortical mass, with an acceleration loss phase during the early stages of the AD, might result in less capability of KTP production and it can explain its dropping levels in the CSF (Sabuncu et al., 2011; Santos et al., 2013). More importantly, the decreased levels of KTP also had an inverse correlation with p-Tau levels in CSF of AD patients, as shown in Figure 6 (A) (Santos et al., 2013). Since p-Tau in CSF acts as a biomarker of neurodegeneration (Schraen-Maschke et al., 2008), being released from senescent neurons, and being KTP also produced in neuronal cells, it is expected that KTP levels naturally fall as neurons die (Santos et al., 2013). Thus, KTP decreased levels in CSF strongly suggest KTP as a candidate for a new AD biomarker (Santos et al., 2013).

This association between AD and pain (Figure 6 (B)), two conditions with extreme epidemiologic relevance, reinforce the need of finding a new therapeutic strategy that

combines both analgesic and neuroprotective effects in one single pharmacological agent. Furthermore, the simultaneously implication of NO in molecular mechanisms subjacent to both KTP-induced analgesia and AD, with the decreased levels of KTP in the brain probably contributing to a decrease in NO synthase activity causing a NO deficit, only reinforced the interest of using KTP as a putative drug for AD therapy.

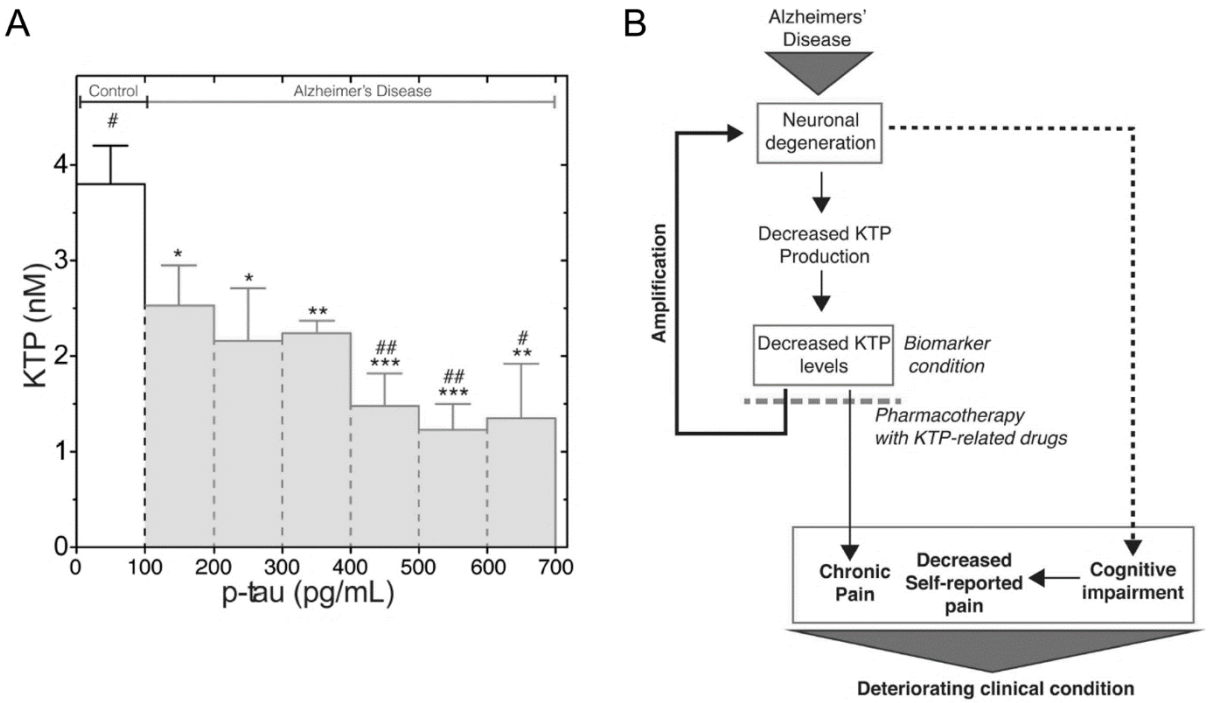

Figure 6. Link between pain and Alzheimer's Disease. (A) Bar graph of kyotorphin (KTP) concentration levels (nM) *versus* hyperphosphorylated tau (p-tau) levels (pg/mL) measured in cerebrospinal fluid (CSF) of Alzheimer's Disease (AD) patients (grey bars) and age-matched controls (white bar). Each bar corresponds to the average of KTP levels of clustering data regarding p-tau levels, using classes with regular intervals of 100 pg/mL. Statistical analysis, using one-way ANOVA with Dunnett's post-hoc test, shows that above 400 pg/mL all AD classes have significantly lower KTP levels when compared to controls (*p <0.04, **p <0.0075,***p <0.0006); and or to the 100- to 200-pg/mL p-tau class (#p <0.04, ##p <0.0046), supporting an inverse correlation between KTP and p-tau levels of AD patients. **(B)** Representation of the potential clinical implications of the link between AD and pain presented in the study of Santos et. al, 2013. The characterized neuronal degeneration observed in AD lead to a decrease of KTP levels, presumably by its production being affected by less available neurons, which increased the possibility of AD patients experiencing chronic pain by decreasing their pain tolerance. In parallel, the cognitive deficits attained by AD patients might also hampered the self-reported pain and, together, these might foster their clinical condition. Finally, given the neuroprotective potential of KTP, decreased levels might result into an amplification of the degenerative scenario, worsening AD progression. Therefore, the authors suggested that a pharmacotherapy with KTP-related drugs might be favorable to AD progression, mainly due to their dual neuroprotective and analgesic action. Adapted from (Santos et al., 2013).

1.3.3.1. Kyotorphin and Amidated-Kyotorphin as neuroprotective agents

During the last years, the potential neuroprotective action of KTP began to be explored in the context of AD and dementia (Figure 7). In summary, after KTP levels were found to be decreased in CSF of AD patients (Santos et al., 2013), the pharmacological use of KTP-related drugs as a dual action in targeting both AD and pain symptoms was suggested to counteract the amplification of the neurodegenerative feedback loop maintained by the lack of KTP (Figure 6 (B)). Among other KTP-derivatives, KTP-NH_2 appeared as an interesting candidate for testing its neuroprotective action, mainly due to its confirmed capability of crossing the BBB.

Besides having an acute and chronic well-characterized analgesic-profile when systemic administrated (see previous topic Functional studies regarding KTP-NH_2), in a mouse model of lipopolysaccharide-induced inflammation, KTP-NH_2 was efficient in decreasing the number of leukocyte rolling, without affecting the microcirculatory environment (Conceição et al., 2016). Systemic KTP-NH_2 treatment also had remarkable effects on ameliorating cognitive symptoms induced in a cerebral hypoperfusion dementia model, possible through neuronal rescue of impaired cells (Sá Santos et al., 2016). Additionally, KTP-NH_2 also showed a systemic glucocorticoid-mediated anti-inflammatory action (Perazzo et al., 2017b). Accordingly, the impact on the glucocorticoid system might account for the molecular link between analgesia, anti-inflammation, and neuroprotection observed by KTP-NH_2 administration (Perazzo et al., 2017b).

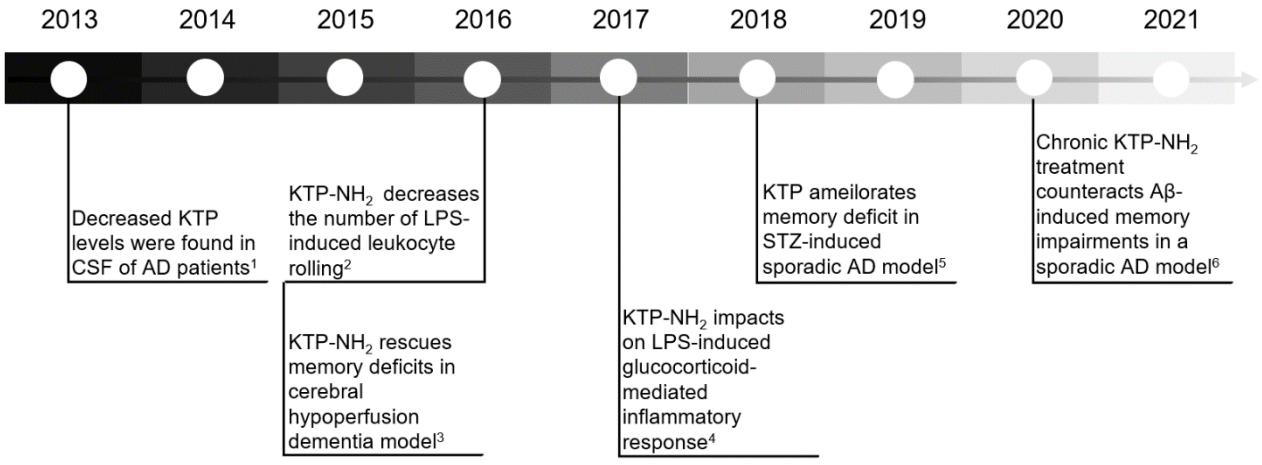

Figure 7. Timeline of studies exploring the neuroprotective potential of Kyotorphin and Amidated-Kyotorphin. These studies explored the therapeutic use of both Kyotorphin (KTP) and Amidated-KTP (KTP-NH_2) in the context of Alzheimer's Disease (AD) and dementia. References: [1](Santos et al., 2013); [2](Conceição et al., 2016); [3](Sá Santos et al., 2016); 4 (Perazzo et al., 2017b); [5](Angelova et al., 2018); [6](Belo et al., 2020); LPS – lipopolysaccharide; STZ – streptozotocin.

Interestingly, i.c.v. injection of KTP in a sporadic AD rat model ameliorated memory impairments without affecting Aβ amyloid deposits in the hippocampus (Angelova et al., 2018). Finally, our recent work was the first to provide evidence for the use of KTP-NH_2 in AD pathophysiology. As such, the chronical i.p. injection of KTP-NH_2 in a sporadic AD rat model was able to counteract Aβ-induced memory impairment, possible by protecting neuronal synapses and plasticity (see Chapter 4).

Chapter 2

Objectives

2.1. General and specifics objectives

Despite the putative therapeutic potential of KTP in pain and AD, its inability to cross the BBB makes its clinical use a challenge. KTP-NH_2, a KTP derivative, was designed to overcome this pharmacokinetic hindrance, which increases its therapeutic value as a CNS drug. In this study, the main goal was to explore the therapeutic use of KTP-NH_2 as a new drug for AD treatment.

Although recent studies have shown a remarkably analgesic, anti-inflammatory, and neuroprotective action of KTP-NH_2, its functional and molecular impacts on synaptic functions are still unknown. Similarly, the synaptic effects of KTP are yet to be uncovered. Thus, the **first specific aim** of this work was to characterize and to compare KTP and KTP-NH_2 effects in synaptic function under non-pathological conditions (Chapter 3).

Then, given the particular interest of this work in AD treatment, the **second specific aim** was to evaluate the neuroprotective potential of both peptides in Aβ-induced AD pathophysiology (Chapter 3). Since Aβ peptide was used as the insult to mimic the *in vitro* AD pathophysiological environment, the neuronal mechanisms known to be impaired by its presence, and that could be potentially protected by KTP and KTP-NH_2 actions, were explored here.

Finally, the **third specific aim** was to correlate the synaptic mechanisms protected by KTP-NH_2 action against Aβ-induced toxicity and the ameliorated memory impairment observed after systemic administration of KTP-NH_2 in a rat model of sporadic AD (Chapter 4).

Chapter 3

Characterization of KTP and KTP-NH_2 effects in synaptic functions under non-pathological conditions and Aβ-induced pathophysiology

3.1. Chapter rationale and publication information

The higher therapeutic interest on KTP-NH_2 - the KTP synthetic derivative especially designed to overcome the BBB, clearly pointed that a comparative study between KTP and KTP-NH_2 was needed. Given their potential in AD treatment, this chapter aimed to characterize and to compare the functional and molecular effects of both peptides in CNS, not only under non-pathological conditions, but also in Aβ-induced pathophysiology conditions. The performed experiments were design to study the impact of exogenous administration of both peptides in synaptic mechanisms that could be either modulated by KTP and KTP-NH_2 action, or that are known to be impaired by Aβ peptide, the elected insult to mimic the AD pathophysiology.

This chapter included the manuscript prepared for an original research article to be submitted soon. Besides having design and conceptualize this study, I performed all experiments and statistical analysis included. Catarina Miranda-Lourenço helped with the electrophysiological recordings and co-performed the glutamate release experiments. Tiago Coelho e Carolina Almeida-Borlido equally contributed to immunocytochemistry analysis under my supervision. Sandra H. Vaz was responsible by both glutamate release and calcium imaging experiments supervision, and results interpretation. Valéria Martins and Beatriz de Alves Pereira helped with technical support and cell cultures manipulation. Clara Pérez-Peinado and Javier Valle helped with KTP_{ant} synthesis under supervision of David Andreu. Hugo Vicente Miranda was responsible for the preparation of the oligomeric species of Aβ. Me, João Fonseca-Gomes and Catarina B. Ferreira were responsible by the neuronal cell cultures. Montserrat Heras and Eduard Bardaji were responsible for the synthetize of both KTP and KTP-NH_2 peptides. Miguel A. R. B. Castanho, Vera Neves, Ana M. Sebastião, and Maria José Diógenes were responsible for the concept and design of the study, interpreted the results and supervised the work.

This study was supported by Santa Casa da Misericórdia de Lisboa (MB37-2017) and FCT: PTDC/NEU-OSD/5644/2014, and PTDC/BIA-VIR/29495/2017. FCT supported Catarina Miranda-Lourenço (SFRH/BD/118238/2016), João Fonseca-Gomes (PD/BD/114441/2016), Catarina B. Ferreira (PD/BD/128390/2017).

3.2. Introduction

Kyotorphin (KTP), a dipeptide constitute by *L*-Arginine-*L*-Tyrosine was discovery in 1979 (Takagi et al., 1979a). It has a described naloxone-reversible opioid-like analgesic effect, which indirectly triggers the release of Met-enkephalin in central nervous system (CNS) (Takagi et al., 1979b; Rackham et al., 1982). The mechanisms underlying this effect remain unclear in several aspects, but it currently accepted that KTP acts through a specific Gi-coupled receptor (KTPr), inducing the Ca^{2+} influx in a phospholipase C-mediated process (Takagi et al., 1979b; Shiomi et al., 1981b; Ueda et al., 1995b, 1995a, 1996). Moreover, KTPr action can be antagonized by the dipeptide *L*-Leucine-*L*-Arginine (KTP_{ant}).

During the last two decades, the vast majority of KTP research has been related to its possible application in pain treatment, but some studies also explored its other non-opioid dependent functions (Dzambazova and Bocheva, 2010; Ueda, 2021). Nowadays, the interest in KTP as a drug for CNS goes behind its analgesic properties, which has recently increased due to its role in neuroprotection, including as a possible drug for Alzheimer's Disease (AD) treatment.

AD has proven to be a highly complex disease and a challenge for drug discovery and development (Bondi et al., 2017). At the molecular level, the presence of brain amyloid plaques, primarily formed by the aggregation of the extracellular misfolded amyloid beta (Aβ) peptide, and neurofibrillary tangles, are the hallmarks of the AD (Citron, 2010; Price et al., 1991). Moreover, excitotoxicity, dysregulation of brain-derived neurotrophic factor (BDNF) signaling, and inflammation are known to be present in this disease (Budni et al., 2015; Jerónimo-Santos et al., 2015; Dansokho and Heneka, 2018). BDNF, an important neurotrophic factor, is involved in synaptic plasticity mechanism (Binder and Scharfman, 2004), enhancing hippocampal long-term potentiation (LTP) and neuronal spine density, through tropomyosin receptor kinase B-full length (TrkB-FL) activation (Fontinha et al., 2008; Minichiello, 2009; Lu et al., 2015). Importantly, Aβ leads to a Ca^{2+}-induced overactivation of calpains, causing the pathological cleavage of TrkB-FL, with the formation of a TrkB truncated form and of an intracellular domain fragment (TrkB-ICD), and consequently affecting synaptic plasticity (Fonseca-Gomes et al., 2019; Jerónimo-Santos et al., 2015; Tanqueiro et al., 2018).

To assess synaptic function, electrophysiological recordings are usually performed, and, in particular, LTP induction in hippocampal CA1 area allows the study the molecular mechanisms of synaptic plasticity that correlate with memory and learning processes (Bliss and Collingridge, 1993). Moreover, hippocampi is one of the most affected brain areas in AD patients (Citron, 2010), which strongly correlates with the progressive memory decline in

these patients. Their limited capacity to verbally express and percept pain can lead to a pain underestimation and, without the adequate treatment, to the worsen of AD progression (Borsook, 2012). Furthermore, AD patients have decreased levels of KTP in cerebrospinal fluid (Santos et al., 2013), which may be a consequence of the disease-specific cortical thinning and hippocampal volume loss. As such, the link between pain and AD, two conditions with extreme epidemiologic relevance, suggested the use of KTP-related drugs as new therapeutic strategies for AD treatment (Santos et al., 2013).

The striking difference in the KTP analgesic effects obtained by systemic and focal intracerebroventricular (i.c.v.) administration assigns its very limited capacity of reach the brain, mainly due to its inability to cross the blood-brain barrier (BBB) and susceptibility to clearance mechanisms (Jiang et al., 2009; Serrano et al., 2014a, 2014b). Within this context, several groups have been working in different strategies to modify and add new function to the original peptide (Perazzo et al., 2017a).

Amidated-Kyotorphin (KTP-NH_2) was synthesized with the substitution of KTP carboxylic group (-OH) with an amine group (-NH_2). This change increased the peptide global net charge, enhancing its interaction with biological membranes, including its capability to cross the BBB (Ribeiro et al., 2011a, 2011b). Besides having an acute and chronic well-characterized analgesic-profile, without major side-effects (Ribeiro et al., 2011a, 2011b), KTP-NH_2 showed remarkably anti-inflammatory effects (Conceição et al., 2016; Perazzo et al., 2017a). Moreover, our recent studies unveiled the neuroprotective effect of KTP-NH_2 on ameliorating cognitive symptoms induced 1) in a cerebral hypoperfusion dementia model, possible through neuronal rescue of impaired cells (Sá Santos et al., 2016), and 2) in a Aβ-induced sporadic AD model, possible by protecting neuronal synapses and plasticity (Belo et al., 2020).

In this work, we aimed to characterize and compare the effects of KTP and KTP-NH_2 to assess possible differences in mediating synaptic activity. More specifically, given our particular interest in unravelling the partially unknown neuroprotective effect of both peptides in Aβ-induced AD pathophysiology, we explored the effects of both peptides in several neuronal mechanisms that are known to be impaired by Aβ action.

3.3. Materials and Methods

3.3.1. Peptides

3.3.1.1. Amyloid β peptide

As previously used in the lab (Belo et al., 2020), *in vitro* experiments using primary cortical cultures were performed using the Amyloid β (Aβ) peptide fragment 25-35 ($Aβ_{25-35}$) (Bachem, Bubendorf, Switzerland). This fragment represents the biologically active region of Aβ, causing similar dysfunctions as the Aβ peptide 1-42 ($Aβ_{1-42}$) (Kaminsky et al., 2010; Pike et al., 1995). Stock solutions of $Aβ_{25-35}$ were prepared in milliQ water to a final concentration of 1 mg/mL. To prepare oligomeric species of $Aβ_{1-42}$ ($Aβ_{olig}$), $Aβ_{1-42}$ (1 mg/ml) (A-42-T, GenicBio, Shanghai, China) was suspended in phosphate-buffered saline (PBS), supplemented with 0.025% ammonia solution, and adjusted to a final pH 7.2 (HCl). Species separation was based on an ultrafiltration process, as previously described (Giuffrida et al., 2009). Briefly, $Aβ_{1-42}$ (220 μM) was set to oligomerize by constant shaking at 600 rpm, at 37ºC for 16 h and ultracentrifuged (40 000 *g*, 30 min) for separation of fibrils (pellet). The supernatant was further separated in centrifugal filters (30 kDa Amicon Ultra). The concentration of the retained fraction, corresponding to oligomers > 30 kDa, was spectrophotometrically determined (ε280 =1490 $M^{-1}cm^{-1}$). These oligomers aliquots (120-220 μM) were immediately stored at -80ºC until further use.

3.3.1.2. KTP, KTP-NH_2 and KTP_{ant}

KTP (*L*-Tyrosine-*L*-Arginine) and KTP-NH_2 (*L*-Tyrosine-*L*-Arginine-NH_2) peptides were synthesized as previously described (Ribeiro et al., 2011b). KTP_{ant} (*L*-Leucine-*L*-Arginine) was synthesized as routinely by our group (Cavaco et al., 2020), using a Prelude synthesizer (Gyros Protein Technologies, Tucson, AZ) running Fmoc (FastMoc) SPPS protocols at 0.1 mmol scale on a fmoc-*L*- Arg(boc)-wang resin. Eight-fold excess of Fmoc-*L*-amino acids and *N*,*N*,*N'*,*N'*-Tetramethyl-O-(1*H*-benzotriazol-1-yl)uronium hexafluorophosphate (HBTU), in the presence of a double molar amount of *N,N*-diisopropylethylamine (DIEA), were used for the coupling steps, with *N*,*N*-dimethylformamide (DMF) as a solvent. After chain assembly, full deprotection and cleavage were carried out with the addition of 3 mL of 95% trifluoroacetic acid (TFA), 2.5% H_2O, 2.5% triisopropylsilane (TIS) (v/v), and the preparation was shacked (200 rpm), for 90 min, at room temperature (RT). After that, the resin was filtered and the peptide was isolated through precipitation with ice-cold diethyl ether, and centrifugation at 4,000 *g*, 4°C for 10 min. Then, the supernatant was removed, and the pellet was dissociated using a vortex. Then, 10 mL of MiliQ water was added, and the peptide was lyophilized inside a vacuum chamber. Analytical reversed-phase HPLC was performed on a Luna C18 column (4.6 × 50 mm, 3 μm; Phenomenex, USA). Linear gradients of solvent B (0.036% TFA

in Acetonitrile) into solvent A (0.045% TFA in H_2O) were used at a flow rate of 1 mL/min and with ultraviolet (UV) detection at 220 nm. Preparative HPLC runs were performed on a Luna C18 column (21.2 × 250 mm, 10 µm; Phenomenex) using linear gradients of solvent B (0.08% TFA in Acetonitrile) into solvent A (0.1% TFA in H_2O) at a flow rate of 25 mL/min and with UV detection at 220 nm. Fractions of adequate HPLC homogeneity and with the expected mass were combined and lyophilized. LC-MS was performed in a LC-MS 2010EV instrument (Shimadzu, Kyoto, Japan) fitted with an XBridge C18 column (4.6 × 150 mm, 3.5 µm; Waters, Spain), eluting with linear gradients of solvent B (0.08% Formic Acid (FA) in Acetonitrile) into solvent A (0.1% FA in H_2O) over 15 min at 1 mL/min. All peptides were prepared in previously filtered and sterile milliQ water and, accordingly of their use in *ex vivo* and *in vitro* experiments, 1 mM and 5 mM stock solutions were stored at -20ºC.

3.3.2. Brain areas dissection and acute hippocampal slices preparation

Brain tissue and acute hippocampal slices were obtained and maintained as routinely in the lab (Belo et al., 2020). Briefly, male C57BL/6J mice (8-11 weeks old), purchased to Charles River Laboratories (Lyon, France), were deeply anesthetized with isoflurane and decapitated. Then, brains were quickly removed and placed in ice-cold artificial cerebral-spinal fluid solution (aCSF; 124 mM NaCl, 3 mM KCl, 1.2 mM NaH_2PO_4, 25 mM $NaHCO_3$, 2 mM $CaCl_2$, 1 mM $MgSO_4$, and 10 mM glucose, pH 7.4), continuously oxygenated (O_2/CO_2: 95%/5%). For the calpain assays and synaptosomes isolation, cortices and hippocampi were respectively dissected in this step. To obtain acute hippocampal slices to conduct electrophysiological recordings, both hippocampi were dissected and placed in a McIlwain tissue chopper, properly oriented to allow the cut of acute hippocampal slices, with a thickness of 400 µm, perpendicularly to the long axis of the hippocampus. Then, to guarantee the functional and energetic tissue recovery, slices were placed in a resting chamber filled with continuously oxygenated aCSF at RT for 1h.

3.3.3. *Ex vivo* electrophysiological recordings

Ex vivo electrophysiological recordings were conducted as routinely in the lab (Belo et al., 2020). Briefly, acute hippocampal slices were placed into a recording chamber continuously superfused with aCSF at 32°C and continuously oxygenated (flow rate of 3 mL/min), unless other way stated below (Figure 8 (A)). Field-excitatory postsynaptic potentials (fEPSP) were extracellularly recorded using a microelectrode filled with aCSF (2–6 MΩ), placed in the *stratum radiatum* of the CA1 area. Stimulation was applied using a bipolar concentric wire electrode placed on Shaffer collateral/commissural fibers in *stratum radiatum* in either one or both independent pathways (S1 or S2). The intensity of stimulation was initially adjusted to obtain the fEPSP slope with a minimal spike contamination and of around 50% of the maximal slope. Recordings were obtained with an Axoclamp 2B amplifier (Axon Instruments,

Foster City, CA, United States), digitized and continuously stored on a personal computer with the *WinLTP* software (Anderson and Collingridge, 2001). Depending on the followed protocol, stimulation pulses were delivered every 10/20 s and individual responses were monitored as the averages of six/eight consecutive signals. Either slopes and/or amplitudes of the fEPSP initial phase, and/or the amplitude of presynaptic fiber volley (PSFV) were quantified. For all electrophysiological recordings, the baseline was defined as the average of 5 points recorded, usually with 10 min duration, immediately *prior* to any followed manipulation known to be liable of perturbing the recorded signal (e.g. changes in stimulation input, and peptides perfusion). This baseline is essential for having an initial stable read-out, working as an internal control, which was used to normalize the respective experiment.

3.3.3.1. Concentration/effect curves

To study the effect of KTP and its amidated form in synaptic transmission, hippocampal slices were superfused with increasing concentrations of the peptides, prepared in continuously oxygenated aCSF, after the obtention of a stable baseline of fEPSP slopes and amplitudes. Every tested concentration (from 5 nM to 5 mM) of each peptide was superfused for 32 min each (16 points), within a close circuitry. After the superfusion of the highest concentrated solution, slices were superfused with aCSF without peptides for 20 min in an open circuitry to assure a complete removal of peptides in circulation (Figure 8 (C)). Both fEPSP slope and amplitude were quantified as the percentage of change in the respective average taken between the last 10 min of each perfused solution (the last 5 points) in relation to the respective average of fEPSP measured during the baseline. Note that peptides physiological concentrations are usually within a nanomolar scale (nM-scale), and similarly to other neurotrophic peptides, a small amount of these molecules is enough to induce a perturbation on the basal synaptic transmission when compared to neurotransmitters (Hökfelt et al., 2003).

3.3.3.2. Input/Output curves

Input/Output (I/O) curves were used to evaluate the synaptic transmission efficacy. Similarly, after obtaining a stable baseline, with an average fEPSP slope around 0.5 mV/ms, the stimulation was decreased to 60 μA, which represents no evoked-fEPSP, and subsequently increased by steps of 20 μA until a supramaximal stimulation of 320 μA. Both fEPSP slope and the amplitude of PSFV were quantified as the average of three consecutive fEPSP recorded for each stimulation intensity. The I/O curves were plotted as 1) the fEPSP slope against the stimulus intensity, 2) the PSFV amplitude against stimulus intensity, and 3) the fEPSP slope against PSFV amplitude, providing a measure of basal synaptic efficiency.

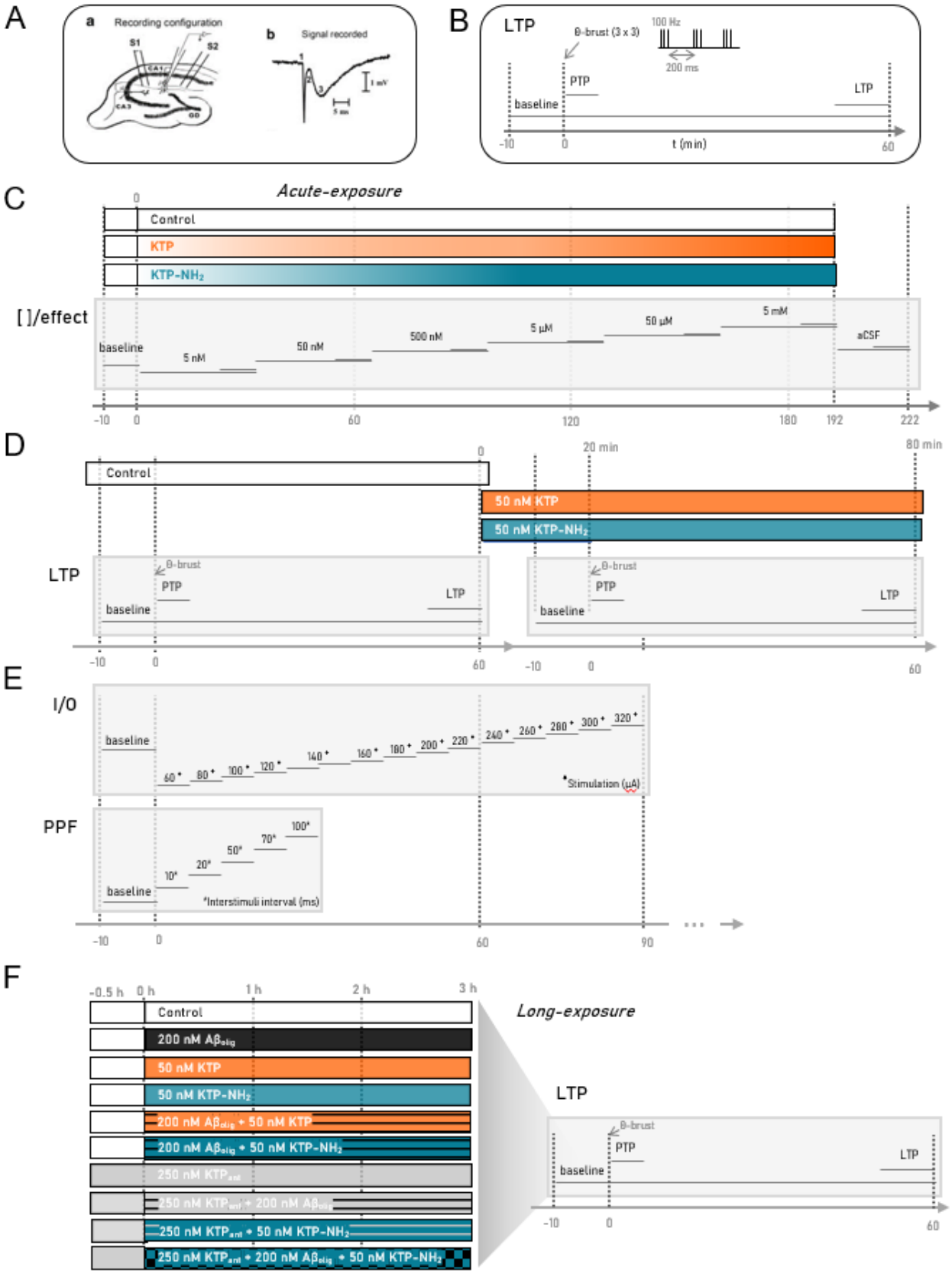

Figure 8. Hippocampal slices treatment and respective electrophysiological recordings protocols used. (A) (a) Schematic representation of an acute hippocampal slice with the electrophysiological recording configuration used to obtain field excitatory postsynaptic potentials

(fEPSP) from CA1 area under the stimulation of two independent Schaffer pathways (S1 and S2). (b) Schematic representation of a recorded signal tracing showing the stimulus artifact (1), the presynaptic volley (2), and the fEPSP (3). Adapted from (Diógenes et al., 2011) **(B)** Representation of the applied long-term potentiation (LTP) protocol for long-exposure treated slices. After a stable baseline (10 min), LTP was induced through a weak θ-burst protocol (3 trains of 100 Hz, 3 stimuli, separated by 200 ms). Post-tetanic potentiation (PTP) was quantified as the average of the first 3 recorded signals (6 min) after LTP induction, whereas LTP magnitude (presented as LTP) was quantified using the last 5 points (10 min) of 1 h of recording. **(C)** Representation of the applied Concentration/effect curves protocol. After obtaining a stable baseline, six solutions of increasing concentration (5 nM, 50 nM, 500 nM, 5 µM, 50 µM, and 5 mM), of each peptide (KTP or KTP-NH_2) were successively superfused during 32 min each, and fEPSP recorded. After the perfusion of the highest concentrated solution, slices were superfused with continuously oxygenated aCSF for 20 min. Both fEPSP slope and amplitude were quantified as the percentage of change in the respective average taken between the last 10 min of each perfused solution (the last 5 points) in relation to the respective average of fEPSPs measured during the baseline. **(D)** Representation of the applied LTP protocol for acute-exposure treated slices. In these experiments, firstly a LTP was induced (control, with aCSF perfusion) in one of the two available stimulation pathways (S1 or S2), and then, the second LTP was induced in the other stimulation pathway (S1 or S2), after peptides superfusion for a minimal of 20 (50 nM KTP or 50 nM KTP-NH_2). Similarly, PTP and LTP were quantified as already described. **(E)** Representation of the applied Input/Output (I/O) curves and Paired-pulse facilitation (PPF) protocols for acute-exposure treated slices. Regarding PTP, after obtaining a stable baseline, the stimulation was decreased to 60 µA, which represents no evoked- fEPSP, and subsequently increased by steps of 20 µA, for 6 min each, until a supramaximal stimulation of 320 µA. Regarding PPF, two consecutive evoked-fEPSP were recorded using a PPF stimulation protocol with successively higher interstimuli intervals (10, 20, 50, 70, and 100 ms), for 6 min each. **(F)** Long-exposure treatment used to evaluate KTP and KTP-NH_2 effect (50 nM) and in the presence or absence of Aβ (200 nM), as well as KTP_{ant} (250 nM). A single LTP was induced as before in S1 pathway.

The maximum slope values were obtained by extrapolation upon nonlinear fitting of the I/O curve. The effects of KTP and KTP-NH_2 were evaluate as the following: an I/O curve was firstly performed in a slice superfused with continuously oxygenated aCSF solution (control condition), in one of independent pathway (S1 or S2); then, a second solution of aCSF with KTP or KTP-NH_2 (50 nM) started to be perfused, and after 20 min, a second I/O curve was performed on the contrary pathway (S2 or S1, respectively) (Figure 8 (D)).

3.3.3.3. Paired-pulse facilitation

Paired-pulse facilitation (PPF) was conducted as routinely in the lab (Diógenes et al., 2014). After obtaining a stable baseline, two consecutive evoked-fEPSP were recorded from hippocampal CA1 area using a PPF stimulation protocol with successively higher interstimuli

intervals (10, 20, 50, 70, and 100 ms), for 6 min each (3 recorded fEPSP-pairs). PPF magnitude was quantified as the slope ratio of the second and the first evoked stimuli (fEPSP2/fEPSP1), as the ratios average of the 3 recorded fEPSP-pairs within the same electrical stimulation range. The superfusion of solutions of continuously oxygenated aCSF (control), with KTP or KTP-NH_2 (50 nM) were also used similarly in PPF recordings to what was described before regarding the I/O curves protocol (Figure 8 (E)).

3.3.3.4. Long-term potentiation and post-tetanic potentiation

LTP induction and quantification were performed as described previously (Belo et al., 2020; Diógenes et al., 2011). After fEPSPs stabilization (baseline), LTP was induced through a weak θ-burst protocol (3 trains of 100 Hz, 3 stimuli, separated by 200 ms). The θ-burst induced LTP pattern of stimulation is considered closer to what physiologically occurs in hippocampi during episodes of learning and memory in living animals (Albensi et al., 2007). We used a mild LTP protocol sensitive to changes in LTP magnitude. LTP magnitude was quantified as the percentage of change in the average slope of fEPSPs taken between 50 to 60 min after LTP induction (last 5 points) in relation to the average slope of fEPSPs measured during the 10 min before θ-burst induced LTP (baseline, 5 points). In addition, post-tetanic potentiation (PTP) magnitude was quantified as the percentage of change in the average fEPSP slopes obtained in the first 6 min (3 recorded points) after LTP induction (Habets and Borst, 2007).

The acute effects of KTP and KTP-NH_2 (50 nM) were evaluate in a context of synaptic plasticity (Figure 8 (C)). Once more, these experiments followed similar protocols concerning slices treatments and time-points. A first LTP (Figure 8 (B)) was induced in a slice superfused with continuously oxygenated aCSF (control condition) in one pathway, and then, after starting the perfusion of aCSF solutions with KTP or KTP-NH_2 (50 nM), a second LTP was induced in the other pathway (Figure 8 (C)). To evaluate the effects of peptides-long exposure, slices were pre-treated for 3h at RT with solutions of continuously oxygenated aCSF with KTP or KTP-NH_2 (50 nM), in the presence or absence of 200 nM $A\beta_{olig}$. In addition, the effect of KTP_{ant} over KTP-NH_2 was evaluated in the same conditions by adding 250 nM KTP_{ant} 30 min prior to co-incubating with 50 nM KTP-NH_2.

3.3.4. Synaptosomes isolation

Hippocampal tissue isolated from adult animals was homogenized using a Potter homogenizer with 5 mL of ice-cold sucrose solution (320 mM sucrose, 1 mM ethylenediaminetetraacetic acid (EDTA), 10 mM 4-(2-hydroxyethyl)-1-piperazineethanesulfonic acid (HEPES), 1 mg/mL bovine serum albumin (BSA), pH 7.40), and a Teflon pestle. Then, after adding an additional 5 mL of the sucrose solution, the

homogenates were centrifuge at 3 000 *g* for 10 min at 4ºC (Avanti J-25I, Beckman Model, rotor: JA-25.50). Supernatants were collected and a new centrifugation was conducted at 14 000 *g* for 12 min at 4ºC. The obtained pellet was resuspended in 2 mL of 45% (v/v) Percoll solution in KHR (140 mM NaCl, 1 mM EDTA, 10 mM HEPES, 5 mM KCl, 5 mM glucose, pH 7.40) and centrifuged at 14 000 *g* for 2 min at 4ºC (Heraues sepatech – Biofuge 28RS centrifuge). The synaptosomal fraction, which was identified as the top layer, was carefully collected through pipette aspiration to a new Eppendorf, washed in 1 mL of KHR solution and centrifuged once more in the same conditions. The synaptosomes were kept on ice and used within 3 hours.

3.3.5. [^{3}H]Glutamate release

Both synaptosomal fraction preparation and [^{3}H]Glutamate release assays were conducted as routinely in the lab (Vaz et al., 2015). The synaptosomes were resuspended in oxygenated aCSF and allowed to equilibrate for 5 min at 37ºC. From this time onward, all solutions used were continuously oxygenated and kept at 37 ºC. The synaptosomes were loaded with 0.2 µM [^{3}H]glutamate (specific activity 30–60 Ci/mmol) for 5 min and equally layered over Whatman GF/C filters (Milipore, MA, USA), onto a six-chamber superfusion apparatus (flow rate, 0.6 ml/min; chamber volume, 90 µl). The effluent was collected for 40 min in 2 min intervals, after a 20 min washout period. Glutamate release from synaptosomes was elicited two times using a high-concentration K^+ solution (15 mM, isomolar substitution of Na^+ with K^+ in the perfusion buffer), with a stimulation period of 2 min each. The first period occurred 5 min after starting the sample collection (S1, first stimulation period) and, the second at the 29th min (S2, second stimulation period). Solutions of 50 nM KTP and 50 nM KTP-NH_2 were prepared in the superfusion medium (control condition), and started to be perfused at 9th min. Each condition (control, KTP and KTP-NH_2) was tested in duplicate within each experiment. After that, aliquots of 500 µL of each sample as well as the filters from each superfusion chamber were analyzed by liquid scintillation counting. The fractional release was expressed as the percentage of the total radioactivity present in the synaptosomes at each time point, and the averages of duplicates of each condition were considered as independent experiments. Then, the amount of radioactivity released by each pulse of K^+ (S1 and S2) was calculated as the difference between the average of the 2 points of the peak, and the average of the 3 points before and the 3 points after the peak. Statistical differences were analyzed using the averaged ratios between the S2 and S1 of each condition.

3.3.6. Primary cortical cultures

Primary cortical cultures were obtained from cortices of Sprague-Dawley fetuses (E18/19), as routinely in the lab (Jerónimo-Santos et al., 2015). Briefly, pregnant animals were deeply

anaesthetised with isoflurane (Esteve, Barcelona, Spain), and decapitated. The collected fetuses were placed in Ca^{2+}- and Mg^{2+}-free Hank's Balanced Salt Solution (HBSS) (Gibco, Paisley, UK), at 4ºC. After brains dissection, and meninges removed, the isolated cortical tissue was mechanically fragmented and enzymatically digested with 0.025% (w/v) of trypsin solution in HBSS for 15 min at 37ºC. A solution of HBSS supplemented with Fetal Bovine Serum (FBS) 20% (w/v) was used to neutralize the action of trypsin, and the cellular suspension was centrifuged at 190g. After discarding the supernatant, the cells were resuspended in the same solution by pipette aspiration to better dissociate cells. This washing process was repeated twice more times. Finally, cells were resuspended in warmed supplemented Neurobasal medium (0.5mM *L*-glutamine, 25mM glutamic acid, 2% B-27, and 25 U/mL penicillin/streptomycin), and filtered (BD Falcon Cell Strainer 70 mM, Thermo Fisher Scientific, Waltham, MA, United States), to unsure a single cells suspension. The cell density was determined using a hemocytometer to count cells in a 0.4% trypan blue solution.

Cells were plated at $1x10^{-5}$ cells/mL in 8-wells Ibidi plates with a glass bottom (ibidi GmbH, Martinsried, Germany), and in96- and 12-wells flat-bottom cell plates covered with glass coverslips (Corning® Costar® TC-treated, Sigma). Both cell plates and coverslips were previously sterilized under UV light, and coated overnight with 10 mg/mL of poly-*D*-lysine (Sigma, St. Louis, MO, United States) and washed with sterile H_2O twice.

For immunocytochemistry and cell viability assays, cells were incubated with 50 nM KTP or 50 nM KTP-NH_2 in the presence or absence of 25 µM $A\beta_{25-35}$, during 24h, after 13 days *in vitro* (DIV13). During this maximum period of 14 days, all cells were maintained at 37ºC in a humidified atmosphere of 95/5% O_2/CO_2.

3.3.7. Calcium imaging

Cortical cultured neurons plated in 8-wells ibidi plates, as described above, were used between 10-14 DIV to conduct the calcium imaging assays. Briefly, at the experiment day, the supplemented Neurobasal medium was removed, and cells were carefully washed twice with external physiological solution Ca^{2+}-HEPES buffer (125 mM NaCl, 1.25 mM NaH_2PO_4, 3 mM KCl, 10 mM D($^+$)-glucose, 2 mM $CaCl_2$, 2 mM $MgCl_2$, 2 mM $MgSO_4$ and 10 mM HEPES; pH 7.4 adjusted with NaOH). Then, cells were loaded with 5 µM of fluorescent dye fura 2-acetoxymethyl (Fura 2AM) in Ca^{2+}-HEPES buffer, for 45 min at 37ºC in a humidified atmosphere of 95/5% O_2/CO_2, and washed three times with Ca^{2+}-HEPES buffer. Fura 2AM is a membrane cell ratiometric dye that binds to intracellular Ca^{2+} allowing to observe its evolution over time.

Then, ibidi plates were placed on a heated chamber where cells were kept at 37ºC in a humidified and oxygenated atmosphere (95/5% O_2/CO_2). This chamber was installed in an

inverted microscope (Axiovert 135TV, Zeiss) with epifluorescent optics and equipped with a high-speed wavelength switcher/multiple excitation fluorimetric system, Lambda DG4 (Sutter Instrument, Novato, CA, USA), with a 175W Xenon arc lamp, and band-pass filters of 340 and 380 nm wavelengths. Data was recorded by a CDD camera (Photometrics CoolSNAP fx), whereas image pairs were obtained every 5-10 s, by sequentially exciting the preparations at 340 nm and 380 nm, for 250 ms at each wavelength, and the emission fluorescence was recorded at 510 nm. These pairs images were processed and analysed by software MetaFluor (Universal Imaging, West Chester, PA, USA), allowing to obtain ratio images for further analysis. Solutions of 50 nM KTP or KTP-NH_2, prepared in Ca^{2+}-HEPES buffer, were carefully applied in the cells medium after establishing a 15 min baseline period. In addition, after 40 min of peptides addition, cells were challenged with 2 µM ionomycin, an effective Ca^{2+} ionophore that induces necrotic cell death (Montagne et al., 2015), by substantially increasing the intracellular calcium levels. As such, this step allows to identify viable cells so that only those cells that responded to ionomycin through a substantial increase of ratio 340/380 nm were considered for statistical analysis. In addition, experiments were performed on cells with a baseline fluorescence ratio around 0.5, which corresponds approximately to the expected intracellular calcium concentration of around 100 nM (Barhoumi et al., 2010; Knot, 2005). Regions of interest were obtained by defining the profile of the cells and averaging the fluorescence intensity within the delimited area. Intensity values were converted to ratio 340/380 nm and the all the values were normalized by the first ratio of each cell.

3.3.8. Immunocytochemistry

In order to evaluate the neuroprotective effect of peptides treatment, spine density was counted as previously reported (Belo et al., 2020). Briefly, after being washed with PBS twice, cells from DIV 14 primary cortical cultures were fixed in 4% paraformaldehyde in PBS (pH 7.4) for 15 min at RT. Firstly, cells were incubated with a blocking solution (3% (w/v) BSA) (Sigma-Aldrich) in PBS with 0.1% (v/v) Triton X-100, cells for 1h at RT; secondly, to specifically detect neurons, cells were incubated with mouse microtubule-associated protein 2 (MAP2) primary antibody (1:200, Millipore), in blocking solution, inside a wet-chamber at 4ºC overnight; thirdly, after washed with PBS twice, cells were co-incubated, also in blocking solution, with goat anti-mouse-Alexa Fluor 568 secondary antibody (1:200, Invitrogen), Alexa Fluor 488 Phalloidin (1:40, Invitrogen) probe, for filamentous actin (F-actin) staining, and Hoechst 33342 (6 µg/mL) for nuclear staining, for 1h at RT inside a dark-wet chamber. Finally, after washing with twice PBS, coverslips were mounted in Mowiol mounting solution. The use of a confocal laser point-scanning microscope LSM 880 with Airyscan (Carl Zeiss MicroImaging, Thornwood, NY, United States), allowed the clear identification of dendritic

protrusions, due to the observed conjugation between MAP2 (568, red), a major cytoskeletal component of neurons (Dinsmore and Solomon, 1991), and F-actin (488, green), an important protein in the constitution of the cytoskeleton of dendritic spines (Koskinen and Hotulainen, 2014). The number of dendritic protrusions allowed to evaluate spine density. As previously reported (Alonso et al., 2004; Ji et al., 2010), each primary culture were considered an independent experiment, and the number of protrusions were counted per parent dendrite, within a 10 µm, and 25 µm apart from the cell body. Independent averages were computed with the number of protrusions counted in 3 different dendrites of each neuron, 6 neurons per condition.

3.3.9. Cell viability assays

Cell viability was assess using the 3-(4,5-dimethylthiazol-2-yl)-2,5-diphenyltetrazolium bromide (MTT) and the cell counting kit-8 (CCK-8) colorimetric assays. The MTT assay allows the global evaluation of cellular metabolic activity by quantifying the bioreduction of the MTT into a formazan (a purple-colored product). Similarly, CCK-8 contains a tetrazolium salt, the 2-(2-methoxy-4-nitrophenyl)-3-(4-nitrophenyl)-5-(2,4-disulfophenyl)-2H-tetrazolium (WST-8), that can be reduced by cellular dehydrogenases to a formazan product (an orange-colored product), which is soluble in Neurobasal medium. The amount of formazan produced in both assays is directly proportional to the number of living and metabolic active cells. To note that although MTT is highly cytotoxic, CCK-8 is very stable, it has little cytotoxicity, with a higher detection sensitivity, and the handling procedure is shorter and less aggressive than when using any other tetrazolium salts such as MTT. The MTT (#CT01, Sigma-Aldrich, MO, USA) stock solution used was prepared as 5 mg/mL in PBS (pH 7.4) and store at -20ºC.

Briefly, primary cortical neurons (DIV 13) cultured in 96-wells plaques were treated with supplemented Neurobasal medium (control), with 25 µM $A\beta_{25-35}$ alone or with 50 nM KTP or 50 nM KTP-NH_2 for 24h at 37ºC in a humidified atmosphere of 95/5% O_2/CO_2. After 24 h, for MTT assays, the cell medium was replaced with 6% (v/v) MTT, and for CCK-8 assays with a solution of 10% (v/v) CCK-8 (Dojindo EU GmbH, Munich, Germany), both prepared in warmed supplemented Neurobasal medium and in a total of 200 µL per well. Cells were incubated for an additional 3h (MTT assays) or 2h (CCK-8 assays), respectively, at 37ºC in a humidified atmosphere of 95/5% O_2/CO_2. Then, the medium solution was removed from plaques incubated with MTT, and 200 µL of dimethylsulfoxide (DMSO) (Merck, Kenilworth, NJ, USA) was added per well, allowing the complete solubilization of the produced formazan product through several pipette aspirations. The absorbance was measured at 570 nm with background subtraction at 650 nm, in a microplate reader Infinite M200 (Tecan, Männedorf, Switzerland). On the other hand, after 2h of incubation with the CCK-8 solution, 100 µL of

each well were transferred onto a new 96-well plate and absorbance at 460 nm was measured using a microplate reader Infinite M200. Cell viability of each condition can reflect the toxicity of each incubation agent. The quantification of cell viability using MTT assays was computed as a ratio between the average of replicated wells of each condition and the average of replicated wells with untreated cells condition (control). On the other hand, the quantification of cell viability using CCK-8 assays was computed as an index between 0 and 1, using the ratio between the difference between the average of replicated wells of each condition and the average of replicated wells incubated with 6% (v/v) isopropanol as the negative control agent, and the absorbance of replicated wells with plated cells without treatment as a positive control [(x – negative control) / positive control].

3.3.10. Calpain enzymatic assay

The collected cortical tissue of 4 animals was homogenized as independent samples, by adding Radio Immuno Precipitation Assay (RIPA) buffer: 50 mM Tris-base (pH 7.5), 150mM NaCl, 5mM EDTA, 0.1% Sodium Dodecyl Sulphate (SDS), and 1% Triton X-100, supplemented with phosphatase inhibitors: 10nM NaF; 5mM Na_3VO_4 and a protease inhibitor cocktail (Complete Mini-EDTA free from Roche, Penzberg, Germany), at 4ºC, and using a Vibracell VC250 Ultrasonic Liquid Processor (Sonics & Materials, CT, USA). Samples were centrifugated at 16 000 *g* for 10ºC at 4ºC and their protein content was quantified using the Bio-Rad DC reagent (Bio-Rad, Berkeley, CA, USA). Then, sample conditions used in the enzymatic assay were prepared with 100 µg of protein, whereas sterile MiliQ water was added to ensure a volume of 100 µL *per* sample. Then, samples were treated with 50 nM KTP or KTP-NH_2, with or without co-treatment of 250 nM KTP_{ant}. After adding the purified rat m-calpain (1 enzymatic unit, EU; Calbiochem, San Diego, CA, USA) and/ or 2 mM $CaCl_2$, samples were incubated for 30 min at RT. Negative controls samples were prepared only with tissue homogenates and sterile MiliQ water. The enzymatic reaction was stopped by rising the temperature of samples to 95ºC and immediately stored at -20ºC until sample preparation for Western Blot.

3.3.11. Western blot (WB)

After conducting calpain *in vitro* enzymatic assay, samples were prepared by adding a loading buffer (350 mM Tris-HCl (pH 6.8), 10% SDS, 30% glycerol, 600 mM Dithiothreitol, 0.06% bromophenol blue), and then boiled at 95°C for 5 min. Next, samples and the molecular weight marker (PageRuler™ Plus Prestained Protein Ladder, 10 to 250 kDa, ThermoFisher Scientific, Massachusetts, USA) were loaded and separated on 12% SDS–polyacrylamide gel electrophoresis (SDS–PAGE) within a standard migration buffer (25 mM Tris-base (pH 8.3), 192 mM Glycine, 10% SDS), at a constant voltage between 80 and 120 mV. Subsequently, proteins were electrotransferred, at 400 mA for 1h30, from the gel to a

polyvinylidene difluoride (PVDF) membrane (GE Healthcare, Buckinghamshire, United Kingdom), previously activated with methanol for 5 min, within the standard buffer (25 mM Tris (pH 8.3), 192 mM glycine, 15% methanol) for wet transfer conditions. Afterwards, membranes were stained with Ponceau S solution (Sigma-Aldrich®) to check for transference efficacy and blocked with a 3% BSA in TBS-T (Tris-Buffered Saline with Tween-20 containing in mM: Tris-base 20; NaCl 137 and 0.1% Tween-20) during 1h at RT to avoid non-specific binding. Membranes were incubated with the primary antibodies overnight at 4°C, and then with the HRP-conjugated secondary antibodies (1:10000, Santa Cruz Biotechnology, Dallas, TX, USA) for 1h at RT, all diluted in 3% BSA solution in TBS-T. The primary antibodies used were the rabbit polyclonal antibody anti-Trk-FL (1:1000, Santa Cruz Biotechnology, Dallas, Texas, USA), raised against the C-terminus (C-14), the mouse monoclonal antibody anti-α*II*-spectrin (C-3), raised against human spectrin (a.a. 2368-2472) (1:2500, Santa Cruz Biotechnology, Dallas, TX, United States), and the mouse monoclonal antibody anti-GAPDH (1:5000, Invitrogen, Carlsbad, California, USA). Chemiluminescent detection was performed with ECL Plus Western Blotting Detection Reagent (GE Healthcare, Buckinghamshire, UK) in the ChemiDoc™ XRS⁺ System from Bio-Rad. The integrated intensity of each band was calculated using computer-assisted densitometry analysis with Image-J 1.45 software (Bethesda Softworks, Bethesda, MD, United States) and normalized to the integrated intensity of the loading control (GAPDH). Images were prepared for printing in Image Lab software 5.2.1 (software available in ChemiDoc XRS⁺ system, Bio-Rad).–The ratio between TrkB-ICD and TrkB-FL was quantified as the average between independent sample conditions.

3.3.12. Ethics

For this study, all C57BL/6J mice were housed in groups of 4/5 per cage and maintained under controlled conditions (21 ± 1ºC; 55 ± 10% humidity; 12:12 h light/dark cycle). Sprague-Dawley pregnant rats were, purchased from Charles River Laboratories (Lyon, France), were housed alone during a maximum period of 4 days, under controlled conditions (20 ± 2ºC; 14:10 h light/dark cycle, lights on between 7 a.m. and 9 p.m.). All animals had unrestricted access to food and water. The handling of animals and all described procedures were conducted according to the European Community (86/609/EEC; 2010/63/EU; 2012/707/EU) and Portuguese (DL 113/2013) legislation for the protection of animals used for scientific purposes, and they were approved by the Ethical Committee for Animal Research of Instituto de Medicina Molecular | João Lobo Antunes, Faculty of Medicine, University of Lisbon, and the Portuguese Competent Authority for Animal Welfare (DGAV) in Portugal.

3.3.13. Statistical Analysis

Data are expressed as mean ± standard error of the mean (mean ± SEM), where *n* is the number of independent experiments. We considered as independent experiments the results obtained 1) from each cell cultures; 2) through electrophysiological recording in hippocampal slices of different animals; 3) from each tissue homogenates prepared from different animals. The data normality was confirmed using the Shapiro-Wilk test.

Results obtained through immunocytochemistry (number of dendritic protrusions), cell viability assays, electrophysiological recordings, namely in LTP magnitude of experiments where Aβ was co-incubated, were analyzed using two-way analysis of variance (ANOVA) followed by Tukey's multiple comparisons test (when comparing all conditions between each other), and/or followed by Sidak's multiple comparisons test (when all condition were compared with the control). In addition, those results obtained through electrophysiological recording where KTP_{ant} was also used were also analyzed using a three-way ANOVA followed by Tukey's multiple comparisons test. The remaining results obtained through calpain enzymatic assay, [^{3}H]Glutamate release, calcium imaging, and electrophysiological recordings where no Aβ was used, namely in LTP, PTP, PPF, concentration/effect curves, and I/O curves, were analyzed using one-way ANOVA followed by Tukey's multiple comparisons test (when comparing all conditions between each other), and/or followed by Dunnett's multiple comparisons test (when all condition were compared with the control

Values of p-value < 0.05 were considered to represent statistically significant differences. All statistical analyses were conducted using the Prism Software (GraphPad Prism®, version 8.0.2, California, USA).

3.4. Results

3.4.1. KTP and KTP-NH_2 caused concentration-dependent changes in synaptic transmission

To better understand the physiological effect of both peptides on basal synaptic transmission, we performed *ex vivo* electrophysiological recordings to obtain their concentration/effect curves. Briefly, we evaluated changes in the average of fEPSP recorded in CA1 hippocampal area of acute slices prepared from adult C57BL/6J male mice, and perfused with successively higher concentrations of each peptide, ranging from 5 nM to 5 mM (see Figure 8 (F)). Table 1 summarizes the averages obtained from the recorded fEPSP slope and amplitude, and the number of independent experiments (N), considering the effect of both KTP and KTP-NH_2.

As observed in Figure 9, both peptides had a concentration-dependent effect on basal synaptic transmission. More specifically, KTP showed a slightly inverted-U shape profile of action , although statistical analysis comparing KTP effect on the averaged fEPSP amplitude or slope revealed no statistical differences between KTP concentrations ($p \geq 0.05$, Mixed-effects model; n = 3-6; Figure 9 (B), (D)). One the other hand, KTP-NH_2 gradually decreased synaptic transmission over the consecutive increase of peptides concentration (Figure 9). Significant differences were detected when analyzing the KTP-NH_2 effect on the averaged fEPSP amplitude (50 nM KTP-NH_2 *vs.* 5 µM KTP-NH_2; 500 nM KTP-NH_2 *vs.* 5 µM KTP-NH_2; $p < 0.05$, Mixed-effects model followed by Tukey's multiple comparisons test; n = 4-5; Figure 9 (B)).

Table 1. The effect of KTP and KTP-NH_2 upon synaptic transmission. Values obtained from the concentration-effect curves. The averaged fEPSP slope and amplitude were recorded from adult C57BL/6J male mice acute hippocampal slices. Slices were perfused with oxygenated aCSF solutions (baseline of 10 min), aCSF solutions with successfully higher concentrations of KTP or KTP-NH_2, ranging from 5 nM to 5 mM (last 10 min of 32 min total), and aCSF washout solution (aCSF, last 10 min of a 20 min total). Data are presented as mean (%) ± SEM.

	KTP			KTP-NH_2		
	Slope (%)	Amplitude (%)	N	Slope (%)	Amplitude (%)	N
baseline	1.05 ± 0.544	0.288 ± 0.393	6	-0.505 ± 0.767	-0.945 ± 0.530	5
5 nM	0.705 ± 3.90	7.47 ± 3.08	6	-1.48 ± 3.49	-2.80 ± 3.26	5
50 nM	2.99 ± 2.03	11.9 ± 2.99	6	1.13 ± 6.46	-3.48 ± 5.07	5
500 nM	3.64 ± 4.61	7.74 ± 1.57	6	-9.21 ± 10.4	-8.51 ± 8.54	4
5 µM	2.86 ± 3.47	8.25 ± 3.6	6	-14.6 ± 8.18	-18.9 ± 6.31	5
50 µM	2.15 ± 9.73	0.626 ± 5.05	3	-24.4 ± 9.60	-27.9 ± 8.09	5
5 mM	-46.2 ± 3.01	-41.1 ± 12.1	3	-50.0 ± 5.94	-53.0 ± 6.92	5
aCSF	8.91 ± 19.8	3.02 ± 16.4	4	-39.1 ± 6.79	-39.6 ± 5.53	5

When peptides were applied in the concentration of 5 mM, a marked decreased of fEPSP slopes and amplitudes were recorded. While the inhibitory effect of KTP-NH_2 (5 mM) was partially washed out by aCSF solution, the effect of the KTP (5 mM) was fully reverted for levels of synaptic transmission higher than the initial basal levels.

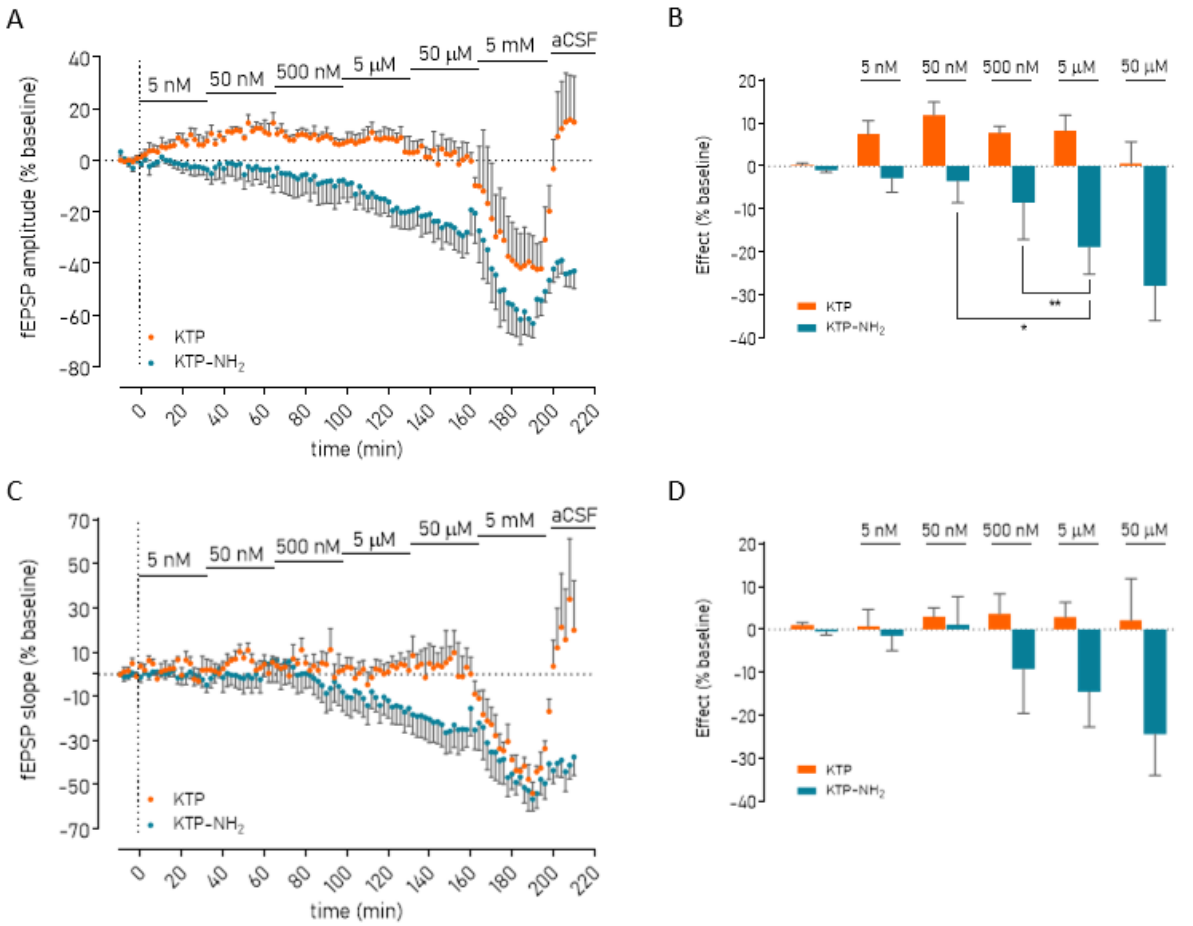

Figure 9. KTP and KTP-NH_2 had a concentration-dependent effects in hippocampal basal synaptic transmission. The averaged time courses changes in field excitatory postsynaptic potential (fEPSP) amplitude **(A)** and slope **(C)**, as % baseline, recorded from adult C57BL/6J male mice acute hippocampal slices. Recordings were measured during slices perfusion of oxygenated aCSF solutions with successfully higher concentrations of either Kyotorphin (KTP, orange points) or Amidated-Kyotorphin (KTP-NH_2, blue points) peptides, ranging from 5 nM to 5 mM, and then washout with aCSF solution. Bar chart depicting the effect of KTP (orange bars) and KTP-NH_2 (blue bars), regarding the different concentration superfused, ranging between 5 nM and 50 µM (% baseline average changes in fEPSP amplitude **(B)** and slope **(D)** at the last 10 min of a total of 32 min). Regarding KTP-NH_2, statistical analysis using Mixed-effects model followed by Tukey's multiple comparisons test revealed differences in fEPSP amplitude between 50 nM *vs*. 5 µM (n = 5), and 500 nM *vs*. 5 µM (n = 4-5), on KTP-NH_2 effect upon. * $p < 0.05$, ** p-value ≤ 0.01. Data are represented as mean ± SEM.

Since peptides physiological concentrations are usually within a nanomolar scale (Hökfelt et al., 2003), 50 nM was the concentration chosen to be use for KTP and KTP-NH_2 in the following experiments. Statistical differences were found between the effect in the averaged fEPSP amplitude of 50 nM KTP (from baseline to 500 nM; $p < 0.05$, Mixed-effects model followed by Dunnett's multiple comparisons test; $n = 6$).

3.4.2. KTP and KTP-NH_2 did not affect synaptic transmission efficiency

The effects of both peptides upon synaptic transmission efficiency were evaluated through I/O recordings (see Figure 8 (E)). Briefly, evoked fEPSP were recorded in CA1 hippocampal area of acute slices prepared from adult C57BL/6J male mice, superfused with oxygenated aCSF (control), or with either 50 nM KTP or 50 nM KTP-NH_2. Figure 10 includes both averaged fEPSP slope (A) and averaged PSFV amplitude (B) *versus* stimulus intensity. Firstly, the amplitude of the PSFV correlates with the number of stimulated fibers and informs about axonal excitability. Secondly, the slope of fEPSP correlates with the activation of postsynaptic receptors, which is triggered by the release of presynaptic neurotransmitters and informs about the level of postsynaptic activation (Burke, 1987).

No statistical differences ($p \geq 0.05$, one-way ANOVA; $n = 4$-7) were observed between conditions when comparing the maximal value obtained through extrapolation upon 1) nonlinear fitting of the fEPSP slope, and the stimulus intensity (control: 3.19 ± 0.492 mV/ms; KTP: 2.15 ± 0.432 mV/ms; KTP-NH_2: 2.29 ± 0.430 mV/ms; Figure 10 (C)), and 2) nonlinear fitting of the PSFV amplitude and stimulus intensity (control: 1.45 ± 0.213 mV; KTP: 0.961 ± 0.135 mV; KTP-NH_2: 1.01 ± 0.220 mV; Figure 10 (D)). Despite the slightly decrease observed for higher stimulus intensity in both fEPSP slope and PSFV amplitude induced by peptides presence, that can be better perceived when fEPSP slope averages were plotted against PSFV amplitude averages were plotted (Figure 10 (E)), the peptides presence did not impact synaptic transmission efficiency.

3.4.3. Long-exposure to KTP impaired θ-burst-induced LTP magnitude

Synaptic plasticity was evaluated through θ-burst LTP-induction in hippocampal CA1 area of acute slices prepared from adult C57BL/6J male mice (Figure 11). Slices were superfused with aCSF (Control), and with KTP or KTP-NH_2 (50 nM) during fEPSP recordings (acute-exposure, Figure 8 (D)), or were pre-incubated for 3 hours with the similar solutions and fEPSP recorded during aCSF superfusion (long-exposure, Figure 8 (F)).

After slices stabilization (baseline), a θ-burst LTP (3x3) was induced, as a synaptic correlate of the basic mechanisms involved in memory and learning processes (Bliss and Collingridge, 1993), and LTP magnitude was assessed as the average fEPSP slopes obtained between 50 and 60 min after LTP induction. No statistical differences were found between the acute-

exposure effect of both peptides on LTP magnitude when compared to control condition (control: 32.8 ± 4.50, n = 13; KTP: 21.0 ± 5.58, n = 8; KTP-NH_2: 29.2 ± 16.4, n = 5; $p \geq 0.05$, one-way ANOVA; n = 5-13; Figure 11 (D)). However, slices pre-incubated with KTP (50 nM) had a significant decreased LTP magnitude when compared to control condition (KTP: -14.9 ± 8.52 *vs.* control: 38.0 ± 8.60, $p < 0.05$, one-way ANOVA with Dunnett's multiple comparisons test; n = 6-11; Figure 11 (H)), but no significant differences were found in slices pre-incubated with KTP-NH_2 (50 nM) (KTP-NH_2: 17.7 ± 7.79, n = 6).

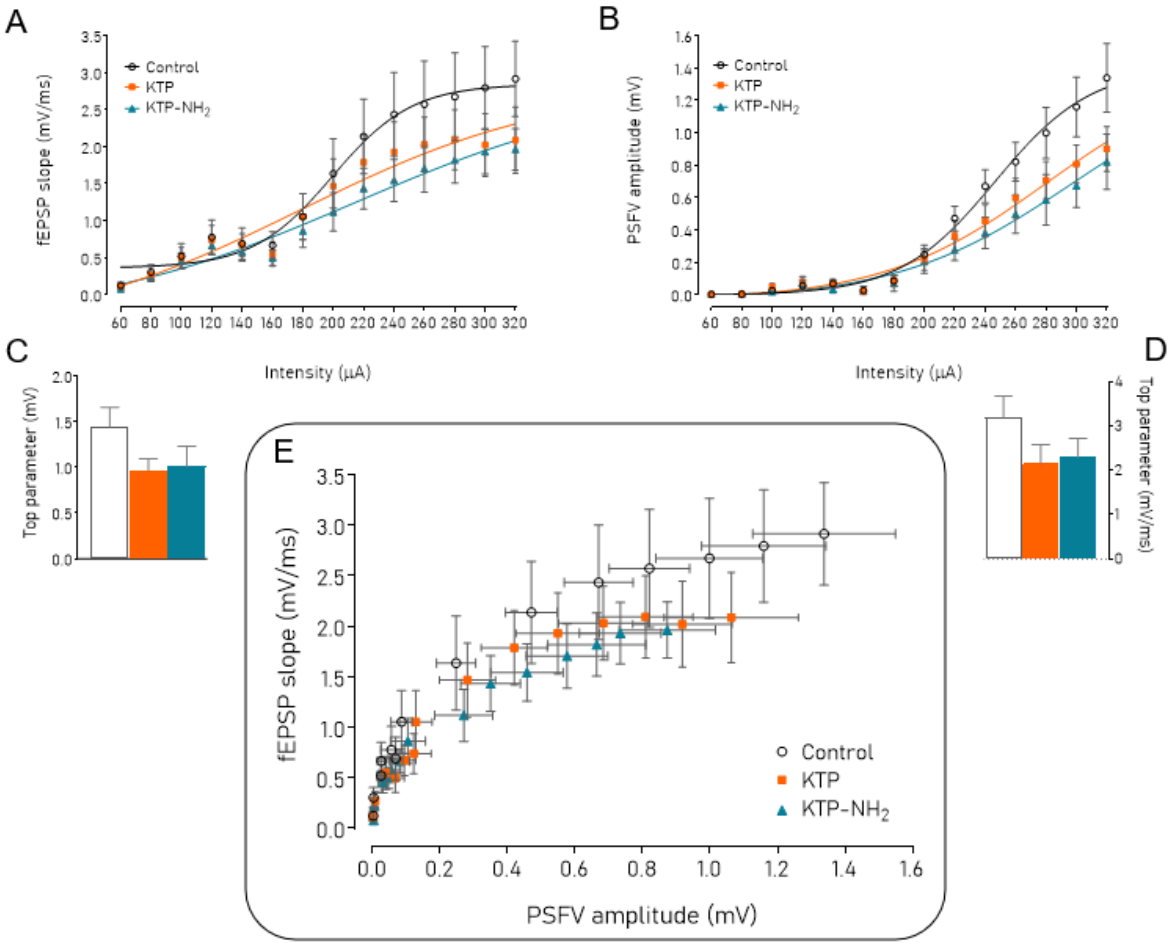

Figure 10. Neither KTP nor KTP-NH_2 affected hippocampal synaptic transmission efficiency. Input/Output (I/O) curves were plotted as **(A)** field excitatory postsynaptic potential (fEPSP) slope, or **(B)** presynaptic fiber volley (PSFV) amplitude, *versus* stimulation intensities (60 – 320 µA), recorded from adult C57BL/6J male mice acute hippocampal slices. These recordings occurred during the perfusion of oxygenated aCSF solution alone (control, black points), or with either 50 nM KTP (orange squares) or 50 nM KTP-NH_2 (blue triangles). Histograms depicting the maximum value (top parameter) obtained through extrapolation upon nonlinear I/O curves fitting, using either **(C)** fEPSP slope, or **(D)** PSFV amplitude, *versus* stimulation intensities, to compare KTP (orange bars), or KTP-NH_2 (blue bars) acute-exposure effect, with control condition (white bars). No statistical differences were found using one-way ANOVA (n = 4-7). **(E)** I/O curves represented as fEPSP slope *versus* PSFV amplitude. Data are represented as mean ± SEM.

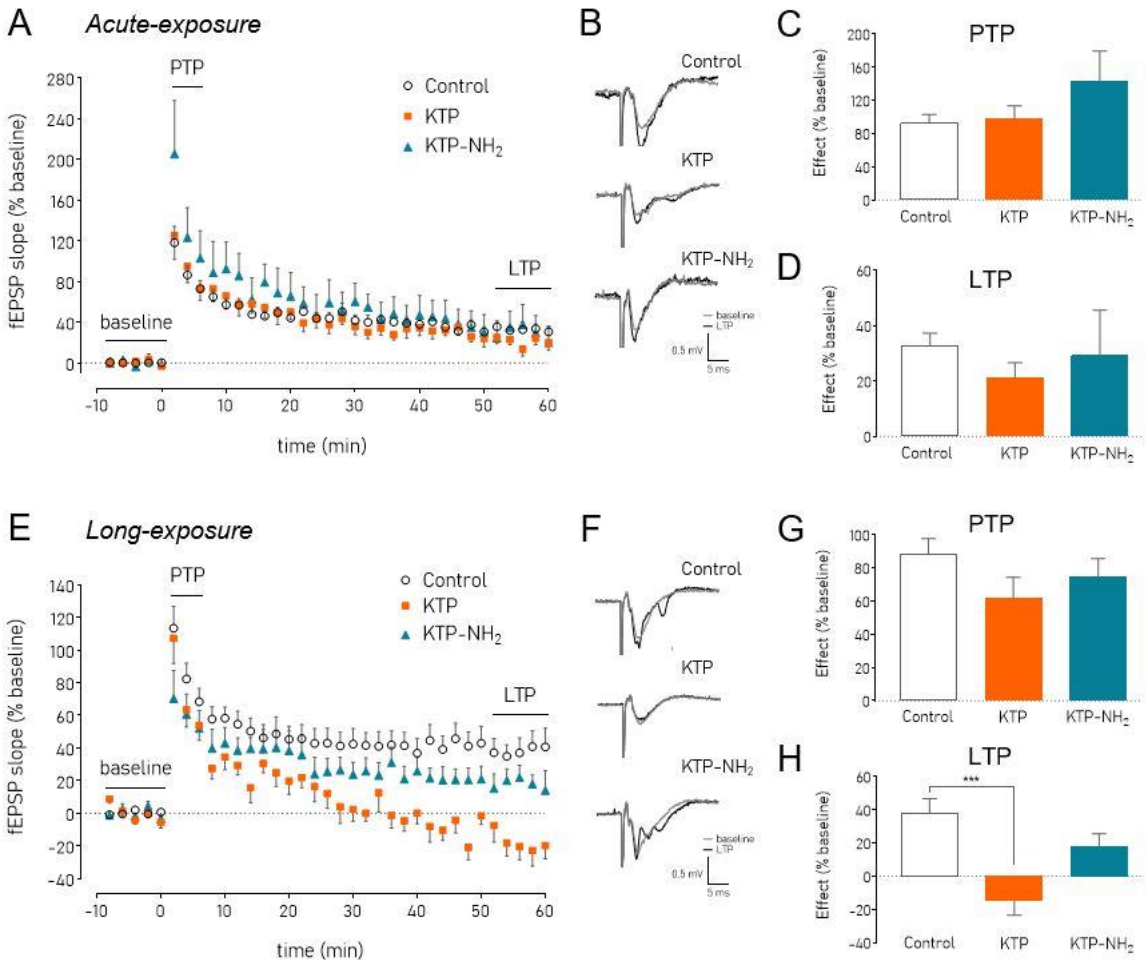

Figure 11. KTP long-exposure, but not KTP-NH_2, decreased θ-burst-induced LTP magnitude. The averaged time courses changes in field excitatory postsynaptic potential (fEPSP) slope (% baseline) induced by a θ-burst stimulation in adult C57BL/6J male mice acute hippocampal slices, during the acute perfusion **(A)** of oxygenated aCSF solution alone (control, black points), or with either 50 nM KTP (orange squares) or 50 nM KTP-NH_2 (blue triangles), or using slices pre-exposure to the same solutions for 3h **(E)**. **(B, F)** Tracings from representative experiments. For each condition, fEPSP tracings recorded at baseline (baseline, grey line) and after θ-burst-induced LTP (LTP, black line) from the same slice are showing overlaid. Bar chart depicting the control (white bars), and KTP (orange bars), or KTP-NH_2 (blue bars) peptides effect on PTP (**C** and **G**) or LTP magnitude (**D** and **H**), as the fEPSP slope, as % baseline, between 0-6 min, or between 50-60 min, after θ-burst LTP induction, respectively. A significant decrease was only found for LTP magnitude on slices pre-exposure to KTP, when compared to control (one-way ANOVA with Dunnett's multiple comparisons test; H). *** p-value ≤ 0.001. Data are represented as mean ± SEM.

3.4.4. KTP and KTP-NH_2 did not affect short-term plasticity

To evaluate the impact of both peptides on short-term plasticity, we assessed their effect upon post-tetanic potentiation (PTP, Figure 11 (C and G)) and paired-pulse facilitation (PPF, Figure 12). These are short-transient changes that occur at the presynaptic neuron and increase the probability of neurotransmitter releasing in an exclusive Ca^{2+}-dependent mechanism (Zucker and Regehr, 2002; Korogod et al., 2007).

PTP was assessed as the average fEPSP slopes obtained in the first 6 min (Habets *et al.*, 2007), after the already described hippocampal θ-burst-induced LTP protocol (Figure 8 (D)). The effects of peptides acute-exposure (control: 92.6 ± 10.3, n = 13; KTP: 97.6 ± 16.0, n = 8; KTP-NH_2: 144 ± 35.8 n = 5; $p > 0.05$, one-way ANOVA; n = 5-13; Figure 11 (C)), or long-exposure (control: 88.0 ± 9.87, n = 11; KTP: 74.5 ± 11.3, n = 6; KTP-NH_2: 61.9 ± 12.5, n = 6; Figure 11 (G)), showed no statistical differences when compared with control conditions ($p \geq 0.05$, one-way ANOVA; n = 5-13).

To assess the paired Ca^{2+}-mediated facilitation, a PPF protocol, with successively higher interstimuli intervals, ranging from 10 to 100 ms (see Figure 8 (D)), was applied in hippocampal CA1 area of acute slices prepared from adult C57BL/6J male mice. PPF were recorded in slices superfused with aCSF alone (Control), and with KTP or KTP-NH_2 (50 nM). Facilitation was evaluated as the ratio between the second and the first evoked fEPSP slope within the same electrical stimulation range. No statistical differences were found when in the presence of peptides ($p > 0.05$, two-way ANOVA; n = 4-9; Figure 12). However, independent significant differences ($p < 0.05$, two-way ANOVA with Tukey's multiple comparisons test; n = 4-9) were found within interstimuli intervals, and within conditions. In fact, KTP-NH_2 effect for 10 ms interstimuli interval is significant lower when compared to control (Figure 12, § symbols). Significant differences between interstimuli intervals effects were found for 1) control condition, between 10 ms and all the other interstimuli intervals; 2) KTP (50 nM), between 10 and 50 ms, and 10 and 70 ms interstimuli intervals; and, 3) KTP-NH_2 (50 nM), between 10 ms and all the other interstimuli intervals and also between 20 and 50 ms, and 20 and 70 ms interstimuli intervals (Figure 12, * symbols).

Additionally, when considering only the 50 ms of interstimuli interval of all conditions, no statistical differences were found when compared to control (p-value ≥ 0.05, one-way ANOVA, n = 4-9). Table 2 summarized the averaged PPF ratio (fEPSP2/fEPSP1), considering peptides presence and interstimuli intervals.

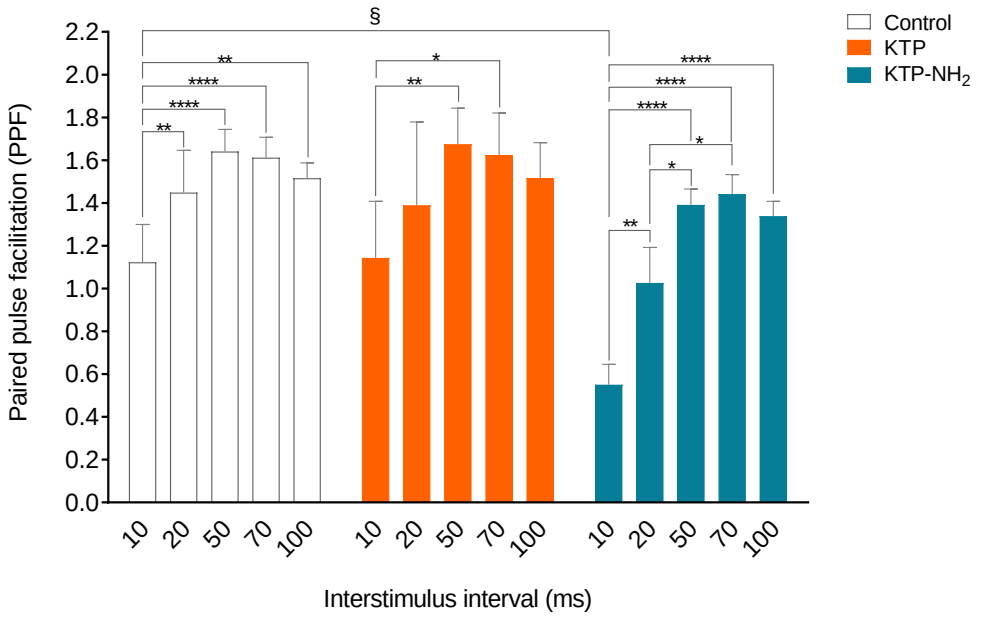

Figure 12. Acute-exposure of either KTP or KTP-NH_2 did not affect hippocampal short-term facilitation. Paired-pulse facilitation (PPF), with consecutively higher interstimuli intervals (10 to 100 ms), were recorded from adult C57BL/6J male mice acute hippocampal slices, during the perfusion of oxygenated aCSF solution alone (control, white bars), or with either 50 nM KTP (orange bars) or 50 nM KTP-NH_2 (blue bars) peptides. Bar graph presents the averaged PPF ratio, measured between the second and the first field excitatory postsynaptic potential (fEPSP) slope signals recorded. Statistical analysis using two-way ANOVA (n = 4-9) did not found differences when considered peptides presence (condition) as the main effect, but differences were found between interstimuli intervals within conditions (*, simple effects within interstimuli intervals) and across conditions (§, simple effects within condition). * p-value ≤ 0.05, ** p-value ≤ 0.01, *** p-value ≤ 0.001, **** p-value ≤ 0.0001, § p-value ≤ 0.05. Data are represented as mean ± SEM.

Table 2. Short-term facilitation evaluated with paired-pulse facilitation upon KTP and KTP-NH_2 effects. Averaged PPF ratios, measured between the second and the first recorded field excitatory postsynaptic potential (fEPSP) slope, considering peptides presence and interstimuli intervals. Values are presented as mean ± SEM.

	Control	KTP	KTP-NH_2
10	1.12 ± 0.177	1.14 ± 0.264	0.550 ± 0.096
20	1.45 ± 0.197	1.40 ± 0.389	1.03 ± 0.165
50	1.64 ± 0.103	1.68 ± 0.168	1.39 ± 0.074
70	1.61 ± 0.094	1.62 ± 0.197	1.44 ± 0.091
100	1.52 ± 0.072	1.52 ± 0.165	1.34 ± 0.069

3.4.5. KTP and KTP-NH_2 did not affect synaptosomal glutamate release

Since glutamate release is directly related to presynaptic activity (Nicholls, 1998), we evaluated whether this process could be modulated by KTP or KTP-NH_2 in synaptosomal fraction of mice hippocampus. As such, the ratio between S1 and S2 peaks of [^{3}H]glutamate fractional release (Figure 13 (A)) was analyzed for each condition. No statistical differences were found between conditions when compared to control condition (control: 0.65 ± 0.125; KTP: 0.95 ± 0.290; KTP-NH_2: 0.607 ± 0.212; ≥ 0.05, one-way ANOVA; n = 4-7; Figure 13 (B)). These results shown that neither 50 nM KTP nor 50 nM KTP-NH_2 affected glutamate release from hippocampal synaptosomes.

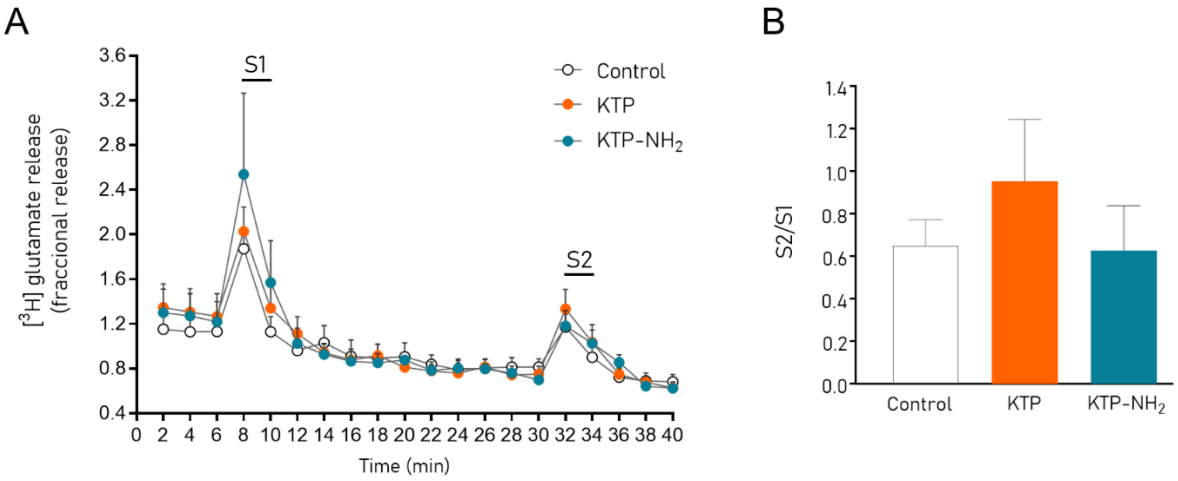

Figure 13. Neither KTP nor KTP-NH_2 affected synaptosomal glutamate release. (A) Average fractional release of [^{3}H]glutamate release from hippocampal synaptosomes prepared from C57BL/6J adult male mice tissue. Both first stimulation (S1) and second (S2) peaks were analyzed as the average of the indicated 2 points and normalized to the respective baseline, which included the average of the precedent and succeeding 3 points. In control condition, both S1 and S2 were obtained using the with the **(B)** Bar chart depicting the ratio between S2 and S1 shown no statistical differences between peptides perfusion when compared to control condition (p-value ≥ 0.05, one-way ANOVA, n = 5). Data are represented as mean ± SEM.

3.4.6. KTP and KTP-NH_2 did not affect calcium homeostasis

To evaluate the impact of both peptides on calcium homeostasis, we measured variations in intracellular calcium concentrations ([Ca^{2+}]i) in cultured cortical neurons. Briefly, through calcium imaging, we recorded changes in [Ca^{2+}]i during 70 min, using Fura 2AM. A baseline period of 15 min was recorded and then, neurons were exposed to KTP or KTP-NH_2 (50 nM). After 40 min, ionomycin (2µM) was added, as a positive control, and recordings were obtained for an additional 15 min period (Figure 14 (A)).

Peptides effects were assessed by the ratio (%) between the average of the normalized calcium fluorescence ratio (340/380 nm) obtained considering two recording periods: 10-15 min (5, 6 and 7th points, baseline in Figure 14 (A)), and 47.5-52.5 min (20, 21 and 22nd points, effect in Figure 14 (A)) after the recordings started. These results showed no detectable variations when peptides were added when compared to control condition (control: 139.10% ± 10.474; KTP: 146.01% ± 9.1052; KTP-NH_2: 173.43% ± 29.574; ≥ 0.05, one-way ANOVA; n = 3-5; Figure 14 (B)). During these experiments, [Ca^{2+}]i levels were progressively increasing in neurons, probably due to hostile recordings conditions. However, adding ionomycin attested neurons viability allowing to measure their responsiveness when Ca^{2+} saturation was elicited, which also induced their eventual death (Morgan and Jacob, 1994).

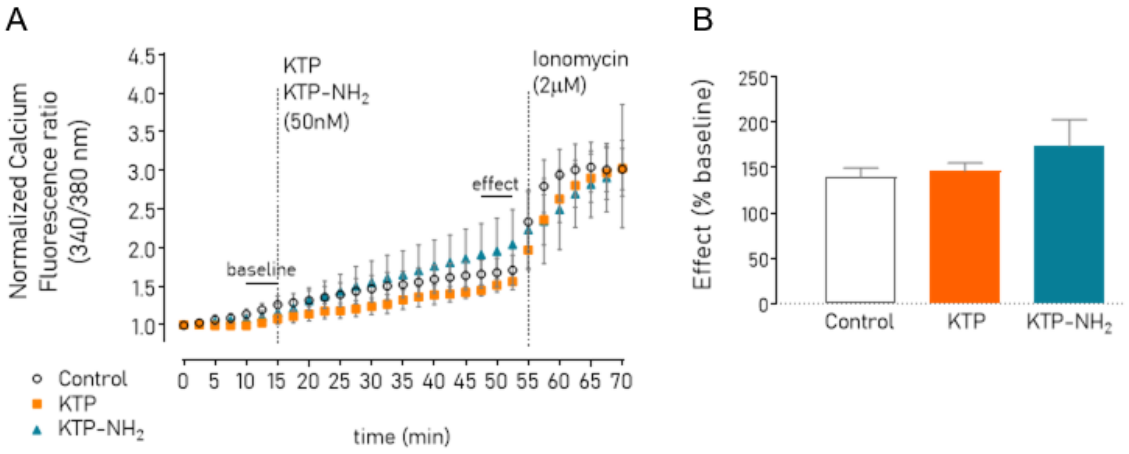

Figure 14. Neither KTP nor KTP-NH_2 affected neuronal calcium homeostasis. (A) Graph showing a 70 min time course of Ca^{2+}-dependent fluorescence recorded and averaged from FURA-2AM in primary neuronal cultures (DIV13). As indicated, 50 nM KTP or KTP-NH_2 were added at the 15th min and 2 µM of ionomycin was added at 55th min. Normalized calcium fluorescence ratio (340/380) were obtained using several reactive cells for each recording. To evaluate the effect (%) of both peptides, the averaged effect (3 indicated points: 20-22nd) was normalized with the averaged baseline (3 indicated points: 5-7th) for each condition. **(B)** Bar chart depicting peptides effect (%) in normalized calcium homeostasis from each condition. Statistical analysis using one-way ANOVA did not indicate significant differences between conditions (n = 5-6). Data are represented as mean ± SEM.

3.4.7. KTP and KTP-NH_2 prevented the Aβ-induced decrease in spine density of primary neuronal cultures without causing toxicity

To address the molecular synaptic mechanisms involved in the neuroprotective action of KTP-NH_2 and to compare the putative differences between its endogenous molecule - the KTP dipeptide, we evaluated the effect of both peptides upon spine density of primary neuronal cultures. Cells were treated for 24h with KTP or KTP-NH_2 (50 nM), in the presence or absence of $A\beta_{25-35}$ peptide (25 µM).

By conjugating MAP2 (red) and Phalloidin (green) labelling in immunocytochemical assays, the dendritic protrusions were identified (yellow). This method allowed to evaluate the effect of both peptides on the number of dendritic spines (Figure 15 (A)). The representative segments of 10 µm of counted dendrites for each analyzed condition are illustrated in Figure 15 (B). As expected, $A\beta_{25-35}$ action significantly decreased the number of dendritic protrusions when compared the control condition ($A\beta_{25-35}$: 6.54 ± 0.324 *vs.* control: 8.06 ± 0.306; $p < 0.05$, two-way ANOVA with Tukey's multiple comparisons test; n = 6), which was prevented when cultures were co-treated with 50 nM KTP-NH_2 ($A\beta_{25-35}$ + KTP-NH_2: 9.60 ± 0.299, n = 6; Figure 15 (C)). In fact, co-treatment with KTP-NH_2 upon Aβ-induced insult significantly increased the number of dendritic protrusions when compared to control condition ($p < 0.05$, two-way ANOVA with Tukey's multiple comparisons test; n = 5-6). Interestingly, co-treatment with 50 nM KTP also prevented the Aβ-induced impairment in the number of dendritic protrusions ($A\beta_{25-35}$ + KTP: 9.08 ± 0.386 *vs.* control: 8.06 ± 0.306; $p > 0.05$, two-way ANOVA with Tukey's multiple comparisons test; n = 6). In addition, KTP alone (KTP: 7.17 ± 0.786; n = 6) did not significantly alter dendritic protrusions when compared to both control and $A\beta_{25-35}$ condition, but KTP-NH_2 alone significantly increase them when compared to control condition (KTP-NH_2: 8.37 ± 0.167 *vs.* control: 8.06 ± 0.306; $p < 0.05$, two-way ANOVA with Tukey's multiple comparisons test; n = 5-6).

To assess the toxicity effect of both peptides, two viability assays were performed using primary neuronal cultures (DIV13) incubated with 25 µM $A\beta_{25-35}$ alone or with 50 nM KTP or 50 nM KTP-NH_2 for 24h: the MTT assay, and the cell counting kit-8 (CCK8) assay (Figure 16). The results showed no significant differences between all conditions for MTT assay (control: 0.87 ± 0.179; $A\beta_{25-35}$: 0.73 ± 0.160; KTP: 0.86 ± 0.146; $A\beta_{25-35}$ + KTP: 0.76 ± 0.115; KTP-NH_2: 0.81 ± 0.165; $A\beta_{25-35}$ + KTP-NH_2: 0.71 ± 0.121; $p > 0.05$, two-way ANOVA, n = 5; Figure 16 (A)).

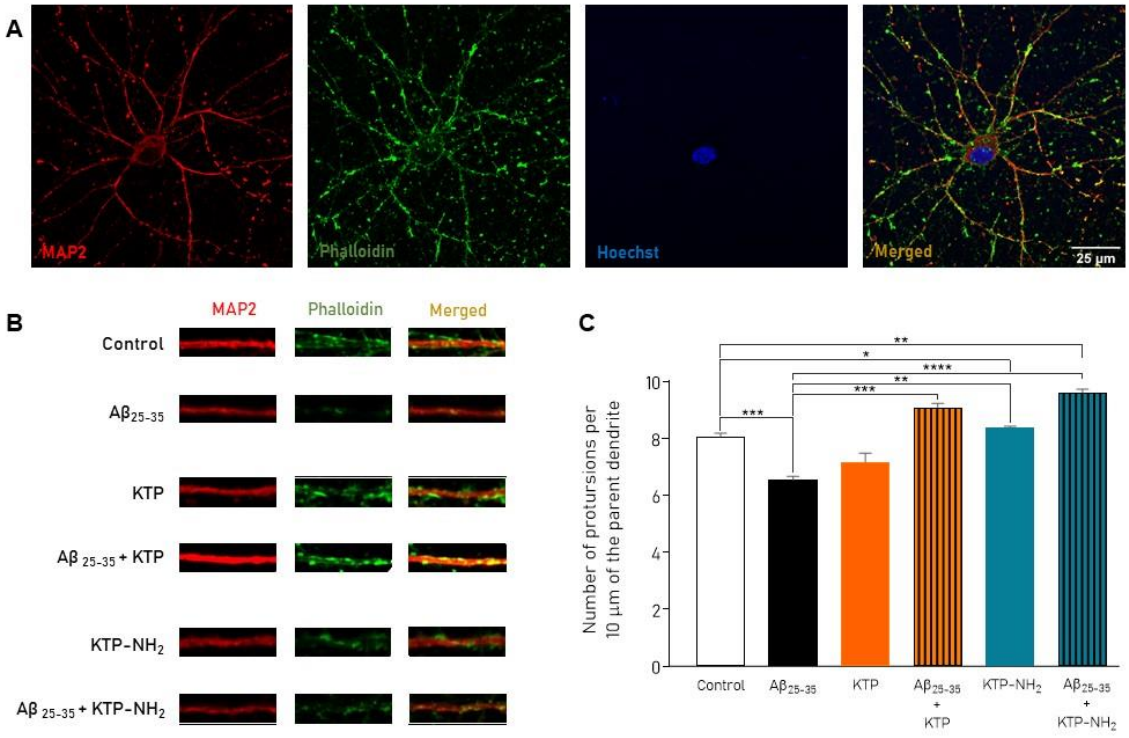

Figure 15. Co-incubation with KTP or KTP-NH_2 prevented Aβ incubation-induced impairments in dendritic spine of primary neuronal cultures. (A) Representative image of an untreated neuron (control) obtained from primary neuronal cultures. Primary neuronal cultures (DIV13) were incubated with 25 µM $Aβ_{25-35}$ and/or with 50 nM KTP or KTP-NH_2 for 24h. MAP2 (red) specifically labels neurons, while phalloidin (green) labels F-actin. The merge between both labels (yellow) allows the identification of dendritic protrusions. To evaluate spine density, the number of protrusions *per* 10 µm of the parent dendrite with a distance of 25 µm from the cell body were counted (3 parent dendrites *per* neuron, 6 neurons *per* condition). **(B)** Treatment effects on synaptic density (10 µm). **(C)** Bar chart depicting spine density as the number of protrusions from each condition. Statistical analysis using two-way ANOVA followed by Tukey's multiple comparisons test indicates a significant difference between conditions (n = 5-6). While 25 µM $Aβ_{25-35}$ treatment ($Aβ_{25-35}$) diminished the number of protrusions in cortical neurons, 50 nM KTP or KTP-NH_2 co-treatment ($Aβ_{25-35}$ + KTP and $Aβ_{25-35}$ + KTP-NH_2, respectively) restored spine density. In addition, 50 nM KTP or KTP-NH_2 treatment alone did not impact spine density. * $p < 0.05$, ** $p \leq 0.01$, *** $p \leq 0.001$, **** $p \leq 0.0001$. Data are represented as mean ± SEM. These results were partially presented in our previous work (Belo et al., 2020).

On the other hand, although the presence of $Aβ_{25-35}$ appeared as a major source of variability when CCK8 assay results were analyzed using a two-way ANOVA (control: 0.60 ± 0.065; $Aβ_{25-35}$: 0.50 ± 0.102; KTP: 0.54 ± 0.111; $Aβ_{25-35}$ + KTP: 0.45 ± 0.153; KTP-NH_2: 0.55 ± 0.120; $Aβ_{25-35}$ + KTP-NH_2: 0.50 ± 0.083; n = 4; $p < 0.05$ (for Aβ), two-way ANOVA; Figure 16 (B)), the post-hoc tests applied were not powerful enough to discriminate the statistical significant differences between specific conditions.

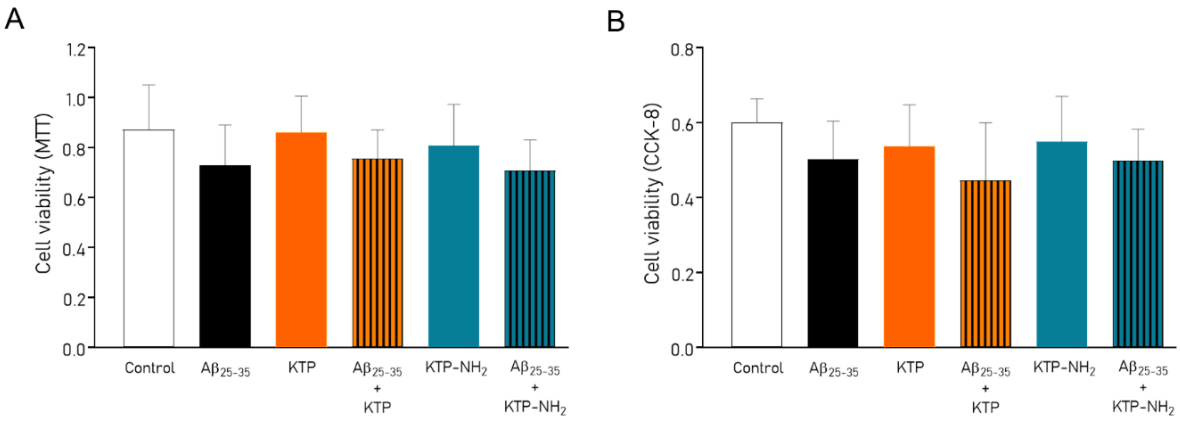

Figure 16. Neither Aβ nor KTP or KTP-NH_2 presented a cytotoxic effect in cortical cultured neurons. Primary neuronal cultures (DIV13) were incubated with 25 μM $Aβ_{25-35}$ and/or with 50 nM KTP or KTP-NH_2 for 24h. **(A)** Bar chart depicting cell viability measured using MTT assays (n = 5). No statistically significant differences were found between conditions using a repeated-measures two-way ANOVA (n = 5). **(B)** Bar chart depicting cell viability measured using CCK-8 assays (n = 4). Statistically analysis using a repeated-measures two-way ANOVA shown a significant difference explained by $Aβ_{25-35}$ presence. Data are represented as mean ± SEM.

Therefore, as expected from previously molecular results regarding spine density, neither 50 nM KTP or KTP-NH_2 incubated for 24h were sufficient to compromise cortical cultured neurons viability. Interestingly, despite the reported Aβ-induced impairments on dendritic spines, in the same controlled environment, $Aβ_{25-35}$ did not affect neurons overall metabolic activity, suggesting that the achieved Aβ-induced toxicity level and time of incubation were also not enough for a significant decreasing on cell viability.

3.4.8. KTP-NH_2, but not KTP, was able to prevent Aβ-induced impairment in LTP magnitude

Since the neuronal spine density has been associated with synaptic reinforcement during hippocampal long-term potentiation (LTP) (Luscher and Malenka, 2012; Toni et al., 1999), we assessed the effect of both KTP and KTP-NH_2 (50 nM) upon hippocampal θ-burst-induced LTP to corroborate the neuroprotective results observed in immunocytochemistry assays. Here, fEPSP were recorded in CA1 hippocampal area of acute slices prepared from adult C57BL/6J male mice, pre-incubated for 3h with $Aβ_{olig}$ (200 nM), a known to be toxic conformational arrangement of Aβ (Giuffrida et al., 2009), and co-incubated with either KTP or KTP-NH_2 (50 nM) (Figure 8 (F)).

As expected, LTP magnitude was significantly decreased in Aβ condition (control: 32.1 ± 5.66 *vs.* Aβ: -4.51 ± 6.53, $p < 0.05$, two-way ANOVA with Tukey's multiple comparisons test; n = 5-9; Figure 17 (B)).

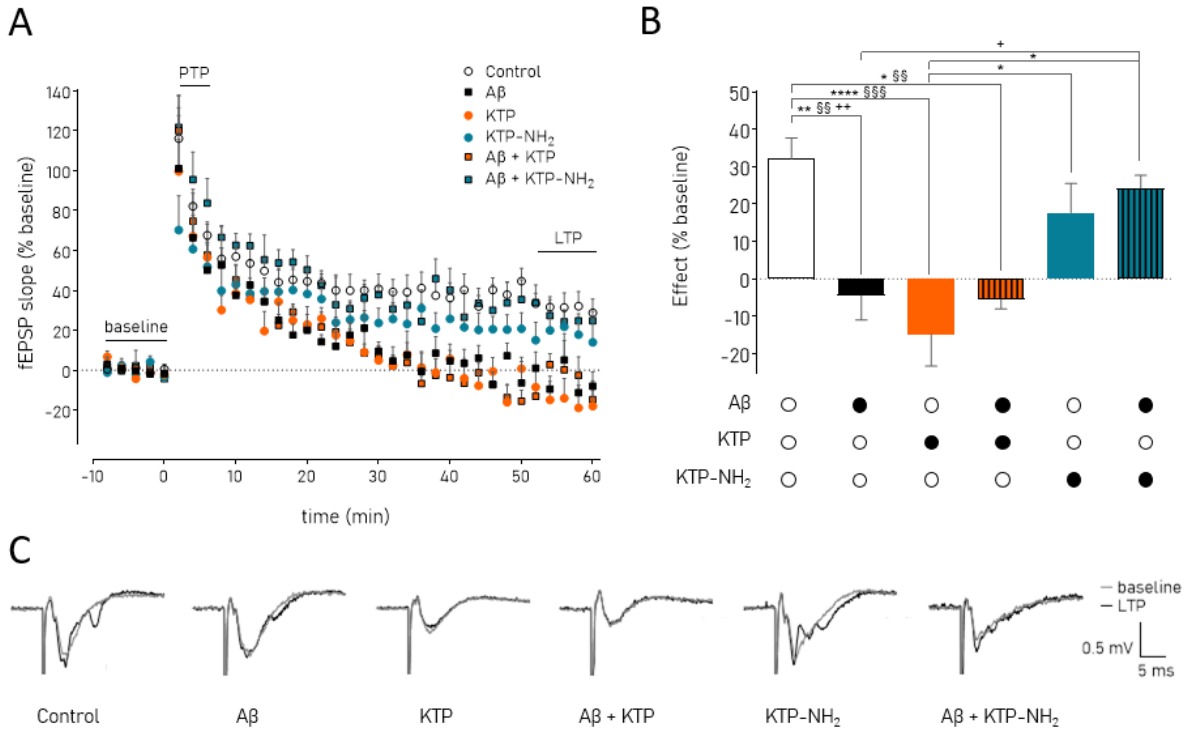

Figure 17. Incubation with KTP-NH_2 (but not with KTP) reduces the impact of Aβ on LTP magnitude. (A) The averaged time courses changes in field excitatory postsynaptic potential (fEPSP) slope (% baseline) induced by a θ-burst stimulation in C57BL/6J adult male mice hippocampal slices with a pre-exposure of 3 h to aCSF solution (Control, n = 9) with 200 nM $Aβ_{olig}$ (Aβ, n = 5), 50 nM KTP (KTP, n = 6), 50 nM KTP-NH_2 (KTP-NH_2, n = 6), 200 nM $Aβ_{olig}$ and 50 nM KTP (Aβ + KTP, n = 5), or 200 nM $Aβ_{olig}$ and 50 nM KTP-NH_2 (Aβ + KTP-NH_2, n = 5). **(B)** Bar chart depicting the effect on LTP magnitude (% average changes in fEPSP slope at 50-60 min normalized to the defined baseline of 10 min immediately before θ-burst stimulation) regarding each group under study (Control, Aβ, KTP, Aβ + KTP, KTP-NH_2, and Aβ + KTP-NH_2). Statistical analysis using two-way ANOVA followed by Tukey's multiple comparisons test indicates a significant difference between all the conditions (n = 5-9). **(C)** Tracings from representative experiments. For each condition, fEPSP tracings recorded at baseline (baseline, grey line) and after θ-burst-induced LTP (LTP, black line) from the same slice are showing overlaid. * or $^{+}$ $p < 0.05$; **, §§ or $^{++}$ $p \leq 0.01$, §§ $p \leq 0.001$; **** $p \leq 0.0001$. Data are represented as mean % ± SEM. These results were already partially presented in Figure 11 regarding peptides long-exposure effects.

Interestingly, LTP magnitudes measured in slices pre-incubated with KTP alone (KTP: -14.9 ± 8.52, n = 6), or in the presence of Aβ (Aβ + KTP: -5.50 ± 2.52, n = 5) were significantly decreased when compared to control condition ($p < 0.05$, two-way ANOVA with Tukey's multiple comparisons test; n = 5-9). On the other hand, LTP magnitudes measured in slices pre-incubated with KTP-NH_2 (KTP-NH_2: 17.7 ± 7.79, n = 6), and co-incubated with Aβ (Aβ + KTP-NH_2: 24.2 ± 3.50, n = 5) were not significantly different from control condition ($p \geq 0.05$,

two-way ANOVA with Tukey's multiple comparisons test; n = 5-9), but they were significantly higher when compared to LTP magnitude obtained with KTP incubation alone ($p < 0.05$, two-way ANOVA with Tukey's multiple comparisons test; n = 5-6; * symbols in Figure 17 (B)).

Moreover, when these effects were independently analyzed according to peptides presence (§ and $^{+}$ symbols for KTP and KTP-NH_2, respectively, in Figure 17 (B)), the results cleared revealed that KTP action was not able to prevent Aβ-induced LTP impairments in slices co-incubated with Aβ (Aβ + KTP *vs.* Aβ, $p \geq 0.05$, two-way ANOVA with Tukey's multiple comparisons test; n = 5-6; § symbols in Figure 17). On the contrary, co-incubation with KTP-NH_2 was able to prevent Aβ-induced impairments on LTP (Aβ + KTP-NH_2 *vs.* Aβ, $p < 0.05$, two-way ANOVA with Tukey's multiple comparisons test; n = 5; $^{+}$ symbols in Figure 17). In summary, although these results clearly indicate that KTP-NH_2 prevented Aβ-induced impairments on LTP, without affecting LTP itself, KTP does not have this action.

3.4.9. KTP_{ant} was able to antagonize the KTP-NH_2 neuroprotective effect against Aβ in LTP magnitude

To evaluate if the KTP-NH_2 neuroprotective effect on synaptic plasticity could be affected by the presence of the KTP_{ant} dipeptide, LTP magnitude was evaluated, as previously described. Hippocampal slices were pre-incubated with KTP_{ant} (250 nM) 30 min before the incubation with the other peptides, and remain up until the end of the pharmacological treatments (Figure 8 (F)).

The statistical analysis comparing the effect between all conditions revealed that significant differences were mainly explained due to 1) the presence of Aβ, 2) the interaction between KTP-NH_2 and Aβ; and 3) the interaction between KTP-NH_2 and KTP_{ant} (Figure 18 (B)). As expected, the presence of Aβ alone caused a significant decrease in LTP magnitude when compared to control condition (p-value < 0.05, three-way ANOVA with Tukey's multiple comparisons test; n = 5-16). KTP_{ant} alone (KTP_{ant}: 31.3 ± 6.19) had no significant effect on LTP magnitude (KTP_{ant} *vs.* control, $p \geq 0.05$, three-way ANOVA with Tukey's multiple comparisons test; n = 4-16), and it was significantly different when compared to Aβ condition ($p < 0.05$, three-way ANOVA with Tukey's multiple comparisons test; n = 4-5). These findings are highlighted in Figure 18 (C).

When incubated 30 min *prior* to the co-incubation with Aβ and KTP-NH_2, KTP_{ant} significantly reduced LTP magnitude when compared to control condition (Aβ + KTP-NH_2 + KTP_{ant}: 9.35 ± 4.70; $p < 0.05$, three-way ANOVA with Tukey's multiple comparisons test, Figure 18 (B), and two-way ANOVA with Sidak's multiple comparisons test, Figure 18 (E); n = 6-16).

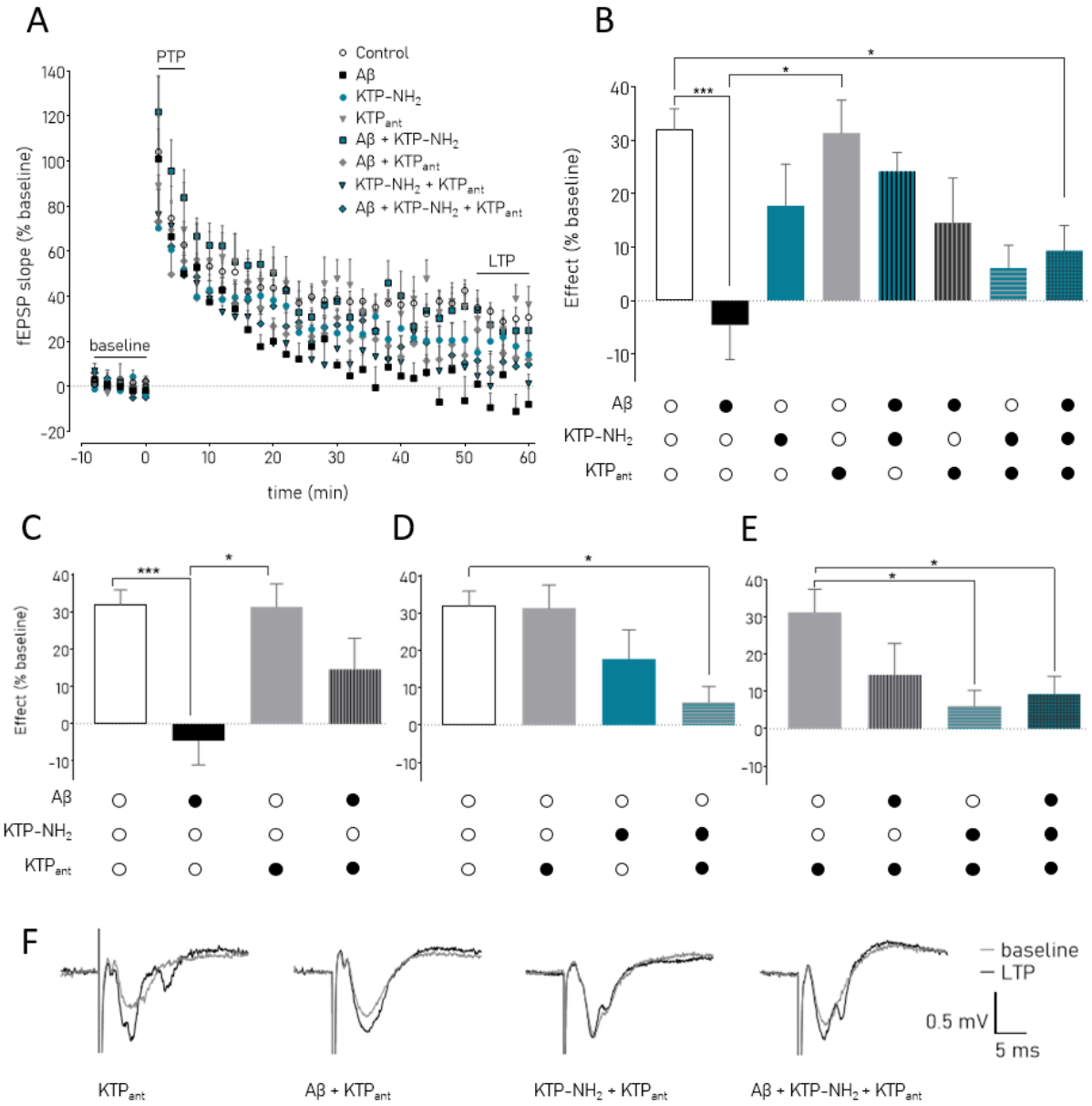

Figure 18. Pre-exposure to KTP_{ant} prevented the neuroprotective effect of KTP-NH_2 against Aβ-induced impairments upon LTP magnitude. (A) The averaged time courses changes in field excitatory postsynaptic potential (fEPSP) slope (% baseline) induced by a θ-burst stimulation in C57BL/6J adult male mice hippocampal slices with a pre-exposure of 30 min of 250 nM KTP_{ant} (KTP_{ant}, n = 4), and 3 h to aCSF solution (Control, n = 16) with 200 nM $Aβ_{olig}$ (Aβ, n = 5), 50 nM KTP-NH_2 (KTP-NH_2, n = 6), 200 nM $Aβ_{olig}$ and 50 nM KTP-NH_2 (Aβ + KTP-NH_2, n = 5), 200 nM $Aβ_{olig}$ and 50 nM KTP_{ant} (Aβ + KTP_{ant}, n = 4), 50 nM KTP-NH_2 and 50 nM KTP_{ant} (KTP-NH_2 + KTP_{ant}, n = 4), or 200 nM $Aβ_{olig}$ and 50 nM KTP-NH_2 and 50 nM KTP_{ant} (Aβ + KTP-NH_2 + KTP_{ant}, n = 6). **(B, C, D, E)** Bar chart depicting the effect on LTP magnitude (% average changes in fEPSP slope at 50-60 min normalized to the defined baseline of 10 min immediately before θ-burst stimulation) regarding each group under study (Control, Aβ, KTP-NH_2, KTP_{ant}, Aβ + KTP-NH_2, Aβ + KTP_{ant}, KTP-NH_2 + KTP_{ant}, Aβ + KTP-NH_2 + KTP_{ant}). Statistical analysis using a three-way ANOVA **(B),** or using a two-way ANOVA

(C, D, E), followed by Tukey's multiple comparisons test indicates a significant difference between all the conditions **(B, C, D)**, or followed by Sidak's multiple comparisons test indicates a significant difference between the control and all conditions **(E)**. **(F)** Tracings from representative experiments (KTP_{ant} conditions). For each condition, fEPSP tracings recorded at baseline (baseline, grey line) and after θ-burst-induced LTP (LTP, black line) from the same slice are showing overlaid. * $p < 0.05$, *** $p \leq 0.001$. Data are represented as mean ± SEM. These results were already partially presented in Figure 11 (long-exposure), and in Figure 17 (control, Aβ, KTP-NH_2 and Aβ + KTP-NH_2 conditions).

Furthermore, when KTP_{ant} was pre-incubated in slices that where then treated with KTP-NH_2 (KTP-NH_2 + KTP_{ant}: 6.12 ± 4.22), the magnitude of LTP was significant lower than in the control condition ($p < 0.05$, two-way ANOVA with Tukey's multiple comparisons test, Figure 18 (D), and with Sidak's multiple comparisons test, Figure 18 (E); n = 4-16). Moreover, despite the finding that LTP magnitude was higher when KTP_{ant} was incubated *prior* to Aβ addition (Aβ + KTP_{ant}: 14.6 ± 8.35, n = 4), than in slices incubated with Aβ only, LTP magnitude was neither different from Aβ, control, nor KTP-NH_2 conditions ($p \geq 0.05$, three-way ANOVA with Tukey's multiple comparisons test; n = 4-16). Although these controversial results point towards KTP_{ant} being able to antagonize the ability of KTP-NH_2 to protect LTP against Aβ, they need to be clarified. On one hand, KTP_{ant} alone had a preventive neuroprotective action against Aβ but, on the other hand, when added *prior* to KTP-NH_2 treatment, LTP magnitude was decreased which may indicate a crosstalk between KTP_{ant} and KTP-NH_2 mechanisms of action.

3.4.10. KTP and KTP-NH_2 did not prevent calpains activation

It is known that in AD calpains are overactivated as a consequence of hyperexcitability induced by Aβ peptide. Calpains are responsible for the cleavage of TrkB-FL, affecting BDNF-mediated role on synaptic plasticity through abolish in LTP and decrease neuronal spine density (Fonseca-Gomes et al., 2019; Jerónimo-Santos et al., 2015; Tanqueiro et al., 2018). As such, the effects of both KTP and KTP-NH_2 (50 nM) in the presence or absence of KTP_{ant} (250 nM) were assessed using calpain *in vitro* enzymatic assays in cortical homogenates (Figure 19).

The concomitant TrkB-FL cleavage and TrkB-ICD production, as well as the production of the calpain-cleaved 145 and 150 kDa α*II*-spectrin breakdown products (SBDP145 and SBDP150, respectively) allowed to assess calpain activation (Zhang et al., 2009). As such, the WB was performed with sample from calpain *in vitro* enzymatic reactions (Figure 19 (B)), and the densitometry analyses was quantified as the ratio between TrkB-ICD and TrkB-FL levels (Figure 19 (A)). These results revealed that, irrespectively of KTP_{ant} presence, neither KTP nor KTP-NH_2 were able to block calpain activation (p-value > 0.05, one-way ANOVA (conditions with m-calpain and $CaCl_2$), n = 4).

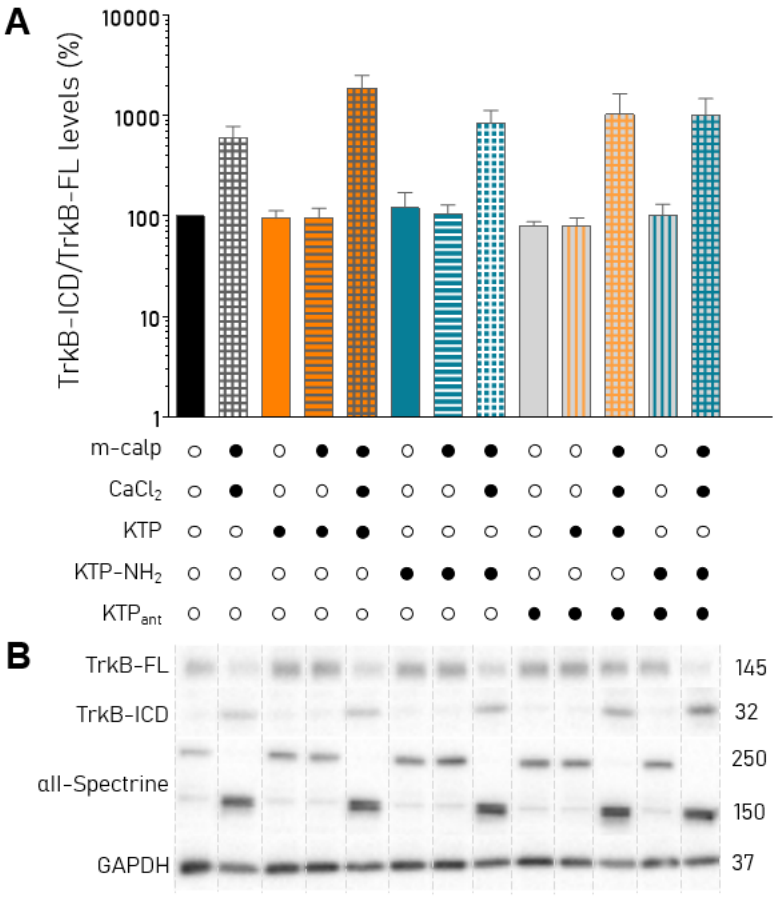

Figure 19. Neither KTP nor KTP-NH_2 prevented calpains activation or calpains-induced TrkB-FL cleavage. Calpain *in vitro* enzymatic assay was conducted using cortical homogenate samples treated with 50 nM KTP or KTP-NH_2 in the presence or absence of KTP_{ant}. As expected, calpain cleavage-activity only occurred in samples with the presence of both m-calp and $CaCl_2$. **(A)** Densiometric analysis of results obtain from western blotting of calpain enzymatic reaction samples as the ratio between TrkB-ICD and TrkB-FL levels. Data are represented as mean ± SEM. Statistical analysis using one-way ANOVA did not found significant differences between conditions with both m-calp and $CaCl_2$. **(B)** Representative immunoblots of TrkB-FL (145 kDa), TrkB-ICD (32 kDa), α*II*-spectrin (250 kDa), 150 kDa α*II*-spectrine breakdown product (SBDP150. 150 kDa), and GAPDH (37 kDa). GAPDH was used as a loading control.

3.5. Discussion

In the present work, we demonstrated significant differences between KTP and KTP-NH_2 actions, especially on their neuroprotective effect upon Aβ-mediated toxicity. More precisely, both peptides presented a recovering action on dendritic spines density in cortical cultured neurons when co-incubated with Aβ peptide, but only KTP-NH_2 was able to counteract Aβ-induced impairments on LTP evaluated in acute hippocampal slices.

Peptides are important regulators, acting as neurotransmitters among others, and their application is already recognized across all biomedical sciences (Santos et al., 2012). Previous studies revealed interesting neuroprotective actions regarding the application of KTP and its synthetic amidated-derivative, the KTP-NH_2. More specifically, KTP i.c.v injection ameliorated memory impairments in a sporadic AD rat model (Angelova et al., 2018), whereas KTP-NH_2 intraperitoneal treatment prevented cognitive symptoms induced in a cerebral hypoperfusion dementia model (Sá Santos et al., 2016), and in a Aβ-induced sporadic AD model (Belo et al., 2020). Nevertheless, none of these studies compared whether KTP and KTP-NH_2 dipeptides have similar effects on the CNS.

Within this work, we profiled the effects of KTP and KTP-NH_2 upon neuronal functions that might be modulated by their action or be impaired by Aβ peptide. Aβ peptide is a neurotoxic agent, and a well-known constitute of senile plaques found in brains of AD patients (Citron, 2010; Price et al., 1991). It is commonly used to trigger AD-related molecular dysfunctions and to mimic the AD pathophysiological environment (Kaminsky et al., 2010; Pike et al., 1995). Nowadays, AD is the neurodegenerative disease with higher impact in society, and the most common cause of dementia in elderly (Alzheimer's Association, 2020). Additionally, the AD-specific cognitive deficits are largely dependent on the hippocampus, an essential brain area for memory and learning processes (Bliss and Collingridge, 1993). In this work, *ex vivo* electrophysiological recordings were used to study neuronal electrical activity (Suter et al., 1999), and fEPSP were recorded from the hippocampal CA1 area. Hippocampal slices were either pre-exposed or acutely superfused with KTP and KTP-NH_2. For testing mimetic AD pathophysiological conditions, slices were pre-treated with oligomeric species of Aβ peptide, one of the most soluble toxic Aβ species (Giuffrida et al., 2009).

Synaptic plasticity, a crucial mechanism for the sustained strengthening of synaptic connections that are essential for several cognitive functions, can be evaluated through LTP, a well-known process related to memory and learning processes (Bliss and Collingridge, 1993). At molecular level, reinforcement of LTP is associated with an increase of neuronal spine density (Luscher and Malenka, 2012; Toni et al., 1999), in a process mediated by BDNF (Figurov et al., 1996; Tyler and Pozzo-Miller, 2001). Importantly, Aβ triggers

excitotoxicity through NMDAR-mediated Ca^{2+} influx, leading to an overactivation of calpains and causing the TrkB-FL cleavage, which impaired plasticity by abolishing LTP and decreasing neuronal spine density (Jerónimo-Santos et al., 2015; Tanqueiro et al., 2018; Fonseca-Gomes et al., 2019).

Our results demonstrate that KTP-NH_2 (50 nM), but not KTP (50 nM), has a neuroprotective effect against Aβ-induced impairments on LTP magnitude. Neither slices pre-exposed or superfused with KTP-NH_2 alone nor superfused with KTP alone have significantly affected LTP. However, LTP is significantly decreased in slices pre-exposed to KTP. These demarked differences observed between KTP and KTP-NH_2 effects contrasted with the fact that both are equally capable to restore Aβ impaired neuronal spine density, and neither of them cause toxicity in cortical cultured neurons. Several factors can possible explain these findings: 1) differences between peptides' membrane permeabilities (Ribeiro et al., 2011a, 2011b), KTP-NH_2 benefits from the added amidation-permeability capacity, which favors its neuroprotection action upon LTP magnitude; 2) different degree of exposure, since cultured neurons are more exposed and accessible to drugs than when comparing to hippocampal slices, KTP molecular action can be more effective in preventing the molecular loss of dendritic spines than in preventing LTP impairments; 3) temporal differences in Aβ peptide toxicity, since there are evidence showing that Aβ may functionally impair LTP mechanism before inducing neuronal spine loss and cell death (Chen et al., 2000). To some extent, the KTP neuroprotective action can counteract Aβ-induced impairments in dendritic spines density but not in LTP, probably because LTP can be more affected by Aβ. However, it is yet to be explained why KTP alone abolished LTP since these findings contrast with the previous study where the neuroprotective action of KTP (i.c.v.) was demonstrated (Angelova et al., 2018). Additionally, to evaluate whether the reported KTP-NH_2 neuroprotective effect on synaptic plasticity could be antagonized by KTP_{ant}, LTP magnitude was studied in slices pre-treated for 30 min with KTP_{ant} (250 nM). The results reveal that KTP_{ant} remarkedly reduced LTP magnitude in slices co-treated with KTP-NH_2 and Aβ peptide, but apparently also attenuated the decrease in LTP magnitude induced by Aβ peptide. However, it is still not clear if KTP_{ant} alone had a preventive neuroprotective action against Aβ, nor which mechanism might prompt toxicity when added *prior* to KTP-NH_2 treatment.

Regarding basal synaptic transmission, under physiologic conditions, our results showed that both peptides presented a concentration-dependent effect. KTP concentrations ranging from 5 nM to 50 μM induced a slight, but not significant, inverted-U shaped-change on synaptic transmission, which is the classical effect of most drugs (Calabrese and Baldwin, 2001). On the other hand, the synaptic transmission decreased when increasing the KTP-NH_2 concentration. Nevertheless, several neuropeptides have been reported to act in the

neuromodulation of glutamatergic synapses and, more specifically, on inhibiting glutamate release from presynaptic terminals (Merighi et al., 2011). Interestingly, some peptides act downstream of axonal excitability through indirectly interacting with G-protein subunits, with neuropeptides receptors coupling more often with G_i/G_o types of G-proteins (Merighi et al., 2011). This is consistent with KTPr being G_i-coupled (Ueda et al., 1989), which can explain the decrease in synaptic transmission caused by KTP-NH_2 action. Additionally, both peptides completely disrupted synaptic transmission at 5 mM, and these disruptive effects were partially or completely washed out with the removal of KTP or KTP-NH_2, respectively. These findings correlated with the structural amidation of KTP, which increased the KTP-NH_2 potential for interacting with biological membranes and it may foster its cellular permeability (Ribeiro et al., 2011a, 2011b). Thus, KTP-NH_2 effect might happen faster, in a more irreversible process, and/or as a consequence for the increased difficulty to completely clear it from the intracellular space. Future experiments with a longer washout period should be conducted to better understand this aspect.

Input/output curves recordings give information about axonal excitability and the level of postsynaptic activation, allowing the study of synaptic efficiency. The results showed that superfusion of both peptides (50 nM) does not affect synaptic efficiency in the CA1 hippocampal area. On the other hand, short-term plasticity is related to short Ca^{2+}-transient changes that occur at the presynaptic neuron and increase the probability of neurotransmitter releasing in an exclusive Ca^{2+}-dependent mechanism. The effects of both peptides were evaluated in phenomena of potentiation and facilitation using, respectively, PTP and PPF electrophysiological recordings. Similarly, the acute superfusion of both peptides (50 nM) do not impact the overall short-term plasticity. However, considering the PPF results obtained at 10 ms interval, KTP-NH_2 slightly decreased synaptic facilitation when compared to control, which is in line with its action in decreasing synaptic transmission. Additionally, glutamate release is directly triggered by presynaptic activation (Nicholls, 1998) and, thus, we evaluated whether this process could be mediated by KTP or KTP-NH_2 presence in the synaptosomal fraction of mice hippocampus. However, as expected from previous studies regarding KTP-mediated vesicular releasing (Janicki and Lipkowski, 1983), both peptides do not impact glutamate release. As such, the suggested decrease in synaptic facilitation induced by KTP-NH_2 was not confirmed. Together, these findings point to a non-mediated effect of both peptides at the presynaptic side.

Elevation of intracellular Ca^{2+} levels are needed to activate KTP-mediated processes, such as in Ca^{2+}-mediated Met-enkephalin release, and even for the release of synaptosomal KTP for neuronal endings (Takagi et al., 1979b; Ueda et al., 1986a). In order to evaluate whether Ca^{2+} increased levels are needed to induce KTP-mediated action or if they are directly

caused by KTP activity, the neuronal calcium homeostasis was assessed upon peptides' addition. Our results revealed that KTP and KTP-NH_2 do not affect the neuronal calcium homeostasis. In addition, we also evaluate *in vitro* peptides action regarding calpain activity. As already mentioned, calpains overactivation is a consequence of hyperexcitability induced by Aβ peptide, however its activation happens due to increased intracellular Ca^{2+} levels. Similarly, neither KTP nor KTP-NH_2 impact calpain activation and, consequently, do not prevent the calpains-induced TrkB-FL cleavage.

Finally, this work was the first to compare the effect of both KTP and KTP-NH_2 upon synaptic functions. It reveals that KTP-NH_2 has a solid neuroprotective effect against Aβ-induced AD pathophysiology, by preventing deficits in LTP magnitude and dendritic spines, whereas KTP action only prevents neuronal spine loss. Remarkably, at the studied concentrations, both peptides maintain most of their synaptic physiological functions. These findings raise their attractiveness as pharmacological tools to be used as neuroprotective drugs for the treatment of neurological diseases such as AD. Furthermore, it will be interesting to assess peptides' anti-inflammatory role in the context of AD. An inflammatory environment might contribute to neurodegeneration and neuronal loss (Dansokho and Heneka, 2018). As such, inflammation has been indicated as a plausible cause for the disease onset and its progression.

Chapter 4

The neuroprotective effect of KTP-NH_2 systemic treatment

4.1. Chapter rationale and publication information

The findings of the previous chapter unveiled the synaptic mechanisms protected by KTP-NH_2 action against Aβ-induced toxicity, namely in LTP and dendritic spines density. In the light of this thesis, in this chapter, the KTP-NH_2 neuroprotection action was correlated with the ameliorated memory impairment observed in an animal model of sporadic AD after the systemic administration of KTP-NH_2.

As such, this chapter included a collaborative study designed to investigate 1) whether the systemic administration of KTP-NH_2 would be effective to ameliorate memory impairment in a rat model of sporadic AD, and 2) correlated with the synaptic mechanisms protected by KTP-NH_2 action against Aβ-induced toxicity. It included the introduction, materials and methods, results and discussion sections of the my peer-revised original research article (Belo et al., 2020). In this work, Margarida and I performed all the experiments, and I wrote the first draft of the manuscript. I performed the electrophysiological recordings, the immunocytochemistry experiments, and all formal statistical analysis presented. Margarida was responsible by the *in vivo* experiments: the surgery was conducted together with Sara Xapelli, the whole animal perfusion fixation procedure with the contribution of Joana E. Coelho, and the animal behavioral studies with Liana Shvachiy. In addition, Margarida did both western-blots and immunohistochemistry procedures under the guidance of Cláudia Valente. Me and João Fonseca-Gomes were responsible by the neuronal cell cultures. Tiago Coelho e Carolina Almeida-Borlido contributed equally to immunocytochemistry analysis under my supervision. Hugo was responsible for preparing the oligomeric species of Aβ. Vera Neves contributed to the interpretation of the results. Maria José Diógenes, Miguel A. R. B. Castanho, and Ana M. Sebastião were responsible for the concept and design of the study, interpreted the results and supervised the work.

This study was supported by Santa Casa da Misericórdia de Lisboa (MB37-2017) and FCT: PTDC/NEU-OSD/5644/2014, and PTDC/BIA-VIR/29495/2017. João Fonseca-Gomes was supported by FCT (PD/BD/114441/2016). Joana E. Coelho was supported by FCT (SFRH/BPD/87647/2012).

4.2. Introduction

Kyotorphin (KTP) is an endogenous dipeptide composed by tyrosine and arginine (*L*-tyrosyl-*L*-arginine) residues, first described as a powerful analgesic molecule (Takagi et al., 1979b, 1979a). Given its analgesic properties, KTP has been investigated as a drug for pain treatment (Ribeiro et al., 2011b; Santos et al., 2013). Although mechanisms underpinning KTP-induced analgesic effects are still not entirely understood, some authors argue that KTP binds to a specific Gi-coupled protein receptor (KTPr), which despite numerous efforts, has never been isolated (Ueda et al., 1989). Nevertheless, it is well-known that KTP triggers the release of met-enkephalins (met-enk) and β-endorphins in a naloxone-reversible opioid receptors mediated-mechanism (Oliveira et al., 2016; Shiomi et al., 1981b; Takagi et al., 1979b; Ueda et al., 1982), an effect antagonized by the dipeptide *L*-Leu-*L*-Arg (a KTPr antagonist) (Ueda et al., 1989; Kawabata et al., 1992).

Interestingly, despite the high expression of KTP in the cortex, the levels of enkephalins and of opioid receptors are low, suggesting other non-opioid physiological actions for KTP (Ueda et al., 1980). Remarkably, KTP has been pointed as a possible neuroprotective factor (Dzambazova and Bocheva, 2010), emerging as a novel drug to be explored for Alzheimer´s disease (AD) and other therapeutic applications.

AD is a chronic progressive neurodegenerative disease and the most common cause of dementia in elderly. The presence of senile plaques (amyloid beta (Aβ) peptide) and neurofibrillary tangles (hyperphosphorylated tau (p-Tau) protein) in the brain are the molecular hallmarks of the disease (Citron, 2010; Price et al., 1991). AD represents a challenge for drug discovery since effective neuroprotective treatments are still needed. It was reported that AD patients present decreased levels of KTP in cerebrospinal fluid (CSF) (Santos et al., 2013) suggesting the increase in KTP levels as a possible therapeutic strategy.

Despite the encouraging recent data showing that intracerebroventricular (i.c.v) injection of KTP ameliorates memory impairments in a sporadic AD rat model (Angelova et al., 2019), its weak activity when administered systemically (Chen et al., 1998) renders KTP as an unrealistic pharmacological tool to fight AD. Amidated-Kyotorphin (KTP-NH_2), is a KTP derivative capable of crossing the blood brain barrier (BBB) (Ribeiro et al., 2011a, 2011b), and with efficacy to decrease neuronal damage induced by cerebral hypoperfusion (Sá Santos et al., 2016). Altogether, these findings prompted us to investigate whether systemic administration of KTP-NH_2 would be effective to ameliorate memory impairment in an animal model of sporadic AD, and if so, which are the synaptic mechanisms operated by KTP-NH_2 to protect synapses against Aβ-induced toxicity.

4.3. Materials and Methods

4.3.1. Drugs

4.3.1.1. Amyloid β peptide

For *in vivo* experiments, Amyloid β (Aβ) peptide 1-42 ($Aβ_{1-42}$) (H-1368, Bachem Bubendorf, Switzerland) was dispersed in water at a concentration of 2.25 mg/mL.

In order to prepare oligomeric species of $Aβ_{1-42}$ ($Aβ_{olig}$), $Aβ_{1-42}$ (1 mg/ml) (A-42-T, GenicBio, Shanghai, China) was suspended in phosphate-buffered saline (PBS), supplemented with 0.025% ammonia solution and adjusted to a final pH 7.2 (HCl). Species separation was based on an ultrafiltration process, as previously described (Giuffrida et al., 2009). Briefly, $Aβ_{1-42}$ (220 μM) was allowed to oligomerize by constant shaking at 600 rpm, at 37ºC for 16 h and ultracentrifuged (40 000 *g*, 30 min) for separation of fibrils (pellet). The supernatant was further separated in centrifugal filters (30 kDa Amicon Ultra). The concentration of the retained fraction, corresponding to oligomers > 30 kDa, was spectrophotometrically determined ($ε_{280}$ =1490 $M^{-1}cm^{-1}$). Oligomers aliquots (120-220 μM) were immediately stored at -80ºC until further use.

In addition, *in vitro* experiments using primary neuronal cultures were performed using the Aβ fragment 25-35 ($Aβ_{25-35}$) (Bachem, Bubendorf, Switzerland). $Aβ_{25-35}$ represents the biologically active region of Aβ and induces the same molecular and cellular dysfunction as $Aβ_{1-42}$ species, being this effect similar to what has been observed in AD brains (Kaminsky et al., 2010; Pike et al., 1995). Stock solutions of $Aβ_{25-35}$ were prepared in milliQ water to a final concentration of 1 mg/mL.

4.3.1.2. KTP-NH_2 peptide

KTP-NH_2 peptide was synthesized as previously described (Ribeiro et al., 2011b). For *in vivo* experiments, KTP-NH_2 was dissolved in physiological saline solution (0.9 % NaCl, vehicle solution), as a 100 mM stock solution, and it was administered at a dose of 32.3 mg/Kg, at a volume of 1 mL/Kg. The selected dose was based on previous results regarding KTP-NH_2 analgesic action profile (Ribeiro et al., 2013, 2011b). For *ex vivo* and *in vitro* experiments, KTP-NH_2 was prepared in previously filtered and sterile milliQ water as 1 mM and 5 mM stock solutions respectively.

4.3.2. Intracerebroventricular injection of Aβ peptide

Male Wistar rats (8-10 weeks), purchased from Charles River Laboratories (Lyon, France), were housed in a group of 2 per cage and maintained under controlled conditions (20 ± 2ºC; 14:10 h light/dark cycle, lights on between 7 a.m. and 9 p.m.). All animals had unrestricted access to food and water. The handling of animals and all described procedures were

conducted according to the European Community (86/609/EEC; 2010/63/EU; 2012/707/EU) and Portuguese (DL 113/2013) legislation for the protection of animals used for scientific purposes, and they were approved by the Ethical Committee for Animal Research of Instituto de Medicina Molecular João Lobo Antunes (iMM), Faculty of Medicine, University of Lisbon, and the Portuguese Competent Authority for Animal Welfare (DGAV) in Portugal.

The animal model of AD was created based on the $A\beta_{1–42}$ i.c.v. injection method, as previously described (Canas et al., 2009; Zhang et al., 2015). Surgical procedures were performed when animals reached 230-320g and during the light period. Briefly, animals were anesthetized with isoflurane (2-3% in O_2) using a RC2 Rodent Anesthesia System (VetEquip Inc., California, USA), firstly using a plexiglas chamber and thereafter maintained via facial mask. EMLA® cream was applied in the ear canal, and Bupivacaine Hydrochloride 0.25% (8 mg/Kg, SC) was administered at the incision site for local anesthetics. Lacryvisc® (Carbomer 974P 0.3%) was applied on the eyes to avoid dehydration. Buprenorphine (0.05 mg/Kg, SC) was also administered pre-emptively for general analgesia, so it would be already in action when animals recovered from anesthesia.

Twelve animals were i.c.v. injected with Aβ peptide (2.25 mg/mL) in 5 µL and fourteen were injected with 5 µL of water (vehicle) at day zero. Injections were performed with a 33-gauge Hamilton microsyringe (Hamilton Company, Nevada, USA) using a microinjection pump (World Precision Instruments, Inc., Florida, USA) with a rate of 500 nL/min, in the right lateral ventricle using a stereotactic system (anteroposterior: -0.84 mm from Bregma, medial/lateral: 1.5 mm and dorsal/ventral: -3.5 mm). Injections lasted 10 min and the needle with the syringe was left in place for 2 min after the injection to ensure complete infusion of Aβ. Animal body temperature was kept constant at 37°C using a heating pad. A timeline of all the experimental events is depicted in Figure 20 (A). Previous work reported soluble forms of Aβ on the hippocampus of i.c.v. Aβ injected animals (Canas et al., 2009), thus showing Aβ diffusion through this brain region. Compared with transgenic models of AD, the i.c.v. Aβ-induced sporadic model of AD is more relevant for the study of Aβ-induced pathophysiological traits of AD. Moreover, the transgenic models of AD are usually used to study the familial form of the disease, which barely represents 5% of AD cases (Lecanu and Papadopoulos, 2013).Chronic intraperitoneal KTP-NH_2 treatment

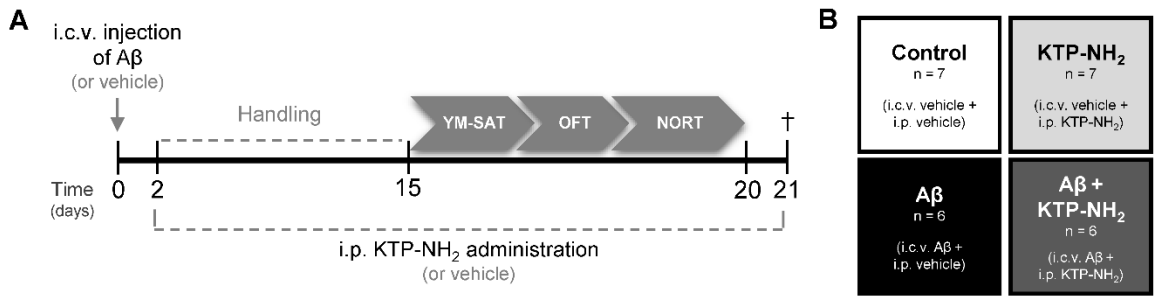

Figure 20. Experimental design. (A) Animals were i.c.v. injected with Aβ ($Aβ_{1-42}$) or vehicle (water) at day 0. On day 2, KTP-NH_2 or vehicle (saline solution) i.p. administration began, simultaneously with handling. Behavioral tests were performed between days 15 and 20: Y-Maze Spontaneous Alternation test (YM-SAT), Open Field test (OFT), and Novel Object Recognition test (NORT). On day 21 animals were sacrificed (†) for molecular analyses (WB and IHC). **(B)** Four experimental groups were tested: Control (i.c.v. and i.p. vehicle administration, n = 7); Aβ (i.c.v. Aβ administration and i.p. vehicle treatment, n = 6); KTP-NH_2 (i.c.v. vehicle administration and i.p. KTP-NH_2 treatment, n = 7), and Aβ + KTP-NH_2 (i.c.v. Aβ administration and i.p. KTP-NH_2 treatment, n = 6).

Thirteen animals underwent a chronic 18-day treatment regimen of KTP-NH_2 (32.3 mg/Kg, single i.p. dose/day), starting the second day after i.c.v. administration of $Aβ_{1–42}$ (Aβ + KTP-NH_2 group, n=6) or vehicle (KTP-NH_2 group, n=7), and lasting until sacrifice. The remaining thirteen animals received the vehicle solution following the same treatment regimen: Aβ + vehicle (Aβ group, n = 6) and vehicle + vehicle (control group, n = 7).The experimental groups of animals are depicted in Figure 20 (B). During the last 5 days of i.p. treatments (KTP-NH_2 or vehicle), animals were tested in the behavioral paradigms identified below. During behavioral assessment days, injections were performed after animal testing and before return to the animal house.

4.3.3. Behavioral testing

Behavioral tests were performed from the fifteenth day after $Aβ_{1–42}$ injection, following a previously described protocol (Canas et al., 2009; Cunha et al., 2008). The handling period coincided with the first 13 days of KTP-NH_2 treatment, where animals were handled for a few minutes before the i.p. injection so that they became used to the experimenter and to the testing room. All behavioral tests were carried out between 9 a.m. and 6 p.m.. All the apparatus used were cleaned with 70% ethanol between animals switching. After placing the animal inside the behavioral apparatus, the experimenter immediately left the room. The experimenter conducting behavioral analysis was blinded to treatment conditions.

Tests were performed in the following order: Y-Maze Spontaneous Alternation Test (YM-SAT), Open Field Test (OFT), and Novel Object Recognition Test (NORT) (Figure 20 (A)). The YM-SAT was performed before the NORT to evaluate working memory for a less

complex paradigm first. Since OFT and NORT use the same testing arena, the OFT was performed during the first 5 min of the first day of NORT habituation period (first contact with the arena).

4.3.4. Y-Maze Spontaneous Alternation Test (YM-SAT)

The spontaneous alternation version of the Y-Maze test evaluates spatial working memory by taking advantage of the willingness of rodents to explore new environments. The testing protocol for YM-SAT has been described in detail previously (Maurice et al., 1996). The wood-made maze used was composed of 3 arms (30 x 10 x 20 cm each), converging to an equal angle. Visual cues were placed on the walls of the maze. Briefly, without prior habituation, animals were individually placed at the end of one arm and allowed to freely move through the maze for 8 min. Two independent investigators visually recorded arm entries, and the comparison between recordings showed total agreement.

An entry was considered valid when all four limbs of the animal were within the arm. An alternation was defined as entries in all three arms on consecutive occasions. The number of maximum possible alternations for each animal was therefore the total number of arm entries minus two. The percentage of spontaneous alternation was calculated as actual alternations/maximum alternations x 100. In addition, the total number of arm entries was used as a measure of locomotor activity.

4.3.5. Open Field Test (OFT)

The OFT is widely used to assess individual spontaneous locomotor activity and anxiety-like behavior when animals are introduced to a novel environment (Bailey and Crawley, 2009; Castanheira et al., 2018; Prut and Belzung, 2003). Importantly, this test allows to detect bias in animal behaviour that could affect performance on NORT, since locomotor activity can impact exploratory drive (Broadhurst, 1958, 1957). The open field arena consisted of an empty square wood box (67 x 67 x 51 cm height), virtually divided into three concentric squares: a peripheral, an intermediate and a central zone. The testing protocol has been described in detail previously (Gould et al., 2009). Briefly, animals were individually placed in the center of the arena and allowed to freely move for 5 min. The behaviour was video-recorded and analyzed by the tracking software Smart® (version 2.5; Panlab, Barcelona, Spain). The reference point used for the animal tracking position was defined as the center of the animal dorsum. Both total travelled distance (cm) and average velocity (cm/s) were measured to assess locomotor activity. In addition, the percentage of time spent in the arena periphery was used as an indicator of the level of anxiety-like behavior. All animals were tested only once.

4.3.6. Novel Object Recognition Test (NORT)

Considering that episodic long-term memory is the predominant cognitive deficit in AD, animals were subjected to the NORT (Antunes and Biala, 2012). To assess long-term memory a retention interval (RI) of 24h was used. This test consists of three phases: habituation, familiarization (training), and test. The habituation phase consisted of 3 sessions of habituation to the arena (15 min each day). During both familiarization and test phases, two objects were added to the same arena, always in the same place. The objects used in this test were translucent glass bottles and brown glass bottles without labels, that were similar in size and shape, but which the animals were able to discriminate between them. To prevent coercion to explore the objects, animals were individually placed in the middle of the opposite wall where objects were, with their backs to them, and allowed to freely move for 5 min. In the familiarization phase, animals were presented with two equal objects, which we herein name as 'familiar' objects. During the familiarization phase, chosen objects were counterbalanced between animals within the same experimental group to reduce any object preference effect. Similarly, object localization was counterbalanced between both arena sides, to eliminate possible preference confounds for a specific side of the arena. Following sample-objects exposure, animals returned to the home cage for 24 h. In the test phase, one of the previously experienced objects (now considered familiar objects) was substituted by a new object (considered the novel object). Exploration was scored when the animal touched an object with its forepaws or snout, bit, licked, or sniffed the object from a distance of no more than 1.5 cm. Running around the object or climbing on it was not recorded as exploration. Animal movements were recorded using the SMART® video-tracking software (version 2.5; Panlab, Barcelona, Spain). A post-analysis was conducted to refine the results obtained by software measures. Two independent investigators made the post-analysis with a high degree of concordance between them.

Three indexes were calculated in order to evaluate both preference between objects and recognition of the novel object: 1) the object preference index, which is the ratio between the time spent exploring one object over the total time spent exploring both objects [object 1 or object 2 / (object 1 + object 2)], and it is assessed both in the training and test phases; 2) the object recognition index, which is the ratio between the time spent exploring the novel object and the total time spent exploring both objects [novel / (novel + familiar)], and it is an index of retention, used for analysis of the test phase performance; and finally, 3) the object discrimination index, which is the ratio between the difference between the time spent exploring the novel and the familiar object, and the total time spent exploring both objects [(novel - familiar) / (novel + familiar)], allowing an easier visualization of data since no memory retention scores as zero (Antunes and Biala, 2012).

4.3.7. Western Blot (WB)

After behavioral tests, three/four animals from each group were deeply anesthetized with isoflurane (Esteve, Barcelona, Spain) and decapitated. Their brains were quickly removed and placed in ice-cold aCSF, continuously oxygenated (O_2/CO_2: 95%/5%) to isolate both hippocampi. The left and the right hippocampi were individually frozen in liquid nitrogen and stored at -80ºC. The two hippocampi were analyzed separately to allow the separate quantification of the hippocampus of the side of the i.c.v. injection (right, ipsilateral) and of the contralateral to it. Since both hippocampi could be differently exposed to Aβ, they could display different degrees of gliosis. Using a Potter homogenizer, tissue homogenates were prepared from frozen samples by solubilizing them in Radio-Immunoprecipitation Assay (RIPA) buffer: 50 mM Tris-base (pH 7.5), 150mM NaCl, 5mM Ethylenediaminetetraacetic Acid (EDTA), 0.1% Sodium Dodecyl Sulphate (SDS), and 1% Triton X-100, supplemented with phosphatase inhibitors: 10nM NaF; 5mM Na_3VO_4 and a protease inhibitor cocktail (Complete Mini-EDTA free from Roche, Penzberg, Germany). Samples were centrifuged at 13 000 *g*, 4°C for 10 min, and the supernatant was collected and placed in fresh tubes. Protein concentration was quantified through Bradford method, using Bio-Rad DC reagent (Bio-Rad Laboratories, Berkeley, CA, United States). All samples were prepared with the same amount of total protein (35 µg), by adding a loading buffer (350 mM Tris-HCl (pH 6.8), 10% SDS, 30% glycerol, 600 mM Dithiothreitol, 0.06% bromophenol blue), and then boiled at 95°C for 5 min. Next, samples and the molecular weight marker (PageRuler™ Plus Prestained Protein Ladder, 10 to 250 kDa, ThermoFisher Scientific, Massachusetts, USA) were loaded and separated on 12% SDS–polyacrylamide gel electrophoresis (SDS-PAGE) within a standard migration buffer (25 mM Tris-base (pH 8.3), 192 mM Glycine, 10% SDS), at a constant voltage between 80 and 120 mV. Subsequently, proteins were electrotransferred, at 400 mA for 1h30, from the gel to a polyvinylidene difluoride (PVDF) membrane (GE Healthcare, Buckinghamshire, United Kingdom), previously activated with methanol for 5 min, within the standard buffer (25 mM Tris (pH 8.3), 192 mM Glycine, 15% methanol) for wet transfer conditions. Afterwards, membranes were stained with Ponceau S solution (Sigma-Aldrich®) to check for transference efficacy, and blocked with a 3% bovine serum albumin (BSA) in TBS-T (Tris-Buffered Saline with Tween-20 containing in mM: Tris base 20; NaCl 137 and 0.1% Tween-20) during 1h at RT to avoid non-specific binding. Membranes were incubated with the primary antibodies overnight at 4°C, and then with the HRP-conjugated secondary antibodies (1:10000, Santa Cruz Biotechnology, Dallas, TX, USA) for 1h at RT, all diluted in 3% BSA solution in TBS-T. The primary antibodies used were rabbit polyclonal antibody anti-GFAP (1:5000, Sigma, St. Louis, MO, USA), goat polyclonal antibody anti-Iba-1 (1:1000, Abcam, Cambridge, UK), and mouse monoclonal

antibody anti-GAPDH (1:5000, Invitrogen, Carlsbad, California, USA). Chemiluminescent detection was performed with ECL Plus Western Blotting Detection Reagent (GE Healthcare, Buckinghamshire, UK) in the ChemiDoc™ XRS+ System from Bio-Rad. The integrated intensity of each band was calculated using computer-assisted densitometry analysis with Image-J 1.45 software (Bethesda Softworks, Bethesda, MD, United States) and normalized to the integrated intensity of the loading control (GAPDH). Images were prepared for printing in Image Lab software 5.2.1 (software available in ChemiDoc XRS+ system, Bio-Rad).

4.3.8. Immunohistochemistry

After behavioral tests, three animals of each group were deeply anesthetized with ketamine/xylazine mixture (120 mg/Kg /16 mg/Kg) at a volume of 1 mL/Kg. After reaching a deep anesthesia state, the animals were perfused transcardially with approximately 200 mL of warmed (37°C) 0.9% saline solution, to clear the blood from the circulatory system, followed by approximately 500 mL of 4% paraformaldehyde (PFA) in PBS, 140mM NaCl, 3mM KCl, 20mM Na_2HPO_4, 1.5mM KH_2PO_4, pH 7.4) (Gage et al., 2012). Animals were then decapitated, and their brains were carefully removed and maintained for post-fixation in the same fixative solution at 4°C overnight. After that, brains were washed twice with PBS, and then cryoprotected at 4°C by immersion in increasing concentrations of sucrose (15% and 30%). Subsequently, brains were gelatin-embedded (7.5% gelatin in 15% sucrose) and then sectioned at a thickness of 12 µm on a cryostat (LEICA CM 3050S, Wetzlar, Germany), by the Histology and Comparative Pathology Laboratory of iMM. Only the coronal sections located at the level of hippocampus (around - 2.92 mm and - 5.04 mm from Bregma) were collected, mounted on SuperFrost® Plus slides (Menzel-Glaser, Braunschweig, Germany) and stored at -20ºC for further use.

For the immunohistochemical analyses, slices were placed in PBS for 10 min at 37ºC to remove the gelatin from brain tissue. Then, each slice was surrounded with DAKO pen (Dako, Glostrup, Denmark) to protect staining areas from drying out and from mixing with each other. After an incubation in glycine (0.1M) for 10 min to remove the small toxic aldehydes originated from PFA degradation, sections were subsequently treated with 0.1% Triton X-100 in PBS (10 min) for membrane permeabilization, washed twice (10 min each time) with PBS in the presence of 0.1% Tween-20 (PBS-T) and then blocked with a blocking solution (10% FBS, 6/10% BSA in PBS-T) for 30 min at RT. Next, slices were incubated with the primary antibodies overnight at 4º C, and with the fluorophores coupled-secondary antibodies for 2h at RT in a humidified dark chamber. The nuclei were stained with Hoechst 33342 (20 µg/mL, Invitrogen) for 10 min at RT. The slices were mounted in Mowiol (Sigma). The primary antibodies used were mouse monoclonal antibody anti-GFAP (1:1000, Millipore,

Burlington, Massachusetts, USA), and goat polyclonal antibody anti-Iba1 (1:1000, Abcam). The secondary antibodies were donkey anti-mouse-Alexa Fluor 568, and donkey anti-goat-Alexa Fluor 488 (1:500, Invitrogen). Images were acquired on an inverted wide field fluorescence microscope (Zeiss Axiovert 200, Zeiss, Oberkochen, Germany), using a monochrome digital camera (AxioCamMR3, Zeiss), with a 40X objective (Zeiss). The software AxioVision 4.7.1 (Carl Zeiss Imaging Systems) was used for image acquisition. Immunofluorescence images were acquired in two areas of the hippocampus: *cornu ammonis* 1 (CA1) and dentate gyrus (DG), of both hemispheres of each animal.

4.3.9. Freshly Prepared Hippocampal Slices and Drug Treatment

Male C57BL/6J mice (8-11 weeks old), purchased to Charles River Laboratories (Lyon, France), were housed in groups of 4/5 per cage and maintained under controlled conditions (21 ± 1ºC; 55 ± 10% humidity; 12:12 h light/dark cycle). Animals were deeply anesthetized with isoflurane (Esteve, Barcelona, Spain) and decapitated to quickly remove their brains. Then, brains were placed in ice-cold artificial cerebral-spinal fluid solution (aCSF; 124 mM NaCl, 3 mM KCl, 1.2 mM NaH_2PO_4, 25 mM $NaHCO_3$, 2 mM $CaCl_2$, 1 mM $MgSO_4$, and 10 mM glucose, pH 7.4), continuously oxygenated (O_2/CO_2: 95%/5%) to dissect both hippocampi. Acute hippocampal slices were cut, with a thickness of 400 µm, perpendicularly to the long axis of the hippocampus using a McIlwain tissue chopper, and placed in a resting chamber filled with continuously oxygenated aCSF at RT for 1h to guarantee the functional and energetic recovery. Slices were incubated for 3h at RT with continuously oxygenated aCSF with 50 nM KTP-NH_2 in the presence or absence of 200 nM $A\beta_{olig}$.

4.3.10. *Ex Vivo* Electrophysiological Recordings

Long-term potentiation (LTP) induction and quantification were performed as described previously (Diógenes et al., 2011). Briefly, hippocampal slices were transferred to a recording chamber continuously superfused with oxygenated aCSF at 32°C (flow rate of 3 mL/min). Stimulation pulses were delivered every 20 s using a bipolar concentric wire electrode placed on Shaffer collateral/commissural fibers in stratum radiatum, and field-excitatory postsynaptic potentials (fEPSPs) were recorded extracellularly through a microelectrode filled with aCSF (2–6 MΩ) placed in the stratum radiatum of the CA1 area. The intensity of stimulation was initially adjusted to obtain a fEPSP slope with a minimal spike contamination and of around 50% of the maximal slope. Recordings were obtained with an Axoclamp 2B amplifier (Axon Instruments, Foster City, CA, United States), digitized and continuously stored on a personal computer with the WinLTP software (Anderson and Collingridge, 2001). Individual responses were monitored, averages of six consecutive responses were obtained, and the slope of the initial phase of the fEPSP was quantified. After fEPSPs stabilization, LTP was induced through a θ-burst protocol (3 trains of 100 Hz, 3

stimuli, separated by 200 ms). The θ-burst induced LTP pattern of stimulation is considered closer to what physiologically occurs in hippocampi during episodes of learning and memory in living animals (Albensi et al., 2007). We used a mild LTP protocol since this proved to be sensitive to synaptic plasticity changes along with aging (Diógenes et al., 2011), and allows assessing both further improvements or impairments on LTP magnitude. LTP magnitude was quantified as the percentage of change in the average slope of fEPSPs taken between 50 to 60 min after LTP induction in relation to the average slope of fEPSPs measured during the 10 min before θ-burst induced LTP (baseline).

4.3.11. Primary Neuronal Cultures and Drug Treatment

Primary neuronal cultures were obtained from fetuses of 18/19-days pregnant Sprague-Dawley females, as routinely in the lab (Jerónimo-Santos et al., 2015). Briefly, animals were deeply anaesthetised with isoflurane and decapitated. The fetuses were collected and placed in cold Ca^{2+}- and Mg^{2+}-free Hank's Balanced Salt Solution (HBSS) (Gibco, Paisley, UK). The brains were dissected, the cerebral cortices were isolated, and the meninges were removed. Then, the tissue was mechanically fragmented, followed by enzymatic digestion with 0.025% (w/v) of trypsin solution in HBSS for 15 min at 37ºC. To neutralize the action of trypsin, HBSS supplemented with FBS 20% (w/v) and cellular suspension was centrifuged at 190g. The supernatant was discarded, and the cells were resuspended in the same solution by pipette aspiration in order to dissociate cells. This process was repeated three times. After washing, cells were resuspended in supplemented Neurobasal medium (0.5mM *L*-glutamine, 25mM glutamic acid, 2% B-27, and 25 U/mL penicillin/streptomycin). Then, cell suspension was filtered (BD Falcon Cell Strainer 70 mM, Thermo Fisher Scientific, Waltham, MA, United States), to obtain single cells and cell density was determined by counting cells in a 0.4% trypan blue solution using a hemocytometer. Cells were plated at $1x10^{-5}$ cells/well on 12-wells flat-bottom cell plates covered with glass coverslips (Corning® Costar® TC-treated, Sigma), and maintained at 37ºC in a humidified atmosphere of 95/5% O_2/CO_2, for 14 days. The coverslips were previously sterilized under UV light, coated overnight with 10 mg/mL of poly-D-lysine (Sigma, St. Louis, MO, United States) and washed with sterile H_2O. After 13 days *in vitro* (DIV13), cells were incubated with 50 nM KTP-NH_2 in the presence or absence of 25 μM $A\beta_{25-35}$, during 24h.

4.3.12. Immunocytochemistry

In order to evaluate the neuroprotective effect of drug treatment, spine density was counted as previously done in our lab (Tanqueiro et al., 2018). Briefly, primary neuronal cultures at DIV14 were fixed in 4% PFA in PBS (pH 7.4) for 15 min at RT, after being washed with PBS twice. Using a blocking solution (3% (w/v) BSA) (Sigma-Aldrich) in PBS with 0.1% (v/v) Triton X-100, cells were incubated for 1h at RT. To specifically detect neurons, cells were

incubated with mouse microtubule-associated protein 2 (MAP2) primary antibody (1:200 in blocking solution) (Millipore), overnight at 4ºC in a wet-chamber. After this, cells were washed with PBS twice and then co-incubated in blocking solution with goat anti-mouse-Alexa Fluor 568 secondary antibody (1:200, Invitrogen), Alexa Fluor 488 Phalloidin (1:40) (Invitrogen), which recognizes filamentous actin (F-actin), and Hoechst 33342 (6 µg/mL) for nuclear staining, for 1h at RT inside a dark-wet chamber. After being washed with PBS twice, coverslips were mounted in Mowiol mounting solution. Using a confocal laser point-scanning microscope LSM 880 with Airyscan (Carl Zeiss MicroImaging, Thornwood, NY, United States), the observed conjugation between MAP2 (568, red) and F-actin (488, green) allowed the clear identification of dendritic protrusions, since F-actin has an important role in the constitution of the cytoskeleton of dendritic spines (Koskinen and Hotulainen, 2014). Spine density was assessed as the number of protrusions, counted per 10 µm of the parent dendrite, as previously reported (Alonso et al., 2004; Ji et al., 2010) with a distance of 25 µm from the cell body. Independent averages were computed with counts of 3 different dendrites of each neuron, 6 neurons per condition, with each primary neuronal culture being considered an independent experiment.

4.3.13. Statistical Analysis

Data are expressed as mean ± standard error of the mean (mean ± SEM), where *n* is the number of independent experiments. Results of each animal per group, and results acquired from different hippocampal slices of different animals were considered independent experiments. The data normality was confirmed using the Shapiro-Wilk test. Results obtained using behavioral paradigms, OFT, YM-SAT, NORT (object recognition index and object discrimination index), through electrophysiological recordings (LTP magnitude), and using immunocytochemistry (number of dendritic protrusions) were analyzed using two-way ANOVA, followed by the Tukey's multiple comparisons test. In addition, significant differences between means of NORT object preference index within each phase were evaluated through unpaired two-tailed Student's *t*-test. Results obtained by western blot were analyzed using two-way ANOVA. Values of $p < 0.05$ were considered to represent statistically significant differences. All statistical analyses were conducted using the Prism Software (GraphPad Prism®, version 8.0.2, California, USA).

4.4. Results

4.4.1. KTP-NH_2 treatment prevented episodic long-term and spatial working memory dysfunction induced by Aβ

To evaluate the influence of KTP-NH_2 in an animal model of AD (Canas et al., 2009; Zhang et al., 2015), KTP-NH_2 (32.3 mg/Kg) or saline solution (vehicle) was i.p. administered for 18 days to rats that had received a 5 µL i.c.v injection of $A\beta_{1–42}$ (2.25 mg/mL) or water (vehicle) (Figure 20 (A)). As such, the experimental groups are the following: control group (vehicles); KTP-NH_2 group (vehicle + KTP-NH_2 treatment); Aβ group (Aβ and vehicle treatment); and Aβ + KTP-NH_2 group (Aβ and KTP-NH_2 treatment) (Figure 20 (B)).

Episodic long-term memory, considered the predominant cognitive deficit in AD, was evaluated through the NORT with a retention time of 24 h (see Methods). As expected, in the training phase (Figure 21, grey bars), the four groups of animals explored approximately the same amount of time the two identical objects. In the test day (Figure 21, black and white bars), animals from the Aβ group did not react to novelty ($p > 0.05$, unpaired two-tailed Student's *t*-test to compare % of time spent with familiar vs. novel object; n = 6; Figure 21 (C)), whereas the control group did ($p \leq 0.0001$, unpaired Student's *t*-test to compare % of time spent with familiar vs. novel object; n = 7; Figure 21 (A) and (C) respectively). Remarkably, the Aβ induced-impairment in the NORT was totally recovered in the animals that had been treated with KTP-NH_2 (Figure 21 (D)). These treated animals showed a clear preference for exploring the novel object more than the familiar one ($p \leq 0.0001$, unpaired Student's *t*-test to compare % of time spent with familiar vs. novel object; n = 6), thus behaving like control animals. The KTP-NH_2 group also behaved like a control group ($p > 0.05$, unpaired two-tailed Student's *t*-test to compare % of time spent with familiar vs. novel object; n = 7; Figure 21 (B)), indicating that *per se* KTP-NH_2, is not a memory enhancer, though markedly ameliorating memory deficits elicited by Aβ.

To better compare performances among the four groups of animals, the time spent exploring each object in the test day was converted into the object recognition index [novel / (novel + familiar)], and the object discrimination index [(novel – familiar) / (novel + familiar)], which were calculated for each animal and averaged within each group (Figure 22 (A), and (B), respectively). The object recognition index ranges from 0 to 1, where obtained values around 0.5 reflect an absence of discrimination between the novel and the familiar objects. The discrimination index ranges from -1 to +1, and obtained values around 0 reflect lack of object discrimination. In both indexes, higher obtained values indicate higher memory performance.

As depicted in Figure 22, the recognition index attained by the Aβ group was significantly different from the control group (Aβ: 0.48 ± 0.046 *vs.* control: 0.71 ± 0.028; $p < 0.05$, two-

way ANOVA with Tukey's multiple comparisons test; n = 6-7). Importantly, the index displayed by the Aβ + KTP-NH_2 group, (0.67 ± 0.020, n = 6) was similar to the control group ($p > 0.05$, two-way ANOVA with Tukey's multiple comparisons test; n = 6-7), and significantly different from Aβ group ($p < 0.05$, two-way ANOVA with Tukey's multiple comparisons test; n = 6-7).

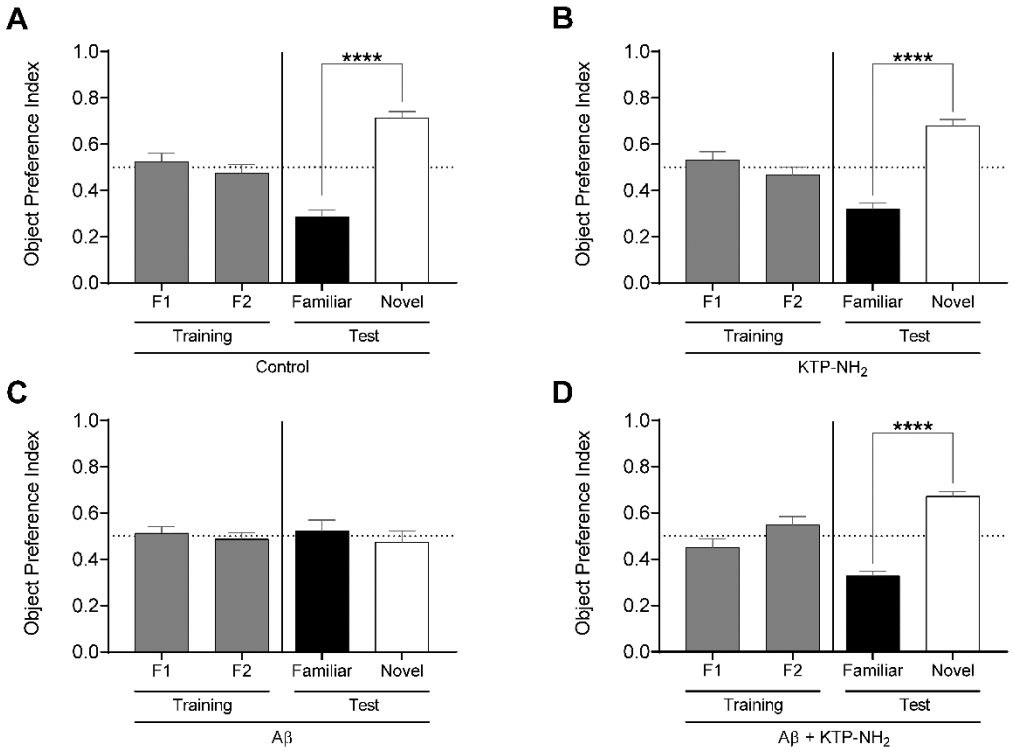

Figure 21. The KTP-NH_2 treatment mitigates Aβ-induced impairments in long-term (24h) episodic memory. Long-term episodic memory was evaluated through the Novel Object Recognition test (NORT). After 3 arena habituation sessions, the training phase consisted of one session with two identical objects (F1 and F2) placed inside the arena. The test phase occurred on the following day (24 h later), where one of the familiar objects (Familiar) was replaced by a novel object (Novel). During both phases, animals freely explore the objects for 5 min and the results are given by the time spent exploring any one of the two objects allows to calculate the Object Preference Index, i.e., F1 or F2 / (F1 + F2) and Familiar or Novel / (Familiar + Novel). A preference index above 0.5 indicates a preference of that specific object, whereas equal to 0.5 represents no preference. Statistical analysis using unpaired two-tailed Student's t-test showed no statistical differences in preference between objects during the training phase (as expected), and revealed a significant preference for the novel objects during the test phase for control **(A)**, KTP-NH_2 **(B)**, and Aβ + KTP-NH_2 **(D)** groups (n = 6-7), which indicates that memory is conserved within these animals. For the Aβ group **(C)**, data showed that there was no preference between familiar and novel objects (n = 6). **** $p \leq 0.0001$. Data are represented as mean ± SEM.

Moreover, the KTP-NH_2 treatment alone (KTP-NH_2 group) did not affect the object recognition index (0.68 ± 0.028, n = 7) when compared to the control group ($p > 0.05$, two-way ANOVA with Tukey's multiple comparisons test; n = 6-7). Thus, this analysis further confirms that KTP-NH_2 treatment had beneficial effects on the performance of Aβ i.c.v. injected animals in long-term memory testing. Similar findings were obtained by calculated scores of the discrimination index (control: 0.43 ± 0.058; Aβ: -0.05 ± 0.091; KTP-NH_2: 0.36 ± 0.053; and Aβ + KTP-NH_2: 0.35 ± 0.039, two-way ANOVA with Tukey's multiple comparisons test; n = 6-7).

To determine whether KTP-NH_2 treatment could counteract the Aβ induced-impairments in spatial working memory, animals were subjected to the YM-SAT and their performance was assessed through the percentage of spontaneous alternation as described in methods (Figure 22 (C)). As expected, animals from Aβ group had a lower percentage of spontaneous alternation when compared with animals from the control group (Aβ: 55 ± 3.5 *vs.* control: 69 ± 2.0, $p < 0.05$, two-way ANOVA with Tukey's multiple comparisons test; n = 6-7), confirming that Aβ i.c.v. injected animals had an impairment in spatial working memory.

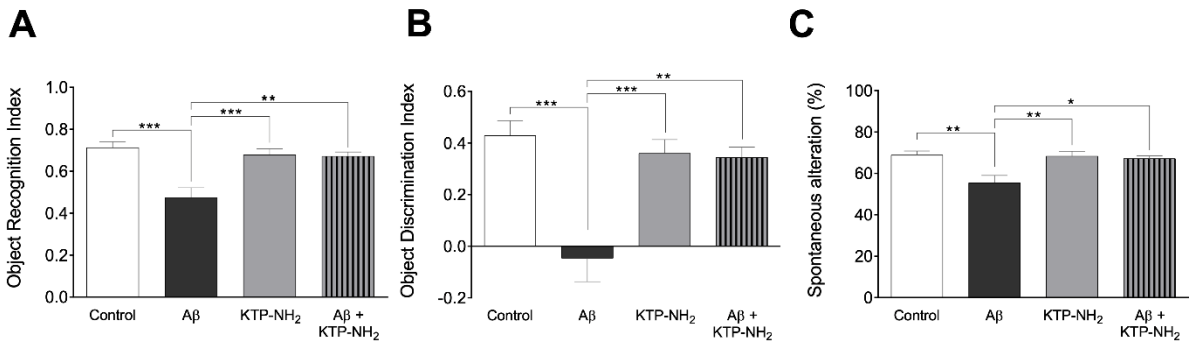

Figure 22. KTP-NH_2 treatment mitigates Aβ-induced impairments in long-term episodic memory and spatial working memory. (A) Object recognition index was calculated from the data obtained in the test day of the Novel Object Recognition test (NORT), as [novel / (novel + familiar)], and it ranges from 0 to 1 (where 1 means only exploration of the novel object and zero exploration only of the familiar object). (B) Object discrimination index was also calculated from the data obtained in the test day of NORT, as [(novel – familiar) / (novel + familiar)], and it ranges from -1 to 1, where zero means no discrimination between both objects. (C) The percentage of spontaneous alternation was calculated from data obtained during the Y-Maze Spontaneous Alternation test (YM-SAT), as actual alternations/maximum alternations x 100. For each statistical analysis, significant differences between the group of Aβ animals (n = 6) and all the other groups (n = 6-7) were assessed using two-way ANOVA followed by Tukey's multiple comparisons test. * $p < 0.05$, ** $p \leq 0.01$, *** $p \leq 0.001$. Data are represented as mean ± SEM.

However, when Aβ i.c.v. injected animals were treated with KTP-NH_2 (Aβ + KTP-NH_2 group) the percentage of spontaneous alternation in the YM-SAT (67 ± 1.3, n = 6) was similar to the control group ($p > 0.05$, two-way ANOVA with Tukey's multiple comparisons test; n = 6-7), and significantly different from that of the Aβ group ($p < 0.05$, two-way ANOVA with Tukey's multiple comparisons test; n = 6-7), implying that KTP-NH_2 treatment reduced the Aβ induced-deficits in YM-SAT. Moreover, KTP-NH_2 alone had no significant effect, since the percentage of spontaneous alternation of animals from KTP-NH_2 group (68 ± 2.4, n = 7) was not significantly different from the control group ($p > 0.05$, two-way ANOVA with Tukey's multiple comparisons test).

Performance in the NORT and in the YM-SAT can be affected by changes in locomotion, by anxiety-like behavior, or by alterations in exploratory drive. To control for these parameters, animals were assessed in the OFT. No statistically significant differences (Figure 23; $p > 0.05$, two-way ANOVA; n = 6-7) were found between any of the experimental groups when analyzing the total distance travelled (Figure 23 (A)), or the average velocity (Figure 23 (B)). In addition, the total number of entries in the YM-SAT arms was also analyzed (control: 26 ± 1.6; Aβ: 23 ± 1.5; KTP-NH_2: 25 ± 2.0; Aβ + KTP-NH_2: 21 ± 1.5), and no significant differences were found between any of the groups ($p > 0.05$, two-way ANOVA; n = 6-7). Together, these results show that neither Aβ, nor KTP-NH_2, alone or in combination, caused appreciable effects in locomotor activity that could mask performance in the NORT or YM-SAT. Similarly, no statistically significant differences ($p > 0.05$, two-way ANOVA, n = 6-7) were found between groups for the percentage of time spent in the periphery of

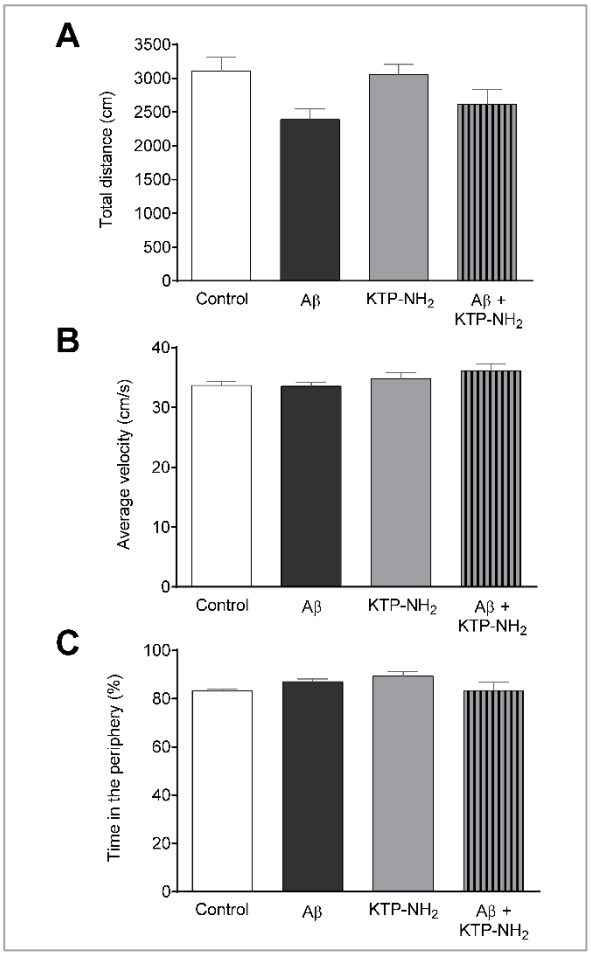

Figure 23. Neither Aβ nor KTP-NH_2 treatment affected locomotor activity or anxiety-like behaviour. Results obtained during the Open-field test performance allow the assessment of locomotor activity through the **(A)** total distance travelled (cm), and **(B)** average velocity (cm/s). **(C)** Anxiety-like behaviour was evaluated through the percentage of time spent in the periphery of the OFT. Statistical analysis using two-way ANOVA did not reveal significant differences ($p < 0.05$) between groups (n = 6-7). Data are represented as mean ± SEM.

the OFT arena (Figure 23 (C)), which also indicates an absence of appreciable changes in anxiety-like behaviour.

4.4.2. Hippocampal gliosis immediately after testing was not different among the groups

To assess if Aβ could lead to an increase in the proliferation of astrocytes and microglia at the time of testing which could suggest gliosis and thus inflammation, WB assays were performed with protein extracts obtained from hippocampal homogenates prepared upon animal sacrifice after behavioral testing. GFAP and Iba-1 were used as markers for astrocytes and microglia, respectively (Figure 24). Densitometry analyses of the WB revealed no significant changes (n=3-4; $p > 0.05$, two-way ANOVA) in samples from Aβ injected animals when compared with control and in response to KTP-NH_2 treatment, thus indicating an absence of proliferation of astrocytes or microglia.

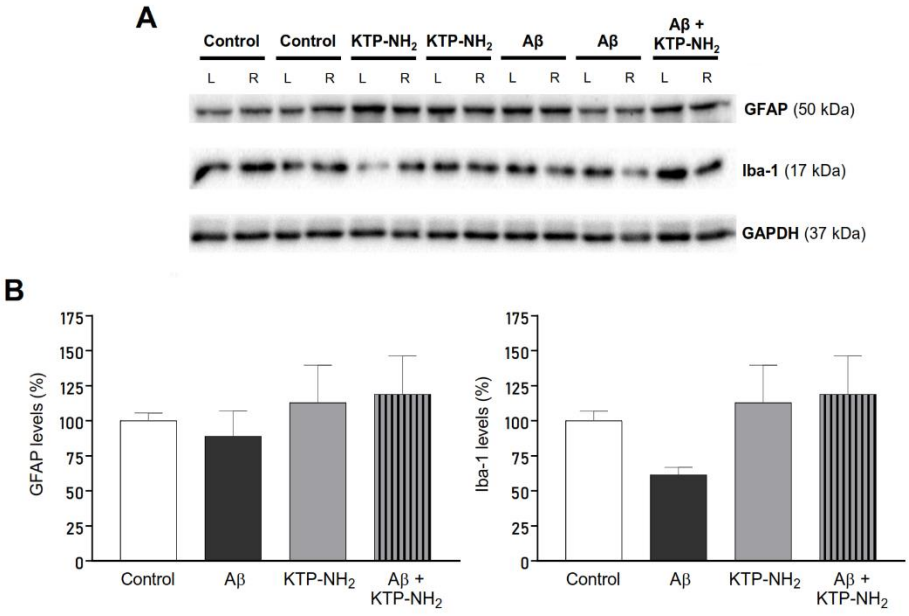

Figure 24. Neither Aβ nor KTP-NH_2 affected hippocampal gliosis assessed by immunoblotting. Protein levels were assessed by western blot using tissue homogenates from each isolated hippocampus of 13 animals, 3-4 for each experimental group (Control, KTP-NH_2, Aβ, and Aβ + KTP-NH_2). **(A)** Representative immunoblots of GFAP (50 kDa), Iba-1 (17 kDa) and GAPDH (37 kDa). GAPDH was used as a loading control. **(B)** Densitometry analysis of the right (R) (side of i.c.v injection) hippocampus, performed for all groups with ImageJ software. No statistically significant differences were found between animal groups regarding GFAP or Iba-1 immunoreactivity and ($p > 0.05$, two-way ANOVA, n = 3-4). Data are represented as mean ± SEM.

Nevertheless, since WB assay did not provide information about morphological changes of astrocytes and microglia, immunohistochemistry analysis of glial cell morphology was performed to further address this issue. As shown in Figure 25, regardless of the hippocampal area analyzed (CA1 or DG), there was no evidence of astrogliosis (evaluated by GFAP immunoreactivity) or microgliosis (evaluated by Iba-1 immunoreactivity), either in control or Aβ animals, treated or untreated with KTP-NH_2, since no morphologic differences in glial cells were noticeable.

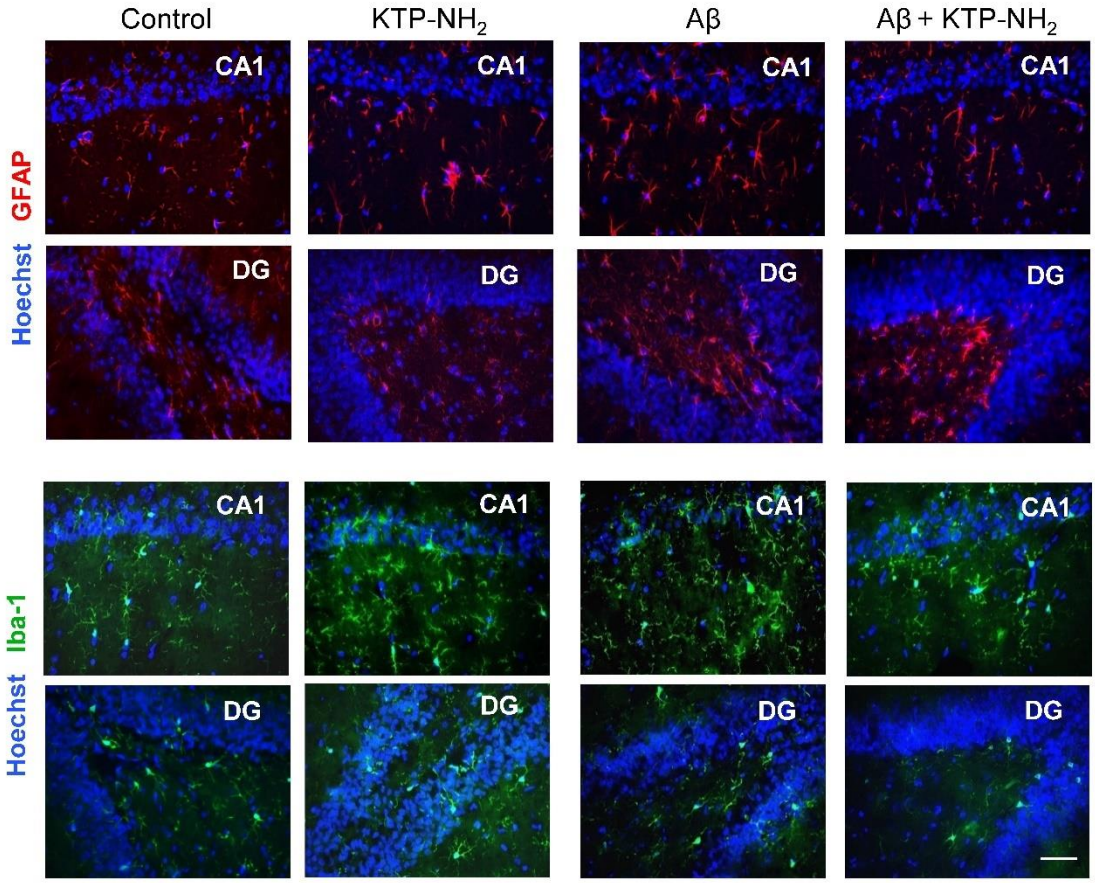

Figure 25. Neither Aβ nor KTP-NH_2 affected hippocampal gliosis assessed by immunohistochemistry labeling. At day 21, thirteen deeply anesthetized animals were transcardially perfused with ice-cold saline and 4% PFA solutions. After decapitation, brains were removed and gelatin-embedded to be sectioned on a cryostat. Coronal sections located at hippocampus level were collected and mounted for labelling with GFAP to stain astrocytes (red) and Iba-1 to stain microglia (green). Nuclei were stained with Hoechst (blue). Images of both CA1 and DG hippocampal areas were acquired on an inverted wide-field fluorescence microscope (Zeiss Axiovert 200), with a 40x objective. The figure includes representative images of each experimental group (Control, KTP-NH_2, Aβ, and Aβ + KTP-NH_2). There was no difference in GFAP or Iba-1 staining between conditions. Scale bar, 50 µm.

4.4.3. KTP-NH_2 prevented the impairment in θ-burst-induced LTP magnitude caused by Aβ

To address the synaptic mechanisms involved in the ability of KTP-NH_2 to mitigate memory impairment in animals injected with Aβ, we assessed the effect of KTP-NH_2 upon θ-burst-induced LTP in hippocampal slices that had been incubated with 200 nM $A\beta_{olig}$, a known to be toxic conformational arrangement of Aβ (Giuffrida et al., 2009).

LTP magnitude (Figure 26 (C)), recorded in slices pre-incubated with 200 nM $A\beta_{olig}$ for 3 h (Aβ) was significantly decreased when compared to that attained in control slices incubated for a similar amount of time in the absence of Aβ (control: 25.4 ± 6.15 *vs.* Aβ: -4.52 ± 6.53, $p < 0.05$, two-way ANOVA with Tukey's multiple comparisons test; n = 5-8).

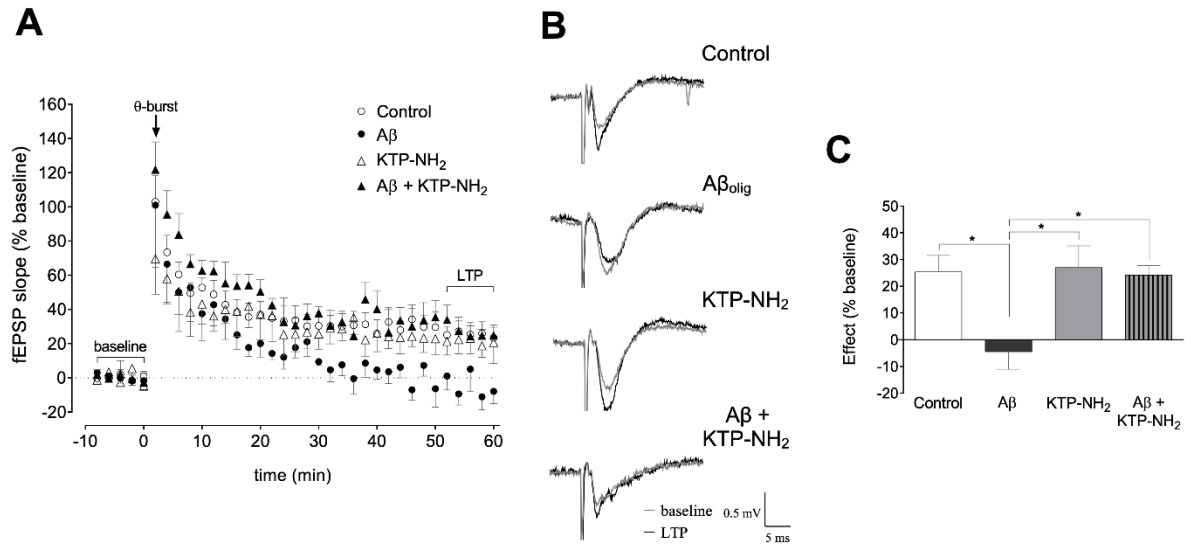

Figure 26. Incubation with KTP-NH_2 reduces the impact of Aβ on LTP magnitude upon θ-burst-induced LTP. (A) The averaged time courses changes in field excitatory postsynaptic potential (fEPSP) slope (% baseline) induced by a θ-burst stimulation in animal hippocampal slices with a pre-exposure of 3 h to aCSF solution (control, n = 8) with 200 nM $A\beta_{olig}$ (Aβ, n = 5), 50 nM KTP-NH_2 (KTP-NH_2, n = 4), or 200 nM $A\beta_{olig}$ and 50 nM KTP-NH_2 (Aβ + KTP-NH_2, n = 5). **(B)** Tracings from representative experiments. For each condition, fEPSP tracings recorded at baseline (baseline, grey line) and after θ-burst-induced LTP (LTP, black line) from the same slice are showing overlaid. **(C)** Histogram depicting the effect on LTP magnitude (% average changes in fEPSP slope at 50-60 min normalized to the defined baseline of 10 min immediately before θ-burst stimulation) regarding each group under study (control, Aβ, KTP-NH_2, Aβ + KTP-NH_2). Statistical analysis using two-way ANOVA followed by Tukey's multiple comparisons test indicates a significant difference between the Aβ condition (n = 5), and all the other groups (n = 4-8). * $p < 0.05$. Data are represented as mean ± SEM.

Remarkable, in slices co-incubated with 200 nM $A\beta_{olig}$ and 50 nM KTP-NH_2 (Aβ + KTP-NH_2), LTP magnitude (24.2 ± 3.50, n = 5) attained values similar to those in control slices ($p > 0.05$, two-way ANOVA with Tukey's multiple comparisons test; n = 5-8). Moreover, LTP magnitude in slices pre-incubated with only 50 nM KTP-NH_2 (KTP-NH_2) was similar (27.0 ± 8.10, n = 4) to that in control slices ($p > 0.05$, two-way ANOVA with Tukey's multiple comparisons test; n = 5-8). Altogether, these results clearly indicate that KTP-NH_2 prevents Aβ-induced impairment of LTP without by itself affecting LTP.

4.4.4. KTP-NH_2 prevented the decrease in spine density caused by Aβ action on cultured cortical neurons

To further investigate the synaptic correlates of the protective action of KTP-NH_2 against Aβ-induced synaptic impairment, we evaluated the effect of KTP-NH_2 on spine density of cultured cortical neurons. The conjugation between MAP2 (red) and Phalloidin (green) labels, allowed the identification of dendritic protrusions (yellow) (Figure 27 (A)), as a morphological readout of the treatment modulation of the number of dendritic spines. The representative segments of 10 µm of counted dendrites for each analysed condition are illustrated in Figure 27 (B).

In accordance with previous studies (Tanqueiro et al., 2018), cultured cortical neurons exposed to $A\beta_{25-35}$ for 24 h, showed a significant decrease in the number of dendritic protrusions when compared to the control condition (Aβ: 6.58 ± 0.153 *vs.* control: 8.07 ± 0.153; $p < 0.05$, two-way ANOVA with Tukey's multiple comparisons test; n = 5) (Figure 27 (C)). Remarkably, the Aβ-induced impairment in the number of dendritic protrusions was absent when neurons were co-treated with 50 nM KTP-NH_2 (Aβ + KTP-NH_2: 9.60 ± 0.134 *vs.* control: 8.07 ± 0.153; $p < 0.05$, two-way ANOVA with Tukey's multiple comparisons test; n = 5). KTP-NH_2 alone did not significantly alter dendritic protrusions when compared to the control condition (KTP-NH_2: 8.41 ± 0.071 *vs.* control: 8.07 ± 0.153; $p > 0.05$, two-way ANOVA with Tukey's multiple comparisons test; n = 5).

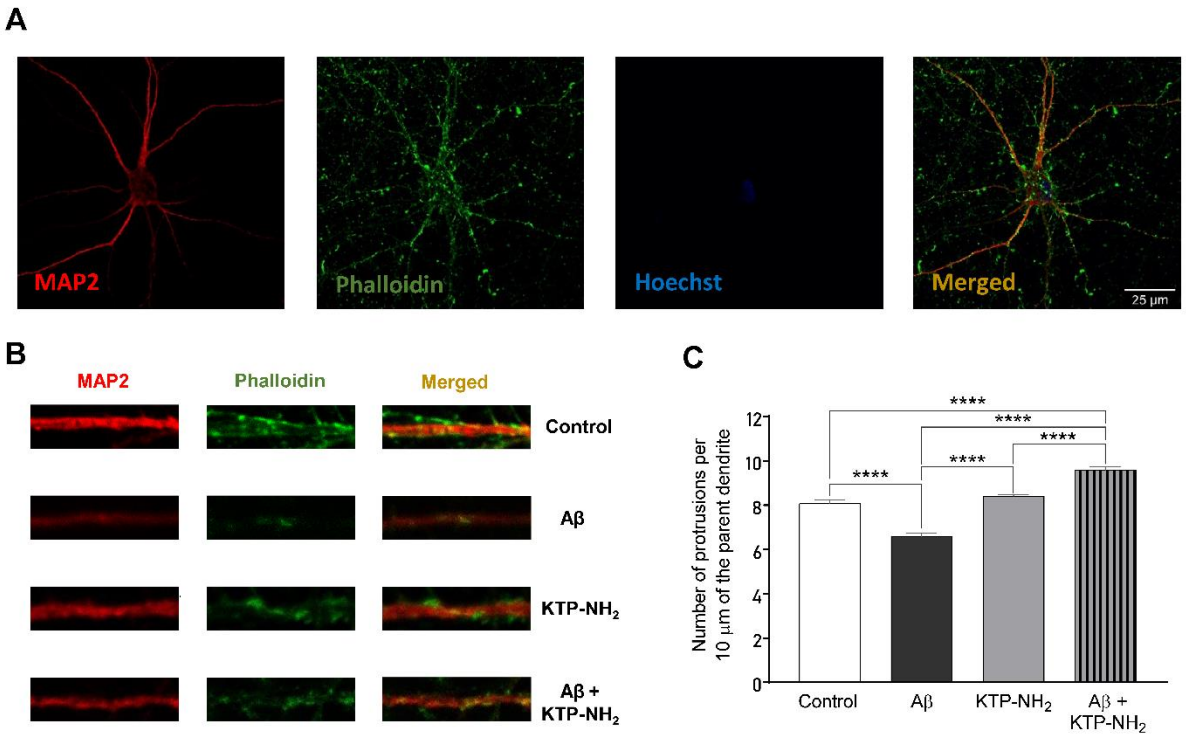

Figure 27. Incubation with KTP-NH_2 mitigates Aβ incubation-induced impairments in spine. **(A)** Representative image of an untreated neuron (control) obtained from primary neuronal cultures. Primary neuronal cultures (DIV13) were incubated with 25 µM $Aβ_{25-35}$ and/or with 50 nM KTP-NH_2 for 24 h. MAP2 (red) specifically labels neurons, while phalloidin (green) labels F-actin. The merge between both labels (yellow) allows the identification of dendritic protrusions. To evaluate spine density, the number of protrusions *per* 10 µm of the parent dendrite with a distance of 25 µm from the cell body were counted (3 parent dendrites *per* neuron, 6 neurons *per* condition). **(B)** Treatment effects on synaptic density (10 µm). **(C)** Histogram depicting spine density as the number of protrusions from each condition. Statistical analysis using two-way ANOVA followed by Tukey's multiple comparisons test indicates a significant difference between conditions (n = 5). While 25 µM $Aβ_{25-35}$ treatment (Aβ) diminished the number of protrusions in cortical neurons, 50 nM KTP-NH_2 co-treatment (Aβ + KTP-NH_2) restored spine density. In addition, 50 nM KTP-NH_2 treatment (KTP-NH_2) did not, by itself, impact spine density. **** $p \leq 0.0001$. Data are represented as mean ± SEM.

4.5. Discussion

A main finding in the present work is that systemically applied KTP-NH_2 prevents memory dysfunction induced by Aβ. At the synaptic level we could demonstrate that KTP-NH_2 prevents synaptic plasticity and spine density impairments caused by Aβ, suggesting that KTP-NH_2 mitigates memory deficits by protecting hippocampal synapses against Aβ-induced toxicity.

Since the hippocampus is required for performance in the NORT (Goulart et al., 2010), this test has been considered a useful tool for basic and preclinical research in the context of AD (Rajagopal et al., 2014). In addition, the sustained strengthening of synaptic connections that characterizes hippocampal long-term potentiation (LTP) is taken as a synaptic correlate of the basic mechanisms involved in memory and learning processes (Bliss and Collingridge, 1993). Accordingly, abnormal performance in memory tasks, especially hippocampal-dependent ones (Figurov et al., 1996; Korte et al., 1998; Pang and Lu, 2004), are associated with impairments in LTP (Morris et al., 1986). Our data showing that KTP-NH_2 prevented the Aβ-induced impairment of hippocampal LTP, strongly suggest that the reestablishment of synaptic plasticity is one of the mechanisms underlying the cognitive actions of KTP-NH_2. Furthermore, at a molecular level, neuronal spine density has been associated with synaptic reinforcement during LTP (Luscher and Malenka, 2012; Toni et al., 1999). In fact, spine density is known to be reduced in cultured cortical neurons incubated with Aβ peptide (Tanqueiro et al., 2018). Our results show that KTP-NH_2 restores Aβ-induced decrease in spine density, further explaining its neuroprotective actions upon synaptic plasticity. These results pave the way for further studies on the mechanism of action of KTP-NH_2 addressing if it reestablishes spine density *in vivo*.

While the presence of episodic memory impairments mimics the clinical hallmarks detected in AD patients in the early stages of the disease (Alescio-Lautier et al., 2007; Gold and Budson, 2008; Huntley and Howard, 2010), motor dysfunctions are better noticed in moderate to severe stages of AD (Zidan et al., 2012). In the present work, we could detect episodic memory dysfunctions through the YM-SAT and NORT, without signs of clear motor dysfunctions, judged by OFT performance. This indicates that the sporadic AD model used mostly mimics the earlier stages of AD. It is known that loss of synapses, mainly in the hippocampus, is one of the earliest consequences of Aβ toxicity (Canas et al., 2009), and that this loss correlates with the initial memory impairments in AD patients (Coleman et al., 2004). Furthermore, compared to the transgenic models of AD available, the use of this sporadic AD model, where the Aβ injection is responsible for the induced-pathophysiological traits of AD, allows us to have a direct understanding of the effect of KTP-NH_2 administration

on the Aβ-induced dysfunction. Our findings that systemic administration of KTP-NH_2 is able to prevent memory loss as well as synaptic plasticity dysfunctions induced by Aβ, highlight the therapeutic potential of BBB permeable KTP analogues in early stages of AD. This may gain particular relevance since the few therapeutic tools so far available for early disease stages are mostly symptomatic to increase cholinergic function. As we show, the KTP derivative is able to enhance synaptic plasticity and, importantly, to prevent retraction of dendritic spines in cultured neurons, thus to prevent synaptic atrophy, a clear sign of neuroprotective ability.

KTP biosynthesis occurs in the nerve terminals (Ueda et al., 1986b), which is especially relevant in AD pathophysiology, where the loss of cortical mass evolves fast during the early stages of the disease (Sabuncu et al., 2011). This cellular death implies less KTP production capability, resulting in a decrease of KTP concentration in the CSF of AD patients (Santos et al., 2013). Accordingly, the increase of KTP levels in the brain emerged as a possible therapeutic tool for AD treatment. However, KTP has pharmacokinetic hindrances, such as its limited capacity to cross the BBB and its high susceptibility to clearance mechanisms, which hampered its clinical use (Serrano et al., 2014b). Our work shows that it is possible to circumvent this problem by using a BBB permeant KTP analogue, KTP-NH_2. The introduced structural change increased the peptide global net charge, increasing its capacity to interact with biological membranes, most notably giving it the ability to cross the BBB (Ribeiro et al., 2011a).

Besides having an acute and chronic well-characterized analgesic-profile when systemically administrated (Ribeiro et al., 2011b, 2011a), this small and cost-effective molecule also showed a remarkable anti-inflammatory effect. Accordingly, independent studies developed by our lab showed that KTP-NH_2 impacts the glucocorticoid system, which might account for the molecular link between analgesia, anti-inflammation, and neuroprotection (Perazzo et al., 2017b). Neuroinflammation caused by Aβ has been commonly linked to the presence of gliosis and, in some studies, to neuronal damage. In the present work, gliosis was evaluated on day 21 after Aβ i.c.v. injection by both immunohistochemistry and western blotting and, in agreement with previous data (Canas et al., 2009), no significant signs of astrogliosis nor microgliosis were detected in the hippocampus. However, it is important to highlight that the peak of the inflammatory response after Aβ injection is one week after injection (McLarnon, 2014). So, we cannot discard initial Aβ-induced neuroinflammation nor an influence of KTP-NH_2 that may have occurred before memory assessment. Nevertheless, our results show that at least immediately after memory testing, there were no signs of gliosis.

In summary, we clearly show that, in a sporadic AD model, systemic administration of KTP-NH_2 protects spatial working- and episodic memory, without affecting motor activity or

inducing anxiety-like behavior. Moreover, KTP-NH_2 prevented Aβ-induced deficits in LTP magnitude and in spine density. We, therefore, highlight a neuroprotective action of KTP-NH_2 against the early stages of AD pathophysiology. While these results are promising as far as pharmacodynamics is concerned, they clearly push towards the need of further studies on the pharmacokinetics of KTP-NH_2 after its systemic administration through different routes, as well as to the need of other studies directed towards other hallmarks of AD. Indeed, in light of the complex pathophysiology of AD, it is important to know whether KTP-NH_2 has a greater potential as a standalone treatment, or rather as part of a broader multidrug treatment regimen.

Chapter 5

Conclusion and Future Perspectives

5.1. Conclusion

This study collected new evidence of KTP and KTP-NH_2 neuromodulatory effects in synaptic function. These peptides were studied not only under non-pathological conditions but also under Aβ-induced AD pathophysiological condition, which provided cumulative insights for their possible use in AD treatment.

Firstly, the characterization between both peptides demonstrates significant differences between their action, especially on their neuroprotective role against Aβ-induced impairments, which were partially unexpected. Briefly, despite both peptides showed a protective action against the decreasing in dendritic spines density of cortical cultured neurons induced by Aβ peptide, only KTP-NH_2 was able to counteracts Aβ-induced impairments on hippocampal LTP. Moreover, apart from slightly differences assessed on basal synaptic transmission, at the studied concentration of 50 nM, both peptides did not impact synaptic physiological functions. This lack of side effects increases their pharmacological attractiveness. These findings highlight the inherent concerns in adapting existing molecules with attractive functions to develop new drugs. The KTP-NH_2 exemplifies that changing the original molecular structure to add or enhance specific characteristics can affect its primordial function. However, the urgent need to find new drugs with a clinical application prioritize studies using synthetic drugs with functional impacts. These functional studies using the new synthetic derivatives can be conducted even before the full understanding of their mechanism of action. Interestingly, studying the effectiveness of a drug in the relief of specific symptoms of a disease can offer new insights regarding the disease itself, the drug action, or both. Nonetheless, the exhaustive study of the original molecule that inspired the production of synthetic derivatives should not be neglected to uncover its mechanisms of action and endogenous function.

Although the massive efforts of the scientific community to unravel the pathophysiological mechanisms of AD, much are yet to be discovery. It is now clear that AD is a very complex and multifactorial disease, which progresses silently many years before the emergence of the first symptoms. In fact, when the first cognitive symptoms appear and patients are diagnosed, the majority of molecular damage (most likely to be unreversible) is already settled. Therefore, not only the treatment time-window should be swift into the early years of the disease progression, but also a more holistic approach should be considered to treat the upcoming patients that are still cognitively healthy. Moreover, given that several neurodegenerative disorders share common symptoms, prospective studies are needed to develop new tools to correctly predict patients' prognosis and promptly reveal which diseases a given person will likely have in the future.

Ageing is a crucial risk factor for the development of several disorders, including neurological disorders such as AD. Apart of encouraging people to adopt and to maintain a healthier lifestyle, where having good eating and sleeping habits, as well as being physical and mental active are considered the pillars, the use of some pharmacologic drugs with a preventive role on the onset of some diseases is already being a common practice. For instance, using low doses of acetylsalicylic acid to prevent cardiovascular diseases (Truong, 2015). Furthermore, elderlies are usually under a heavier pharmacological regimen mainly due to common comorbidities, and pharmacological interaction cannot be lightly discarded (Boparai and Korc-Grodzicki, 2011). As such, drugs with multiple proposes can offer a solution to target symptoms with similar origins or that are commonly manifested together.

In that sense, KTP-related drugs can emerge as a pharmacological solution. Although additional studies are still needed to fully understand the therapeutic value of these peptides, KTP-NH_2 already presented remarkably results as an analgesic molecule, with anti-inflammatory properties, and an impressive neuroprotective role. In fact, KTP-NH_2 had a neuroprotective effect against Aβ-induced memory impairments associated to AD pathophysiology. The systemic administration of KTP-NH_2 in a sporadic AD model revealed to be crucial for the protection of spatial working memory and episodic memory, without affecting motor activity or inducing anxiety-like behavior in animals. In addition, this work reported that the neuroprotective action of KTP-NH_2 presumably acted in the prevention of Aβ-induced deficits in LTP magnitude and spine density (Chapter 4).Thus, the molecular findings presented in this work regarding KTP-NH_2 neuroprotective effect in Aβ-induced AD pathophysiology (Chapter 3) supported the neuroprotective results obtained through its systemic administration in a rat model of sporadic AD (Chapter 4), which provided important evidence for the use of KTP-NH_2 as a drug for AD treatment.

In summary, this work paves the way for future studies comparing KTP and KTP-NH_2 effects in CNS and, more specifically, for studying new applications regarding KTP-NH_2 neuroprotective action. As such, to identify the therapeutic time-window for using KTP-NH_2 in the treatment of AD will allow us to better understand whether the action of this peptide relies on the prevention, or on the recovery, of molecular and cognitive deficits present in AD pathophysiology. Moreover, the characterization of KTP-NH_2 effect in the AD-specific inflammatory process can also provide new evidence for how this peptide protects against Aβ-induced deficits. Finally, it is remarkable that in small molecules such as dipeptides, a unique change on their structure can severely impact their function. In that sense, studying both molecular structures and its physical-chemical properties can reveal which of them are of utmost important for the desirable effects.

5.2. Future Perspectives

Despite this work unveiled some interesting findings, several questions remained to be answered. As such, during this work, I also participated in additional KTP-related projects of which I will present next.

5.2.1. KTP-NH_2 treatment in 5xFAD transgenic mice model of AD

To better understand the neuroprotective role of KTP-NH_2 in AD, we designed an *in vivo* study to evaluate the effect of chronical treatment of KTP-NH_2 in a 5xFAD transgenic AD mice model. This AD model is characterized by having five AD-related mutations expressed in two human transgenes: the Swedish (K670N/M671L), Florida (I716V), and London (V717I) mutations in *APP* gene, and the M146L and L286V mutations in *PSEN1* gene (5xFAD (B6SJL) | Alzforum, 2019). Accordingly, these animals are expected to rapidly develop severe amyloid pathology, starting to manifest cognitive symptoms at 4-months old.

A colony of this 5xFAD model was stablished at Rodent Facility of iMM, FMUL. The handling of animals and all the applied procedures were conducted according to the European Community (86/609/EEC; 2010/63/EU; 2012/707/EU) and Portuguese (DL 113/2013) legislation for the protection of animals used for scientific purposes, and they were approved by the Ethical Committee for Animal Research of iMM, FMUL, and the Portuguese Competent Authority for Animal Welfare (DGAV) in Portugal.

Briefly, animals of 4-months old underwent a chronic treatment regimen of KTP-NH_2 (32.3 mg/Kg in saline solution, single i.p. dose/day) or of the respective saline solution, for at least 10 weeks (except weekends), and until animals' sacrifice. A battery of behavioral tests was applied to all animals to evaluate memory and learning processes, among others. These tests were applied when animals were 6-month-old, having received the treatment for about 1.5 months. Then, animals were sacrificed, and the brain collected. In some animals, the hippocampus was isolated and acute hippocampal slices were prepared for conducting electrophysiological recordings, such as LTP. The remaining brain areas were independently dissected (hippocampus, cortex, striatum, brainstem, and cerebellum), raised in PBS, and rapidly frozen for future molecular studies. Alternatively, some animals were perfused transcardially with PBS solution, followed by a 4% PFA solution, their brains removed, and half hemisphere was used to dissect and isolate the brain areas as before, and the other half was maintained intact, and its tissue was prepared for immunohistochemistry studies. All animal tissue was stored at -80ºC for future use. Tail's samples of all animals were collected to confirm animals' genotype, which was performed by polymerase chain reaction (PCR).

Although all behavioral and electrophysiological experiments were concluded by the time that this dissertation was written, due to time constrains, the results are still being carefully

analyzed and they were not included in this thesis. Nevertheless, we are now planning the remaining molecular analysis, such as protein levels quantification by western-blot and immunohistochemistry analysis, to study the impact of this KTP-NH_2 treatment in synaptic functions and neuroinflammation processes of this model. Finally, we expect that the results of this study will offer some additional evidence to better understand the KTP-NH_2-induced neuroprotective effect. As such, we aimed to perceived if the chronical treatment of KTP-NH_2 is able to sustain, at some level, its appreciated neuroprotective effect to counteract the cognitive deficits onset or the worsening of them through disease progression in the 5xFAD model. Moreover, the molecular studies will be used to assess the anti-inflammatory potential of KTP-NH_2 in the Aβ-induced inflammation.

5.2.2. Effect of KTP and KTP-NH_2 in Aβ-induced inflammatory *in vitro* models

Given that KTP-NH_2 has an anti-inflammatory action with a proposed dual mechanism regarding the glucocorticoid-mediated effect or its independent mechanism (Perazzo et al., 2017b), exploring KTP and KTP-NH_2 impact in Aβ-induced inflammatory can reveal additional insights regarding KTP-NH_2 neuroprotective effect. As such, the use of *in vitro* Aβ-induced inflammatory models using neuronal cortical cultures and co-cultures of astrocytes and microglia offer the opportunity to study the impact of both peptides on an induced inflammatory environment, which can be related with AD-specific inflammation (Dansokho and Heneka, 2018). Specifically, the expected astrogliosis and microgliosis phenomena can be evaluated, as well as their progression followed overtime, through the molecular quantification of inflammatory biomarkers using western-blot, immunocytochemistry, and/or ELISA assays. Unfortunately, this study was not started due to time constrains.

5.2.3. Structural relevance of KTP-related drugs

As briefly mentioned, see previous section Synthetic derivatives, KTP and its derivatives are essential composed by two a.a. (in *L*- or *D*-form), linked to small chemical relevant groups or other larger molecules. To better understand if the observed functional effects of KTP and KTP-NH_2 are precisely obtained due to their chemical structure (*L*-Tyr-*L*-Arg-OH and *L*-Tyr-*L*-Arg-NH_2, respectively), or are a direct consequence of the chemical properties of the a.a. included in their structures, other dipeptides were study (Figure 28 (C)). As such, six new dipeptides were synthetized as the following:

- Tyrosine-Lysine (*L*-Tyr-*L*-Lys). Changing the arginine (Figure 28 (B)) by other similar cationic a.a., such as the lysine (Figure 28 (B)), kept a similar chemical structure. However, the lack of arginine prevents the Arg-induced NO production. Thus, studying these peptides in the context of analgesia will offer new evidence to better

understand the role of KTP in NO production (more about this topic in previous section Nitric Oxide);

- Phenylalanine-Arginine (*L*-Phe-*L*-Arg). The substitution of tyrosine by another phenolic a.a. removed the similarities with morphine (Figure 28 (A)), but maintained the phenolic ring.
- Phenylalanine--Lysine (*L*-Phe-*L*-Lys). These peptides included both explained changes.

Note that the amidated form of all above mentioned peptides were also synthesize for a comparison study: *L*-Tyr-*L*-Lys-NH_2, *L*-Phe-*L*-Arg-NH_2, and *L*-Phe-*L*-Lys-NH_2. Additionally, KTP, KTP-NH_2, and KTP_{ant} were also synthesized. Interestingly, KTP_{ant} (Leucine-Arginine, *L*-Leu-*L*-Arg) only differed from KTP in one a.a. - the leucine, that, unlike tyrosine and phenylalanine, does not present a phenolic ring, not sharing a similar structure. Furthermore, as an attempted to study the peptides' interaction with cell membranes and their possible intracellular trajectory, additional peptides were synthetized. As such, a fluorophore, the $Quasar_{570}$, was used to label KTP, KTP-NH_2 and KTP_{ant}, allowing their identification by confocal microscopy. However, the fluorophore addition not only doubled the final size of peptides, but it also changed their hydrophobic properties.

Preliminary MTT results, using undifferentiated SHY-Y5Y neuroblastoma cells incubated with not only these six peptides, but also KTP, KTP-NH_2 and KTP_{ant}, indicated that, regardless of the applied concentration (5 nM, 50 nM, 500 nM, 5 µM), or incubation period (30 min, 2 h, 4 h, and 24 h), these peptides did not induce significant toxicity. Additionally, an exploratory imaging experiment with undifferentiated SHY-Y5Y neuroblastoma cells incubated for 30 min with the $Quasar_{570}$-labeled KTP, KTP-NH_2 or KTP_{ant}, revealed lower level of fluorescence in cells incubated with KTP. These results can be partially explained by the differences between peptides capability to enter inside cells.

Additionally, these preliminary findings were obtained with a reduce number of independent samples (N=3), and they need to be supported with additional control experiments to confirm the suggested findings. As such, these reasons were taken into consideration for not include them in this dissertation.

Note that, all of this work was developed during a two-month internship at Dr. David Andreu's Laboratory, Universitat Pompeu Fabra, Barcelona Biomedical Research Park (Barcelona), with the help of Dr. Javier Valle and Dr. Clara Pérez-Peinado.

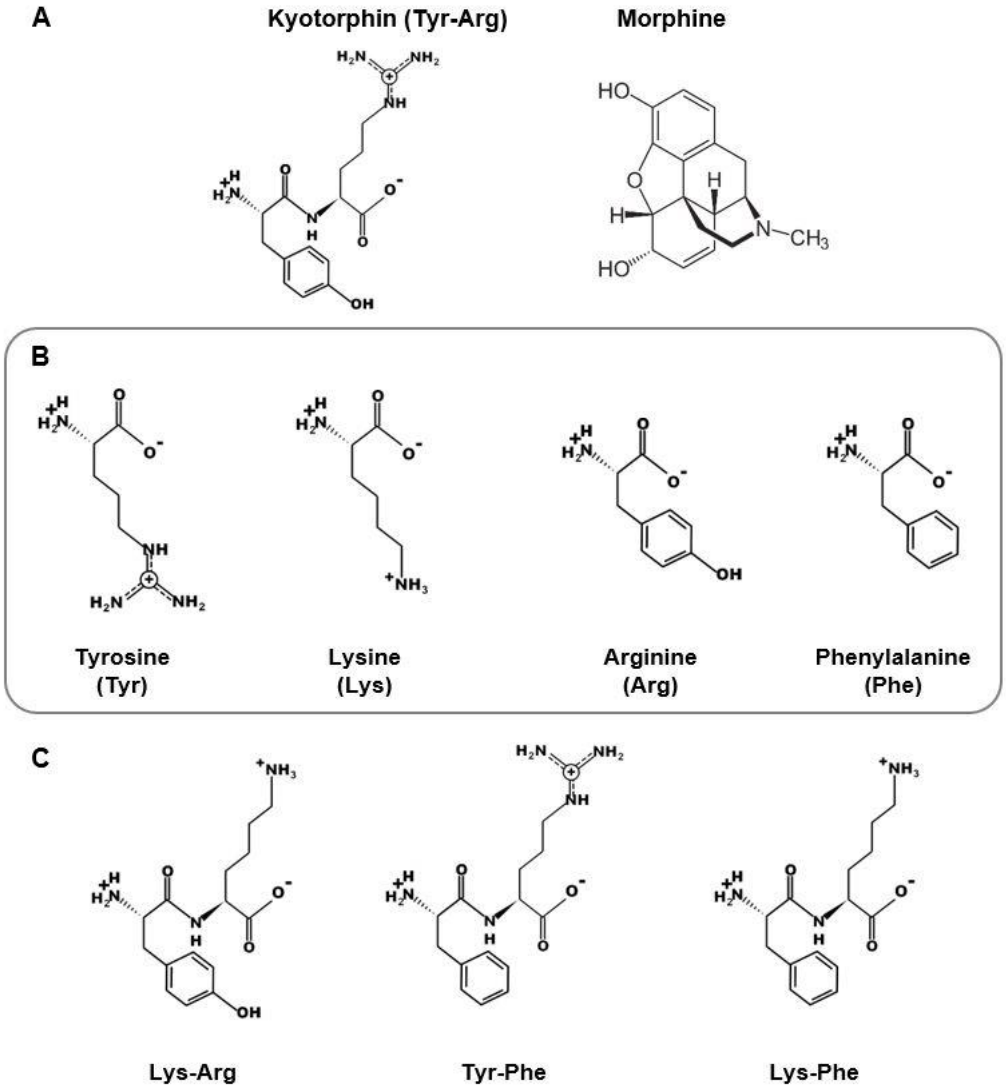

Figure 28. Chemical structure of synthetized peptides and their aminoacids. (A) Kyotorphin (KTP) and morphine; **(B)** The four aminoacids used to synthetize the studied peptides; **(C)** Studied peptides. Figures were obtained using PepDraw (Freeman, 2015) and (Wikimedia Foundation, 2021); Tyr-Arg – Kyotorphin; Tyr – Tyrosine; Lys – Lysine; Arg – Arginine; Phe – Phenylalanine.

Chapter 6

References

5xFAD (B6SJL) | Alzforum. Alzforum 2019. https://www.alzforum.org/research-models/5xfad-b6sjl (accessed September 7, 2021).

Akasaki K, Nakamura A, Shiomi H, Tsuji H. Identification and characterization of two distinct kyotorphin-hydrolyzing enzymes in rat brain. Neuropeptides 1991;20:103–7. https://doi.org/10.1016/0143-4179(91)90059-R.

Akasaki K, Tsuji H. An Enkephalin-Degrading Aminopeptidase from Rat Brain Catalyzes the Hydrolysis of a Neuropeptide, Kyotorphin (L-Tyr-L-Arg). Chem Pharm Bull (Tokyo) 1991;39:1883–5. https://doi.org/10.1248/cpb.39.1883.

Akasaki K, Yoshimoto H, Nakamura A, Shiomi H, Tsuji H. Purification and Characterization of a Major Kyotorphin-Hydrolyzing Peptidase of Rat Brain1. J Biochem (Tokyo) 1995;117:897–902. https://doi.org/10.1093/oxfordjournals.jbchem.a124793.

Albensi BC, Oliver DR, Toupin J, Odero G. Electrical stimulation protocols for hippocampal synaptic plasticity and neuronal hyper-excitability: Are they effective or relevant? Exp Neurol 2007;204:1–13. https://doi.org/10.1016/j.expneurol.2006.12.009.

Alescio-Lautier B, Michel BF, Herrera C, Elahmadi A, Chambon C, Touzet C, et al. Visual and visuospatial short-term memory in mild cognitive impairment and Alzheimer disease: Role of attention. Neuropsychologia 2007;45:1948–60. https://doi.org/10.1016/j.neuropsychologia.2006.04.033.

Alois Alzheimer Biography. Biogr Website 2016. https://www.biography.com/people/alois-alzheimer-21216461 (accessed August 17, 2021).

Alonso M, Medina JH, Pozzo-Miller L. ERK1/2 activation is necessary for BDNF to increase dendritic spine density in hippocampal CA1 pyramidal neurons. Learn Mem Cold Spring Harb N 2004;11:172–8. https://doi.org/10.1101/lm.67804.

Alzheimer's Association. 2020 Alzheimer's disease facts and figures. Alzheimers Dement 2020;16:391–460. https://doi.org/10.1002/alz.12068.

Alzheimer's Association. 2019 Alzheimer's Disease Facts and Figures. Alzheimers Dement 2019 2019;15:321–87.

Anderson WW, Collingridge GL. The LTP Program: a data acquisition program for on-line analysis of long-term potentiation and other synaptic events. J Neurosci Methods 2001;108:71–83. https://doi.org/10.1016/S0165-0270(01)00374-0.

Angelova H, Pechlivanova D, Dzhambazova E, Landzhov B. Effects of kyotorphin on the early behavioural and histological changes induced by an experimental model of Alzheimer's disease in rats. Comptes Rendus Acad Bulg Sci 2018;71:424–30. https://doi.org/10.7546/CRABS.2018.03.16.

Angelova H, Pechlivanova D, Krumova E, Miteva-Staleva J, Kostadinova N, Dzhambazova E, et al. Moderate protective effect of Kyotorphin against the late consequences of intracerebroventricular streptozotocin model of Alzheimer's disease. Amino Acids 2019. https://doi.org/10.1007/s00726-019-02784-5.

Antunes M, Biala G. The novel object recognition memory: neurobiology, test procedure, and its modifications. Cogn Process 2012;13:93–110. https://doi.org/10.1007/s10339-011-0430-z.

Area-Gomez E, de Groof A, Bonilla E, Montesinos J, Tanji K, Boldogh I, et al. A key role for MAM in mediating mitochondrial dysfunction in Alzheimer disease. Cell Death Dis 2018;9:335. https://doi.org/10.1038/s41419-017-0215-0.

Area-Gomez E, Schon EA. On the Pathogenesis of Alzheimer's Disease: The MAM Hypothesis. FASEB J 2017;31:864–7. https://doi.org/10.1096/fj.201601309.

Arima J, Uesugi Y, Uraji M, Iwabuchi M, Hatanaka T. Dipeptide Synthesis by an Aminopeptidase from Streptomyces septatus TH-2 and Its Application to Synthesis of Biologically Active Peptides. Appl Environ Microbiol 2006;72:4225–31. https://doi.org/10.1128/AEM.00150-06.

Arima T. Kyotorphin (L-tyrosyl-L-arginine) as a possible substrate for inducible nitric oxide synthase in rat glial cells. Neurosci Lett 1996;212:1–4.

Arima T, Kitamura Y, Nishiya T, Takagi H, Nomura Y. Kyotorphin (l-tyrosyl-l-arginine) as a possible substrate for inducible nitric oxide synthase in rat glial cells. Neurosci Lett 1996;212:1–4. https://doi.org/10.1016/0304-3940(96)12758-0.

Axelrod J, Gordon E, Hertting G, Kopin IJ, Potter LT. On the mechanism of tachyphylaxis to tyramine in the isolated rat heart. Br J Pharmacol Chemother 1962;19:56–63. https://doi.org/10.1111/j.1476-5381.1962.tb01426.x.

Bailey KR, Crawley JN. Anxiety-Related Behaviors in Mice. In: Buccafusco JJ, editor. Methods Behav. Anal. Neurosci. 2nd ed., Boca Raton (FL): CRC Press/Taylor & Francis; 2009.

Bali J, Gheinani AH, Zurbriggen S, Rajendran L. Role of genes linked to sporadic Alzheimer's disease risk in the production of β-amyloid peptides. Proc Natl Acad Sci 2012;109:15307–11. https://doi.org/10.1073/pnas.1201632109.

Barhoumi R, Qian Y, Burghardt RC, Tiffany-Castiglioni E. Image analysis of Ca2+ signals as a basis for neurotoxicity assays: Promises and challenges. Neurotoxicol Teratol 2010;32:16–24. https://doi.org/10.1016/j.ntt.2009.06.002.

Bekris LM, Yu C-E, Bird TD, Tsuang DW. Genetics of Alzheimer Disease. J Geriatr Psychiatry Neurol 2010;23:213–27. https://doi.org/10.1177/0891988710383571.

Belo RF, Martins MLF, Shvachiy L, Costa-Coelho T, de Almeida-Borlido C, Fonseca-Gomes J, et al. The Neuroprotective Action of Amidated-Kyotorphin on Amyloid β Peptide-Induced Alzheimer's Disease Pathophysiology. Front Pharmacol 2020;11:985. https://doi.org/10.3389/fphar.2020.00985.

Benyamin R, Trescot AM, Datta S, Buenaventura R, Adlaka R, Sehgal N, et al. Opioid complications and side effects. Pain Physician 2008;11:S105-120.

Berger UV, Hediger MA. Distribution of peptide transporter PEPT2 mRNA in the rat nervous system. Anat Embryol (Berl) 1999;199:439–49. https://doi.org/10.1007/s004290050242.

Binder DK, Scharfman HE. Brain-derived neurotrophic factor. Growth Factors Chur Switz 2004;22:123–31. https://doi.org/10.1016/j.bbi.2008.05.010.

Birks J, Grimley Evans J, Iakovidou V, Tsolaki M. Rivastigmine for Alzheimer's disease. In: The Cochrane Collaboration, editor. Cochrane Database Syst. Rev., Chichester, UK: John Wiley & Sons, Ltd; 2009, p. CD001191.pub2. https://doi.org/10.1002/14651858.CD001191.pub2.

Birks J, Harvey RJ. Donepezil for dementia due to Alzheimer's disease. Cochrane Database Syst Rev 2006. https://doi.org/10.1002/14651858.CD001190.pub2.

Blennow K, Zetterberg H. Biomarkers for Alzheimer's disease: current status and prospects for the future. J Intern Med 2018;284:643–63. https://doi.org/10.1111/joim.12816.

Bliss TV, Collingridge GL. A synaptic model of memory: long-term potentiation in the hippocampus. Nature 1993;361:31–9. https://doi.org/10.1038/361031a0.

Bobkova N, Vorobyov V. The brain compensatory mechanisms and Alzheimer′s disease progression: a new protective strategy. Neural Regen Res 2015;10:696. https://doi.org/10.4103/1673-5374.156954.

Bocheva AI, Dzambazova E, Pajpanova TI. Is nitric oxide involved in the antinociceptive effects of kyotorphin, Tyr-Cav and MIF's analogues in rats? Collect. Symp. Ser., Prague: Institute of Organic

Chemistry and Biochemistry, Academy of Sciences of the Czech Republic; 2003, p. 1–3. https://doi.org/10.1135/css200306001.

Bocheva AI, Dzambazova-Maximova EB. Effects of kyotorphin and analogues on nociception and pentylenetetrazole seizures. Folia Med (Plovdiv) 2004;46:40–4.

Bocheva AI, Lazarova M. Involvement of nitric oxide in the nociception of kyotorphin, TYR-CAV and MIF-s analogues in the rat spinal cord. Methods Find Exp Clin Pharmacol 2003;25:91. https://doi.org/10.1358/mf.2003.25.2.723682.

Bondi MW, Edmonds EC, Salmon DP. Alzheimer's Disease: Past, Present, and Future. J Int Neuropsychol Soc 2017;23:818–31. https://doi.org/10.1017/S135561771700100X.

Boparai MK, Korc-Grodzicki B. Prescribing for Older Adults. Mt Sinai J Med J Transl Pers Med 2011;78:613–26. https://doi.org/10.1002/msj.20278.

Borsook D. Neurological diseases and pain. Brain 2012;135:320–44. https://doi.org/10.1093/brain/awr271.

Braak H, Braak E. Neuropathological stageing of Alzheimer-related changes. Acta Neuropathol (Berl) 1991;82:239–59. https://doi.org/10.1007/BF00308809.

Broadhurst PL. Determinants of emotionality in the rat: II. Antecedent factors*. Br J Psychol 1958;49:12–20. https://doi.org/10.1111/j.2044-8295.1958.tb00632.x.

Broadhurst PL. Determinants of emotionality in rat: I. Situational factors. Br J Psychol 1957;48:1–12. https://doi.org/10.1111/j.2044-8295.1957.tb00594.x.

Bronnikov G, Dolgacheva L, Zhang S-J, Galitovskaya E, Kramarova L, Zinchenko V. The effect of neuropeptides kyotorphin and neokyotorphin on proliferation of cultured brown preadipocytes. FEBS Lett 1997;407:73–7. https://doi.org/10.1016/S0014-5793(97)00298-6.

Bronnikov GE, Kolaeva SG, Dolgacheva LP, Kramarova LI. Kyotorphin suppresses proliferation and Ca2+ signaling in brown preadipocytes. Bull Exp Biol Med 2006;141:223–5. https://doi.org/10.1007/s10517-006-0133-0.

Budni J, Bellettini-Santos T, Mina F, Garcez ML, Zugno AI. The involvement of BDNF, NGF and GDNF in aging and Alzheimer's disease. Aging Dis 2015;6:331–41. https://doi.org/10.14336/AD.2015.0825.

Burke RE. Synaptic efficacy and the control of neuronal input-output relations. Trends Neurosci 1987;10:42–5. https://doi.org/10.1016/0166-2236(87)90124-X.

Calabrese EJ, Baldwin LA. U-Shaped Dose-Responses in Biology, Toxicology, and Public Health. Annu Rev Public Health 2001;22:15–33. https://doi.org/10.1146/annurev.publhealth.22.1.15.

Calignano A, Moncada S, Di Rosa M. Endogenous nitric oxide modulates morphine-induced constipation. Biochem Biophys Res Commun 1991;181:889–93. https://doi.org/10.1016/0006-291X(91)91274-G.

Canas PM, Porciuncula LO, Cunha GMA, Silva CG, Machado NJ, Oliveira JMA, et al. Adenosine A2A Receptor Blockade Prevents Synaptotoxicity and Memory Dysfunction Caused by -Amyloid Peptides via p38 Mitogen-Activated Protein Kinase Pathway. J Neurosci 2009;29:14741–51. https://doi.org/10.1523/JNEUROSCI.3728-09.2009.

Canevelli M, Piscopo P, Talarico G, Vanacore N, Blasimme A, Crestini A, et al. Familial Alzheimer's disease sustained by presenilin 2 mutations: Systematic review of literature and genotype–phenotype correlation. Neurosci Biobehav Rev 2014;42:170–9. https://doi.org/10.1016/j.neubiorev.2014.02.010.

Castanheira L, Ferreira MF, Sebastião AM, Telles-Correia D. Anxiety Assessment in Pre-clinical Tests and in Clinical Trials: A Critical Review. Curr Top Med Chem 2018;18:1656–76. https://doi.org/10.2174/1568026618666181115102518.

Cavaco M, Valle J, da Silva R, Correia JDG, Castanho MARB, Andreu D, et al. DPepH3, an Improved Peptide Shuttle for Receptor-independent Transport Across the Blood-Brain Barrier. Curr Pharm Des 2020;26:1495–506. https://doi.org/10.2174/1381612826666200213094556.

Chen G, Xu T, Yan Y, Zhou Y, Jiang Y, Melcher K, et al. Amyloid beta: structure, biology and structure-based therapeutic development. Acta Pharmacol Sin 2017;38:1205–35. https://doi.org/10.1038/aps.2017.28.

Chen P, Bodor N, Wu W-M, Prokai L. Strategies to target Kyotorphin analogues to the brain. J Med Chem 1998;41:3773–81. https://doi.org/10.1021/jm970715l.

Chen QS, Kagan BL, Hirakura Y, Xie CW. Impairment of hippocampal long-term potentiation by Alzheimer amyloid beta-peptides. J Neurosci Res 2000;60:65–72. https://doi.org/10.1002/(SICI)1097-4547(20000401)60:1<65::AID-JNR7>3.0.CO;2-Q.

Citron M. Alzheimer's disease: strategies for disease modification. Nat Rev Drug Discov 2010;9:387–98. https://doi.org/10.1038/nrd2896.

Clark WG, Ponder SW. Thermoregulatory effects of (D-ala2)-methionine-enkephalinamide in the cat. Evidence for multiple naloxone-sensitive opioid receptors. Brain Res Bull 1980;5:415–20. https://doi.org/10.1016/S0361-9230(80)80011-6.

Coleman P, Federoff H, Kurlan R. A focus on the synapse for neuroprotection in Alzheimer disease and other dementias. Neurology 2004;63:1155–62. https://doi.org/10.1212/01.WNL.0000140626.48118.0A.

Conceição K, Magalhães PR, Campos SRR, Domingues MM, Ramu VG, Michalek M, et al. The anti-inflammatory action of the analgesic kyotorphin neuropeptide derivatives: insights of a lipid-mediated mechanism. Amino Acids 2016;48:307–18. https://doi.org/10.1007/s00726-015-2088-9.

Corder E, Saunders A, Strittmatter W, Schmechel D, Gaskell P, Small G, et al. Gene dose of apolipoprotein E type 4 allele and the risk of Alzheimer's disease in late onset families. Science 1993;261:921–3. https://doi.org/10.1126/science.8346443.

Cunha GMA, Canas PM, Melo CS, Hockemeyer J, Müller CE, Oliveira CR, et al. Adenosine A2A receptor blockade prevents memory dysfunction caused by β-amyloid peptides but not by scopolamine or MK-801. Exp Neurol 2008;210:776–81. https://doi.org/10.1016/j.expneurol.2007.11.013.

Dansokho C, Heneka MT. Neuroinflammatory responses in Alzheimer's disease. J Neural Transm 2018;125:771–9. https://doi.org/10.1007/s00702-017-1831-7.

Davatzikos C, Bhatt P, Shaw LM, Batmanghelich KN, Trojanowski JQ. Prediction of MCI to AD conversion, via MRI, CSF biomarkers, and pattern classification. Neurobiol Aging 2011;32:2322.e19-2322.e27. https://doi.org/10.1016/j.neurobiolaging.2010.05.023.

Dieck ST, Heuer H, Ehrchen J, Otto C, Bauer K. The peptide transporter PepT2 is expressed in rat brain and mediates the accumulation of the fluorescent dipeptide derivative beta-Ala-Lys-Nepsilon-AMCA in astrocytes. Glia 1999;25:10–20. https://doi.org/10.1002/(sici)1098-1136(19990101)25:1<10::aid-glia2>3.0.co;2-y.

Dinsmore JH, Solomon F. Inhibition of MAP2 expression affects both morphological and cell division phenotypes of neuronal differentiation. Cell 1991;64:817–26. https://doi.org/10.1016/0092-8674(91)90510-6.

Diógenes MJ, Costenla AR, Lopes LV, Jerónimo-Santos A, Sousa VC, Fontinha BM, et al. Enhancement of LTP in Aged Rats is Dependent on Endogenous BDNF. Neuropsychopharmacology 2011;36:1823–36. https://doi.org/10.1038/npp.2011.64.

Diógenes MJ, Neves-Tome R, Fucile S, Martinello K, Scianni M, Theofilas P, et al. Homeostatic Control of Synaptic Activity by Endogenous Adenosine is Mediated by Adenosine Kinase. Cereb Cortex 2014;24:67–80. https://doi.org/10.1093/cercor/bhs284.

Dzambazova EB, Bocheva AI. The unique brain dipeptide kyotorphin - from discovery to nowadays. J Biomed Clin Res 2010;3:3–11.

Dzhambazova E. Possible Anti-Stressor Effects of Kyotorphin and its Optical Isomer. Pharmacologia 2015;6:413–20. https://doi.org/10.5567/pharmacologia.2015.413.420.

Dzimbova TA, Bocheva A, Pajpanova T. Kyotorphin analogues containing unnatural amino acids: synthesis, analgesic activity and computer modeling of their interactions with μ-receptor. Med Chem Res 2014;23:3694–704. https://doi.org/10.1007/s00044-014-0953-9.

Epperly T, Dunay MA, Boice JL. Alzheimer Disease: Pharmacologic and Nonpharmacologic Therapies for Cognitive and Functional Symptoms. Am Fam Physician 2017;95:771–8.

Escott-Price V, Sims R, Bannister C, Harold D, Vronskaya M, Majounie E, et al. Common polygenic variation enhances risk prediction for Alzheimer's disease. Brain 2015;138:3673–84. https://doi.org/10.1093/brain/awv268.

Figurov A, Pozzo-Miller LD, Olafsson P, Wang T, Lu B. Regulation of synaptic responses to high-frequency stimulation and LTP by neurotrophins in the hippocampus. Nature 1996;381:706–9. https://doi.org/10.1038/381706a0.

Finnerup NB, Scholz J, First MB, Barke A, Cohen M, Smith BH, et al. Chronic pain as a symptom or a disease. Pain 2018;160:19–27. https://doi.org/10.1097/j.pain.0000000000001384.

Fonseca-Gomes J, Jerónimo-Santos A, Lesnikova A, Casarotto P, Castrén E, Sebastião AM, et al. TrkB-ICD fragment, originating from BDNF receptor cleavage, is translocated to cell nucleus and phosphorylates nuclear and axonal proteins. Front Mol Neurosci 2019;12:4. https://doi.org/10.3389/fnmol.2019.00004.

Fontinha BM, Diógenes MJ, Ribeiro JA, Sebastião AM. Enhancement of long-term potentiation by brain-derived neurotrophic factor requires adenosine A2A receptor activation by endogenous adenosine. Neuropharmacology 2008;54:924–33. https://doi.org/10.1016/j.neuropharm.2008.01.011.

Forner S, Baglietto-Vargas D, Martini AC, Trujillo-Estrada L, LaFerla FM. Synaptic Impairment in Alzheimer's Disease: A Dysregulated Symphony. Trends Neurosci 2017;40:347–57. https://doi.org/10.1016/j.tins.2017.04.002.

Freeman TC. PepDraw 2015. http://pepdraw.com/ (accessed July 29, 2021).

Fujita T, Kishida T, Okada N, Ganapathy V, Leibach H, Yamamoto A. Interaction of kyotorphin and brain peptide transporter in synaptosomes prepared from rat cerebellum: implication of high af®nity type H1/peptide transporter PEPT2 mediated transport system. Neurosci Lett 1999:4.

Fujita T, Kishida T, Wada M, Okada N, Yamamoto A, Leibach FH, et al. Functional characterization of brain peptide transporter in rat cerebral cortex: identification of the high-affinity type H+/peptide transporter PEPT2. Brain Res 2004;997:52–61. https://doi.org/10.1016/j.brainres.2003.10.049.

Gage GJ, Kipke DR, Shain W. Whole Animal Perfusion Fixation for Rodents. J Vis Exp 2012:3564. https://doi.org/10.3791/3564.

Giuffrida ML, Caraci F, Pignataro B, Cataldo S, De Bona P, Bruno V, et al. B-Amyloid Monomers Are Neuroprotective. J Neurosci 2009;29:10582–7. https://doi.org/10.1523/JNEUROSCI.1736-09.2009.

Glowinski J, Iversen LL. Regional studies of catecholamines in the rat brain. I. The disposition of [3H]norepinephrine, [3H]dopamine and [3H]dopa in various regions of the brain. J Neurochem 1966;13:655–69. https://doi.org/10.1111/j.1471-4159.1966.tb09873.x.

Godlevsky LS, Shandra AA, Mikhaleva II, Vastyanov RS, Mazarati AM. Seizure-protecting effects of kyotorphin and related peptides in an animal model of epilepsy. Brain Res Bull 1995;37:223–6. https://doi.org/10.1016/0361-9230(94)00274-5.

Gold CA, Budson AE. Memory loss in Alzheimer's disease: implications for development of therapeutics. Expert Rev Neurother 2008;8:1879–91. https://doi.org/10.1586/14737175.8.12.1879.

Gómez-Isla T, Growdon WB, McNamara MJ, Nochlin D, Bird TD, Arango JC, et al. The impact of different presenilin 1 andpresenilin 2 mutations on amyloid deposition, neurofibrillary changes and neuronal loss in the familial Alzheimer's disease brain. Brain 1999;122:1709–19. https://doi.org/10.1093/brain/122.9.1709.

Goulart BK, de Lima MNM, de Farias CB, Reolon GK, Almeida VR, Quevedo J, et al. Ketamine impairs recognition memory consolidation and prevents learning-induced increase in hippocampal brain-derived neurotrophic factor levels. Neuroscience 2010;167:969–73. https://doi.org/10.1016/j.neuroscience.2010.03.032.

Gould TD, Dao DT, Kovacsics CE. The Open Field Test. In: Gould TD, editor. Mood Anxiety Relat. Phenotypes Mice, vol. 42, Totowa, NJ: Humana Press; 2009, p. 1–20. https://doi.org/10.1007/978-1-60761-303-9_1.

Gouras GK, Olsson TT, Hansson O. β-amyloid Peptides and Amyloid Plaques in Alzheimer's Disease. Neurotherapeutics 2015;12:3–11. https://doi.org/10.1007/s13311-014-0313-y.

Guerreiro R, Wojtas A, Bras J, Carrasquillo M, Rogaeva E, Majounie E, et al. TREM2 Variants in Alzheimer's Disease. N Engl J Med 2013;368:117–27. https://doi.org/10.1056/NEJMoa1211851.

Habets RLP, Borst JGG. Dynamics of the readily releasable pool during post-tetanic potentiation in the rat calyx of Held synapse: RRP increase during post-tetanic potentiation. J Physiol 2007;581:467–78. https://doi.org/10.1113/jphysiol.2006.127365.

Hardy J, Higgins G. Alzheimer's disease: the amyloid cascade hypothesis. Science 1992;256:184–5. https://doi.org/10.1126/science.1566067.

Hazato T, Kase R, Ueda H, Takagi H, Katayama T. Inhibitory effects of the analgesic neuropeptides kyotorphin and neo-kyotorphin on enkephalin-degrading enzymes from monkey brain. Biochem Int 1986;12:379–83.

Hebert LE, Bienias JL, Aggarwal NT, Wilson RS, Bennett DA, Shah RC, et al. Change in risk of Alzheimer disease over time. Neurology 2010;75:786–91. https://doi.org/10.1212/WNL.0b013e3181f0754f.

Hirai K, Katayama Y. Effect of the endogenous analgesic dipeptide, kyotorphin, on transmitter release in sympathetic ganglia. Br J Pharmacol 1985;85:629–34. https://doi.org/10.1111/j.1476-5381.1985.tb10557.x.

Hökfelt T, Bartfai T, Bloom F. Neuropeptides: opportunities for drug discovery. Lancet Neurol 2003;2:463–72. https://doi.org/10.1016/S1474-4422(03)00482-4.

Hort J, O'Brien JT, Gainotti G, Pirttila T, Popescu BO, Rektorova I, et al. EFNS guidelines for the diagnosis and management of Alzheimer's disease. Eur J Neurol 2010;17:1236–48. https://doi.org/10.1111/j.1468-1331.2010.03040.x.

Huang Y, Mucke L. Alzheimer Mechanisms and Therapeutic Strategies. Cell 2012;148:1204–22. https://doi.org/10.1016/j.cell.2012.02.040.

Hughes J, Smith TW, Kosterlitz HW, Fothergill LA, Morgan BA, Morris HR. Identification of two related pentapeptides from the brain with potent opiate agonist activity. Nature 1975;258:577–9. https://doi.org/10.1038/258577a0.

Huntley JD, Howard RJ. Working memory in early Alzheimer's disease: a neuropsychological review. Int J Geriatr Psychiatry 2010;25:121–32. https://doi.org/10.1002/gps.2314.

Hyman BT, Marzloff K, Arriagada PV. The Lack of Accumulation of Senile Plaques or Amyloid Burden in Alzheimer's Disease Suggests a Dynamic Balance Between Amyloid Deposition and Resolution: J Neuropathol Exp Neurol 1993;52:594–600. https://doi.org/10.1097/00005072-199311000-00006.

Ignat'ev DA, Vorob'ev VV, Ziganshin RKh. Effects of a number of short peptides isolated from the brain of the hibernating ground squirrel on the EEG and behavior in rats. Neurosci Behav Physiol 1998;28:158–66. https://doi.org/10.1007/BF02461962.

Ikonomovic MD, Buckley CJ, Heurling K, Sherwin P, Jones PA, Zanette M, et al. Post-mortem histopathology underlying β-amyloid PET imaging following flutemetamol F 18 injection. Acta Neuropathol Commun 2016;4:130. https://doi.org/10.1186/s40478-016-0399-z.

Ingelsson M, Fukumoto H, Newell KL, Growdon JH, Hedley-Whyte ET, Frosch MP, et al. Early Aβ accumulation and progressive synaptic loss, gliosis, and tangle formation in AD brain. Neurology 2004;62:925–31. https://doi.org/10.1212/01.WNL.0000115115.98960.37.

Inoue M, Nakayamada H, Tokuyama S, Ueda H. Peripheral non-opioid analgesic effects of kyotorphin in mice. Neurosci Lett 1997;236:60–2. https://doi.org/10.1016/S0304-3940(97)00760-X.

Inoue M, Yamada T, Ueda H. Low dose of kyotorphin (tyrosine–arginine) induces nociceptive responses through a substance P release from nociceptor endings. Mol Brain Res 1999;69:302–5. https://doi.org/10.1016/S0169-328X(99)00133-3.

Jack CR, Knopman DS, Jagust WJ, Petersen RC, Weiner MW, Aisen PS, et al. Tracking pathophysiological processes in Alzheimer's disease: an updated hypothetical model of dynamic biomarkers. Lancet Neurol 2013;12:207–16. https://doi.org/10.1016/S1474-4422(12)70291-0.

Janicki PK, Jeske-Janicka M. Relevance of nitric oxide in pain mechanisms and pain management. Curr Rev Pain 1998;2:211–6. https://doi.org/10.1007/s11916-998-0022-5.

Janicki PK, Lipkowski AW. Kyotorphin and d-kyotorphin stimulate Met-enkephalin release from rat striatum in vitro. Neurosci Lett 1983;43:73–7. https://doi.org/10.1016/0304-3940(83)90131-3.

Jerónimo-Santos A, Vaz SH, Parreira S, Rapaz-Lérias S, Caetano AP, Buée-Scherrer V, et al. Dysregulation of TrkB Receptors and BDNF Function by Amyloid-β Peptide is Mediated by Calpain. Cereb Cortex 2015;25:3107–21. https://doi.org/10.1093/cercor/bhu105.

Ji Y, Lu Y, Yang F, Shen W, Tang TT-T, Feng L, et al. Acute and gradual increases in BDNF concentration elicit distinct signaling and functions in neurons. Nat Neurosci 2010;13:302–9. https://doi.org/10.1038/nn.2505.

Jiang H, Hu Y, Keep RF, Smith DE. Enhanced antinociceptive response to intracerebroventricular kyotorphin in Pept2 null mice. J Neurochem 2009;109:1536–43. https://doi.org/10.1111/j.1471-4159.2009.06090.x.

Johnson J, Kotermanski S. Mechanism of action of memantine. Curr Opin Pharmacol 2006;6:61–7. https://doi.org/10.1016/j.coph.2005.09.007.

Jonsson T, Stefansson H, Steinberg S, Jonsdottir I, Jonsson PV, Snaedal J, et al. Variant of TREM2 Associated with the Risk of Alzheimer's Disease. N Engl J Med 2013;368:107–16. https://doi.org/10.1056/NEJMoa1211103.

Kaminsky YG, Marlatt MW, Smith MA, Kosenko EA. Subcellular and metabolic examination of amyloid-beta peptides in Alzheimer disease pathogenesis: evidence for Abeta(25-35). Exp Neurol 2010;221:26–37. https://doi.org/10.1016/j.expneurol.2009.09.005.

Karch CM, Goate AM. Alzheimer's Disease Risk Genes and Mechanisms of Disease Pathogenesis. Biol Psychiatry 2015;77:43–51. https://doi.org/10.1016/j.biopsych.2014.05.006.

Kastin AJ, Honour LC, Coy DH. Kyotorphins affect aversive pecking in chicks. Physiol Behav 1981;27:1073–6. https://doi.org/10.1016/0031-9384(81)90372-3.

Kavirajan H. Memantine: a comprehensive review of safety and efficacy. Expert Opin Drug Saf 2009;8:89–109. https://doi.org/10.1517/14740330802528420.

Kawabata A, Muguruma H, Tanaka M, Takagi H. Kyotorphin synthetase activity in rat adrenal glands and spinal cord. Peptides 1996;17:407–11. https://doi.org/10.1016/0196-9781(96)00026-5.

Kawabata A, Nishimura Y, Takagi H. L-Leucyl-L-arginine, naltrindole and d-arginine block antinociception elicited by L-arginine in mice with carrageenin-induced hyperalgesia. Br J Pharmacol 1992;107:1096–101. https://doi.org/10.1111/j.1476-5381.1992.tb13413.x.

Kawabata A, Umeda N, Takagi H. L-Arginine exerts a dual role in nociceptive processing in the brain: involvement of the kyotorphin-Met-enkephalin pathway and NO-cyclic GMP pathway. Br J Pharmacol 1993;109:73–9. https://doi.org/10.1111/j.1476-5381.1993.tb13533.x.

Kaye AD, Baluch A, Scott JT. Pain Management in the Elderly Population: A Review 2010;10:9.

Kitabatake S, Tsurutani R, Nakajima H, Tomita K, Yoshihara Y, Ueda H, et al. A Novel Method for the Synthesis of Kyotorphin, Tyr-Arg, and 3H-Tyr-Arg, Catalyzed by Tyrosyl-tRNA Synthetase from Bacillus stearothermophilus. Pharm Res 1987;04:154–7. https://doi.org/10.1023/A:1016479305603.

Knot HJ. Twenty Years of Calcium Imaging: Cell Physiology to Dye For. Mol Interv 2005;5:112–27. https://doi.org/10.1124/mi.5.2.8.

Kolaeva SG, Semenova TP, Santalova IM, Moshkov DA, Anoshkina IA, Golozubova V. Effects of L-thyrosyl - L-arginine (kyotorphin) on the behavior of rats and goldfish. Peptides 2000;21:1331–6. https://doi.org/10.1016/S0196-9781(00)00275-8.

Korogod N, Lou X, Schneggenburger R. Posttetanic potentiation critically depends on an enhanced Ca2+ sensitivity of vesicle fusion mediated by presynaptic PKC. Proc Natl Acad Sci 2007;104:15923–8. https://doi.org/10.1073/pnas.0704603104.

Korte M, Kang H, Bonhoeffer T, Schuman E. A role for BDNF in the late-phase of hippocampal long-term potentiation. Neuropharmacology 1998;37:553–9. https://doi.org/10.1016/S0028-3908(98)00035-5.

Koskinen M, Hotulainen P. Measuring F-actin properties in dendritic spines. Front Neuroanat 2014;8. https://doi.org/10.3389/fnana.2014.00074.

De La Torre JC, Stefano GB. Evidence that Alzheimer's disease is a microvascular disorder: The role of constitutive nitric oxide. Brain Res Rev 2000;34:119–36. https://doi.org/10.1016/S0165-0173(00)00043-6.

Lane CA, Hardy J, Schott JM. Alzheimer's disease. Eur J Neurol 2018;25:59–70. https://doi.org/10.1111/ene.13439.

Lanoiselée H-M, Nicolas G, Wallon D, Rovelet-Lecrux A, Lacour M, Rousseau S, et al. APP, PSEN1, and PSEN2 mutations in early-onset Alzheimer disease: A genetic screening study of familial and sporadic cases. PLOS Med 2017;14:e1002270. https://doi.org/10.1371/journal.pmed.1002270.

Lecanu L, Papadopoulos V. Modeling Alzheimer's disease with non-transgenic rat models. Alzheimers Res Ther 2013;5:17. https://doi.org/10.1186/alzrt171.

Lewis R V, Stern AS. Biosynthesis of the Enkephalins and Enkephalin-Containing Polypeptides. Annu Rev Pharmacol Toxicol 1983;23:353–72. https://doi.org/10.1146/annurev.pa.23.040183.002033.

Li Y, Saito Y, Suzuki M, Ueda H, Endo M, Maruyama K. Kyotorphin has a novel action on rat cardiac muscle. Biochem Biophys Res Commun 2006;339:805–9. https://doi.org/10.1016/j.bbrc.2005.11.081.

Liu W, Liang R, Ramamoorthy S, Fei Y-J, Ganapathy ME, Hediger MA, et al. Molecular cloning of PEPT 2, a new member of the H+/peptide cotransporter family, from human kidney. Biochim Biophys Acta BBA - Biomembr 1995;1235:461–6. https://doi.org/10.1016/0005-2736(95)80036-F.

Lopes SCDN, Fedorov A, Castanho MARB. Chiral Recognition of D-Kyotorphin by Lipidic Membranes: Relevance Toward Improved Analgesic Efficiency. ChemMedChem 2006a;1:723–8. https://doi.org/10.1002/cmdc.200600096.

Lopes SCDN, Soares CM, Baptista AM, Goormaghtigh E, Costa Cabral BJ, Castanho MARB. Conformational and Orientational Guidance of the Analgesic Dipeptide Kyotorphin Induced by Lipidic Membranes: Putative Correlation toward Receptor Docking. J Phys Chem B 2006b;110:3385–94. https://doi.org/10.1021/jp053651w.

Lott IT, Head E. Dementia in Down syndrome: unique insights for Alzheimer disease research. Nat Rev Neurol 2019;15:135–47. https://doi.org/10.1038/s41582-018-0132-6.

Loy C, Schneider L. Galantamine for Alzheimer's disease and mild cognitive impairment. Cochrane Database Syst Rev 2006. https://doi.org/10.1002/14651858.CD001747.pub3.

Lu B, Nagappan G, Lu Y. BDNF and synaptic plasticity, cognitive function, and dysfunction. Handb Exp Pharmacol 2015;220:223–50. https://doi.org/10.1007/978-3-642-45106-5_9.

Luscher C, Malenka RC. NMDA Receptor-Dependent Long-Term Potentiation and Long-Term Depression (LTP/LTD). Cold Spring Harb Perspect Biol 2012;4:a005710–a005710. https://doi.org/10.1101/cshperspect.a005710.

Machuqueiro M, Baptista AM. The pH-Dependent Conformational States of Kyotorphin: A Constant-pH Molecular Dynamics Study. Biophys J 2007;92:1836–45. https://doi.org/10.1529/biophysj.106.092445.

Marinov BS, Ziganshin RK. [Redox properties of peptides potentially regulating animal hibernation]. Biofizika 1997;42:147–53.

Massoud F, Léger GC. Pharmacological Treatment of Alzheimer Disease. Can J Psychiatry 2011;56:579–88. https://doi.org/10.1177/070674371105601003.

Masters CL, Bateman R, Blennow K, Rowe CC, Sperling RA, Cummings JL. Alzheimer's disease. Nat Rev Dis Primer 2015;1:15056. https://doi.org/10.1038/nrdp.2015.56.

Matsubayashi K, Kojima C, Kawajiri S, Ono K, Takegoshi T, Ueda H, et al. Hydrolytic deactivation of kyotorphin by the rodent brain homogenates and sera. J Pharmacobiodyn 1984;7:479–84. https://doi.org/10.1248/bpb1978.7.479.

Maurice T, Lockhart BP, Privat A. Amnesia induced in mice by centrally administered beta-amyloid peptides involves cholinergic dysfunction. Brain Res 1996;706:181–93. https://doi.org/10.1016/0006-8993(95)01032-7.

Mayeux R, Stern Y. Epidemiology of Alzheimer Disease. Cold Spring Harb Perspect Med 2012;2:a006239–a006239. https://doi.org/10.1101/cshperspect.a006239.

McLarnon JG. Correlated inflammatory responses and neurodegeneration in peptide-injected animal models of Alzheimer's disease. BioMed Res Int 2014;2014. https://doi.org/10.1155/2014/923670.

Merighi A, Salio C, Ferrini F, Lossi L. Neuromodulatory function of neuropeptides in the normal CNS. J Chem Neuroanat 2011;42:276–87. https://doi.org/10.1016/j.jchemneu.2011.02.001.

Mielke MM, Ferretti MT, Iulita MF, Hayden K, Khachaturian AS. Sex and gender in Alzheimer's disease - Does it matter? Alzheimers Dement 2018;14:1101–3. https://doi.org/10.1016/j.jalz.2018.08.003.

Minichiello L. TrkB signalling pathways in LTP and learning. Nat Rev Neurosci 2009;10:850–60. https://doi.org/10.1038/nrn2738.

Montagne R, Berbon M, Doublet L, Debreuck N, Baranzelli A, Drobecq H, et al. Necrosis- and apoptosis-related Met cleavages have divergent functional consequences. Cell Death Dis 2015;6:e1769–e1769. https://doi.org/10.1038/cddis.2015.132.

Morgan AJ, Jacob R. Ionomycin enhances Ca2+ influx by stimulating store-regulated cation entry and not by a direct action at the plasma membrane. Biochem J 1994;300:665–72. https://doi.org/10.1042/bj3000665.

Morris RG, Anderson E, Lynch GS, Baudry M. Selective impairment of learning and blockade of long-term potentiation by an N-methyl-D-aspartate receptor antagonist, AP5. Nature 1986;319:774–6. https://doi.org/10.1038/319774a0.

Mucke L. Alzheimer's disease. Nature 2009;461:895–7. https://doi.org/10.1038/461895a.

Mufson EJ, Malek-Ahmadi M, Snyder N, Ausdemore J, Chen K, Perez SE. Braak stage and trajectory of cognitive decline in noncognitively impaired elders. Neurobiol Aging 2016;43:101–10. https://doi.org/10.1016/j.neurobiolaging.2016.03.003.

Murison R. The Neurobiology of Stress. Neurosci. Pain Stress Emot., Elsevier; 2016, p. 29–49. https://doi.org/10.1016/B978-0-12-800538-5.00002-9.

Neyama H, Hamada Y, Tsukahara R, Narita M, Tsukamoto K, Ueda H. Blockade of analgesic effects following systemic administration of N-methyl-kyotorphin, NMYR and arginine in mice deficient of preproenkephalin or proopiomelanocortin gene. Peptides 2018;107:10–6. https://doi.org/10.1016/j.peptides.2018.06.010.

Nicholls DG. Chapter 2 Presynaptic modulation of glutamate release. Prog. Brain Res., vol. 116, Elsevier; 1998, p. 15–22. https://doi.org/10.1016/S0079-6123(08)60427-6.

Nishimura K, Kaya K, Hazato T, Ueda H, Satoh M, Takagi H. [Kyotorphin like substance in human cerebrospinal fluid of patients with persistent pain]. Masui 1991;40:1686–90.

Noguchi-Shinohara M, Komatsu J, Samuraki M, Matsunari I, Ikeda T, Sakai K, et al. Cerebral Amyloid Angiopathy-Related Microbleeds and Cerebrospinal Fluid Biomarkers in Alzheimer's Disease. J Alzheimers Dis 2016;55:905–13. https://doi.org/10.3233/JAD-160651.

Oliveira MC, Gano L, Santos I, Correia JDG, Serrano ID, Santos SS, et al. Improvement of the pharmacological properties of amidated kyotorphin by means of iodination. MedChemComm 2016;7:906–13. https://doi.org/10.1039/C6MD00028B.

Olsson B, Lautner R, Andreasson U, Öhrfelt A, Portelius E, Bjerke M, et al. CSF and blood biomarkers for the diagnosis of Alzheimer's disease: a systematic review and meta-analysis. Lancet Neurol 2016;15:673–84. https://doi.org/10.1016/S1474-4422(16)00070-3.

Onor ML, Trevisiol M, Aguglia E. Rivastigmine in the treatment of Alzheimer's disease: an update. Clin Interv Aging 2007;2:17–32. https://doi.org/10.2147/ciia.2007.2.1.17.

Orawski AT, Simmons WH. Dipeptidase activities in rat brain synaptosomes can be distinguished on the basis of inhibition by bestatin and amastatin: Identification of a kyotorphin (Tyr-Arg)-degrading enzyme. Neurochem Res 1992;17:817–20. https://doi.org/10.1007/BF00969018.

Overk CR, Masliah E. Pathogenesis of synaptic degeneration in Alzheimer's disease and Lewy body disease. Biochem Pharmacol 2014;88:508–16. https://doi.org/10.1016/j.bcp.2014.01.015.

Pang PT, Lu B. Regulation of late-phase LTP and long-term memory in normal and aging hippocampus: role of secreted proteins tPA and BDNF. Ageing Res Rev 2004;3:407–30. https://doi.org/10.1016/j.arr.2004.07.002.

Perazzo J, Castanho MARB, Sá Santos S. Pharmacological Potential of the Endogenous Dipeptide Kyotorphin and Selected Derivatives. Front Pharmacol 2017a;7. https://doi.org/10.3389/fphar.2016.00530.

Perazzo J, Lima C, Heras M, Bardají E, Lopes-Ferreira M, Castanho M. Neuropeptide Kyotorphin Impacts on Lipopolysaccharide-Induced Glucocorticoid-Mediated Inflammatory Response. A Molecular Link to Nociception, Neuroprotection, and Anti-Inflammatory Action. ACS Chem Neurosci 2017b;8:1663–7. https://doi.org/10.1021/acschemneuro.7b00007.

Pike CJ, Walencewicz-Wasserman AJ, Kosmoski J, Cribbs DH, Glabe CG, Cotman CW. Structure-activity analyses of beta-amyloid peptides: contributions of the beta 25-35 region to aggregation and neurotoxicity. J Neurochem 1995;64:253–65. https://doi.org/10.1046/j.1471-4159.1995.64010253.x.

Potter R, Patterson BW, Elbert DL, Ovod V, Kasten T, Sigurdson W, et al. Increased in Vivo Amyloid- 42 Production, Exchange, and Loss in Presenilin Mutation Carriers. Sci Transl Med 2013;5:189ra77-189ra77. https://doi.org/10.1126/scitranslmed.3005615.

Price JL, Davis PB, Morris JC, White DL. The distribution of tangles, plaques and related immunohistochemical markers in healthy aging and Alzheimer's disease. Neurobiol Aging 1991;12:295–312. https://doi.org/10.1016/0197-4580(91)90006-6.

Prut L, Belzung C. The open field as a paradigm to measure the effects of drugs on anxiety-like behaviors: a review. Eur J Pharmacol 2003;463:3–33. https://doi.org/10.1016/S0014-2999(03)01272-X.

Rackham A, Wood PL, Hudgin RL. Kyotorphin (tyrosine-arginine): Further evidence for indirect opiate receptor activation. Life Sci 1982;30:1337–42. https://doi.org/10.1016/0024-3205(82)90017-0.

Raja SN, Carr DB, Cohen M, Finnerup NB, Flor H, Gibson S, et al. The revised International Association for the Study of Pain definition of pain: concepts, challenges, and compromises. Pain 2020;161:1976–82. https://doi.org/10.1097/j.pain.0000000000001939.

Rajagopal L, Massey B, Huang M, Oyamada Y, Meltzer H. The Novel Object Recognition Test in Rodents in Relation to Cognitive Impairment in Schizophrenia. Curr Pharm Des 2014;20:5104–14. https://doi.org/10.2174/1381612819666131216114240.

Ribeiro MMB. IMPROVED ANALGESIC KYOTORPHIN DERIVATIVES – CORRELATING MEMBRANE INTERACTIONS, BRAIN TARGETING AND PHARMACOLOGICAL ACTIVITIES. 2012. https://doi.org/10.1017/CBO9781107415324.004.

Ribeiro MMB, Pinto ART, Domingues MM, Serrano I, Heras M, Bardaji ER, et al. Chemical Conjugation of the Neuropeptide Kyotorphin and Ibuprofen Enhances Brain Targeting and Analgesia. Mol Pharm 2011a;8:1929–40. https://doi.org/10.1021/mp2003016.

Ribeiro MMB, Pinto ART, Pinto M, Heras M, Martins I, Correia A, et al. Inhibition of nociceptive responses after systemic administration of amidated kyotorphin: Kyotorphin-amide: a new analgesic peptide. Br J Pharmacol 2011b;163:964–73. https://doi.org/10.1111/j.1476-5381.2011.01290.x.

Ribeiro MMB, Santos SS, Sousa DSC, Oliveira M, Santos SM, Heras M, et al. Side-effects of analgesic kyotorphin derivatives: advantages over clinical opioid drugs. Amino Acids 2013;45:171–8. https://doi.org/10.1007/s00726-013-1484-2.

Robinson DM, Plosker GL. Galantamine Extended Release in Alzheimer's Disease. Drugs Aging 2006;23:839–42. https://doi.org/10.2165/00002512-200623100-00006.

Rybal'chenko VK, Ostrovskaya GV, Poralo IV, Rybal'chenko TV, Mel'nik YuM. Membranotropic activity of optical isomers of the neuropeptide kyotorphin and a cardiotonic agent, suphan. Neurophysiology 1999;31:223–5. https://doi.org/10.1007/BF02515077.

Sá Santos S, Santos SM, Pinto ART, Ramu VG, Heras M, Bardaji E, et al. Amidated and Ibuprofen-Conjugated Kyotorphins Promote Neuronal Rescue and Memory Recovery in Cerebral Hypoperfusion Dementia Model. Front Aging Neurosci 2016;8. https://doi.org/10.3389/fnagi.2016.00001.

Sabuncu MR, Desikan RS, Sepulcre J, Yeo BTT, Liu H, Schmansky NJ, et al. The dynamics of cortical and hippocampal atrophy in Alzheimer disease. Arch Neurol 2011;68:1040–8. https://doi.org/10.1001/archneurol.2011.167.

Sakurada T, Sakurada S, Watanabe S, Matsumura H, Kisara K, Akutsu Y, et al. Actions of intracerebroventricular administration of kyotorphin and an analog on thermoregulation in the mouse. Peptides 1983;4:859–63. https://doi.org/10.1016/0196-9781(83)90081-5.

Salio C, Lossi L, Ferrini F, Merighi A. Neuropeptides as synaptic transmitters. Cell Tissue Res 2006;326:583–98. https://doi.org/10.1007/s00441-006-0268-3.

Santos S, Torcato I, Castanho MARB. Biomedical applications of dipeptides and tripeptides. Biopolymers 2012;98:288–93. https://doi.org/10.1002/bip.22067.

Santos SM, Garcia-Nimo L, Sá Santos S, Tavares I, Cocho JA, Castanho MARB. Neuropeptide Kyotorphin (Tyrosyl-Arginine) has Decreased Levels in the Cerebro-Spinal Fluid of Alzheimer's Disease Patients: Potential Diagnostic and Pharmacological Implications. Front Aging Neurosci 2013;5. https://doi.org/10.3389/fnagi.2013.00068.

Satoh M, Kawajiri S, Yamamoto M, Akaike A, Ukai Y, Takagi H. Effects of tyrosyl-arginine (kyotorphin), a new opioid dipeptide, on single neurons in the spinal dorsal horn of rabbits and the nucleus reticularis paragigantocellularis of rats. Neurosci Lett 1980;16:319–22. https://doi.org/10.1016/0304-3940(80)90018-X.

Schmidt JA, Rinaldi S, Scalbert A, Ferrari P, Achaintre D, Gunter MJ, et al. Plasma concentrations and intakes of amino acids in male meat-eaters, fish-eaters, vegetarians and vegans: a cross-sectional analysis in the EPIC-Oxford cohort. Eur J Clin Nutr 2016;70:306–12. https://doi.org/10.1038/ejcn.2015.144.

Schmitz R. Friedrich Wilhelm Sertürner and the Discovery of Morphine. Pharm Hist 1985;27:61–74.

Schraen-Maschke S, Sergeant N, Dhaenens CM, Bombois S, Deramecourt V, Caillet-Boudin ML, et al. Tau as a biomarker of neurodegenerative diseases. Biomark Med 2008;2:363–84. https://doi.org/10.2217/17520363.2.4.363.

Seltzer B. Donepezil: an update. Expert Opin Pharmacother 2007;8:1011–23. https://doi.org/10.1517/14656566.8.7.1011.

Sengoku R. Aging and Alzheimer's disease pathology. Neuropathology 2020;40:22–9. https://doi.org/10.1111/neup.12626.

Serrano ID, Freire J, Carvalho M, Neves M, Melo M, Castanho MARB. The Mechanisms and Quantification of the Selective Permeability in Transport Across Biological Barriers: the Example of

Kyotorphin. Mini-Rev Med Chem 2014a;14:99–110. https://doi.org/10.2174/1389557514666140123130058.

Serrano ID, Ramu VG, Pinto ART, Freire JM, Tavares I, Heras M, et al. Correlation between membrane translocation and analgesic efficacy in kyotorphin derivatives: Membrane Translocation and Analgesic Efficacy. Biopolymers 2014b;104:1–10. https://doi.org/10.1002/bip.22580.

Serrano-Pozo A, Frosch MP, Masliah E, Hyman BT. Neuropathological Alterations in Alzheimer Disease. Cold Spring Harb Perspect Med 2011;1:a006189–a006189. https://doi.org/10.1101/cshperspect.a006189.

Shi LY, Ku BS, Yao HY. [Studies on antidepressant effects of several overshort peptides (OSP)]. Yao Xue Xue Bao 1991;26:546–7.

Shiomi H, Kuraishi Y, Ueda H, Harada Y, Amano H, Takagi H. Mechanism of kyotorphin-induced release of Met-enkephalin from guinea pig striatum and spinal cord. Brain Res 1981a;221:161–9. https://doi.org/10.1016/0006-8993(81)91070-2.

Shiomi H, Ueda H. Isolation and Analgesic Mechanism of Opioid Analgesic Neuropeptide, Kyotorphin (Tyr-Arg). YAKUGAKU ZASSHI 1985;105:531–41. https://doi.org/10.1248/yakushi1947.105.6_531.

Shiomi H, Ueda H, Takagi H. Isolation and identification of an analgesic opioid dipeptide kyotorphin (TYR-ARG) from bovine brain. Neuropharmacology 1981b;20:633–8. https://doi.org/10.1016/0028-3908(81)90109-X.

Sims R, Hill M, Williams J. The multiplex model of the genetics of Alzheimer's disease. Nat Neurosci 2020;23:311–22. https://doi.org/10.1038/s41593-020-0599-5.

Strittmatter WJ, Weisgraber KH, Huang DY, Dong LM, Salvesen GS, Pericak-Vance M, et al. Binding of human apolipoprotein E to synthetic amyloid beta peptide: isoform-specific effects and implications for late-onset Alzheimer disease. Proc Natl Acad Sci 1993;90:8098–102. https://doi.org/10.1073/pnas.90.17.8098.

Summy–Long JY, Bui V, Gestl S, Koehler-Stec E, Liu H, Terrell ML, et al. Effects of Central Injection of Kyotorphin and l-Arginine on Oxytocin and Vasopressin Release and Blood Pressure in Conscious Rats. Brain Res Bull 1998;45:395–403. https://doi.org/10.1016/S0361-9230(97)00341-9.

Suter KJ, Smith BN, Dudek FE. Electrophysiological Recording from Brain Slices. Methods 1999;18:86–90. https://doi.org/10.1006/meth.1999.0761.

Takagi H, Harima A, Shimizu H. A novel clinical treatment of persistent pain with L-arginine. Eur J Pharmacol 1990;183:1443. https://doi.org/10.1016/0014-2999(90)94580-Q.

Takagi H, Inukai T, Nakama M. A modification of Haffner's method for testing analgesics. Jpn J Pharmacol 1966;16:287–94. https://doi.org/10.1254/jjp.16.287.

Takagi H, Nomura Y. EFFECTS OF KYOTORPHIN (L-TYROSYL-L-ARGININE) ON [3H]Ng-NITRO-L-ARGININE BINDING TO NEURONAL NITRIC OXIDE SYNTHASE IN RAT BRAIN. Neurochem Int 1997;30:605–11.

Takagi H, Shiomi H, Ueda H, Amano H. Morphine-like analgesia by a new dipeptide, L-Tyrosyl-L-Arginine (kyotorphin) and its analogue. Eur J Pharmacol 1979a;55:109–11. https://doi.org/10.1016/0014-2999(79)90154-7.

Takagi H, Shiomi H, Ueda H, Amano H. A novel analgesic dipeptide from bovine brain is a possible Met-enkephalin releaser. Nature 1979b;282:410–2. https://doi.org/10.1038/282410a0.

Takahashi RH, Nagao T, Gouras GK. Plaque formation and the intraneuronal accumulation of β-amyloid in Alzheimer's disease: Intraneuronal accumulation of β-amyloid. Pathol Int 2017;67:185–93. https://doi.org/10.1111/pin.12520.

Tanqueiro SR, Ramalho RM, Rodrigues TM, Lopes LV, Sebastião AM, Diógenes MJ. Inhibition of NMDA Receptors Prevents the Loss of BDNF Function Induced by Amyloid β. Front Pharmacol 2018;9:237. https://doi.org/10.3389/fphar.2018.00237.

Terry AV, Buccafusco JJ. The Cholinergic Hypothesis of Age and Alzheimer's Disease-Related Cognitive Deficits: Recent Challenges and Their Implications for Novel Drug Development. J Pharmacol Exp Ther 2003;306:821–7. https://doi.org/10.1124/jpet.102.041616.

Terstappen GC, Meyer AH, Bell RD, Zhang W. Strategies for delivering therapeutics across the blood–brain barrier. Nat Rev Drug Discov 2021;20:362–83. https://doi.org/10.1038/s41573-021-00139-y.

Thakkar SV, Miyauchi S, Prasad PD, Ganapathy V. Stimulation of Na+/Cl−-coupled Opioid Peptide Transport System in SK-N-SH Cells by L-kyotorphin, an Endogenous Substrate for H+-coupled Peptide Transporter PEPT2. Drug Metab Pharmacokinet 2008;23:254–62. https://doi.org/10.2133/dmpk.23.254.

Thal DR, Rüb U, Orantes M, Braak H. Phases of Aβ-deposition in the human brain and its relevance for the development of AD. Neurology 2002;58:1791–800. https://doi.org/10.1212/WNL.58.12.1791.

Toni N, Buchs P-A, Nikonenko I, Bron CR, Muller D. LTP promotes formation of multiple spine synapses between a single axon terminal and a dendrite. Nature 1999;402:421–5. https://doi.org/10.1038/46574.

Tripathi MK, Kartawy M, Amal H. The role of nitric oxide in brain disorders: Autism spectrum disorder and other psychiatric, neurological, and neurodegenerative disorders. Redox Biol 2020;34:101567. https://doi.org/10.1016/j.redox.2020.101567.

Truong C. Low-dose acetylsalicylic acid for primary prevention of cardiovascular disease: Do not misinterpret the recommendations. Can Fam Physician Med Fam Can 2015;61:971–5.

Tsukahara T, Yamagishi S, Neyama H, Ueda H. Tyrosyl-tRNA synthetase: A potential kyotorphin synthetase in mammals. Peptides 2018;101:60–8. https://doi.org/10.1016/j.peptides.2017.12.026.

Tyler WJ, Pozzo-Miller LD. BDNF enhances quantal neurotransmitter release and increases the number of docked vesicles at the active zones of hippocampal excitatory synapses. J Neurosci Off J Soc Neurosci 2001;21:4249–58.

Ueda H. Review of Kyotorphin Research: A Mysterious Opioid Analgesic Dipeptide and Its Molecular, Physiological, and Pharmacological Characteristics. Front Med Technol 2021;3:662697. https://doi.org/10.3389/fmedt.2021.662697.

Ueda H, Amano H, Shiomi H, Takagi H. Comparison of the analgesic effects of various opioid peptides by a newly devised intracisternal injection technique in conscious mice. Eur J Pharmacol 1979;56:265–8. https://doi.org/10.1016/0014-2999(79)90181-X.

Ueda H, Fukushima N, Yoshihara Y, Takagi H. A Met-enkephalin releaser (kyotorphin)-induced release of plasma membrane-bound Ca2+ from rat brain synaptosomes. Brain Res 1987a;419:197–200. https://doi.org/10.1016/0006-8993(87)90583-X.

Ueda H, Harada H, Nozaki M, Katada T, Ui M, Satoh M, et al. Reconstitution of rat brain mu opioid receptors with purified guanine nucleotide-binding regulatory proteins, Gi and Go. Proc Natl Acad Sci 1988;85:7013–7. https://doi.org/10.1073/pnas.85.18.7013.

Ueda H, Inoue M. In vivo signal transduction of nociceptive response by kyotorphin (tyrosine-arginine) through Galpha(i)- and inositol trisphosphate-mediated Ca(2+) influx. Mol Pharmacol 2000;57:108–15.

Ueda H, Inoue M, Weltrowska G, Schiller PW. An enzymatically stable kyotorphin analog induces pain in subattomol doses☆. Peptides 2000;21:717–22. https://doi.org/10.1016/S0196-9781(00)00190-X.

Ueda H, Matsumoto S, Yoshihara Y, Fukushima N, Takagi H. Uptake and release of kyotorphin in rat brain synaptosomes. Life Sci 1986a;38:2405–11. https://doi.org/10.1016/0024-3205(86)90609-0.

Ueda H, Ming G, Hazato T, Katayama T, Takagi H. Degradation of kyotorphin by a purified membrane-bound-aminopeptidase from monkey brain: potentiation of kyotorphin-induced analgesia by a highly effective inhibitor, bestatin. Life Sci 1985a;36:1865–71. https://doi.org/10.1016/0024-3205(85)90160-2.

Ueda H, Misawa H, Katada T, Ui M, Takagi H, Satoh M. Functional Reconstitution of Purified Gi and Go with u-Opioid Receptors in Guinea Pig Striatal Membranes Pretreated with Micromolar Concentrations of N-Ethylmaleimide. J Neurochem 1990;54:841–8. https://doi.org/10.1111/j.1471-4159.1990.tb02328.x.

Ueda H, Miyamae T, Hayashi C, Watanabe S, Fukushima N, Sasaki Y, et al. Protein kinase C involvement in homologous desensitization of delta-opioid receptor coupled to Gi-phospholipase C activation in Xenopus oocytes. J Neurosci 1995a;15:7485–99. https://doi.org/10.1523/JNEUROSCI.15-11-07485.1995.

Ueda H, Miyamae T, Nobuyuki F, Watanabe S, Misu Y. Evidence for a metabostatic opioid ϰ-receptor inhibiting pertussis toxin-sensitive metabotropic glutamate receptor-currents in Xenopus oocytes. FEBS Lett 1995b;375:201–5. https://doi.org/10.1016/0014-5793(95)01204-R.

Ueda H, Shiomi H, Takagi H. Regional distribution of a novel analgesic dipeptide kyotorphin (Tyr-Arg) in the rat brain and spinal cord. Brain Res 1980;198:460–4. https://doi.org/10.1016/0006-8993(80)90761-1.

Ueda H, Tamura S, Fukushima N, Katada T, Ui M, Satoh M. Inositol 1,4,5-Trisphosphate-Gated Calcium Transport through Plasma Membranes in Nerve Terminals. J Neurosci 1996;16:2891–900. https://doi.org/10.1523/JNEUROSCI.16-09-02891.1996.

Ueda H, Tatsumi K, Shiomi H, Takagi H. Analgesic dipeptide, kyotorphin (Tyr-Arg), is highly concentrated in the synaptosomal fraction of the rat brain. Brain Res 1982;231:222–4. https://doi.org/10.1016/0006-8993(82)90023-3.

Ueda H, Yoshihara Y, Fukushima N, Shiomi H, Nakamura A, Takagi H. Kyotorphin (tyrosine-arginine) synthetase in rat brain synaptosomes. J Biol Chem 1987b;262:8165–73.

Ueda H, Yoshihara Y, Misawa H, Fukushima N, Katada T, Ui M, et al. The kyotorphin (tyrosine-arginine) receptor and a selective reconstitution with purified Gi, measured with GTPase and phospholipase C assays. J Biol Chem 1989;264:3732–41.

Ueda H, Yoshihara Y, Nakamura A, Shiomi H, Satoh M, Takagi H. How is kyotorphin (Tyr-Arg) generated in the brain? Neuropeptides 1985b;5:525–8. https://doi.org/10.1016/0143-4179(85)90070-8.

Ueda H, Yoshihara Y, Takagi H. A putative met-enkephalin releaser, kyotorphin enhances intracellular Ca2+ in the synaptosomes. Biochem Biophys Res Commun 1986b;137:897–902. https://doi.org/10.1016/0006-291x(86)91164-2.

Vaught JL, Chipkin RE. A characterization of kyotorphin (Tyr-Arg)-induced antinociception. Eur J Pharmacol 1982;79:167–73. https://doi.org/10.1016/0014-2999(82)90622-7.

Vaz SH, Lérias SR, Parreira S, Diógenes MJ, Sebastião AM. Adenosine A2A receptor activation is determinant for BDNF actions upon GABA and glutamate release from rat hippocampal synaptosomes. Purinergic Signal 2015. https://doi.org/10.1007/s11302-015-9476-1.

Wang C, Zhao M, Yang J, Peng S. Synthesis and analgesic effects of kyotorphin-steroid linkers. Steroids 2001;66:811–5. https://doi.org/10.1016/S0039-128X(01)00112-X.

Wikimedia Foundation. Morphine. Morphine 2021. https://en.wikipedia.org/wiki/Morphine (accessed September 7, 2021).

Xiang J, Jiang H, Hu Y, Smith DE, Keep RF. Kyotorphin transport and metabolism in rat and mouse neonatal astrocytes. Brain Res 2010;1347:11–8. https://doi.org/10.1016/j.brainres.2010.05.094.

Xu W, Tan Lan, Wang H-F, Jiang T, Tan M-S, Tan Lin, et al. Meta-analysis of modifiable risk factors for Alzheimer's disease. J Neurol Neurosurg Psychiatry 2015:jnnp-2015-310548. https://doi.org/10.1136/jnnp-2015-310548.

Yamamoto M, Kawamuki K, Satoh M, Takagi H. Kyotorphin (L-TYR-L-ARG) inhibits extinction of pole-jumping avoidance response in the rat. Neurosci Lett 1982;31:175–9. https://doi.org/10.1016/0304-3940(82)90112-4.

Yaribeygi H, Panahi Y, Sahraei H, Johnston TP, Sahebkar A. The impact of stress on body function: a review. EXCLI J 16Doc1057 ISSN 1611-2156 2017. https://doi.org/10.17179/EXCLI2017-480.

Yoshihara Y, Ueda H, Fujii N, Shide A, Yajima H, Satoh M. Purification of a novel type of calcium-activated neutral protease from rat brain. Possible involvement in production of the neuropeptide kyotorphin from calpastatin fragments. J Biol Chem 1990;265:5809–15.

Yoshihara Y, Ueda H, Imajoh S, Satoh M, Takagi H. Calcium-activated neutral protease (CANP), a putative processing enzyme of the neuropeptide, kyotorphin, in the brain. Biochem Biophys Res Commun 1988;155:546–53. https://doi.org/10.1016/S0006-291X(88)80529-1.

Zarayskiy VV, Monje F, Peter K, Csutora P, Khodorov B, Bolotina VM. Store-Operated Orai1 and IP 3 Receptor-Operated TRPC1 Channel: Separation of the Siamese Twins. Channels 2007;1:246–52. https://doi.org/10.4161/chan.4835.

Zhang L, Fang Y, Lian Y, Chen Y, Wu T, Zheng Y, et al. Brain-Derived Neurotrophic Factor Ameliorates Learning Deficits in a Rat Model of Alzheimer's Disease Induced by Aβ1-42. PLOS ONE 2015;10:e0122415. https://doi.org/10.1371/journal.pone.0122415.

Zhang Z, Larner SF, Liu MC, Zheng W, Hayes RL, Wang KKW. Multiple alphaII-spectrin breakdown products distinguish calpain and caspase dominated necrotic and apoptotic cell death pathways. Apoptosis 2009;14:1289–98. https://doi.org/10.1007/s10495-009-0405-z.

Zidan M, Arcoverde C, Araújo NB de, Vasques P, Rios A, Laks J, et al. Alterações motoras e funcionais em diferentes estágios da doença de Alzheimer. Arch Clin Psychiatry São Paulo 2012;39:161–5. https://doi.org/10.1590/S0101-60832012000500003.

Zucchella C, Sinforiani E, Tamburin S, Federico A, Mantovani E, Bernini S, et al. The Multidisciplinary Approach to Alzheimer's Disease and Dementia. A Narrative Review of Non-Pharmacological Treatment. Front Neurol 2018;9:1058. https://doi.org/10.3389/fneur.2018.01058.

Zucker RS, Regehr WG. Short-Term Synaptic Plasticity. Annu Rev Physiol 2002;64:355–405. https://doi.org/10.1146/annurev.physiol.64.092501.114547.

Agradecimentos/Acknowledgments

Porque como tudo na vida, este trabalho não seria possível sem o [desi]equilíbrio de determinadas forças e energias do universo. Num tétris de decisões, momentos e pessoas, foi possível construir-se este trabalho. Apesar de ser um grão de areia num imenso areal, a parte romântica da pessoa que há em mim quer acreditar que dedicou algum tempo da sua vida a aumentar o conhecimento cientifico da humanidade...

Um especial obrigada às minhas orientadoras, sempre disponíveis. À Professora Ana Sebastião, agradeço por me ter acolhido no seu fantástico laboratório, recheado com tantas pessoas incríveis, e com o qual sempre me irei sentir orgulhosamente ligada. Por tornar a ciência de todos, para todos e sempre tão excitante. À Vera Neves, o meu elo com a bioquímica, obrigada por teres apoiado todas as nossas (neuro)decisões e estares sempre disponível para me receber. Por fim, à Mizé, que em muitos momentos foi a minha mãe científica. O "esforço" que faz pelos seus estudantes é admirável. É o verdadeiro exemplo de que tudo se consegue fazer com um pouco de fé e muito amor. Obrigada por ter apoiado todas as minhas aventuras paralelas a este trabalho, por ter partilhado tantas experiências comigo e pela paciência neste longo final que durou a escrita deste trabalho. Agradeço também ao Professor Miguel Castanho que, apesar de não ser formalmente um co-orientador, sempre desempenhou esse papel, possibilitando a minha estadia em Barcelona. Um obrigada ao Professor David Andreu e a toda a sua equipa do PRBB por me terem acolhido tão bem em Barcelona. Também agradeço aos membros do meu comité de tese, os professores Francisco Enguita, Susana Solá e Raquel Dias, pela sua disponibilidade em discutir os resultados do meu trabalho, pelos conselhos, palavras de conforto e motivação extra na recta final. Agradeço também a todos os meus colegas do Programa Doutoral M2B pela partilha científica, e convívio divertido nos nossos encontros.

Um obrigada a todos os meus colegas do iMM (ASebastião, MCastanho, LLopes, MRemondes e VMorais Labs), à Alexandra Botelho, Cristina Varandas e Sr. João, que, directa ou indirectamente, contribuiram para a realização deste trabalho.. Ao João e à Beatriz pelos anos/meses em que fomos a "AD team" (agora já foi noutra vida). Aos restantes *Mizeses*, por me terem recebido tão bem, e por terem partilhado a bancada e tantas experiências comigo (em especial à Catarina, ao Tiago, Carolina e Mafalda); aos *Astropeople* e aos *Xapellis* por tornarem o lab muito mais diversificado! Ao Adam por me ajudar a expandir ideias que julguei que nunca passariam disso mesmo. Um enorme obrigada à Filipa Nunes e Sofia Santos, pela ajuda, suporte, e por terem sido uma luzinha de presença, que fez toda a diferença para navegar durante o final esta aventura. Agradeço também à Sara Xapelli e à Sandra Vaz por, juntamente com a Mizé e a Professora Ana, me mostrarem a força que é ser-se mulher neste mundo tão exigente! Ao Nuno Morais agradeço o voto de confiança em mim, por ter apoiado as minhas ideias, por me inspirar a ser uma melhor pessoa. Foi um prazer imenso fazer parte desta equipa durante este último ano e meio, e presenciar a dedicação e profissionalismo de todos. Aprendi muito convosco e foram (e ainda são) uma lufada de ar fresco nesta pandemia! Adorei todos os nossos projectos paralelos e partilhar um pouquinho dessa amizade simples que vos une. Obrigada Mariana, Nuno, Miguel, Marta, Rita e Zé. Por tudo.

Obrigada à Catarina Lourenço e à Nádia Rei, pelo exemplo de mulheres de armas que são; ao Miguel Ferreira, pessoinha completamente desajustada, obrigada pela ajuda na revião dos meus textos, animais sacrificados, e tantos cafés; ao Rui, pelas gargalhadas, encorajamento no nomadismo, e por me teres confiado a tua ideia inicial do “Fala-me Neuro”! Essencialmente, obrigada pela vossa amizade pura, sem filtros e sem outros demais interesses.

A todos aqueles que irei levar comigo desta aventura, obrigada! Porque a ciência (e a vida no geral) é difícil; é um mar de emoções com tantas derrotas e conquistas, lágrimas e gargalhadas (daquelas que chegam a ser forçadas para reprimir a angústia), e teria sido tudo demasiado solitário sem vocês. Como não me quero esquecer de ninguém, obrigada a todos aqueles que de alguma forma contribuiram para me ajudar a viver durante esta etapa de sobrevivência constante. Obrigada pelas pausas para cafés, lanches, chocolates e gelados partilhados, jantares com copos de vinho ou chá, somersbys em frente ao hospital, fatias picadas e krebs preparado, abraços roubados, apontamentos organizados, exercícios resolvidos e trabalhos de grupo (aos “the 4 nearest neighbours”); pelos almoços na cantina, aulas de ioga e braçadas na piscina (aos “[Covidando]Cantina&Gym”), pela nossa “semana pijama”, trotinetes na califórnia, ovos moles, e churrascadas, enfim... obrigada pelo exemplo de boas pessoas que são e por me inspirarem a ser melhor todos os dias! Agradeço a todos no “Fala-me Neuro”, pela companhia virtual que passei a ansiar todas as semanas! Assistir ao crescer da vossa dedicação ao projecto fez de mim uma pessoa sem dúvida mais feliz.

Por fim, agradeço àqueles que partiram comigo para esta brincadeira... Obrigada pela vossa amizade, por me mostrarem que a vida é muito mais do que esta dimensão. Em especial, a todos aqueles que partilharam conversas, quilometros dentro do carro, praias, auroras, cervejas e cidras, lagos, grutas, cascatas, iguarias, cantorias, contagens de final de anos, estórias, fotos, conselhos, lágrimas, gargalhadas, babyshowers e aniversários, trilhos e mergulhos, pizzas, e sucessos! A todos vocês, e em especial ao “bando dos cinco”: Gonçalo, Mariana, Diana e Tiago - obrigada por existirem e tornarem tudo tão simples, orgânico e natural!

Um enorme obrigada à minha familia! Aos meus pais, sempre disponíveis e amigos, por compreenderem o meu carácter, respeitarem o meu tempo, o meu espaço e as minhas decisões, pela preocupação e por todo o amor e miminhos constantes. Tornam a minha vida muito mais leve e completa. À minha irmã Inês, às amigas que sempre seremos, à mulher que se tornou e que me irei sempre orgulhar. Nunca deixes ninguém diminuir os teus sonhos. E, por fim, à minha nova família, aquela que veio como um embrulho bonito em volta da melhor prenda que a vida me deu.

Ao Gonçalo, agradeço por simplesmente existires na minha vida. És o meu equilíbrio constante e tornas-me numa melhor pessoa. Obrigada por me manteres segura (pelo “abrigo e comida”), por me desafiares e tirares da zona de conforto. Obrigada por me continuares a deixar sonhar, sonhares comigo, e por me manteres na terra... Sei que tens o melhor e o pior de mim. Desculpa por este percurso ter sido tão atribulado e demorado. Prometo tentar fazer [e ser] melhor daqui para a frente!

Termina aqui esta fantástica aventura de mais de 5 anos (sempre em “hard mode”, porque nem tinha piada se não fosse). Obrigada por terem ficado desse lado até ao fim. Que venha a próxima!

Appendix

frontiers in Pharmacology

ORIGINAL RESEARCH
published: 09 July 2020
doi: 10.3389/fphar.2020.00985

The Neuroprotective Action of Amidated-Kyotorphin on Amyloid β Peptide-Induced Alzheimer's Disease Pathophysiology

Rita F. Belo[1,2†], Margarida L. F. Martins[1,2†], Liana Shvachiy[3], Tiago Costa-Coelho[1,2], Carolina de Almeida-Borlido[1,2], João Fonseca-Gomes[1,2], Vera Neves[2,4], Hugo Vicente Miranda[5], Tiago F. Outeiro[5,6,7,8], Joana E. Coelho[2], Sara Xapelli[1,2], Cláudia A. Valente[1,2], Montserrat Heras[9], Eduard Bardaji[9], Miguel A. R. B. Castanho[2,4‡], Maria José Diógenes[1,2‡] and Ana M. Sebastião[1,2‡]*

[1] Instituto de Farmacologia e Neurociências, Faculdade de Medicina, Universidade de Lisboa, Lisbon, Portugal, [2] Instituto de Medicina Molecular João Lobo Antunes, Faculdade de Medicina, Universidade de Lisboa, Lisbon, Portugal, [3] Cardiovascular Autonomic Function Lab, Centro Cardiovascular da Universidade de Lisboa, Lisbon, Portugal, [4] Instituto de Bioquímica, Faculdade de Medicina, Universidade de Lisboa, Lisbon, Portugal, [5] CEDOC, Chronic Diseases Research Center, NOVA Medical School, Faculdade de Ciências Médicas, Universidade Nova de Lisboa, Lisboa, Portugal, [6] Department of Experimental Neurodegeneration, Center for Biostructural Imaging of Neurodegeneration, University Medical Center Göttingen, Göttingen, Germany, [7] Max Planck Institute for Experimental Medicine, Göttingen, Germany, [8] Translational and Clinical Research Institute, Faculty of Medical Sciences, Newcastle University, Framlington Place, Newcastle Upon Tyne, United Kingdom, [9] Laboratori d'Innovació en Processos i Productes de Síntesi Orgànica (LIPPSO), Departament de Química, Universitat de Girona, Girona, Spain

Kyotorphin (KTP, L-tyrosyl-L-arginine) is an endogenous dipeptide initially described to have analgesic properties. Recently, KTP was suggested to be an endogenous neuroprotective agent, namely for Alzheimer's disease (AD). In fact, KTP levels were shown to be decreased in the cerebrospinal fluid of patients with AD, and recent data showed that intracerebroventricular (i.c.v.) injection of KTP ameliorates memory impairments in a sporadic rat model of AD. However, this administration route is far from being a suitable therapeutic strategy. Here, we evaluated if the blood-brain permeant KTP-derivative, KTP-NH_2, when systemically administered, would be effective in preventing memory deficits in a sporadic AD animal model and if so, which would be the synaptic correlates of that action. The sporadic AD model was induced in male Wistar rats through i.c.v. injection of amyloid β peptide (Aβ). Animals were treated for 20 days with KTP-NH_2 (32.3 mg/kg, intraperitoneally (i.p.), starting at day 3 after Aβ administration) before memory testing (Novel object recognition (NOR) and Y-maze (YM) tests). Animals were then sacrificed, and markers for gliosis were assessed by immunohistochemistry and Western blot analysis. Synaptic correlates were assessed by evaluating theta-burst induced long term potentiation (LTP) of field excitatory synaptic potentials (fEPSPs) recorded from hippocampal slices and cortical spine density analysis. In the absence of KTP-NH_2 treatment, Aβ-injected rats had clear memory deficits, as assessed through NOR or YM tests. Importantly, these memory deficits were absent in Aβ-injected rats that

OPEN ACCESS

Edited by:
Jacob Raber, Oregon Health and Science University, United States

Reviewed by:
Christian Hölscher, Lancaster University, United Kingdom
Romain Goutagny, UMR7364 Laboratoire de Neurosciences Cognitives et Adaptatives (LNCA), France

***Correspondence:**
Ana M. Sebastião
anaseb@medicina.ulisboa.pt

[†]*These authors share first authorship*

[‡]*These authors share senior authorship*

Specialty section:
This article was submitted to Neuropharmacology, a section of the journal Frontiers in Pharmacology

Received: *09 March 2020*
Accepted: *18 June 2020*
Published: *09 July 2020*

Citation:
Belo RF, Martins MLF, Shvachiy L, Costa-Coelho T, de Almeida-Borlido C, Fonseca-Gomes J, Neves V, Vicente Miranda H, Outeiro TF, Coelho JE, Xapelli S, Valente CA, Heras M, Bardaji E, Castanho MARB, Diógenes MJ and Sebastião AM (2020) The Neuroprotective Action of Amidated-Kyotorphin on Amyloid β Peptide-Induced Alzheimer's Disease Pathophysiology. Front. Pharmacol. 11:985. doi: 10.3389/fphar.2020.00985

had been treated with KTP-NH_2, which scored in memory tests as control (sham i.c.v. injected) rats. No signs of gliosis could be detected at the end of the treatment in any group of animals. LTP magnitude was significantly impaired in hippocampal slices that had been incubated with Aβ oligomers (200 nM) in the absence of KTP-NH_2. Co-incubation with KTP-NH_2 (50 nM) rescued LTP toward control values. Similarly, Aβ caused a significant decrease in spine density in cortical neuronal cultures, and this was prevented by co-incubation with KTP-NH_2 (50 nM). In conclusion, the present data demonstrate that i.p. KTP-NH_2 treatment counteracts Aβ-induced memory impairments in an AD sporadic model, possibly through the rescuing of synaptic plasticity mechanisms.

Keywords: amidated-kyotorphin, Alzheimer's disease, amyloid β peptide, novel object recognition test, Y-Maze alternation test, long-term potentiation, memory, synaptic plasticity

INTRODUCTION

Kyotorphin (KTP) is an endogenous dipeptide composed by tyrosine and arginine (L-tyrosyl-L-arginine) residues, first described as a powerful analgesic molecule (Takagi et al., 1979a; Takagi et al., 1979b). Given its analgesic properties, KTP has been investigated as a drug for pain treatment (Ribeiro et al., 2011b; Santos et al., 2013). Although mechanisms underpinning KTP-induced analgesic effects are still not entirely understood, some authors argue that KTP binds to a specific Gi-coupled protein receptor (KTPr), which despite numerous efforts, has never been isolated (Ueda et al., 1989). Nevertheless, it is well-known that KTP triggers the release of met-enkephalins (met-enk) and β-endorphins in a naloxone-reversible opioid receptors mediated-mechanism (Takagi et al., 1979a; Shiomi et al., 1981; Ueda et al., 1982; Oliveira et al., 2016), an effect antagonized by the dipeptide L-Leu-L-Arg (a KTPr antagonist) (Ueda et al., 1989; Kawabata et al., 1992).

Interestingly, despite the high expression of KTP in the cortex, the levels of enkephalins and of opioid receptors are low, suggesting other non-opioid physiological actions for KTP (Ueda et al., 1980). Remarkably, KTP has been pointed as a possible neuroprotective factor (Dzambazova and Bocheva, 2010), emerging as a novel drug to be explored for Alzheimer´s disease (AD) and other therapeutic applications.

AD is a chronic progressive neurodegenerative disease and the most common cause of dementia in elderly. The presence of senile plaques (amyloid beta (Aβ) peptide) and neurofibrillary tangles (hyperphosphorylated tau (p-Tau) protein) in the brain are the molecular hallmarks of the disease (Price et al., 1991; Citron, 2010). AD represents a challenge for drug discovery since effective neuroprotective treatments are still needed. It was reported that AD patients present decreased levels of KTP in cerebrospinal fluid (CSF) (Santos et al., 2013) suggesting the increase in KTP levels as a possible therapeutic strategy.

Despite the encouraging recent data showing that intracerebroventricular (i.c.v) injection of KTP ameliorates memory impairments in a sporadic AD rat model (Angelova et al., 2019), its weak activity when administered systemically (Chen et al., 1998) renders KTP as an unrealistic pharmacological tool to fight AD. Amidated-kyotorphin (KTP-NH_2), is a KTP derivative capable of crossing the blood brain barrier (BBB) (Ribeiro et al., 2011a; Ribeiro et al., 2011b), and with efficacy to decrease neuronal damage induced by cerebral hypoperfusion (Sá Santos et al., 2016). Altogether, these findings prompted us to investigate whether systemic administration of KTP-NH_2 would be effective to ameliorate memory impairment in an animal model of sporadic AD, and if so, which are the synaptic mechanisms operated by KTP-NH_2 to protect synapses against Aβ-induced toxicity.

MATERIALS AND METHODS

Drugs

Amyloid β Peptide

For *in vivo* experiments, Amyloid β (Aβ) peptide 1 to 42 ($Aβ_{1–42}$) (H-1368, Bachem Bubendorf, Switzerland) was dispersed in water at a concentration of 2.25 mg/ml.

In order to prepare oligomeric species of $Aβ_{1–42}$ ($Aβ_{olig}$), $Aβ_{1–42}$ (1 mg/ml) (A-42-T, GenicBio, Shanghai, China) was suspended in phosphate-buffered saline (PBS), supplemented with 0.025% ammonia solution and adjusted to a final pH 7.2 (HCl). Species separation was based on an ultrafiltration process, as previously described (Giuffrida et al., 2009). Briefly, $Aβ_{1–42}$ (220 μM) was allowed to oligomerize by constant shaking at 600 rpm, at 37°C for 16 h and ultracentrifuged (40,000*g*, 30 min) for separation of fibrils (pellet). The supernatant was further separated in centrifugal filters (30 kDa Amicon Ultra). The concentration of the retained fraction, corresponding to oligomers > 30 kDa, was spectrophotometrically determined (ϵ_{280} = 1490 M^{-1} cm^{-1}). Oligomers aliquots (120–220 μM) were immediately stored at −80°C until further use.

In addition, *in vitro* experiments using primary neuronal cultures were performed using the Aβ fragment 25–35 ($Aβ_{25–35}$) (Bachem, Bubendorf, Switzerland). $Aβ_{25–35}$ represents the biologically active region of Aβ and induces the same molecular and cellular dysfunction as $Aβ_{1–42}$ species, being this effect similar to what has been observed in AD brains (Pike et al., 1995; Kaminsky et al., 2010). Stock solutions of $Aβ_{25–35}$ were prepared in MilliQ water to a final concentration of 1 mg/ml.

KTP-NH_2 Peptide

KTP-NH_2 peptide was synthesized as previously described (Ribeiro et al., 2011b). For *in vivo* experiments, KTP-NH_2 was dissolved in physiological saline solution (0.9% NaCl, vehicle solution), as a 100 mM stock solution, and it was administered at a dose of 32.3 mg/kg, at a volume of 1 ml/kg. The selected dose was based on previous results regarding KTP-NH_2 analgesic action profile (Ribeiro et al., 2011b; Ribeiro et al., 2013). For *ex vivo* and *in vitro* experiments, KTP-NH_2 was prepared in previously filtered and sterile milliQ water as 1 and 5 mM stock solutions, respectively.

Intracerebroventricular Injection of Aβ Peptide

Male Wistar rats (8–10 weeks), purchased from Charles River Laboratories (Lyon, France), were housed in a group of 2 per cage and maintained under controlled conditions (20 ± 2°C; 14:10 h light/dark cycle, lights on between 7:00 AM and 9:00 PM). All animals had unrestricted access to food and water. The handling of animals and all described procedures were conducted according to the European Community (86/609/EEC; 2010/63/EU; 2012/707/EU) and Portuguese (DL 113/2013) legislation for the protection of animals used for scientific purposes, and they were approved by the Ethical Committee for Animal Research of Instituto de Medicina Molecular João Lobo Antunes (iMM), Faculty of Medicine, University of Lisbon, and the Portuguese Competent Authority for Animal Welfare (DGAV) in Portugal.

The animal model of AD was created based on the $A\beta_{1-42}$ i.c.v. injection method, as previously described (Canas et al., 2009; Zhang et al., 2015). Surgical procedures were performed when animals reached 230 to 320 g and during the light period. Briefly, animals were anesthetized with isoflurane (2–3% in O_2) using a RC2 Rodent Anesthesia System (VetEquip Inc., California, USA), firstly using a plexiglas chamber and thereafter maintained *via* facial mask. EMLA® cream was applied in the ear canal, and Bupivacaine Hydrochloride 0.25% (8 mg/kg, SC) was administered at the incision site for local anesthetics. Lacryvisc® (Carbomer 974P 0.3%) was applied on the eyes to avoid dehydration. Buprenorphine (0.05 mg/kg, SC) was also administered pre-emptively for general analgesia, so it would be already in action when animals recovered from anesthesia.

Twelve animals were i.c.v. injected with Aβ peptide (2.25 mg/ml) in 5 µl and 14 were injected with 5 µl of water (vehicle) at day zero. Injections were performed with a 33-gauge Hamilton microsyringe (Hamilton Company, Nevada, USA) using a microinjection pump (World Precision Instruments, Inc., Florida, USA) with a rate of 500 nl/min, in the right lateral ventricle using a stereotactic system (anteroposterior, −0.84 mm from bregma; medial/lateral, 1.5 mm; and dorsal/ventral, −3.5 mm). Injections lasted 10 min, and the needle with the syringe was left in place for 2 min after the injection to ensure complete infusion of Aβ. Animal body temperature was kept constant at 37°C using a heating pad. A timeline of all the experimental events is depicted in **Figure 1A**. Previous work reported soluble forms of Aβ on the hippocampus of i.c.v. Aβ injected animals (Canas et al., 2009), thus showing Aβ diffusion through this brain region. Compared with transgenic models of AD, the i.c.v. Aβ-induced sporadic model of AD is more relevant for the study of Aβ-induced pathophysiological traits of AD. Moreover, the transgenic models of AD are usually used to study the familial form of the disease, which barely represents 5% of AD cases (Lecanu and Papadopoulos, 2013).

Chronic Intraperitoneal KTP-NH_2 Treatment

Thirteen animals underwent a chronic 18-day treatment regimen of KTP-NH_2 (32.3 mg/kg, single i.p. dose/day), starting the second day after i.c.v. administration of $A\beta_{1-42}$ (Aβ + KTP-NH_2 group, n=6) or vehicle (KTP-NH_2 group, n=7), and lasting until sacrifice. The remaining thirteen animals received the vehicle solution following the same treatment regimen: Aβ + vehicle (Aβ group, n = 6) and vehicle + vehicle (control group, n = 7). The experimental groups of animals are depicted in **Figure 1B**. During the last 5 days of i.p. treatments (KTP-NH_2 or vehicle), animals were tested in the behavioral paradigms identified below. During behavioral

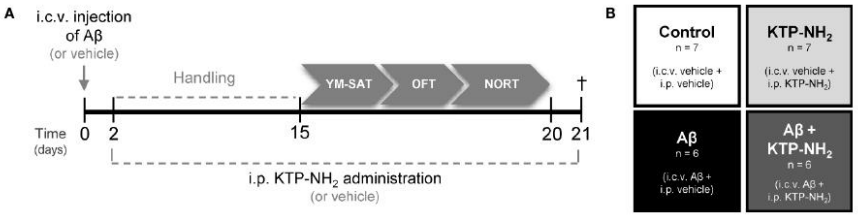

FIGURE 1 | Experimental design. **(A)** Animals were i.c.v. injected with Aβ ($A\beta_{1-42}$) or vehicle (water) at day 0. On day 2, KTP-NH_2 or vehicle (saline solution) i.p. administration began, simultaneously with handling. Behavioral tests were performed between days 15 and 20: Y-Maze Spontaneous Alternation test (YM-SAT), Open Field test (OFT), and Novel Object Recognition test (NORT). On day 21 animals were sacrificed (†) for molecular analyses (WB and IHC). **(B)** Four experimental groups were tested: Control (i.c.v. and i.p. vehicle administration, n = 7); Aβ (i.c.v. Aβ administration and i.p. vehicle treatment, n = 6); KTP-NH_2 (i.c.v. vehicle administration and i.p. KTP-NH_2 treatment, n = 7), and Aβ + KTP-NH_2 (i.c.v. Aβ administration and i.p. KTP-NH_2 treatment, n = 6).

assessment days, injections were performed after animal testing and before return to the animal house.

Behavioral Testing

Behavioral tests were performed from the fifteenth day after $A\beta_{1-42}$ injection, following a previously described protocol (Cunha et al., 2008; Canas et al., 2009). The handling period coincided with the first 13 days of KTP-NH_2 treatment, where animals were handled for a few minutes before the i.p. injection so that they became used to the experimenter and to the testing room. All behavioral tests were carried out between 9:00 AM and 6:00 PM. All the apparatus used were cleaned with 70% ethanol between animals switching. After placing the animal inside the behavioral apparatus, the experimenter immediately left the room. The experimenter conducting behavioral analysis was blinded to treatment conditions.

Tests were performed in the following order: Y-Maze Spontaneous Alternation Test (YM-SAT), Open Field Test (OFT), and Novel Object Recognition Test (NORT) (**Figure 1A**). The YM-SAT was performed before the NORT to evaluate working memory for a less complex paradigm first. Since OFT and NORT use the same testing arena, the OFT was performed during the first 5 min of the first day of NORT habituation period (first contact with the arena).

Y-Maze Spontaneous Alternation Test (YM-SAT)

The spontaneous alternation version of the Y-Maze test evaluates spatial working memory by taking advantage of the willingness of rodents to explore new environments. The testing protocol for YM-SAT has been described in detail previously (Maurice et al., 1996). The wood-made maze used was composed of 3 arms (30 x 10 x 20 cm each), converging to an equal angle. Visual cues were placed on the walls of the maze. Briefly, without prior habituation, animals were individually placed at the end of one arm and allowed to freely move through the maze for 8 min. Two independent investigators visually recorded arm entries, and the comparison between recordings showed total agreement.

An entry was considered valid when all four limbs of the animal were within the arm. An alternation was defined as entries in all three arms on consecutive occasions. The number of maximum possible alternations for each animal was therefore the total number of arm entries minus two. The percentage of spontaneous alternation was calculated as actual alternations/maximum alternations ×100. In addition, the total number of arm entries was used as a measure of locomotor activity.

Open Field Test (OFT)

The OFT is widely used to assess individual spontaneous locomotor activity and anxiety-like behavior when animals are introduced to a novel environment (Prut and Belzung, 2003; Bailey and Crawley, 2009; Castanheira et al., 2018). Importantly, this test allows to detect bias in animal behaviour that could affect performance on NORT, since locomotor activity can impact exploratory drive (Broadhurst, 1957; Broadhurst, 1958). The open field arena consisted of an empty square wood box (67 x 67 x 51 cm height), virtually divided into three concentric squares: a peripheral, an intermediate and a central zone. The testing protocol has been described in detail previously (Gould et al., 2009). Briefly, animals were individually placed in the center of the arena and allowed to freely move for 5 min. The behaviour was video-recorded and analyzed by the tracking software Smart® (version 2.5; Panlab, Barcelona, Spain). The reference point used for the animal tracking position was defined as the center of the animal dorsum. Both total travelled distance (cm) and average velocity (cm/s) were measured to assess locomotor activity. In addition, the percentage of time spent in the arena periphery was used as an indicator of the level of anxiety-like behavior. All animals were tested only once.

Novel Object Recognition Test (NORT)

Considering that episodic long-term memory is the predominant cognitive deficit in AD, animals were subjected to the NORT (Antunes and Biala, 2012). To assess long-term memory a retention interval (RI) of 24 h was used. This test consists of three phases: habituation, familiarization (training), and test. The habituation phase consisted of 3 sessions of habituation to the arena (15 min each day). During both familiarization and test phases, two objects were added to the same arena, always in the same place. The objects used in this test were translucent glass bottles and brown glass bottles without labels, that were similar in size and shape, but which the animals were able to discriminate between them. To prevent coercion to explore the objects, animals were individually placed in the middle of the opposite wall where objects were, with their backs to them, and allowed to freely move for 5 min. In the familiarization phase, animals were presented with two equal objects, which we herein name as 'familiar' objects. During the familiarization phase, chosen objects were counterbalanced between animals within the same experimental group to reduce any object preference effect. Similarly, object localization was counterbalanced between both arena sides, to eliminate possible preference confounds for a specific side of the arena. Following sample-objects exposure, animals returned to the home cage for 24 h. In the test phase, one of the previously experienced objects (now considered familiar objects) was substituted by a new object (considered the novel object). Exploration was scored when the animal touched an object with its forepaws or snout, bit, licked, or sniffed the object from a distance of no more than 1.5 cm. Running around the object or climbing on it was not recorded as exploration. Animal movements were recorded using the SMART® video-tracking software (version 2.5; Panlab, Barcelona, Spain). A post-analysis was conducted to refine the results obtained by software measures. Two independent investigators made the post-analysis with a high degree of concordance between them.

Three indexes were calculated in order to evaluate both preference between objects and recognition of the novel object: 1) the object preference index, which is the ratio between the time spent exploring one object over the total time spent exploring both objects [object 1 or object 2/(object 1 + object 2)], and it is assessed both in the training and test phases; 2) the object recognition index, which is the ratio between the time spent exploring the novel object and the total time spent exploring both objects [novel/(novel + familiar)], and it is an index of retention, used for analysis of the test phase

performance; and finally, 3) the object discrimination index, which is the ratio between the difference between the time spent exploring the novel and the familiar object, and the total time spent exploring both objects [(novel − familiar)/(novel + familiar)], allowing an easier visualization of data since no memory retention scores as zero (Antunes and Biala, 2012).

Western Blot

After behavioral tests, three/four animals from each group were deeply anesthetized with isoflurane (Esteve, Barcelona, Spain) and decapitated. Their brains were quickly removed and placed in ice-cold aCSF, continuously oxygenated (O_2/CO_2: 95%/5%) to isolate both hippocampi. The left and the right hippocampi were individually frozen in liquid nitrogen and stored at −80°C. The two hippocampi were analyzed separately to allow the separate quantification of the hippocampus of the side of the i.c.v. injection (right, ipsilateral) and of the contralateral to it. Since both hippocampi could be differently exposed to Aβ, they could display different degrees of gliosis. Using a Potter homogenizer, tissue homogenates were prepared from frozen samples by solubilizing them in Radio-Immunoprecipitation Assay (RIPA) buffer: 50 mM Tris-base (pH 7.5), 150 mM NaCl, 5 mM Ethylenediaminetetraacetic Acid (EDTA), 0.1% *Sodium Dodecyl Sulphate* (SDS), and 1% Triton X-100, supplemented with phosphatase inhibitors: 10 nM NaF; 5 mM Na_3VO_4 and a protease inhibitor cocktail (Complete Mini-EDTA free from Roche, Penzberg, Germany). Samples were centrifuged at 13,000*g*, 4°C for 10 min, and the supernatant was collected and placed in fresh tubes. Protein concentration was quantified through Bradford method, using Bio-Rad DC reagent (Bio-Rad Laboratories, Berkeley, CA, United States). All samples were prepared with the same amount of total protein (35 μg), by adding a loading buffer (350 mM Tris-HCl (pH 6.8), 10% SDS, 30% glycerol, 600 mM Dithiothreitol, 0.06% bromophenol blue), and then boiled at 95°C for 5 min. Next, samples and the molecular weight marker (PageRuler™ Plus Prestained Protein Ladder, 10 to 250 kDa, ThermoFisher Scientific, Massachusetts, USA) were loaded and separated on 12% SDS–polyacrylamide gel electrophoresis (SDS–PAGE) within a standard migration buffer (25 mM Tris-base (pH 8.3), 192 mM Glycine, 10% SDS), at a constant voltage between 80 and 120 mV. Subsequently, proteins were electrotransferred, at 400 mA for 1 h 30 min, from the gel to a polyvinylidene difluoride (PVDF) membrane (GE Healthcare, Buckinghamshire, United Kingdom), previously activated with methanol for 5 min, within the standard buffer (25 mM Tris (pH 8.3), 192 mM Glycine, 15% methanol) for wet transfer conditions. Afterward, membranes were stained with Ponceau S solution (Sigma-Aldrich®) to check for transference efficacy, and blocked with a 3% bovine serum albumin (BSA) in TBS-T (Tris-Buffered Saline with Tween-20 containing in mM: Tris base 20; NaCl 137 and 0.1% Tween-20) during 1 h at RT to avoid non-specific binding. Membranes were incubated with the primary antibodies overnight at 4°C, and then with the HRP-conjugated secondary antibodies (1:10000, Santa Cruz Biotechnology, Dallas, TX, USA) for 1 h at RT, all diluted in 3% BSA solution in TBS-T. The primary antibodies used were rabbit polyclonal antibody anti-GFAP (1:5000, Sigma, St. Louis, MO, USA), goat polyclonal antibody anti-Iba-1 (1:1000, Abcam, Cambridge, UK), and mouse monoclonal antibody anti-GAPDH (1:5000, Invitrogen, Carlsbad, California, USA). Chemiluminescent detection was performed with ECL Plus Western Blotting Detection Reagent (GE Healthcare, Buckinghamshire, UK) in the ChemiDoc™ XRS+ System from Bio-Rad. The integrated intensity of each band was calculated using computer-assisted densitometry analysis with Image-J 1.45 software (Bethesda Softworks, Bethesda, MD, United States) and normalized to the integrated intensity of the loading control (GAPDH). Images were prepared for printing in Image Lab software 5.2.1 (software available in ChemiDoc XRS+ system, Bio-Rad).

Immunohistochemistry

After behavioral tests, three animals of each group were deeply anesthetized with ketamine/xylazine mixture (120 mg/kg/16 mg/kg) at a volume of 1 ml/kg. After reaching a deep anesthesia state, the animals were perfused transcardially with approximately 200 ml of warmed (37°C) 0.9% saline solution, to clear the blood from the circulatory system, followed by approximately 500 ml of 4% paraformaldehyde (PFA) in phosphate buffer (PBS, 140 mM NaCl, 3 mM KCl, 20 mM Na_2HPO_4, 1.5 mM KH_2PO_4, pH 7.4) (Gage et al., 2012). Animals were then decapitated, and their brains were carefully removed and maintained for post-fixation in the same fixative solution at 4°C overnight. After that, brains were washed twice with PBS, and then cryoprotected at 4°C by immersion in increasing concentrations of sucrose (15% and 30%). Subsequently, brains were gelatin-embedded (7.5% gelatin in 15% sucrose) and then sectioned at a thickness of 12 μm on a cryostat (LEICA CM 3050S, Wetzlar, Germany), by the Histology and Comparative Pathology Laboratory of iMM. Only the coronal sections located at the level of hippocampus (around −2.92 mm and −5.04 mm from Bregma) were collected, mounted on SuperFrost® Plus slides (Menzel-Glaser, Braunschweig, Germany) and stored at −20°C for further use.

For the immunohistochemical analyses, slices were placed in PBS for 10 min at 37°C to remove the gelatin from brain tissue. Then, each slice was surrounded with DAKO pen (Dako, Glostrup, Denmark) to protect staining areas from drying out and from mixing with each other. After an incubation in glycine (0.1 M) for 10 min to remove the small toxic aldehydes originated from PFA degradation, sections were subsequently treated with 0.1% Triton X-100 in PBS (10 min) for membrane permeabilization, washed twice (10 min each time) with PBS in the presence of 0.1% Tween-20 (PBS-T) and then blocked with a blocking solution (10% Fetal Bovine Serum (FBS), 6/10% BSA in PBS-T) for 30 min at RT. Next, slices were incubated with the primary antibodies overnight at 4°C, and with the fluorophores coupled-secondary antibodies for 2 h at RT in a humidified dark chamber. The nuclei were stained with Hoechst 33342 (20 μg/ml, Invitrogen) for 10 min at RT. The slices were mounted in Mowiol (Sigma). The primary antibodies used were mouse monoclonal antibody anti-GFAP (1:1000, Millipore, Burlington, Massachusetts, USA), and goat polyclonal antibody anti-Iba1 (1:1000, Abcam). The secondary antibodies were donkey anti-mouse-Alexa Fluor 568, and donkey anti-goat-Alexa Fluor 488

(1:500, Invitrogen). Images were acquired on an inverted wide field fluorescence microscope (Zeiss Axiovert 200, Zeiss, Oberkochen, Germany), using a monochrome digital camera (AxioCamMR3, Zeiss), with a 40× objective (Zeiss). The software AxioVision 4.7.1 (Carl Zeiss Imaging Systems) was used for image acquisition. Immunofluorescence images were acquired in two areas of the hippocampus: cornu ammonis 1 (CA1) and dentate gyrus (DG), of both hemispheres of each animal.

Freshly Prepared Hippocampal Slices and Drug Treatment

Male C57BL/6J mice (8–11 weeks old), purchased to Charles River Laboratories (Lyon, France), were housed in groups of 4/5 per cage and maintained under controlled conditions (21 ± 1°C; 55 ± 10% humidity; 12:12 h light/dark cycle). Animals were deeply anesthetized with isoflurane (Esteve, Barcelona, Spain) and decapitated to quickly remove their brains. Then, brains were placed in ice-cold artificial cerebral-spinal fluid solution (aCSF; 124 mM NaCl, 3 mM KCl, 1.2 mM NaH_2PO_4, 25 mM $NaHCO_3$, 2 mM $CaCl_2$, 1 mM $MgSO_4$, and 10 mM glucose, pH 7.4), continuously oxygenated (O_2/CO_2: 95%/5%) to dissect both hippocampi. Acute hippocampal slices were cut, with a thickness of 400 μm, perpendicularly to the long axis of the hippocampus using a McIlwain tissue chopper, and placed in a resting chamber filled with continuously oxygenated aCSF at RT for 1 h to guarantee the functional and energetic recovery. Slices were incubated for 3 h at RT with continuously oxygenated aCSF with 50 nM KTP-NH_2 in the presence or absence of 200 nM $A\beta_{olig}$.

Ex Vivo Electrophysiological Recordings

Long-term potentiation (LTP) induction and quantification were performed as described previously (Diógenes et al., 2011). Briefly, hippocampal slices were transferred to a recording chamber continuously superfused with oxygenated aCSF at 32°C (flow rate of 3 ml/min). Stimulation pulses were delivered every 20 s using a bipolar concentric wire electrode placed on Shaffer collateral/commissural fibers in stratum radiatum, and field-excitatory post-synaptic potentials (fEPSPs) were recorded extracellularly through a microelectrode filled with aCSF (2–6 MΩ) placed in the stratum radiatum of the CA1 area. The intensity of stimulation was initially adjusted to obtain a fEPSP slope with a minimal spike contamination and of around 50% of the maximal slope. Recordings were obtained with an Axodamp 2B amplifier (Axon Instruments, Foster City, CA, United States), digitized, and continuously stored on a personal computer with the WinLTP software (Anderson and Collingridge, 2001). Individual responses were monitored, averages of six consecutive responses were obtained, and the slope of the initial phase of the fEPSP was quantified. After fEPSPs stabilization, LTP was induced through a θ-burst protocol (3 trains of 100 Hz, 3 stimuli, separated by 200 ms). The θ-burst induced LTP pattern of stimulation is considered closer to what physiologically occurs in hippocampi during episodes of learning and memory in living animals (Albensi et al., 2007). We used a mild LTP protocol since this proved to be sensitive to synaptic plasticity changes along with aging (Diógenes et al., 2011), and allows assessing both further improvements or impairments on LTP magnitude. LTP magnitude was quantified as the percentage of change in the average slope of fEPSPs taken between 50 to 60 min after LTP induction in relation to the average slope of fEPSPs measured during the 10 min before θ-burst induced LTP (baseline).

Primary Neuronal Cultures and Drug Treatment

Primary neuronal cultures were obtained from fetuses of 18/19-days pregnant Sprague-Dawley females, as routinely in the lab (Jerónimo-Santos et al., 2015). Briefly, animals were deeply anaesthetised with isoflurane and decapitated. The fetuses were collected and placed in cold Ca^{2+}- and Mg^{2+}-free Hank's Balanced Salt Solution (HBSS) (Gibco, Paisley, UK). The brains were dissected, the cerebral cortices were isolated, and the meninges were removed. Then, the tissue was mechanically fragmented, followed by enzymatic digestion with 0.025% (w/v) of trypsin solution in HBSS for 15 min at 37°C. To neutralize the action of trypsin, HBSS supplemented with FBS 20% (w/v) and cellular suspension was centrifuged at 190*g*. The supernatant was discarded, and the cells were resuspended in the same solution by pipette aspiration in order to dissociate cells. This process was repeated three times. After washing, cells were resuspended in supplemented Neurobasal medium (0.5 mM L-glutamine, 25 mM glutamic acid, 2% B-27, and 25 U/ml penicillin/streptomycin). Then, cell suspension was filtered (BD Falcon Cell Strainer 70 mM, Thermo Fisher Scientific, Waltham, MA, United States) to obtain single cells, and cell density was determined by counting cells in a 0.4% trypan blue solution using a hemocytometer. Cells were plated at 1×10^{-5} cells/well on 12-wells flat-bottom cell plates covered with glass coverslips (Corning® Costar® TC-treated, Sigma), and maintained at 37°C in a humidified atmosphere of 95/5% O_2/CO_2, for 14 days. The coverslips were previously sterilized under UV light, coated overnight with 10 mg/ml of poly-D-lysine (Sigma, St. Louis, MO, United States) and washed with sterile H_2O. After 13 days *in vitro* (DIV13), cells were incubated with 50 nM KTP-NH_2 in the presence or absence of 25 μM $A\beta_{25-35}$, during 24 h.

Immunocytochemistry

In order to evaluate the neuroprotective effect of drug treatment, spine density was counted as previously done in our lab (Tanqueiro et al., 2018). Briefly, primary neuronal cultures at DIV14 were fixed in 4% PFA in PBS (pH 7.4) for 15 min at RT, after being washed with PBS twice. Using a blocking solution (3% (w/v) BSA) (Sigma-Aldrich) in PBS with 0.1% (v/v) Triton X-100, cells were incubated for 1 h at RT. To specifically detect neurons, cells were incubated with mouse microtubule-associated protein 2 (MAP2) primary antibody (1:200 in blocking solution) (Millipore), overnight at 4°C in a wet-chamber. After this, cells were washed with PBS twice and then co-incubated in blocking solution with goat anti-mouse-Alexa Fluor 568 secondary antibody (1:200, Invitrogen), Alexa Fluor 488 Phalloidin (1:40) (Invitrogen), which recognizes filamentous actin (F-actin), and Hoechst 33342 (6 μg/ml) for

nuclear staining, for 1 h at RT inside a dark-wet chamber. After being washed with PBS twice, coverslips were mounted in Mowiol mounting solution. Using a confocal laser point-scanning microscope LSM 880 with Airyscan (Carl Zeiss MicroImaging, Thornwood, NY, United States), the observed conjugation between MAP2 (568, red) and F-actin (488, green) allowed the clear identification of dendritic protrusions, since F-actin has an important role in the constitution of the cytoskeleton of dendritic spines (Koskinen and Hotulainen, 2014). Spine density was assessed as the number of protrusions, counted per 10 μm of the parent dendrite, as previously reported (Alonso et al., 2004; Ji et al., 2010) with a distance of 25 μm from the cell body. Independent averages were computed with counts of 3 different dendrites of each neuron, 6 neurons per condition, with each primary neuronal culture being considered an independent experiment.

Statistical Analysis

Data are expressed as mean ± standard error of the mean (mean ± SEM), where *n* is the number of independent experiments. Results of each animal per group, and results acquired from different hippocampal slices of different animals were considered independent experiments. The data normality was confirmed using the Shapiro-Wilk test. Results obtained using behavioral paradigms, OFT, YM-SAT, NORT (object recognition index and object discrimination index), through electrophysiological recordings (LTP magnitude), and using immunocytochemistry (number of dendritic protrusions) were analyzed using two-way ANOVA, followed by the Tukey's multiple comparisons test. In addition, significant differences between means of NORT object preference index within each phase were evaluated through unpaired two-tailed Student's *t*-test. Results obtained by Western blot (WB) were analyzed using two-way ANOVA. Values of $p < 0.05$ were considered to represent statistically significant differences. All statistical analyses were conducted using the Prism Software (GraphPad Prism®, version 8.0.2, California, USA).

RESULTS

KTP-NH_2 Treatment Prevented Episodic Long-Term and Spatial Working Memory Dysfunction Induced by Aβ

To evaluate the influence of KTP-NH_2 in an animal model of AD (Canas et al., 2009; Zhang et al., 2015), KTP-NH_2 (32.3 mg/kg) or saline solution (vehicle) was i.p. administered for 18 days to rats that had received a 5 μl i.c.v injection of $A\beta_{1-42}$ (2.25 mg/ml) or water (vehicle) (**Figure 1A**). As such, the experimental groups are the following: control group (vehicles); KTP-NH_2 group (vehicle + KTP-NH_2 treatment); Aβ group (Aβ and vehicle treatment); and Aβ + KTP-NH_2 group (Aβ and KTP-NH_2 treatment) (**Figure 1B**).

Episodic long-term memory, considered the predominant cognitive deficit in AD, was evaluated through the NORT with a retention time of 24 h (see Methods). As expected, in the training phase (**Figure 2**, gray bars), the four groups of animals explored approximately the same amount of time the two identical objects. In the test day (**Figure 2**, black and white bars), animals from the Aβ group did not react to novelty ($p > 0.05$, unpaired two-tailed Student's *t*-test to compare % of time spent with familiar *vs.* novel object; n = 6; **Figure 2C**), whereas the control group did ($p \leq 0.0001$, unpaired Student's *t*-test to compare % of time spent with familiar *vs.* novel object; n = 7; **Figure 2A**). Remarkably, the Aβ induced-impairment in the NORT was totally recovered in the animals that had been treated with KTP-NH_2 (**Figure 2D**). These treated animals showed a clear preference for exploring the novel object more than the familiar one ($p \leq 0.0001$, unpaired Student's *t*-test to compare % of time spent with familiar *vs.* novel object; n = 6), thus behaving like control animals. The KTP-NH_2 group also behaved like a control group ($p > 0.05$, unpaired two-tailed Student's *t*-test to compare % of time spent with familiar *vs.* novel object; n = 7; **Figure 2B**), indicating that *per se* KTP-NH_2, is not a memory enhancer, though markedly ameliorating memory deficits elicited by Aβ.

To better compare performances among the four groups of animals, the time spent exploring each object in the test day was converted into the object recognition index [novel/(novel + familiar)], and the object discrimination index [(novel – familiar)/(novel + familiar)], which were calculated for each animal and averaged within each group (**Figures 3A, B**, respectively). The object recognition index ranges from 0 to 1, where obtained values around 0.5 reflect an absence of discrimination between the novel and the familiar objects. The discrimination index ranges from −1 to +1, and obtained values around 0 reflect lack of object discrimination. In both indexes, higher obtained values indicate higher memory performance. As depicted in **Figure 3**, the recognition index attained by the Aβ group was significantly different from the control group (Aβ: 0.48 ± 0.046 *vs.* control: 0.71 ± 0.028; $p < 0.05$, two-way ANOVA with Tukey's multiple comparisons test; n = 6–7). Importantly, the index displayed by the Aβ + KTP-NH_2 group, (0.67 ± 0.020, n = 6) was similar to the control group ($p > 0.05$, two-way ANOVA with Tukey's multiple comparisons test; n = 6–7), and significantly different from Aβ group ($p < 0.05$, two-way ANOVA with Tukey's multiple comparisons test; n = 6–7). Moreover, the KTP-NH_2 treatment alone (KTP-NH_2 group) did not affect the object recognition index (0.68 ± 0.028, n = 7) when compared to the control group ($p > 0.05$, two-way ANOVA with Tukey's multiple comparisons test; n = 6–7). Thus, this analysis further confirms that KTP-NH_2 treatment had beneficial effects on the performance of Aβ i.c.v. injected animals in long-term memory testing. Similar findings were obtained by calculated scores of the discrimination index (control: 0.43 ± 0.058; Aβ: −0.05 ± 0.091; KTP-NH_2: 0.36 ± 0.053; and Aβ + KTP-NH_2: 0.35 ± 0.039, two-way ANOVA with Tukey's multiple comparisons test; n = 6–7).

To determine whether KTP-NH_2 treatment could counteract the Aβ induced-impairments in spatial working memory, animals were subjected to the YM-SAT, and their performance was assessed through the percentage of spontaneous alternation as described in

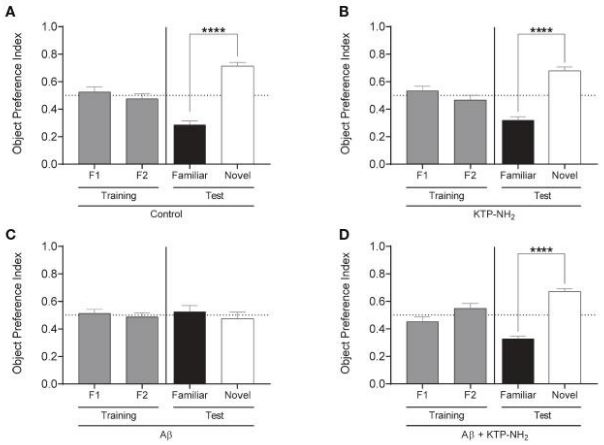

FIGURE 2 | The KTP-NH_2 treatment mitigates Aβ-induced impairments in long-term (24 h) episodic memory. Long-term episodic memory was evaluated through the Novel Object Recognition test (NORT). After 3 arena habituation sessions, the training phase consisted of one session with two identical objects (F1 and F2) placed inside the arena. The test phase occurred on the following day (24 h later), where one of the familiar objects (Familiar) was replaced by a novel object (Novel). During both phases, animals freely explore the objects for 5 min and the results are given by the time spent exploring any one of the two objects allows to calculate the Object Preference Index, i.e., F1 or F2 / (F1 + F2) and Familiar or Novel / (Familiar + Novel). A preference index above 0.5 indicates a preference of that specific object, whereas equal to 0.5 represents no preference. Statistical analysis using unpaired two-tailed Student's t-test showed no statistical differences in preference between objects during the training phase (as expected), and revealed a significant preference for the novel objects during the test phase for control **(A)**, KTP-NH_2 **(B)**, and Aβ + KTP-NH_2 **(D)** groups (n = 6–7), which indicates that memory is conserved within these animals. For the Aβ group **(C)**, data showed that there was no preference between familiar and novel objects (n = 6). ****p ≤ 0.0001. Data are represented as mean ± SEM.

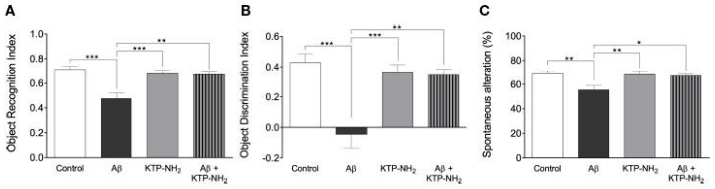

FIGURE 3 | KTP-NH_2 treatment mitigates Aβ-induced impairments in long-term episodic memory and spatial working memory. **(A)** Object recognition index was calculated from the data obtained in the test day of the Novel Object Recognition test (NORT), as [novel / (novel + familiar)], and it ranges from 0 to 1 (where 1 means only exploration of the novel object and zero means only exploration of the familiar object). **(B)** Object discrimination index was also calculated from the data obtained in the test day of NORT, as [(novel – familiar) / (novel + familiar)], and it ranges from –1 to 1, where zero means no discrimination between both objects. **(C)** The percentage of spontaneous alternation was calculated from data obtained during the Y-Maze Spontaneous Alternation test (YM-SAT), as actual alternations/maximum alternations x 100. For each statistical analysis, significant differences between the group of Aβ animals (n = 6) and all the other groups (n = 6–7) were assessed using two-way ANOVA followed by Tukey's multiple comparisons test. *p < 0.05, **p ≤ 0.01, ***p ≤ 0.001. Data are represented as mean ± SEM.

methods (**Figure 3B**). As expected, animals from Aβ group had a lower percentage of spontaneous alternation when compared with animals from the control group (Aβ: 55 ± 3.5 *vs.* control: 69 ± 2.0, $p < 0.05$, two-way ANOVA with Tukey's multiple comparisons test; n = 6–7), confirming that Aβ i.c.v. injected animals had an impairment in spatial working memory. However, when Aβ i.c.v. injected animals were treated with KTP-NH_2 (Aβ + KTP-NH_2 group) the percentage of spontaneous alternation in the YM-SAT (67 ± 1.3, n = 6) was similar to the control group ($p > 0.05$, two-way ANOVA with Tukey's multiple comparisons test; n = 6–7), and significantly different from that of the Aβ group ($p < 0.05$, two-way ANOVA with Tukey's multiple comparisons test; n = 6–7), implying that KTP-NH_2 treatment reduced the Aβ induced-deficits in YM-SAT. Moreover, KTP-NH_2 alone had no significant effect, since the percentage of spontaneous alternation of animals from KTP-NH_2 group (68 ± 2.4, n = 7) was not

significantly different from the control group ($p > 0.05$, two-way ANOVA with Tukey's multiple comparisons test).

Performance in the NORT and in the YM-SAT can be affected by changes in locomotion, by anxiety-like behavior, or by alterations in exploratory drive. To control for these parameters, animals were assessed in the OFT. No statistically significant differences (**Figure 4**; $p > 0.05$, two-way ANOVA; $n = 6–7$) were found between any of the experimental groups when analyzing the total distance travelled (**Figure 4A**), or the average velocity (**Figure 4B**). In addition, the total number of entries in the YM-SAT arms was also analyzed (control: 26 ± 1.6; Aβ: 23 ± 1.5; KTP-NH_2: 25 ± 2.0; Aβ + KTP-NH_2: 21 ± 1.5), and no significant differences were found between any of the groups ($p > 0.05$, two-way ANOVA; $n = 6–7$). Together, these results show that neither Aβ, nor KTP-NH_2, alone or in combination, caused appreciable effects in locomotor activity that could mask performance in the NORT or YM-SAT. Similarly, no statistically significant differences ($p > 0.05$, two-way ANOVA, $n = 6–7$) were found between groups for the percentage of time spent in the periphery of the OFT arena (**Figure 4C**), which also indicates an absence of appreciable changes in anxiety-like behaviour.

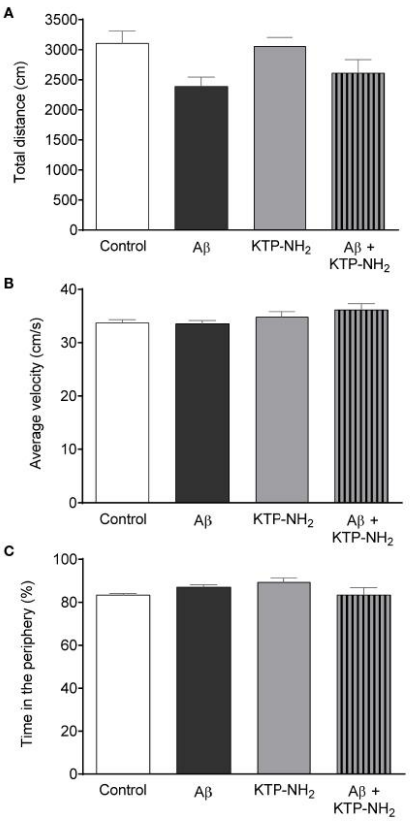

FIGURE 4 | Neither Aβ nor KTP-NH_2 treatment affected locomotor activity or anxiety-like behaviour. Results obtained during the Open-field test (OFT) performance allow the assessment of locomotor activity through the **(A)** total distance travelled (cm), and **(B)** average velocity (cm/s). **(C)** Anxiety-like behaviour was evaluated through the percentage of time spent in the periphery of the OFT. Statistical analysis using two-way ANOVA did not reveal significant differences ($p < 0.05$) between groups ($n = 6-7$). Data are represented as mean ± SEM.

Hippocampal Gliosis Immediately After Testing Was Not Different Among the Groups

To assess if Aβ could lead to an increase in the proliferation of astrocytes and microglia at the time of testing, which could suggest gliosis and thus inflammation, WB assays were performed with protein extracts obtained from hippocampal homogenates prepared upon animal sacrifice after behavioral testing. GFAP and Iba-1 were used as markers for astrocytes and microglia, respectively (**Figure 5**). Densitometry analyses of the WB revealed no significant changes ($n=3–4$; $p > 0.05$, two-way ANOVA) in samples from Aβ injected animals when compared with control, and in response to KTP-NH_2 treatment, thus indicating an absence of proliferation of astrocytes and microglia cells. Nevertheless, since WB assay did not provide information about morphological changes of astrocytes and microglia, immunohistochemistry analysis of glial cell morphology was performed to further address this issue. As shown in **Figure 6**, regardless of the hippocampal area analyzed (CA1 or DG), there was no evidence of astrogliosis (evaluated by GFAP immunoreactivity) or microgliosis (evaluated by Iba-1 immunoreactivity), either in control or Aβ animals, treated or untreated with KTP-NH_2, since no morphologic differences in glial cells were noticeable.

KTP-NH_2 Prevented the Impairment in θ-Burst-Induced LTP Magnitude Caused by Aβ

To address the synaptic mechanisms involved in the ability of KTP-NH_2 to mitigate memory impairment in animals injected with Aβ, we assessed the effect of KTP-NH_2 upon θ-burst-induced LTP in hippocampal slices that had been incubated with 200 nM $Aβ_{olig}$ (**Figures 7A, B**), a known to be toxic conformational arrangement of Aβ (Giuffrida et al., 2009).

LTP magnitude (**Figure 7C**), recorded in slices pre-incubated with 200 nM $Aβ_{olig}$ for 3 h (Aβ) was significantly decreased when compared to that attained in control slices incubated for a similar amount of time in the absence of Aβ (control: 25.4 ± 6.15 *vs.* Aβ: −4.52 ± 6.53, $p < 0.05$, two-way ANOVA with Tukey's multiple comparisons test; $n = 5–8$). Remarkable, in slices co-incubated with 200 nM $Aβ_{olig}$ and 50 nM KTP-NH_2 (Aβ + KTP-NH_2), LTP magnitude (24.2 ± 3.50, $n = 5$) attained values similar to those in control slices ($p > 0.05$, two-way ANOVA with Tukey's multiple comparisons test; $n = 5–8$). Moreover, LTP

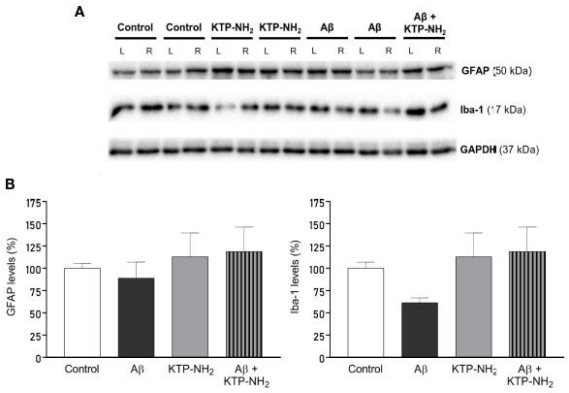

FIGURE 5 | Neither Aβ nor KTP-NH_2 affected hippocampal gliosis assessed by immunoblotting. Protein levels were assessed by western blotting using tissue homogenates from each isolated hippocampus of 13 animals, 3-4 for each experimental group (Control, KTP-NH_2, Aβ, and Aβ + KTP-NH_2). **(A)** Representative immunoblots of GFAP (50 kDa), Iba-1 (17 kDa) and GAPDH (37 kDa). GAPDH was used as a loading control. **(B)** Densitometry analysis of the right (R) (side of i.c.v injection) hippocampus, performed for all groups with ImageJ software. No statistically significant differences were found between animal groups regarding GFAP or Iba-1 immunoreactivity and ($p > 0.05$, two-way ANOVA, $n = 3$-4). Data are represented as mean ± SEM.

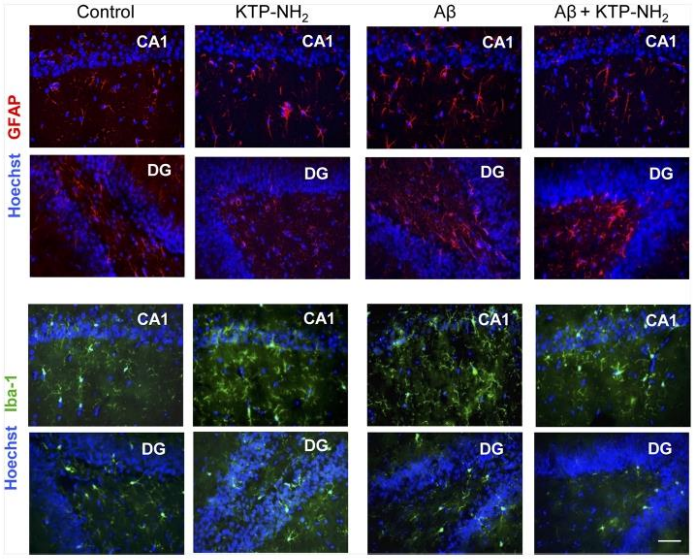

FIGURE 6 | Neither Aβ nor KTP-NH_2 affected hippocampal gliosis assessed by immunohistochemistry labeling. At day 21, thirteen deeply anesthetized animals were transcardially perfused with ice-cold saline and 4% PFA solutions. After decapitation, brains were removed and gelatin-embedded to be sectioned on a cryostat. Coronal sections located at hippocampus level were collected and mounted for labelling with GFAP to stain astrocytes (red) and Iba-1 to stain microglia (green). Nuclei were stained with Hoechst (blue). Images of both CA1 and DG hippocampal areas were acquired on an inverted wide-field fluorescence microscope (Zeiss Axiovert 200), with a 40x objective. The figure includes representative images of each experimental group (Control, KTP-NH_2, Aβ, and Aβ + KTP-NH_2). There was no difference in GFAP or Iba-1 staining between conditions. Scale bar, 50 µm.

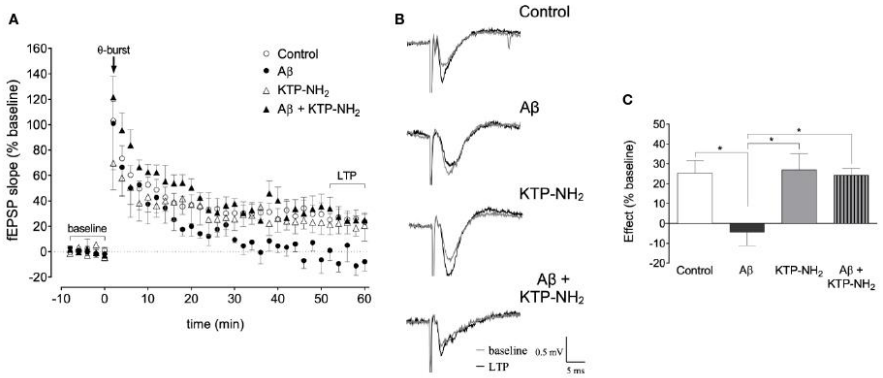

FIGURE 7 | Incubation with KTP-NH_2 reduces the impact of Aβ on LTP magnitude upon θ-burst-induced LTP. **(A)** The averaged time courses changes in field excitatory post-synaptic potential (fEPSP) slope (% baseline) induced by a θ-burst stimulation in animal hippocampal slices with a pre-exposure of 3 h to aCSF solution (control, n = 8) with 200 nM $Aβ_{olig}$ (Aβ, n = 5), 50 nM KTP-NH_2 (KTP-NH_2, n = 4), or 200 nM $Aβ_{olig}$ and 50 nM KTP-NH_2 (Aβ + KTP-NH_2, n = 5). **(B)** Tracings from representative experiments. For each condition, fEPSP tracings recorded at baseline (baseline, grey line) and after θ-burst-induced LTP (LTP, black line) from the same slice are showing overlaid. **(C)** Histogram depicting the effect on LTP magnitude (% average changes in fEPSP slope at 50-60 min normalized to the defined baseline of 10 min immediately before θ-burst stimulation) regarding each group under study (control, Aβ, KTP-NH_2, Aβ + KTP-NH_2). Statistical analysis using two-way ANOVA followed by Tukey's multiple comparisons test indicates a significant difference between the Aβ condition (n = 5), and all the other groups (n = 4-8). *p < 0.05. Data are represented as mean ± SEM.

magnitude in slices pre-incubated with only 50 nM KTP-NH_2 (KTP-NH_2) was similar (27.0 ± 8.10, n = 4) to that in control slices (p > 0.05, two-way ANOVA with Tukey's multiple comparisons test; n = 5–8). Altogether, these results clearly indicate that KTP-NH_2 prevents Aβ-induced impairment of LTP without by itself affecting LTP.

KTP-NH_2 Prevented the Decrease in Spine Density Caused by Aβ Action on Cultured Cortical Neurons

To further investigate the synaptic correlates of the protective action of KTP-NH_2 against Aβ-induced synaptic impairment, we evaluated the effect of KTP-NH_2 on spine density of cultured cortical neurons. The conjugation between MAP2 (red) and Phalloidin (green) labels, allowed the identification of dendritic protrusions (yellow) (**Figure 8A**), as a morphological readout of the treatment modulation of the number of dendritic spines. The representative segments of 10 μm of counted dendrites for each analysed condition are illustrated in **Figure 8B**.

In accordance with previous studies (Tanqueiro et al., 2018), cultured cortical neurons exposed to $Aβ_{25–35}$ for 24 h, showed a significant decrease in the number of dendritic protrusions when compared to the control condition (Aβ: 6.58 ± 0.153 *vs.* control: 8.07 ± 0.153; p < 0.05, two-way ANOVA with Tukey's multiple comparisons test; n = 5) (**Figure 8C**). Remarkably, the Aβ-induced impairment in the number of dendritic protrusions was absent when neurons were co-treated with 50 nM KTP-NH_2 (Aβ + KTP-NH_2: 9.60 ± 0.134 *vs.* control: 8.07 ± 0.153; p < 0.05, two-way ANOVA with Tukey's multiple comparisons test; n = 5). KTP-NH_2 alone did not significantly alter dendritic protrusions when compared to the control condition (KTP-NH_2: 8.41 ± 0.071 *vs.* control: 8.07 ± 0.153; p > 0.05, two-way ANOVA with Tukey's multiple comparisons test; n = 5).

DISCUSSION

A main finding in the present work is that systemically applied KTP-NH_2 prevents memory dysfunction induced by Aβ. At the synaptic level we could demonstrate that KTP-NH_2 prevents synaptic plasticity and spine density impairments caused by Aβ, suggesting that KTP-NH_2 mitigates memory deficits by protecting hippocampal synapses against Aβ-induced toxicity.

Since the hippocampus is required for performance in the NORT (Goulart et al., 2010), this test has been considered a useful tool for basic and preclinical research in the context of AD (Rajagopal et al., 2014). In addition, the sustained strengthening of synaptic connections that characterizes hippocampal long-term potentiation (LTP) is taken as a synaptic correlate of the basic mechanisms involved in memory and learning processes (Bliss and Collingridge, 1993). Accordingly, abnormal performance in memory tasks, especially hippocampal-dependent ones (Figurov et al., 1996; Korte et al., 1998; Pang and Lu, 2004), are associated with impairments in LTP (Morris et al., 1986). Our data showing that KTP-NH_2 prevented the Aβ-induced impairment of hippocampal LTP, strongly suggest that the reestablishment of synaptic plasticity is one of the mechanisms underlying the cognitive actions of KTP-NH_2.

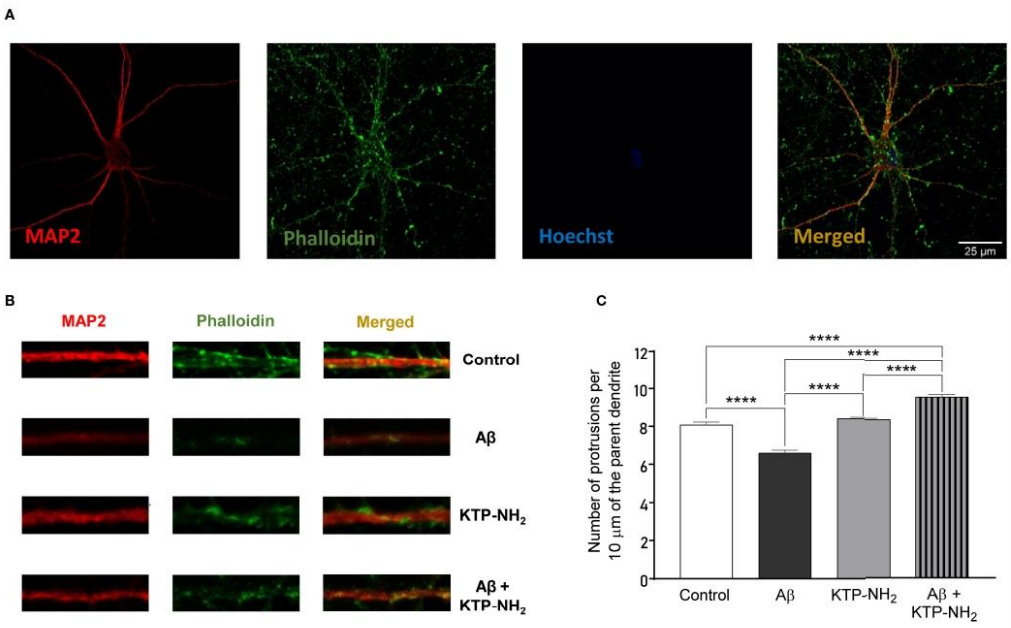

FIGURE 8 | Incubation with KTP-NH_2 mitigates Aβ incubation-induced impairments in spine. **(A)** Representative image of an untreated neuron (control) obtained from primary neuronal cultures. Primary neuronal cultures (DIV13) were incubated with 25 µM $Aβ_{25-35}$ and/or with 50 nM KTP-NH_2 for 24 h. MAP2 (red) specifically labels neurons, while phalloidin (green) labels F-actin. The merge between both labels (yellow) allows the identification of dendritic protrusions. To evaluate spine density, the number of protrusions *per* 10 µm of the parent dendrite with a distance of 25 µm from the cell body were counted (3 parent dendrites *per* neuron, 6 neurons *per* condition). **(B)** Treatment effects on synaptic density (10 µm). **(C)** Histogram depicting spine density as the number of protrusions from each condition. Statistical analysis using two-way ANOVA followed by Tukey's multiple comparisons test indicates a significant difference between conditions (n = 5). While 25 µM $Aβ_{25-35}$ treatment (Aβ) diminished the number of protrusions in cortical neurons, 50 nM KTP-NH_2 co-treatment (Aβ + KTP-NH_2) restored spine density. In addition, 50 nM KTP-NH_2 treatment (KTP-NH_2) did not, by itself, impact spine density. ****$p \leq 0.0001$. Data are represented as mean ± SEM.

Furthermore, at a molecular level, neuronal spine density has been associated with synaptic reinforcement during LTP (Toni et al., 1999; Luscher and Malenka, 2012). In fact, spine density is known to be reduced in cultured cortical neurons incubated with Aβ peptide (Tanqueiro et al., 2018). Our results show that KTP-NH_2 restores Aβ-induced decrease in spine density, further explaining its neuroprotective actions upon synaptic plasticity. These results pave the way for further studies on the mechanism of action of KTP-NH_2 addressing if it reestablishes spine density *in vivo*.

While the presence of episodic memory impairments mimics the clinical hallmarks detected in AD patients in the early stages of the disease (Alescio-Lautier et al., 2007; Gold and Budson, 2008; Huntley and Howard, 2010), motor dysfunctions are better noticed in moderate to severe stages of AD (Zidan et al., 2012). In the present work, we could detect episodic memory dysfunctions through the YM-SAT and NORT, without signs of clear motor dysfunctions, judged by OFT performance. This indicates that the sporadic AD model used mostly mimics the earlier stages of AD. It is known that loss of synapses, mainly in the hippocampus, is one of the earliest consequences of Aβ toxicity (Canas et al., 2009), and that this loss correlates with the initial memory impairments in AD patients (Coleman et al., 2004). Furthermore, compared to the transgenic models of AD available, the use of this sporadic AD model, where the Aβ injection is responsible for the induced-pathophysiological traits of AD, allows us to have a direct understanding of the effect of KTP-NH_2 administration on the Aβ-induced dysfunction. Our findings support that systemic administration of KTP-NH_2 is able to prevent memory loss as well as synaptic plasticity dysfunctions induced by Aβ, highlight the therapeutic potential of BBB permeable KTP analogues in early stages of AD. This may gain particular relevance since the few therapeutic tools so far available for early disease stages are mostly symptomatic to increase cholinergic function. As we show, the KTP derivative is able to enhance synaptic plasticity

and, importantly, to prevent retraction of dendritic spines in cultured neurons, thus to prevent synaptic atrophy, a clear sign of neuroprotective ability.

Furthermore, KTP biosynthesis occurs in the nerve terminals (Ueda et al., 1986), which is especially relevant in AD pathophysiology, where the loss of cortical mass evolves fast during the early stages of the disease (Sabuncu, 2011). This cellular death implies less KTP production capability, resulting in a decrease of KTP concentration in the CSF of AD patients (Santos et al., 2013). Accordingly, the increase of KTP levels in the brain emerged as a possible therapeutic tool for AD treatment. However, KTP has pharmacokinetic hindrances, such as its limited capacity to cross the BBB and its high susceptibility to clearance mechanisms, which hampered its clinical use (Serrano et al., 2015). Our work shows that it is possible to circumvent this problem by using a BBB permeant KTP analogue, KTP-NH_2. The introduced structural change increased the peptide global net charge, increasing its capacity to interact with biological membranes, most notably giving it the ability to cross the BBB (Ribeiro et al., 2011a).

Besides having an acute and chronic well-characterized analgesic-profile when systemically administrated (Ribeiro et al., 2011a; Ribeiro et al., 2011b), this small and cost-effective molecule also showed a remarkable anti-inflammatory effect. Accordingly, independent studies developed by our lab showed that KTP-NH_2 impacts the glucocorticoid system, which might account for the molecular link between analgesia, anti-inflammation, and neuroprotection (Perazzo et al., 2017). Neuroinflammation caused by Aβ has been commonly linked to the presence of gliosis and, in some studies, to neuronal damage. In the present work, gliosis was evaluated on day 21 after Aβ i.c.v. injection by both immunohistochemistry and Western blotting and, in agreement with previous data (Canas et al., 2009), no significant signs of astrogliosis nor microgliosis were detected in the hippocampus. However, it is important to highlight that the peak of the inflammatory response after Aβ injection is one week after injection (McLarnon, 2014). So, we cannot discard initial Aβ-induced neuroinflammation nor an influence of KTP-NH_2 that may have occurred before memory assessment. Nevertheless, our results show that at least immediately after memory testing, there were no signs of gliosis.

In summary, we clearly show that, in a sporadic AD model, systemic administration of KTP-NH_2 protects spatial working- and episodic memory, without affecting motor activity or inducing anxiety-like behavior. Moreover, KTP-NH_2 prevented Aβ-induced deficits in LTP magnitude and in spine density. We, therefore, highlight a neuroprotective action of KTP-NH_2 against the early stages of AD pathophysiology. While these results are promising as far as pharmacodynamics is concerned, they clearly push toward the need of further studies on the pharmacokinetics of KTP-NH_2 after its systemic administration through different routes, as well as to the need of other studies directed toward other hallmarks of AD. Indeed, in light of the complex pathophysiology of AD, it is important to know whether KTP-NH_2 has a greater potential as a standalone treatment, or rather as part of a broader multidrug treatment regimen.

DATA AVAILABILITY STATEMENT

The raw data supporting the conclusions of this article will be made available by the authors, without undue reservation, to any qualified researcher.

ETHICS STATEMENT

The animal study was reviewed and approved by Ethical Committee for Animal Research of Instituto de Medicina Molecular João Lobo Antunes (iMM), Faculty of Medicine, University of Lisbon, and the Portuguese Competent Authority for Animal Welfare (DGAV) in Portugal.

AUTHOR CONTRIBUTIONS

RFB and MLFM contributed equally to this work. Both performed the experiments, interpreted the results, and wrote the initial draft of the manuscript. RFB performed electrophysiological recordings and immunocytochemistry experiments as well as all statistical analyses. MLFM performed the i.c.v. injection of Aβ together with SX and JEC, the animal behavioral studies with LS under the supervision of JEC, and Western blots and immunohistochemistry procedures under the guidance of CAV. RFB and JF-G were responsible by the neuronal cell cultures. TC-C and CA-B contributed equally to immunocytochemistry analysis. HVM was responsible for preparing oligomeric species of Aβ with the supervision of TFO. CAV contributed to the interpretation of Western blot and immunohistochemistry experiments. VN contributed to the interpretation of the results. MH and EB were responsible for the synthetize of the KTP-NH_2 peptide. MJD was responsible for the concept and design of the study regarding electrophysiological and immunocytochemistry experiments, contributed to the interpretation of the results. MARBC and AMS were responsible for the study design, interpreted the results and supervised the work. All authors contributed to the article and approved the submitted version.

FUNDING

This study was supported by Santa Casa da Misericórdia de Lisboa (MB37-2017) and Fundação para a Ciência e Tecnologia (FCT): PTDC/NEU-OSD/5644/2014, and PTDC/BIA-VIR/29495/2017. RFB was supported by FCT (PD/BD/114337/2016). JF-G was supported by FCT (PD/BD/114441/2016). JEC was supported by FCT (SFRH/BPD/87647/2012).

ACKNOWLEDGMENTS

The authors would like to thank Rodents, Comparative Pathology and Bioimaging Units of iMM for the support along

with this study. Catarina Beatriz Ferreira, Adam Armada-Moreira and Filipa F. Ribeiro for being part of the cortical neuronal culture team at Ana Sebastião Lab. Francisco M. Mouro for helping to set up the behavioral tests and how to properly interpret the results of those tests. Sara R. Tanqueiro and Rita M. Ramalho for helping with immunocytochemistry technique and analysis. Miguel Ferreira for the document proof-reading.

REFERENCES

Albensi, B. C., Oliver, D. R., Toupin, J., and Odero, G. (2007). Electrical stimulation protocols for hippocampal synaptic plasticity and neuronal hyper-excitability: Are they effective or relevant? *Exp. Neurol.* 204, 1–13. doi: 10.1016/j.expneurol.2006.12.009

Alescio-Lautier, B., Michel, B. F., Herrera, C., Elahmadi, A., Chambon, C., Touzet, C., et al. (2007). Visual and visuospatial short-term memory in mild cognitive impairment and Alzheimer disease: Role of attention. *Neuropsychologia* 45, 1948–1960. doi: 10.1016/j.neuropsychologia.2006.04.033

Alonso, M., Medina, J. H., and Pozzo-Miller, L. (2004). ERK1/2 activation is necessary for BDNF to increase dendritic spine density in hippocampal CA1 pyramidal neurons. *Learn. Mem. Cold Spring Harb. N.* 11, 172–178. doi: 10.1101/lm.67804

Anderson, W. W., and Collingridge, G. L. (2001). The LTP Program: a data acquisition program for on-line analysis of long-term potentiation and other synaptic events. *J. Neurosci. Methods* 108, 71–83. doi: 10.1016/S0165-0270(01)00374-0

Angelova, H., Pechlivanova, D., Krumova, E., Miteva-Staleva, J., Kostadinova, N., Dzhambazova, E., et al. (2019). Moderate protective effect of Kyotorphin against the late consequences of intracerebroventricular streptozotocin model of Alzheimer's disease. *Amino Acids* 51 (10–12), 1501–1513. doi: 10.1007/s00726-019-02784-5

Antunes, M., and Biala, G. (2012). The novel object recognition memory: neurobiology, test procedure, and its modifications. *Cogn. Process.* 13, 93–110. doi: 10.1007/s10339-011-0430-z

Bailey, K. R., and Crawley, J. N. (2009). "Anxiety-Related Behaviors in Mice," in *Methods of Behavior Analysis in Neuroscience Frontiers in Neuroscience*. Ed. J. J. Buccafusco (Boca Raton (FL): CRC Press/Taylor & Francis). Available at: [Accessed February 20, 2020].

Bliss, T. V., and Collingridge, G. L. (1993). A synaptic model of memory: long-term potentiation in the hippocampus. *Nature* 361, 31–39. doi: 10.1038/361031a0

Broadhurst, P. L. (1957). Determinants of emotionality in rat: I. Situational factors. *Br. J. Psychol.* 48, 1–12. doi: 10.1111/j.2044-8295.1957.tb00594.x

Broadhurst, P. L. (1958). Determinants of emotionality in the rat: II. Antecedent factors*. *Br. J. Psychol.* 49, 12–20. doi: 10.1111/j.2044-8295.1958.tb00632.x

Canas, P. M., Porciuncula, L. O., Cunha, G. M. A., Silva, C. G., Machado, N. J., Oliveira, J. M. A., et al. (2009). Adenosine A2A Receptor Blockade Prevents Synaptotoxicity and Memory Dysfunction Caused by -Amyloid Peptides via p38 Mitogen-Activated Protein Kinase Pathway. *J. Neurosci.* 29, 14741–14751. doi: 10.1523/JNEUROSCI.3728-09.2009

Castanheira, L., Ferreira, M. F., Sebastião, A. M., and Telles-Correia, D. (2018). Anxiety Assessment in Pre-clinical Tests and in Clinical Trials: A Critical Review. *Curr. Top. Med. Chem.* 18, 1656–1676. doi: 10.2174/1568026618666181115102518

Chen, P., Bodor, N., Wu, W.-M., and Prokai, L. (1998). Strategies to target Kyotorphin analogues to the brain. *J. Med. Chem.* 41, 3773–3781. doi: 10.1021/jm970715l

Citron, M. (2010). Alzheimer's disease: strategies for disease modification. *Nat. Rev. Drug Discov.* 9, 387–398. doi: 10.1038/nrd2896

Coleman, P., Federoff, H., and Kurlan, R. (2004). A focus on the synapse for neuroprotection in Alzheimer disease and other dementias. *Neurology* 63, 1155–1162. doi: 10.1212/01.WNL.0000140626.48118.0A

Cunha, G. M. A., Canas, P. M., Melo, C. S., Hockemeyer, J., Müller, C. E., Oliveira, C. R., et al. (2008). Adenosine A2A receptor blockade prevents memory dysfunction caused by β-amyloid peptides but not by scopolamine or MK-801. *Exp. Neurol.* 210, 776–781. doi: 10.1016/j.expneurol.2007.11.013

Diógenes, M. J., Costenla, A. R., Lopes, L. V., Jerónimo-Santos, A., Sousa, V. C., Fontinha, B. M., et al. (2011). Enhancement of LTP in Aged Rats is Dependent on Endogenous BDNF. *Neuropsychopharmacology* 36, 1823–1836. doi: 10.1038/npp.2011.64

Dzambazova, E. B., and Bocheva, A.II (2010). The unique brain dipeptide kyotorphin - from discovery to nowadays. *J. Biomed. Clin. Res.* 3, 3–11.

Figurov, A., Pozzo-Miller, L. D., Olafsson, P., Wang, T., and Lu, B. (1996). Regulation of synaptic responses to high-frequency stimulation and LTP by neurotrophins in the hippocampus. *Nature* 381, 706–709. doi: 10.1038/381706a0

Gage, G. J., Kipke, D. R., and Shain, W. (2012). Whole Animal Perfusion Fixation for Rodents. *J. Vis. Exp.* 3564. doi: 10.3791/3564

Giuffrida, M. L., Caraci, F., Pignataro, B., Cataldo, S., De Bona, P., Bruno, V., et al. (2009). B-Amyloid Monomers Are Neuroprotective. *J. Neurosci.* 29, 10582–10587. doi: 10.1523/JNEUROSCI.1736-09.2009

Gold, C. A., and Budson, A. E. (2008). Memory loss in Alzheimer's disease: implications for development of therapeutics. *Expert Rev. Neurother.* 8, 1879–1891. doi: 10.1586/14737175.8.12.1879

Goulart, B. K., de Lima, M. N. M., de Farias, C. B., Reolon, G. K., Almeida, V. R., Quevedo, J., et al. (2010). Ketamine impairs recognition memory consolidation and prevents learning-induced increase in hippocampal brain-derived neurotrophic factor levels. *Neuroscience* 167, 969–973. doi: 10.1016/j.neuroscience.2010.03.032

Gould, T. D., Dao, D. T., and Kovacsics, C. E. (2009). "The Open Field Test," in *Mood and Anxiety Related Phenotypes in Mice*. Ed. T. D. Gould (Totowa, NJ: Humana Press), 1–20. doi: 10.1007/978-1-60761-303-9_1

Huntley, J. D., and Howard, R. J. (2010). Working memory in early Alzheimer's disease: a neuropsychological review. *Int. J. Geriatr. Psychiatry* 25, 121–132. doi: 10.1002/gps.2314

Jerónimo-Santos, A., Vaz, S. H., Parreira, S., Rapaz-Lérias, S., Caetano, A. P., Buée-Scherrer, V., et al. (2015). Dysregulation of TrkB Receptors and BDNF Function by Amyloid-β Peptide is Mediated by Calpain. *Cereb. Cortex* 25, 3107–3121. doi: 10.1093/cercor/bhu105

Ji, Y., Lu, Y., Yang, F., Shen, W., Tang, T. T.-T., Feng, L., et al. (2010). Acute and gradual increases in BDNF concentration elicit distinct signaling and functions in neurons. *Nat. Neurosci.* 13, 302–309. doi: 10.1038/nn.2505

Kaminsky, Y. G., Marlatt, M. W., Smith, M. A., and Kosenko, E. A. (2010). Subcellular and metabolic examination of amyloid-beta peptides in Alzheimer disease pathogenesis: evidence for Abeta(25-35). *Exp. Neurol.* 221, 26–37. doi: 10.1016/j.expneurol.2009.09.005

Kawabata, A., Nishimura, Y., and Takagi, H. (1992). L-Leucyl-L-arginine, naltrindole and d-arginine block antinociception elicited by L-arginine in mice with carrageenin-induced hyperalgesia. *Br. J. Pharmacol.* 107, 1096–1101. doi: 10.1111/j.1476-5381.1992.tb13413.x

Korte, M., Kang, H., Bonhoeffer, T., and Schuman, E. (1998). A role for BDNF in the late-phase of hippocampal long-term potentiation. *Neuropharmacology* 37, 553–559. doi: 10.1016/S0028-3908(98)00035-5

Koskinen, M., and Hotulainen, P. (2014). Measuring F-actin properties in dendritic spines. *Front. Neuroanat.* 8, 1–14. doi: 10.3389/fnana.2014.00074

Lecanu, L., and Papadopoulos, V. (2013). Modeling Alzheimer's disease with non-transgenic rat models. *Alzheimers Res. Ther.* 5, 17. doi: 10.1186/alzrt171

Luscher, C., and Malenka, R. C. (2012). NMDA Receptor-Dependent Long-Term Potentiation and Long-Term Depression (LTP/LTD). *Cold Spring Harb. Perspect. Biol.* 4, a005710–a005710. doi: 10.1101/cshperspect.a005710

Maurice, T., Lockhart, B. P., and Privat, A. (1996). Amnesia induced in mice by centrally administered beta-amyloid peptides involves cholinergic dysfunction. *Brain Res.* 706, 181–193. doi: 10.1016/0006-8993(95)01032-7

McLarnon, J. G. (2014). Correlated inflammatory responses and neurodegeneration in peptide-injected animal models of Alzheimer's disease. *BioMed. Res. Int.* 2014 1–9. doi: 10.1155/2014/923670

Morris, R. G., Anderson, E., Lynch, G. S., and Baudry, M. (1986). Selective impairment of learning and blockade of long-term potentiation by an N-methyl-D-aspartate receptor antagonist, AP5. *Nature* 319, 774–776. doi: 10.1038/319774a0

Oliveira, M. C., Gano, L., Santos, I., Correia, J. D. G., Serrano, I. D., Santos, S. S., et al. (2016). Improvement of the pharmacological properties of amidated kyotorphin by means of iodination. *MedChemComm* 7, 906–913. doi: 10.1039/C6MD00028B

Pang, P. T., and Lu, B. (2004). Regulation of late-phase LTP and long-term memory in normal and aging hippocampus: role of secreted proteins tPA and BDNF. *Ageing Res. Rev.* 3, 407–430. doi: 10.1016/j.arr.2004.07.002

Perazzo, J., Lima, C., Heras, M., Bardají, E., Lopes-Ferreira, M., and Castanho, M. (2017). Neuropeptide Kyotorphin Impacts on Lipopolysaccharide-Induced Glucocorticoid-Mediated Inflammatory Response. A Molecular Link to Nociception, Neuroprotection, and Anti-Inflammatory Action. *ACS Chem. Neurosci.* 8, 1663–1667. doi: 10.1021/acschemneuro.7b00007

Pike, C. J., Walencewicz-Wasserman, A. J., Kosmoski, J., Cribbs, D. H., Glabe, C. G., and Cotman, C. W. (1995). Structure-activity analyses of beta-amyloid peptides: contributions of the beta 25-35 region to aggregation and neurotoxicity. *J. Neurochem.* 64, 253–265. doi: 10.1046/j.1471-4159.1995.64010253.x

Price, J. L., Davis, P. B., Morris, J. C., and White, D. L. (1991). The distribution of tangles, plaques and related immunohistochemical markers in healthy aging and Alzheimer's disease. *Neurobiol. Aging* 12, 295–312. doi: 10.1016/0197-4580(91)90006-6

Prut, L., and Belzung, C. (2003). The open field as a paradigm to measure the effects of drugs on anxiety-like behaviors: a review. *Eur. J. Pharmacol.* 463, 3–33. doi: 10.1016/S0014-2999(03)01272-X

Rajagopal, L., Massey, B., Huang, M., Oyamada, Y., and Meltzer, H. (2014). The Novel Object Recognition Test in Rodents in Relation to Cognitive Impairment in Schizophrenia. *Curr. Pharm. Des.* 20, 5104–5114. doi: 10.2174/1381612819666131216114240

Ribeiro, M. M. B., Pinto, A. R. T., Domingues, M. M., Serrano, I., Heras, M., Bardaji, E. R., et al. (2011a). Chemical Conjugation of the Neuropeptide Kyotorphin and Ibuprofen Enhances Brain Targeting and Analgesia. *Mol. Pharm.* 8, 1929–1940. doi: 10.1021/mp2003016

Ribeiro, M. M. B., Pinto, A. R. T., Pinto, M., Heras, M., Martins, I., Correia, A., et al. (2011b). Inhibition of nociceptive responses after systemic administration of amidated kyotorphin: Kyotorphin-amide: a new analgesic peptide. *Br. J. Pharmacol.* 163, 964–973. doi: 10.1111/j.1476-5381.2011.01290.x

Ribeiro, M. M. B., Santos, S. S., Sousa, D. S. C., Oliveira, M., Santos, S. M., Heras, M., et al. (2013). Side-effects of analgesic kyotorphin derivatives: advantages over clinical opioid drugs. *Amino Acids* 45, 171–178. doi: 10.1007/s00726-013-1484-2

Sá Santos, S., Santos, S. M., Pinto, A. R. T., Ramu, V. G., Heras, M., Bardají, E., et al. (2016). Amidated and Ibuprofen-Conjugated Kyotorphins Promote Neuronal Rescue and Memory Recovery in Cerebral Hypoperfusion Dementia Model. *Front. Aging Neurosci.* 8, 1–11. doi: 10.3389/fnagi.2016.00001

Sabuncu, M. R. (2011). The Dynamics of Cortical and Hippocampal Atrophy in Alzheimer Disease. *Arch. Neurol.* 68, 1040. doi: 10.1001/archneurol.2011.167

Santos, S. M., Garcia-Nimo, L., Sá Santos, S., Tavares, I., Cocho, J. A., and Castanho, M. A. R. B. (2013). Neuropeptide Kyotorphin (Tyrosyl-Arginine) has Decreased Levels in the Cerebro-Spinal Fluid of Alzheimer's Disease Patients: Potential Diagnostic and Pharmacological Implications. *Front. Aging Neurosci.* 5, 1–6. doi: 10.3389/fnagi.2013.00068

Serrano, I. D., Ramu, V. G., Pinto, A. R. T., Freire, J. M., Tavares, I., Heras, M., et al. (2015). Correlation between membrane translocation and analgesic efficacy in kyotorphin derivatives: Membrane Translocation and Analgesic Efficacy. *Biopolymers* 104, 1–10. doi: 10.1002/bip.22580

Shiomi, H., Ueda, H., and Takagi, H. (1981). Isolation and identification of an analgesic opioid dipeptide kyotorphin (TYR-ARG) from bovine brain. *Neuropharmacology* 20, 633–638. doi: 10.1016/0028-3908(81)90109-X

Takagi, H., Shiomi, H., Ueda, H., and Amano, H. (1979a). A novel analgesic dipeptide from bovine brain is a possible Met-enkephalin releaser. *Nature* 282, 410–412. doi: 10.1038/282410a0

Takagi, H., Shiomi, H., Ueda, H., and Amano, H. (1979b). Morphine-like analgesia by a new dipeptide, L-Tyrosyl-L-Arginine (kyotorphin) and its analogue. *Eur. J. Pharmacol.* 55, 109–111. doi: 10.1016/0014-2999(79)90154-7

Tanqueiro, S. R., Ramalho, R. M., Rodrigues, T. M., Lopes, L. V., Sebastião, A. M., and Diógenes, M. J. (2018). Inhibition of NMDA Receptors Prevents the Loss of BDNF Function Induced by Amyloid β. *Front. Pharmacol.* 9, 237. doi: 10.3389/fphar.2018.00237

Toni, N., Buchs, P.-A., Nikonenko, I., Bron, C. R., and Muller, D. (1999). LTP promotes formation of multiple spine synapses between a single axon terminal and a dendrite. *Nature* 402, 421–425. doi: 10.1038/46574

Ueda, H., Shiomi, H., and Takagi, H. (1980). Regional distribution of a novel analgesic dipeptide kyotorphin (Tyr-Arg) in the rat brain and spinal cord. *Brain Res.* 198, 460–464. doi: 10.1016/0006-8993(80)90761-1

Ueda, H., Tatsumi, K., Shiomi, H., and Takagi, H. (1982). Analgesic dipeptide, kyotorphin (Tyr-Arg), is highly concentrated in the synaptosomal fraction of the rat brain. *Brain Res.* 231, 222–224. doi: 10.1016/0006-8993(82)90023-3

Ueda, H., Yoshihara, Y., and Takagi, H. (1986). A putative met-enkephalin releaser, kyotorphin enhances intracellular Ca2+ in the synaptosomes. *Biochem. Biophys. Res. Commun.* 137, 897–902. doi: 10.1016/0006-291x(86)91164-2

Ueda, H., Yoshihara, Y., Misawa, H., Fukushima, N., Katada, T., Ui, M., et al. (1989). The kyotorphin (tyrosine-arginine) receptor and a selective reconstitution with purified Gi, measured with GTPase and phospholipase C assays. *J. Biol. Chem.* 264, 3732–3741.

Zhang, L., Fang, Y., Lian, Y., Chen, Y., Wu, T., Zheng, Y., et al. (2015). Brain-Derived Neurotrophic Factor Ameliorates Learning Deficits in a Rat Model of Alzheimer's Disease Induced by Aβ1-42. *PLoS One* 10, e0122415. doi: 10.1371/journal.pone.0122415

Zidan, M., Arcoverde, C., Araújo, , N.B.de, Vasques, P., Rios, A., Laks, J., et al. (2012). Alterações motoras e funcionais em diferentes estágios da doença de Alzheimer. *Arch. Clin. Psychiatry São Paulo* 39, 161–165. doi: 10.1590/S0101-60832012000500003

Conflict of Interest: The authors declare that the research was conducted in the absence of any commercial or financial relationships that could be construed as a potential conflict of interest.